

Molecular markers in breast cancer:  
new tools in imaging and prognosis

Jeroen Vermeulen



Coverart: 'Natural Pose',

© Joe Bonita, 2012

Used with permission.

ISBN: 978-90-393-5861-0

© J.F. Vermeulen, 2012

Printed by: Gildeprint Drukkerijen - Enschede, The Netherlands

Financial support for the publication of this thesis was kindly provided by: Department of Pathology University Medical Center Utrecht, A. Menarini Diagnostics, Novartis Oncology, Roche Nederland.

# Molecular markers in breast cancer: new tools in imaging and prognosis

**Moleculaire markers in borstkanker:  
nieuwe mogelijkheden voor beeldvorming en prognose**

*(met een samenvatting in het Nederlands)*

## **Proefschrift**

ter verkrijging van de graad van doctor aan de Universiteit Utrecht  
op gezag van de rector magnificus, prof. dr. G.J. van der Zwaan,  
ingevolge het besluit van het college voor promoties  
in het openbaar te verdedigen op vrijdag 14 december 2012  
des middags te 2.30 uur

door

**Johannes Frederikus Vermeulen**

geboren op 8 december 1984

te Gouda

Promotoren: Prof. dr. E. van der Wall  
Prof. dr. P.J. van Diest

Co-promotor: Dr. P.W.B. Derksen

# Contents

<b>Chapter 1</b>	General introduction	7
PART 1:	MOLECULAR MARKERS FOR IMAGING OF BREAST CANCER	
<b>Chapter 2</b>	The potential of hypoxia markers for molecular imaging of breast cancer - a systematic review and meta-analysis <i>Manuscript in preparation</i>	13
<b>Chapter 3</b>	Immunophenotyping invasive breast cancer: paving the road for molecular imaging <i>BMC Cancer 2012; 12(1): 240</i>	57
<b>Chapter 4</b>	Differential expression of growth factor receptors and membrane-bound tumor markers for imaging in male and female breast cancer <i>Submitted</i>	75
<b>Chapter 5</b>	Expression of membrane markers for molecular imaging of ductal carcinoma in situ of the breast <i>Submitted</i>	91
<b>Chapter 6</b>	Near-infrared fluorescence molecular imaging of ductal carcinoma in situ with CD44v6-specific antibodies in mice: a preclinical study <i>Submitted</i>	103
PART 2:	BIOMARKERS PREDICTING METASTASIS AND THERAPY RESISTANCE	
<b>Chapter 7</b>	Nuclear Kaiso expression is associated with high grade and triple-negative invasive breast cancer <i>PLOS One 2012; 7(5): e:37864</i>	123
<b>Chapter 8</b>	FER kinase promotes breast cancer growth and metastasis through inhibition of cell adhesion and anchorage dependence <i>Submitted</i>	143

<b>Chapter 9</b>	Nuclear SOX4 expression in breast cancer predicts resistance towards adjuvant chemo- and radiotherapy <i>Manuscript in preparation</i>	173
<b>Chapter 10</b>	Summary and future perspectives	191
ADDENDUM		
	Nederlandse samenvatting	198
	Dankwoord	202
	About the Author	205
	List of Publications	207

# One

**General introduction**

## General introduction

The life time risk to develop breast cancer is 1 in 8 for women and 1 in 1,000 for men, resulting that breast cancer is the most prevalent cancer in women worldwide [1]. In The Netherlands, 13,257 women and 94 men were diagnosed with breast cancer in 2010 [2, 3]. The incidence of breast cancer is still increasing every year, due to increased life expectancy and because of the age composition of the Dutch population. However, the number of breast cancer-related deaths has been stable for the last decades; annually around 3,200 women and 32 men. Due to improved diagnostics and therapeutic strategies, the 5-years survival rate increased to 86% ([www.i knl.nl](http://www.i knl.nl)) in last 20 years, but eventually one third of patients will still develop distant metastases [4].

The majority of breast cancers in The Netherlands are detected by mammographic based population screening. Since the introduction of digital mammography, breast cancers are more often detected in an early stage, resulting in better survival rates. However, the detection rate of ductal carcinoma *in situ* (DCIS) and columnar cell lesions also increased, resulting that DCIS being increasingly the sole target of surgery [5, 6]. Since mammography is not ultimately sensitive in younger patients and patients with dense breasts [7-12], other imaging modalities like ultrasonography, MRI and PET are increasingly used for diagnosis of breast cancer.

The most recent developments in the field of molecular imaging comprise the application of near-infrared fluorescent labeled (NIRF) tracers for detection of breast cancer. The oldest NIRF tracer, indocyanine green (ICG), was applied for detection of breast cancer in the early 2000s by Ntziachristos et al. when they showed that ICG uptake in the tumor overlapped with MRI images [13]. The disadvantages of ICG are the relatively low quantum yield, the stability, and that ICG is not targeted which resulted in limited resolution. The new generation of near-infrared dyes, including IRDye800CW, have solved these problems and allow the generation of tumor-specific imaging tracers based on antibodies, antibody-fragments etc., resulting in higher sensitivity and specificity. Thus far, only a few molecular imaging tracers have been taken to the clinic.

In addition to improved detection of breast cancer, increased survival was obtained by targeted therapies. Since the molecular characteristics of breast cancer are being elucidated over the last few decades, the potential for targeted therapeutics in predefined subgroups of patients increased. Improved patient survival was obtained with e.g. tamoxifen/aromatase inhibitors in hormone receptor positive disease and Herceptin in HER2-



positive breast cancer. Currently, multiple other membrane targets are considered as targets for therapy such as EGFR, IGF1-R and vascular endothelial growth factor (VEGF). This also means that patient stratification based on tumor characteristics becomes crucial, and that loss of expression of the target directly affects the sensitivity for therapy and is a determinant for acquired therapy resistance. Therefore, diagnostic imaging and targeted therapy increasingly go hand in hand and will become an integral part of clinical decision making (“theranostics”).

## Outline of the thesis

The first part of the thesis focuses on biomarkers for molecular imaging of breast cancer. In **chapter 2** the prevalence of hypoxia-related markers CAIX, GLUT1, CXCR4, and IGF1-R in breast cancer and their potential for molecular imaging strategies is systematically reviewed, to unravel the most suitable targets for molecular imaging. **Chapter 3** reports expression profiles of membrane-bound markers for molecular imaging in histological and molecular subtypes of female breast cancer. In **chapter 4** the growth factor receptor expression profiles of male breast cancer are studied in search of a marker panel for molecular imaging of male breast cancer. **Chapter 5** explores whether identified markers for imaging of female breast cancer can be used for image-guided surgery of ductal carcinoma *in situ* (DCIS) using molecular imaging and whether expression differs between DCIS and adjacent invasive breast cancer. In **Chapter 6** we explore for the first time optical imaging using CD44v6-specific antibodies for non-invasive and intra-operative imaging of DCIS lesions *in vivo* in a preclinical study.

The second part of the thesis focuses on markers determining aggressiveness, metastasis, and predicting therapy resistance of breast cancer. The role of the transcription factor Kaiso in ductal and lobular breast cancer in relation to grade, estrogen receptor expression and molecular type is described in **chapter 7**. The role of FER kinase in breast cancer metastasis is examined in **chapter 8**. **Chapter 9** reports SOX4 expression in breast cancer and explores its relation to prognosis and resistance to chemotherapy and radiotherapy.

Finally, in **chapter 10** the results of this thesis are summarized and discussed, including the future directions.

## References

1. Howlader N, Noone A, Krapcho M, *et al.* SEER Cancer Statistics Review, 1975-2009, based on November 2011 SEER data submission. 2012.
2. Integraal KankerCentrum Nederland. Sterfte aan kanker (1989-2010). [www.cijfersoverkanker.nl](http://www.cijfersoverkanker.nl). Accessed: 30 June 2012.
3. Integraal KankerCentrum Nederland. Incidentie van invasieve tumoren (1989-2010). [www.cijfersoverkanker.nl](http://www.cijfersoverkanker.nl). Accessed: 30 June 2012.
4. Siegel R, Naishadham D and Jemal A. Cancer statistics, 2012. *CA Cancer J Clin* 2012; 62(1):10-29.
5. Verschuur-Maes AH, van Gils CH, van den Bosch MA, De Bruin PC and van Diest PJ. Digital mammography: more microcalcifications, more columnar cell lesions without atypia. *Mod Pathol* 2011; 24(9):1191-7.
6. Wong H, Lau S, Leung R, *et al.* Coexisting ductal carcinoma in situ independently predicts lower tumor aggressiveness in node-positive luminal breast cancer. *Med Oncol* 2011.
7. Brewer NT, Salz T and Lillie SE. Systematic review: the long-term effects of false-positive mammograms. *Ann Intern Med* 2007; 146(7):502-10.
8. Brown ML, Houn F, Sickles EA and Kessler LG. Screening mammography in community practice: positive predictive value of abnormal findings and yield of follow-up diagnostic procedures. *Am J Roentgenol* 1995; 165(6):1373-7.
9. Elmore JG, Armstrong K, Lehman CD and Fletcher SW. Screening for breast cancer. *JAMA* 2005; 293(10):1245-56.
10. Kerlikowske K, Grady D, Barclay J, *et al.* Positive predictive value of screening mammography by age and family history of breast cancer. *JAMA* 1993; 270(20):2444-50.
11. Lidbrink E, Elfving J, Frisell J and Jonsson E. Neglected aspects of false positive findings of mammography in breast cancer screening: analysis of false positive cases from the Stockholm trial. *BMJ* 1996; 312(7026):273-6.
12. Moadel RM. Breast cancer imaging devices. *Semin Nucl Med* 2011; 41(3):229-41.
13. Ntziachristos V, Yodanis AG, Schnall M and Chance B. Concurrent MRI and diffuse optical tomography of breast after indocyanine green enhancement. *Proc Natl Acad Sci U S A* 2000; 97(6):2767-72.



# Part 1



# Two

## **The potential of hypoxia markers for molecular imaging of breast cancer - a systematic review and meta-analysis**

Jeroen F. Vermeulen<sup>1\*</sup>, Arthur Adams<sup>2\*</sup>, Aram S.A. van Brussel<sup>1\*</sup>,  
Willem P.Th.M. Mali<sup>2</sup>, Elsken van der Wall<sup>3</sup>, Paul J. van Diest<sup>1</sup>, Sjoerd G. Elias<sup>2,4</sup>

<sup>1</sup> Department of Pathology, University Medical Center Utrecht, Utrecht, The Netherlands,

<sup>2</sup> Department of Radiology, University Medical Center Utrecht, Utrecht, The Netherlands,

<sup>3</sup> Division of Internal Medicine and Dermatology, University Medical Center Utrecht, Utrecht,  
The Netherlands,

<sup>4</sup> Julius Center of Health Sciences and Primary Care, University Medical Center Utrecht,  
Utrecht, The Netherlands

\* These authors contributed equally to this study

***Manuscript in preparation***

## Abstract

**Background:** Molecular imaging of breast cancer with tumor-specific tracers has several potential advantages over the currently used anatomical imaging modalities. As hypoxia is a common phenomenon in breast cancer, hypoxia-upregulated membrane proteins could be valuable targets for molecular imaging. We performed a comprehensive systematic review and meta-analysis of the literature to assess immunohistochemical expression patterns of hypoxia-upregulated membrane proteins in breast cancer, to evaluate their potential for molecular imaging strategies.

**Materials and Methods:** A systematic search of the database of MEDLINE and EMBASE was performed to identify articles describing CAIX, or GLUT1, or CXCR4, or IGF1R expression in breast cancer evaluated by immunohistochemistry. We pooled prevalence estimates across studies using a random-effects linear mixed model, allowing for between-study heterogeneity, and used meta-regression to assess the relation between hypoxia marker expression and histological grade, tumor size, histological type, and specimen handling.

**Results:** The search yielded 1,705 articles, of which 126 articles were included, comprising 28,478 specimens. Pooled expression prevalences were 35% (95% Confidence Interval (CI): 26%-46%) for CAIX, 51% (95% CI 40%-62%) for GLUT1, 46% (95% CI: 33%-59%) for CXCR4, and 46% (95% CI: 35%-57%) for IGF1R, respectively. The expression prevalence of CAIX, GLUT1, and CXCR4 was significantly higher for grade III compared to grade I cancers (all  $p < 0.001$ ). Further, the prevalence of all markers was significantly lower in lobular breast cancer ( $p < 0.001$ ). Tissue microarray-based studies reported a lower prevalence for CAIX ( $p = 0.006$ ) and GLUT1 ( $p = 0.007$ ), and a higher prevalence for IGF1R ( $p = 0.032$ ) than studies using whole slides.

**Conclusion:** We have shown that expression patterns of hypoxia markers are in the range of other targets for molecular imaging of breast cancer, but are individually insufficiently expressed to be used for screening or diagnostic purposes. Future studies should incorporate data on expression patterns in normal tissue, benign lesions, and DCIS, as such information is currently lacking in the literature.

## Introduction

In the past decades, conventional breast cancer imaging modalities such as (digital) mammography, breast ultrasound, and more recently dynamic contrast enhanced magnetic resonance imaging (DCE-MRI) and  $^{18}\text{F}$ -fluorodeoxyglucose Positron Emission Tomography ( $^{18}\text{F}$ FDG-PET), have improved the detection, characterization, and management of breast cancer. Although these imaging modalities are valuable in clinical practice, molecular imaging of breast cancer with tumor-specific tracers such as antibodies or antibody-based molecules has several potential advantages. These include high sensitivity and specificity, the potential of early detection, detection of distant metastases, intra-operative guidance, 'in vivo' receptor status determination, and, in the case of fluorescent molecular imaging, no use of ionizing radiation [1-5].

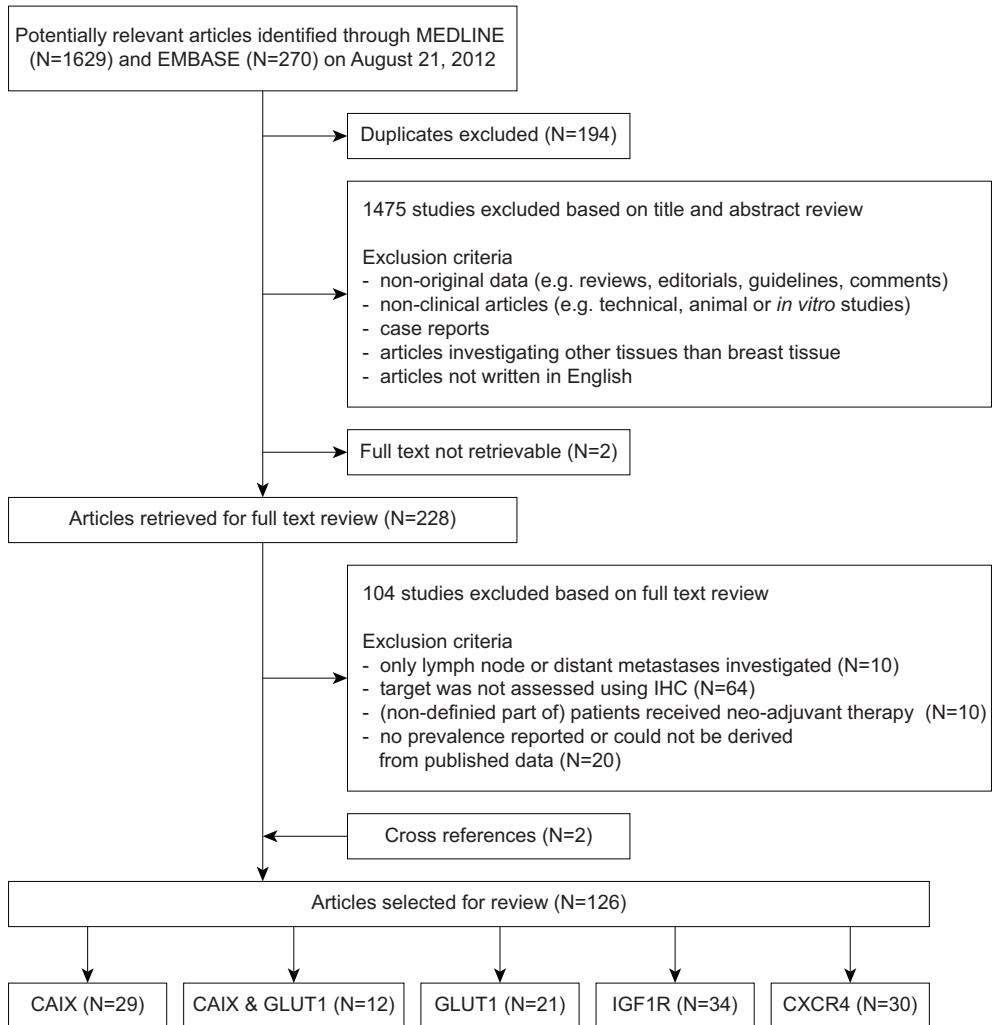
Besides growth factor receptors (e.g. EGFR, HER2), that have been exploited in several (pre)clinical studies as molecular imaging targets [6-9], hypoxia-upregulated proteins could be valuable for molecular imaging. Hypoxia is involved in neo-angiogenesis (one of the hallmarks of cancer [10]) and is present in about half of all breast cancers [11]. In ductal carcinoma *in situ* (DCIS) and in larger tumors, tumor hypoxia arises due to limited perfusion [12, 13]. This results in focal expression of hypoxia inducible factor 1 $\alpha$  (HIF-1 $\alpha$ ), the key regulator of the hypoxia response [11, 12, 14].

Successful clinical implementation of molecular imaging depends on several aspects, including the expression of the targeted tumor antigen. In general, extracellularly located targets such as plasma membrane markers are most attractive, as these are easier accessible for most tracers compared to intracellular targets that are shielded from the extracellular environment by the plasma membrane [15]. The downstream targets of HIF-1 $\alpha$ , carbonic anhydrase IX (CAIX), glucose transporter 1 (GLUT1) and C-X-C chemokine receptor type 4 (CXCR4) [16-19], and insulin-like growth factor 1 receptor (IGF1R) that maintains the hypoxia response via HIF-1 $\alpha$  stabilization [20-22], are expressed on the plasma membrane and can therefore be suitable candidates for molecular imaging purposes.

Despite the high potential of these hypoxia-upregulated proteins, it is not well known in what proportion of breast cancers these targets are present, as reported prevalences of these targets vary widely in literature. Furthermore, variation of marker expression between cancer patients, levels of expression in normal breast tissue and benign lesions, expression in tumor margins, and intra-tumor heterogeneity [23-25] could potentially limit successful clinical implementation.

To evaluate whether molecular imaging using these targets could be clinically relevant, we performed a systematic literature review and meta-analysis to quantify expression prevalences of these hypoxia markers in breast cancer as assessed by immunohistochemistry, and to determine the significance of clinicopathological characteristics (tumor size, histological grade, and histological type) on these expression rates.

**Figure 1.** Flowchart of the selection procedure.





## Methods

### Literature search

We performed a comprehensive systematic search in the databases of MEDLINE and EMBASE on August 21, 2012. Search terms included synonyms for the targets of interest (CXCR4, GLUT1, CAIX, and IGF1R), combined with 'breast' and 'mamm\*'. The full search syntax can be found in Table 1. We applied no restrictions on publication date. The search in the database of EMBASE was limited to articles that were not indexed with a MEDLINE ID, and conference abstracts were excluded. Duplicate articles were manually removed from the search results.

**Table 1.** Search strategy used to identify publications of interest.

Target	Synonyms used
CAIX	CAIX OR CA-IX OR "CA IX" OR CA9 OR CA-9 OR "CA 9" OR "carbonic anhydrase IX" OR "carbonic anhydrase 9"
GLUT1	GLUT1 OR GLUT-1 OR "Glucose transporter 1"
CXCR4	CXCR4 OR CXCR-4 OR CXC-R4 OR "CXC chemokine receptor-4"
IGF1R	"insulin like growth factor 1 receptor" OR IGF-1R OR IGF1R OR IGF1-R OR "insulin like growth factor I receptor" OR IGFR OR IGF-IR

Search terms were combined with 'breast' and 'mamm\*'. For MEDLINE, '[tiab]' was added to each search term, and for EMBASE, 'ti;ab;' was added.

### Selection of articles

Article eligibility was reviewed by three reviewers (ASAvB, AA, and JFV) by screening all titles and abstracts from the search result independently. We excluded articles based on predefined criteria and disagreements were resolved by discussion. An overview of the selection procedure is shown in Figure 1. Reasons for exclusion of articles based on title or abstract were: (1) non-original data (e.g. reviews, editorials, guidelines, and comments), (2) non-clinical articles (e.g. technical, animal, or *in vitro* studies), (3) case reports, (4) articles investigating other tissues than breast tissue, or (5) articles not written in English. The full texts of the remaining articles were reviewed for information on prevalences of expression of the targets of interest. Studies were excluded if (1) lymph node or distant metastases were investigated only (N=10), (2) the target of interest was assessed using another method than immunohistochemistry (e.g. qPCR or Western Blot) (N=64), (3) all or a non-definable part of patients received neo-adjuvant therapy (N=10), or (4) the prevalence of the target of interest was not reported and could not be derived from the published data (N=20). All references of the remaining articles were reviewed to retrieve articles initially missed in the search syntax.

### *Data extraction and statistical analysis*

We extracted relevant information of each study (e.g. study and population characteristics, patient and tumor characteristics, and immunohistochemical methodology). Then, for each study and per target of interest, we annotated the number of lesions stated as target-positive and the total number of lesions, either directly or through recalculation based on the information stated in the article. Lesions of interest were invasive breast cancer, DCIS, benign breast lesions, or normal breast tissue.

For invasive cancers, we grouped studies based on similar cut-off values used for calling a result positive. If patient data was used in multiple articles (e.g. when articles referred to the same study, or assessed a comparable number of patients from the same hospital in the same inclusion period to evaluate the expression of the same hypoxia marker), then only the article with the largest number of patients was included in the review and meta-analysis. Subgroups were defined for expression prevalences in relation to tumor size, histological grade, and histological type, when stated. Furthermore, studies were grouped according to specimen handling, i.e. if whole slides or TMAs were investigated. Then, for the total group of invasive cancers and the defined subgroups (i.e. tumor size, histological grade, histological type, specimen handling), we pooled prevalence estimates across studies using a random-effects model, allowing for between-study heterogeneity. For this, a linear mixed model was fit to the data using the exact binomial approach with the restricted maximum likelihood method [26]. Then, we tested for subgroup differences using meta-regression analysis (linear mixed model with subgroup indicators as fixed and the individual studies as random effects).

Analyses were performed with R (version 2.15.1, R Foundation for Statistical Computing, Vienna, Austria) [27]; with the package 'lme4' [28]. All statistical tests were two-sided and a p-value of <0.05 was considered statistically significant. Prevalence estimates are reported with corresponding 95% logit confidence intervals.

## Results

The search yielded 1,629 articles in MEDLINE and 270 articles in EMBASE. After removal of 194 duplicates, 1,705 unique articles were left for evaluation. Of these, we excluded 1,475 articles based on title and abstract, and 104 articles based on full text screening (Figure 1). The full text of two articles could not be retrieved. Reference cross-checking of the selected articles yielded two additional studies that were initially missed, as (synonyms) for 'breast' were not included in the title or abstract [29, 30]. Of the 126 selected studies, 11 studies [31-41] described both GLUT1 and CAIX expression, and one study [23] described IGF1R, CAIX, and GLUT1 expression. We excluded eight articles [42-49], from our meta-analysis due to (suspected) patient overlap with other articles. Also, one article [40] was excluded because we could not distinguish between *in situ* and invasive breast cancer. Study characteristics of the included studies are shown in Table S1.

Included studies were heterogeneous with respect to the applied immunohistochemistry methodology. For assessment of CAIX expression, 3 different antibodies were used, and 11 (31%) studies did not specify the used clone. For GLUT1, 6 different antibodies were used and for 23 (72%) studies only the manufacturer was stated. For CXCR4, 8 different antibodies were used and in 8 (29%) studies the antibody data was not reported, and for IGF1R, 11 different antibodies were used, and 6 (19%) studies did not specify either the clone or the manufacturer.

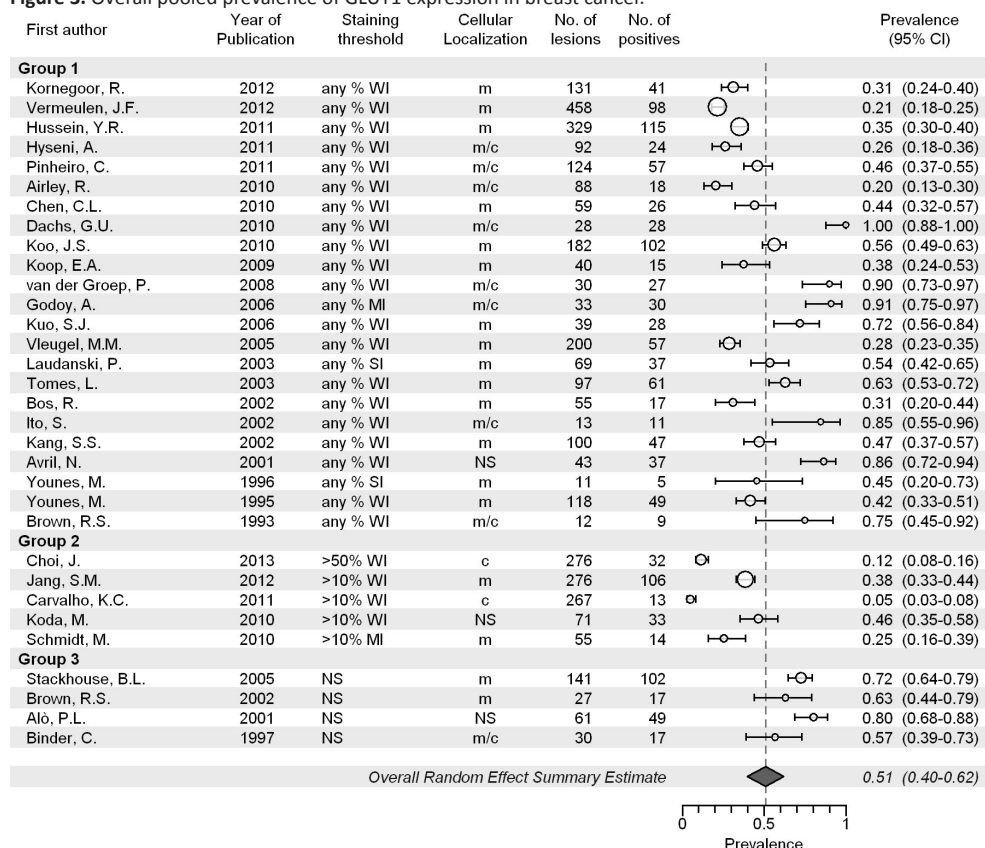
In addition, 44% of the studies used tissue microarrays (TMAs) to evaluate the expression of the target of interest. However, only 31 (62%) studies using TMAs reported the number of cores and 36 (72%) studies reported the diameter of the cores. In 37% of the studies, no information was available on who evaluated the staining intensity and localization and in 38% of the studies it was explicitly stated that evaluation was performed by one or more pathologists.



### GLUT1

A total of 32 articles including 3,555 invasive cancers reported on GLUT1 expression (range of 11-458 cancers per study). The overall pooled prevalence of GLUT1 expression was 51% (95% CI 40-62%; Figure 3), but the reported prevalence varied substantially between studies (range 5%-100%). GLUT1 prevalences were significantly higher in grade III tumors (58% vs. 23% in grade I tumors,  $p < 0.001$ ). Furthermore, ILC was associated with a significantly lower GLUT1 prevalence compared to IDC (9% vs. 48%,  $p < 0.001$ ). Studies using TMAs had a significantly lower prevalence of GLUT1 expression compared to studies using whole slides (33% vs. 66%,  $p = 0.007$ ). The pooled prevalences and the results from the meta-regression are summarized in Table 2, and the individual study estimates and pooling results per subgroup are shown in Figures S5-8.

**Figure 3.** Overall pooled prevalence of GLUT1 expression in breast cancer.

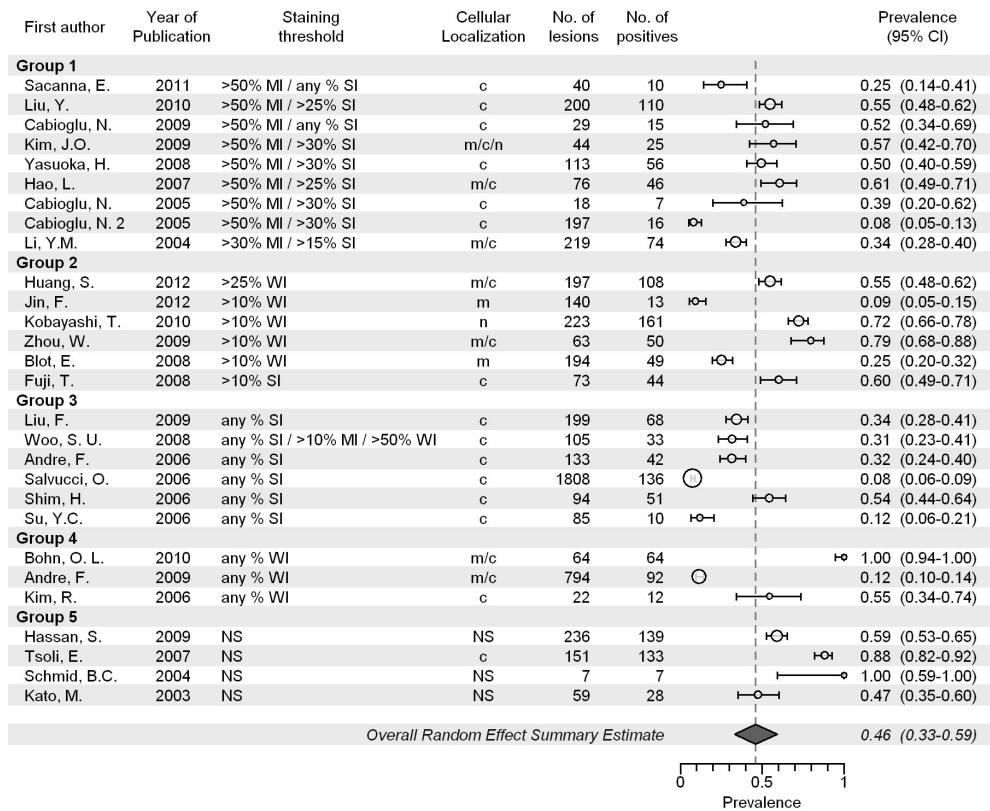


Dashed line represents overall random effect summary prevalence estimate. Abbreviations: Staining threshold: weak intensity (WI), moderate intensity (MI), strong intensity (SI); Localization: cytoplasm (c), membrane (m); confidence interval (CI); not stated (NS)

## CXCR4

A total of 28 articles including 5,583 invasive cancers reported on CXCR4 expression (range of 7-1,808 cancers per study). The pooled prevalence of CXCR4 expression was 46% (95% CI 33-59%; Figure 4), with a range between studies of 8-100%. CXCR4 prevalence increased with histological grade (pooled prevalence of 32% in grade II ( $p=0.049$ ) and 44% in grade III ( $p<0.001$ ) cancer compared to 26% in grade I cancers). Furthermore, the prevalence of CXCR4 in IDC was significantly higher than in ILC, (46% vs. 35%,  $p=0.001$ ). However, no significant relation of CXCR4 prevalence was found with respect to tumor size and the slide construction method. The pooled prevalences and the results from the meta-regression are summarized in Table 2, and the individual study estimates and pooling results per subgroup are shown in Figures S9-12.

**Figure 4.** Overall pooled prevalence of CXCR4 expression in breast cancer.

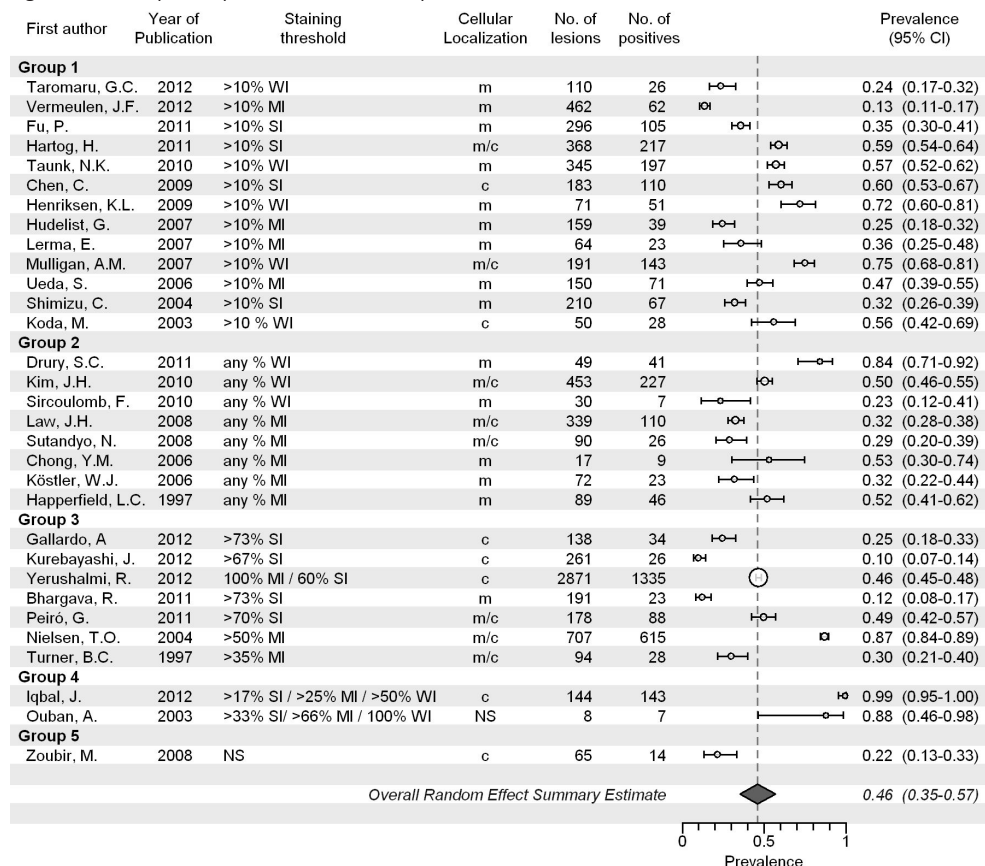


Dashed line represents overall random effect summary prevalence estimate. Abbreviations: Staining threshold: weak intensity (WI), moderate intensity (MI), strong intensity (SI); Localization: cytoplasm (c), membrane (m), nuclear (n); confidence interval (CI); not stated (NS)

## IGF1R

We analyzed a total of 31 articles including 8,455 breast cancer specimens (range of 8-2,871 cancers per study). The pooled prevalence of IGF1R expression was 46% (95% CI 35-57%) with a range between studies of 10%-99%. (Figure 5). Prevalence of IGF1R was higher in IDC compared to ILC (42% vs. 25%,  $p<0.001$ ). In contrast to CAIX, GLUT1, and CXCR4, the pooled prevalence of IGF1R was significantly lower in grade III tumors vs. grade I cancers (41% vs. 57%,  $p<0.001$ ) and in lower in T3 cancers compared to T1 cancers (39% vs. 45%,  $p=0.047$ ). Furthermore, the pooled prevalence was higher in studies using TMAs compared to studies using whole slides (57% vs. 34%,  $p=0.032$ ). The pooled prevalences and the results from the meta-regression are summarized in Table 2, and the individual study estimates and pooling results per subgroup are shown in Figures S13-16.

**Figure 5.** Overall pooled prevalence of IGF1R expression in breast cancer.



Dashed line represents overall random effect summary prevalence estimate. Abbreviations: Staining threshold: weak intensity (WI), moderate intensity (MI), strong intensity (SI); Localization: cytoplasm (c), membrane (m); confidence interval (CI); not stated (NS)

*Expression of hypoxia markers in normal tissue, benign and in situ lesions*

In 19 studies, expression of hypoxia markers in normal breast tissue, benign or ductal carcinoma *in situ* lesions was described. Individual study estimates are shown in Figures S17-20. In normal breast tissue, expression frequencies ranged from 0% to 74% for CAIX (4 studies), 0% to 35% for GLUT1 (5 studies), 0% to 7% for CXCR4 (4 studies), and 62% to 74% for IGF1R (2 studies), respectively. Expression of hypoxia markers in benign lesions was comparable to normal breast tissue. For DCIS, CAIX expression was described in four studies, with prevalences ranging from 25% to 71%; GLUT1 in three studies with prevalences ranging from 42% to 64%; CXCR4 in two studies with prevalences ranging from 44% to 93%, and IGF1R in two studies with prevalences ranging from 24 to 53%, respectively.



**Table 2.** Systematic review and meta-analysis of the prevalence of hypoxia markers in breast cancer in relation to clinicopathological features.

Clinicopathological features	CAIX			GLUT1			CKC4			IGF1R					
	N	Prevalence	95% CI	p-value	N	Prevalence	95% CI	p-value	N	Prevalence	95% CI	p-value			
Overall	36	0.35	0.26-0.46		32	0.51	0.40-0.62		28	0.46	0.33-0.59		31	0.46	0.35-0.70
Histological grade	12				9				13				5		
I		0.04	0.02-0.08	Ref		0.23	0.17-0.31	Ref		0.26	0.13-0.44	Ref		0.57	0.51-0.63
II		0.16	0.10-0.24	<b>&lt;0.001</b>		0.30	0.17-0.47	0.090		0.32	0.17-0.52	<b>0.049</b>		0.51	0.49-0.54
III		0.30	0.22-0.39	<b>&lt;0.001</b>		0.58	0.44-0.70	<b>&lt;0.001</b>		0.44	0.26-0.63	<b>&lt;0.001</b>		0.41	0.39-0.43
Tumor size	7				6				12				4		
T1		0.12	0.11-0.14	Ref		0.37	0.31-0.42	Ref		0.48	0.28-0.69	Ref		0.45	0.39-0.51
T2		0.15	0.11-0.20	<b>&lt;0.001</b>		0.36	0.29-0.43	0.64		0.52	0.28-0.74	0.62		0.47	0.44-0.49
T3		0.30	0.17-0.47	<b>&lt;0.001</b>		0.30	0.14-0.53	0.18		0.68	0.53-0.80	0.12		0.39	0.32-0.47
Histological type	13				13				10				6		
IDC		0.34	0.20-0.52	Ref		0.48	0.32-0.64	Ref		0.46	0.22-0.72	Ref		0.42	0.28-0.57
ILC		0.01	0.00-0.05	<b>0.001</b>		0.09	0.01-0.40	<b>&lt;0.001</b>		0.35	0.00-0.98	<b>0.001</b>		0.25	0.08-0.55
Specimen handling	36				32				28				31		
Whole slides		0.50	0.36-0.64	Ref		0.61	0.48-0.72	Ref		0.39	0.28-0.51	Ref		0.34	0.26-0.42
Tissue Microarray		0.26	0.17-0.36	<b>0.006</b>		0.33	0.20-0.48	<b>0.007</b>		0.61	0.29-0.85	0.17		0.57	0.39-0.73

p-values obtained using meta-regression (linear mixed model with subgroup indicators as fixed and the individual studies as random effects)

## Discussion

In this comprehensive systematic review and meta-analysis, we reported on the prevalence of expression of the hypoxia-upregulated proteins GLUT1, CAIX, CXCR4, and IGF1R in breast cancer. We included a total of 126 articles, were able to pool results on 28,478 investigated specimens, and found clinicopathological features significantly influencing expression rates. The expression prevalences of the hypoxia-upregulated proteins were in the range of other potential targets for molecular imaging (e.g. EGFR, 48%) [50] and were much higher than for example HER2. Given the known heterogeneity of breast cancer, the investigated hypoxia proteins have high potential for molecular imaging purposes.

However, our reported pooled prevalences might not reflect true expression rates of the investigated targets, as between-study variation was substantial. There are several possible causes responsible for this variation. First, by using meta-regression we found that clinicopathological features of breast cancer significantly influenced the expression rate of hypoxia markers. Second, we found large variability in used staining and assessment methodology, and third, differences in study populations and study settings might have had influence on the expression prevalences. We will elaborate on these three factors below.

CAIX, GLUT1 and CXCR4 were more frequently expressed in high grade tumors, consistent with the hypothesis that high grade tumors have a higher proliferation rate, which causes the formation of new blood vessels to lag behind the expanding tumor mass. The resulting inadequate nutrient and oxygen supply results in tumor hypoxia and upregulation of CAIX, GLUT1 and CXCR4 [51, 52]. This could also suggest that larger tumors express hypoxia markers more frequently. However, we could only find this relation for CAIX in our meta-analysis. In addition, we found that hypoxia proteins are infrequently expressed in lobular carcinomas. This might suggest that hypoxia is not a common phenomenon in ILC. Another study reported that only 3% of lobular carcinomas expressed HIF1 $\alpha$ , compared to 39% of ductal carcinomas [53], indicating that hypoxia is rare in ILC and thereby explains the low prevalence of hypoxia proteins in lobular carcinomas. Also, results of <sup>18</sup>F-FDG-PET showed that lobular carcinomas had a lower Standardized Uptake Value (SUV) compared to ductal carcinomas [54, 55], indicating that tumor metabolism is lower in these tumors. Whether the absence of hypoxia and lower SUV found in ILC can be related to the diffuse growth pattern of ILC, the lack of growth factor receptor expression in ILC [23] or to an intrinsic phenomenon of ILC remains to be elucidated. For molecular imaging of lobular carcinoma, other markers than hypoxia proteins should be considered.

Among the investigated articles, different cut-off values were chosen for calling a result positive. Unlike HER2 for which the scoring system is standardized, the cut-off for the hypoxia markers was either arbitrarily chosen, chosen on local experience, or not reported at all. In case of CAIX and GLUT1 expression, the majority of studies used the presence of any staining in any percentage of cells as cut-off, whereas for CXCR4 the cut-off differed regarding the intensity of staining and the percentage of positive cells. For IGF1R, cytoplasmic staining was considered positive and specific in several investigated studies, while IGF1R is known as a plasma membrane receptor. Cytoplasmic expression patterns might be found in studies using antibodies with low specificity for their antigen. Therefore, validation of these antibodies is required using positive and negative controls (e.g. formalin-fixed paraffin embedded cell lines overexpressing or with a knockdown for the target of interest). Still, it remains unclear if any of these cut-off values are valid to represent the expression patterns that will be obtained using molecular imaging in a clinical setting.

An increasing number of recent studies evaluated the expression of hypoxia markers using tissue microarrays (TMAs). Although TMAs allow for higher throughput evaluation of more samples than whole slide analyses, a major drawback is misreading of biomarker status when intra-tumor heterogeneity is present. We found that the prevalence of CAIX and GLUT1 was significantly lower among studies that used TMAs. This underestimation is presumably due to sampling errors during TMA construction, because hypoxia and thus hypoxia-upregulated proteins are expressed next to necrotic tumor regions, which are commonly avoided during construction of TMAs. Although TMAs are convenient for evaluation of large patient cohorts, the value for assessment of hypoxia (and other) markers needs to be reconsidered given significant differences between prevalences found in our meta-analysis. Future studies should report better on intra-tumoral expression patterns (diffuse vs. perinecrotic [39]), as well as the observed intra-tumoral heterogeneity. Surprisingly, we found an opposite effect for IGF1R, in which significantly higher prevalences were found for studies using TMAs.

The interpretation of the staining result was not conducted by a pathologist in all studies, and none of the studies reported inter- or intra-observer agreement of pathologists. In addition, further improvements are required in reporting on patient and tumor characteristics, since many recent studies lacked important data like age, gender, neo-adjuvant treatment and/or tumor characteristics like histological grade, tumor size, and histological type. Future studies investigating hypoxia targets should therefore use standardized staining protocols and reproducible assessment of marker status, and should investigate co-expression patterns of hypoxia proteins as well.

Last, other factors, i.e. demographical differences, gender, genetic differences (e.g. BRCA1 or BRCA2 mutations) and selection of molecular types of breast cancer (e.g. selected on HER2 expression), which we could not correct for, will have accounted for heterogeneity between study populations as well.

In conclusion, we have shown that expression patterns of the hypoxia markers GLUT1, CAIX, CXCR4, and IGF1R are in the range of other relevant targets for molecular imaging of breast cancer. However, these single targets are insufficiently expressed for screening or diagnostic purposes using molecular imaging, although they are potential candidates for a multi-targeted approach. To evaluate this concept, studies need to be conducted investigating co-expression patterns of candidate molecular imaging markers. Furthermore, these studies should also incorporate data on expression patterns in benign breast lesions and normal and precancerous tissue, as such information is currently essentially lacking in the literature.

## Acknowledgements

This work was supported by the MAMmary carcinoma MOlecular imaging for diagnostics and THerapeutics (MAMMOTH) project of the Dutch Center for Translational Molecular Medicine, by an unrestricted research grant of AEGON Inc., and by the Dutch Cancer Society KWF by a research fellowship to S.G.E.

## References

1. Sampath L, Wang W and Sevick-Muraca EM. Near infrared fluorescent optical imaging for nodal staging. *J Biomed Opt* 2008; 13(4):041312.
2. Goldenberg DM and Nabi HA. Breast cancer imaging with radiolabeled antibodies. *Semin Nucl Med* 1999; 29(1):41-8.
3. Mann RM, Hoogeveen YL, Blickman JG and Boetes C. MRI compared to conventional diagnostic work-up in the detection and evaluation of invasive lobular carcinoma of the breast: a review of existing literature. *Breast Cancer Res Treat* 2008; 107(1):1-14.
4. Leung JW. New modalities in breast imaging: digital mammography, positron emission tomography, and sestamibi scintimammography. *Radiol Clin North Am* 2002; 40(3):467-82.
5. Petralia G, Bonello L, Priolo F, Summers P and Bellomi M. Breast MR with special focus on DW-MRI and DCE-MRI. *Cancer Imaging* 2011; 11:76-90.
6. Meng X, Loo BW, Jr, Ma L, et al. Molecular imaging with 11C-PD153035 PET/CT predicts survival in non-small cell lung cancer treated with EGFR-TKI: a pilot study. *J Nucl Med* 2011; 52(10):1573-9.
7. Miao Z, Ren G, Liu H, et al. PET of EGFR expression with an 18F-labeled antibody molecule. *J Nucl Med* 2012; 53(7):1110-8.
8. Wallberg H, Grafstrom J, Cheng Q, et al. HER2-Positive Tumors Imaged Within 1 Hour Using a Site-Specifically 11C-Labeled Sel-Tagged Antibody Molecule. *J Nucl Med* 2012; 53(9):1446-53.
9. Terwisscha van Scheltinga AG, van Dam GM, Nagengast WB, et al. Intraoperative near-infrared fluorescence tumor imaging with vascular endothelial growth factor and human epidermal growth factor receptor 2 targeting antibodies. *J Nucl Med* 2011; 52(11):1778-85.
10. Hanahan D and Weinberg RA. Hallmarks of cancer: the next generation. *Cell* 2011; 144(5):646-74.
11. Bos R, van der Groep P, Greijer AE, et al. Levels of hypoxia-inducible factor-1 $\alpha$  independently predict prognosis in patients with lymph node negative breast carcinoma. *Cancer* 2003; 97(6):1573-81.
12. Bos R, Zhong H, Hanrahan CF, et al. Levels of hypoxia-inducible factor-1  $\alpha$  during breast carcinogenesis. *J Natl Cancer Inst* 2001; 93(4):309-14.
13. Wykoff CC, Beasley N, Watson PH, et al. Expression of the hypoxia-inducible and tumor-associated carbonic anhydrases in ductal carcinoma in situ of the breast. *Am J Pathol* 2001; 158(3):1011-9.
14. Li XF and O'Donoghue JA. Hypoxia in microscopic tumors. *Cancer Lett* 2008; 264(2):172-80.
15. Taroni P. Diffuse optical imaging and spectroscopy of the breast: a brief outline of history and perspectives. *Photochem Photobiol Sci* 2012; 11(2):241-50.
16. Vaupel P, Thews O and Hoeckel M. Treatment resistance of solid tumors: role of hypoxia and anemia. *Med Oncol* 2001; 18(4):243-59.
17. Vaupel P, Mayer A, Briest S and Hockel M. Hypoxia in breast cancer: role of blood flow, oxygen diffusion distances, and anemia in the development of oxygen depletion. *Adv Exp Med Biol* 2005; 566:333-42.
18. Staller P, Sulitkova J, Lisztwan J, et al. Chemokine receptor CXCR4 downregulated by von Hippel-Lindau tumour suppressor pVHL. *Nature* 2003; 425(6955):307-11.
19. Cronin PA, Wang JH and Redmond HP. Hypoxia increases the metastatic ability of breast cancer cells via upregulation of CXCR4. *BMC Cancer* 2010; 10:225.
20. Peretz S, Kim C, Rockwell S, Baserga R and Glazer PM. IGF1 receptor expression protects against microenvironmental stress found in the solid tumor. *Radiat Res* 2002; 158(2):174-80.
21. Treins C, Giorgetti-Peraldi S, Murdaca J, Monthouel-Kartmann MN and Van Obberghen E. Regulation of hypoxia-inducible factor (HIF)-1 activity and expression of HIF hydroxylases in response to insulin-like growth factor I. *Mol Endocrinol* 2005; 19(5):1304-17.
22. Riedemann J and Macaulay VM. IGF1R signalling and its inhibition. *Endocr Relat Cancer* 2006; 13 Suppl 1:S33-43.
23. Vermeulen JF, van Brussel AS, van der Groep P, et al. Immunophenotyping invasive breast cancer: paving the road for molecular imaging. *BMC Cancer* 2012; 12(1):240.
24. Potts SJ, Krueger JS, Landis ND, et al. Evaluating tumor heterogeneity in immunohistochemistry-stained breast cancer tissue. *Lab Invest* 2012; 92(9):1342-57.
25. Lewis JT, Ketterling RP, Halling KC, et al. Analysis of intratumoral heterogeneity and amplification status in breast carcinomas with equivocal (2+) HER-2 immunostaining. *Am J Clin Pathol* 2005; 124(2):273-81.
26. Hamza TH, van Houwelingen HC and Stijnen T. The binomial distribution of meta-analysis was preferred to model within-study variability. *J Clin Epidemiol* 2008; 61(1):41-51.
27. R Core Team. R: A language and environment for statistical computing, R Foundation for Statistical Computing, Vienna, Austria, 2012.
28. Bates D, Maechleer M and Bolker B. lme4: Linear mixed-effects models using Eigen and syntax. R package version 0.999999-0. 2012.
29. Ito S, Fukusato T, Nemoto T, et al. Coexpression of glucose transporter 1 and matrix metalloproteinase-2 in human cancers. *J Natl Cancer Inst* 2002; 94(14):1080-91.

30. Younes M, Lechago LV, Somoano JR, Mosharaf M and Lechago J. Wide expression of the human erythrocyte glucose transporter Glut1 in human cancers. *Cancer Res* 1996; 56(5):1164-7.
31. Choi J, Jung WH and Koo JS. Metabolism-Related Proteins Are Differentially Expressed according to the Molecular Subtype of Invasive Breast Cancer Defined by Surrogate Immunohistochemistry. *Pathobiology* 2013; 80(1):41-52.
32. Kornegoor R, Verschuur-Maes AH, Buerger H, et al. Fibrotic focus and hypoxia in male breast cancer. *Mod Pathol* 2012; 25(10):1397-404.
33. Hyseni A, van der Groep P, van der Wall E and van Diest PJ. Subcellular FIH-1 expression patterns in invasive breast cancer in relation to HIF-1alpha expression. *Cell Oncol (Dordr)* 2011; 34(6):565-70.
34. Pinheiro C, Sousa B, Albergaria A, et al. GLUT1 and CAIX expression profiles in breast cancer correlate with adverse prognostic factors and MCT1 overexpression. *Histol Histopathol* 2011; 26(10):1279-86.
35. Chen CL, Chu JS, Su WC, Huang SC and Lee WY. Hypoxia and metabolic phenotypes during breast carcinogenesis: expression of HIF-1alpha, GLUT1, and CAIX. *Virchows Arch* 2010; 457(1):53-61.
36. Dachs GU, Kano M, Volkova E, et al. A profile of prognostic and molecular factors in European and Maori breast cancer patients. *BMC Cancer* 2010; 10:543.
37. Koop EA, van Laar T, van Wichen DF, et al. Expression of BNIP3 in invasive breast cancer: correlations with the hypoxic response and clinicopathological features. *BMC Cancer* 2009; 9:175.
38. van der Groep P, Bouter A, Menko FH, van der Wall E and van Diest PJ. High frequency of HIF-1alpha overexpression in BRCA1 related breast cancer. *Breast Cancer Res Treat* 2008; 111(3):475-80.
39. Vleugel MM, Greijer AE, Shvarts A, et al. Differential prognostic impact of hypoxia induced and diffuse HIF-1alpha expression in invasive breast cancer. *J Clin Pathol* 2005; 58(2):172-7.
40. Cooper C, Liu GY, Niu YL, et al. Intermittent hypoxia induces proteasome-dependent down-regulation of estrogen receptor alpha in human breast carcinoma. *Clin Cancer Res* 2004; 10(24):8720-7.
41. Tomes L, Emberley E, Niu Y, et al. Necrosis and hypoxia in invasive breast carcinoma. *Breast Cancer Res Treat* 2003; 81(1):61-9.
42. Fox SB, Generali D, Berruti A, et al. The prolyl hydroxylase enzymes are positively associated with hypoxia-inducible factor-1alpha and vascular endothelial growth factor in human breast cancer and alter in response to primary systemic treatment with epirubicin and tamoxifen. *Breast Cancer Res* 2011; 13(1):R16.
43. Ibrahim T, Sacanna E, Gaudio M, et al. Role of RANK, RANKL, OPG, and CXCR4 tissue markers in predicting bone metastases in breast cancer patients. *Clin Breast Cancer* 2011; 11(6):369-75.
44. Yan M, Jene N, Byrne D, et al. Recruitment of regulatory T cells is correlated with hypoxia-induced CXCR4 expression, and is associated with poor prognosis in basal-like breast cancers. *Breast Cancer Res* 2011; 13(2):R47.
45. Peiro G, Benlloch S, Sanchez-Tejada L, et al. Low activation of Insulin-like Growth Factor 1-Receptor (IGF1R) is associated with local recurrence in early breast carcinoma. *Breast Cancer Res Treat* 2009; 117(2):433-41.
46. Yasuoka H, Tsujimoto M, Yoshidome K, et al. Cytoplasmic CXCR4 expression in breast cancer: induction by nitric oxide and correlation with lymph node metastasis and poor prognosis. *BMC Cancer* 2008; 8:340.
47. Henriksen KL, Rasmussen BB, Lykkesfeldt AE, et al. Semi-quantitative scoring of potentially predictive markers for endocrine treatment of breast cancer: a comparison between whole sections and tissue microarrays. *J Clin Pathol* 2007; 60(4):397-404.
48. Generali D, Berruti A, Brizzi MP, et al. Hypoxia-inducible factor-1alpha expression predicts a poor response to primary chemoendocrine therapy and disease-free survival in primary human breast cancer. *Clin Cancer Res* 2006; 12(15):4562-8.
49. Vleugel MM, Shvarts D, van der Wall E and van Diest PJ. p300 and p53 levels determine activation of HIF-1 downstream targets in invasive breast cancer. *Hum Pathol* 2006; 37(8):1085-92.
50. Klijn JG, Berns PM, Schmitz PI and Foekens JA. The clinical significance of epidermal growth factor receptor (EGF-R) in human breast cancer: a review on 5232 patients. *Endocr Rev* 1992; 13(1):3-17.
51. Brahimi-Horn MC, Chiche J and Pouyssegur J. Hypoxia and cancer. *J Mol Med (Berl)* 2007; 85(12):1301-7.
52. Semenza GL. Targeting HIF-1 for cancer therapy. *Nat Rev Cancer* 2003; 3(10):721-32.
53. Ercan C, Vermeulen JF, Hoefnagel L, et al. HIF-1alpha and NOTCH signaling in ductal and lobular carcinomas of the breast. *Cell Oncol (Dordr)* 2012.
54. Groheux D, Giacchetti S, Moretti JL, et al. Correlation of high 18F-FDG uptake to clinical, pathological and biological prognostic factors in breast cancer. *Eur J Nucl Med Mol Imaging* 2011; 38(3):426-35.
55. Heudel P, Cimarelli S, Montella A, Bouteille C and Mognetti T. Value of PET-FDG in primary breast cancer based on histopathological and immunohistochemical prognostic factors. *Int J Clin Oncol* 2010; 15(6):588-93.
56. Betof AS, Rabbani ZN, Hardee ME, et al. Carbonic anhydrase IX is a predictive marker of doxorubicin resistance in early-stage breast cancer independent of HER2 and TOP2A amplification. *Br J Cancer* 2012; 106(5):916-22.
57. Tafreshi NK, Bui MM, Bishop K, et al. Noninvasive detection of breast cancer lymph node metastasis

- using carbonic anhydrases IX and XII targeted imaging probes. *Clin Cancer Res* 2012; 18(1):207-19.
58. Beketic-Oreskovic L, Ozretic P, Rabbani ZN, *et al.* Prognostic significance of carbonic anhydrase IX (CA-IX), endoglin (CD105) and 8-hydroxy-2'-deoxyguanosine (8-OHdG) in breast cancer patients. *Pathol Oncol Res* 2011; 17(3):593-603.
59. Khurana A, Liu P, Mellone P, *et al.* HSulf-1 modulates FGF2- and hypoxia-mediated migration and invasion of breast cancer cells. *Cancer Res* 2011; 71(6):2152-61.
60. Lou Y, McDonald PC, Oloumi A, *et al.* Targeting tumor hypoxia: suppression of breast tumor growth and metastasis by novel carbonic anhydrase IX inhibitors. *Cancer Res* 2011; 71(9):3364-76.
61. Zanetti JS, Soave DF, Oliveira-Costa JP, *et al.* The role of tumor hypoxia in MUC1-positive breast carcinomas. *Virchows Arch* 2011; 459(4):367-75.
62. Jubb AM, Soilleux EJ, Turley H, *et al.* Expression of vascular notch ligand delta-like 4 and inflammatory markers in breast cancer. *Am J Pathol* 2010; 176(4):2019-28.
63. Lancashire LJ, Powe DG, Reis-Filho JS, *et al.* A validated gene expression profile for detecting clinical outcome in breast cancer using artificial neural networks. *Breast Cancer Res Treat* 2010; 120(1):83-93.
64. Rakha EA, Elsheikh SE, Aleskandarany MA, *et al.* Triple-negative breast cancer: distinguishing between basal and nonbasal subtypes. *Clin Cancer Res* 2009; 15(7):2302-10.
65. Tan EY, Yan M, Campo L, *et al.* The key hypoxia regulated gene CAIX is upregulated in basal-like breast tumours and is associated with resistance to chemotherapy. *Br J Cancer* 2009; 100(2):405-11.
66. Crabb SJ, Bajdik CD, Leung S, *et al.* Can clinically relevant prognostic subsets of breast cancer patients with four or more involved axillary lymph nodes be identified through immunohistochemical biomarkers? A tissue microarray feasibility study. *Breast Cancer Res* 2008; 10(1):R6.
67. Kyndi M, Sorensen FB, Knudsen H, *et al.* Carbonic anhydrase IX and response to postmastectomy radiotherapy in high-risk breast cancer: a subgroup analysis of the DBCG82 b and c trials. *Breast Cancer Res* 2008; 10(2):R24.
68. Garcia S, Dales JP, Charafe-Jauffret E, *et al.* Poor prognosis in breast carcinomas correlates with increased expression of targetable CD146 and c-Met and with proteomic basal-like phenotype. *Hum Pathol* 2007; 38(6):830-41.
69. Hussain SA, Ganesan R, Reynolds G, *et al.* Hypoxia-regulated carbonic anhydrase IX expression is associated with poor survival in patients with invasive breast cancer. *Br J Cancer* 2007; 96(1):104-9.
70. Tan EY, Campo L, Han C, *et al.* Cytoplasmic location of factor-inhibiting hypoxia-inducible factor is associated with an enhanced hypoxic response and a shorter survival in invasive breast cancer. *Breast Cancer Res* 2007; 9(6):R89.
71. Trastour C, Benizri E, Ettore F, *et al.* HIF-1alpha and CA IX staining in invasive breast carcinomas: prognosis and treatment outcome. *Int J Cancer* 2007; 120(7):1451-8.
72. Brennan DJ, Jirstrom K, Kronblad A, *et al.* CA IX is an independent prognostic marker in premenopausal breast cancer patients with one to three positive lymph nodes and a putative marker of radiation resistance. *Clin Cancer Res* 2006; 12(21):6421-31.
73. Generali D, Fox SB, Berruti A, *et al.* Role of carbonic anhydrase IX expression in prediction of the efficacy and outcome of primary epirubicin/tamoxifen therapy for breast cancer. *Endocr Relat Cancer* 2006; 13(3):921-30.
74. Van den Eynden GG, Van der Auwera I, Van Laere SJ, *et al.* Angiogenesis and hypoxia in lymph node metastases is predicted by the angiogenesis and hypoxia in the primary tumour in patients with breast cancer. *Br J Cancer* 2005; 93(10):1128-36.
75. Kuijper A, van der Groep P, van der Wall E and van Diest PJ. Expression of hypoxia-inducible factor 1 alpha and its downstream targets in fibroepithelial tumors of the breast. *Breast Cancer Res* 2005; 7(5):R808-18.
76. Blackwell KL, Dewhirst MW, Liotcheva V, *et al.* HER-2 gene amplification correlates with higher levels of angiogenesis and lower levels of hypoxia in primary breast tumors. *Clin Cancer Res* 2004; 10(12 Pt 1):4083-8.
77. Colpaert CG, Vermeulen PB, Benoy I, *et al.* Inflammatory breast cancer shows angiogenesis with high endothelial proliferation rate and strong E-cadherin expression. *Br J Cancer* 2003; 88(5):718-25.
78. Bartosova M, Parkkila S, Pohlodek K, *et al.* Expression of carbonic anhydrase IX in breast is associated with malignant tissues and is related to overexpression of c-erbB2. *J Pathol* 2002; 197(3):314-21.
79. Chia SK, Wykoff CC, Watson PH, *et al.* Prognostic significance of a novel hypoxia-regulated marker, carbonic anhydrase IX, in invasive breast carcinoma. *J Clin Oncol* 2001; 19(16):3660-8.
80. Jang SM, Han H, Jang KS, *et al.* The Glycolytic Phenotype is Correlated with Aggressiveness and Poor Prognosis in Invasive Ductal Carcinomas. *J Breast Cancer* 2012; 15(2):172-80.
81. Carvalho KC, Cunha IW, Rocha RM, *et al.* GLUT1 expression in malignant tumors and its use as an immunodiagnostic marker. *Clinics (Sao Paulo)* 2011; 66(6):965-72.
82. Hussein YR, Bandyopadhyay S, Semaan A, *et al.* Glut-1 Expression Correlates with Basal-like Breast Cancer. *Transl Oncol* 2011; 4(6):321-7.

83. Airley R, Evans A, Mobasheri A and Hewitt SM. Glucose transporter Glut-1 is detectable in peri-necrotic regions in many human tumor types but not normal tissues: Study using tissue microarrays. *Ann Anat* 2010; 192(3):133-8.
84. Koda M, Kanczuga-Koda L, Sulkowska M, Surmacz E and Sulkowski S. Relationships between hypoxia markers and the leptin system, estrogen receptors in human primary and metastatic breast cancer: effects of preoperative chemotherapy. *BMC Cancer* 2010; 10:320.
85. Koo JS and Jung W. Alteration of REDD1-mediated mammalian target of rapamycin pathway and hypoxia-inducible factor-1alpha regulation in human breast cancer. *Pathobiology* 2010; 77(6):289-300.
86. Schmidt M, Voelker HU, Kapp M, et al. Glycolytic phenotype in breast cancer: activation of Akt, up-regulation of GLUT1, TKTL1 and down-regulation of M2PK. *J Cancer Res Clin Oncol* 2010; 136(2):219-25.
87. Godoy A, Ulloa V, Rodriguez F, et al. Differential subcellular distribution of glucose transporters GLUT1-6 and GLUT9 in human cancer: ultrastructural localization of GLUT1 and GLUT5 in breast tumor tissues. *J Cell Physiol* 2006; 207(3):614-27.
88. Kuo SJ, Wu YC, Chen CP, Tseng HS and Chen DR. Expression of glucose transporter-1 in Taiwanese patients with breast carcinoma--a preliminary report. *Kaohsiung J Med Sci* 2006; 22(7):339-45.
89. Stackhouse BL, Williams H, Berry P, et al. Measurement of glut-1 expression using tissue microarrays to determine a race specific prognostic marker for breast cancer. *Breast Cancer Res Treat* 2005; 93(3):247-53.
90. Laudanski P, Koda M, Kozlowski L, et al. Expression of glucose transporter GLUT-1 and estrogen receptors ER-alpha and ER-beta in human breast cancer. *Neoplasma* 2004; 51(3):164-8.
91. Bos R, van der Hoeven JJ, van der Wall E, et al. Biologic correlates of (18)fluorodeoxyglucose uptake in human breast cancer measured by positron emission tomography. *J Clin Oncol* 2002; 20(2):379-87.
92. Brown RS, Goodman TM, Zasadny KR, Greenson JK and Wahl RL. Expression of hexokinase II and Glut-1 in untreated human breast cancer. *Nucl Med Biol* 2002; 29(4):443-53.
93. Kang SS, Chun YK, Hur MH, et al. Clinical significance of glucose transporter 1 (GLUT1) expression in human breast carcinoma. *Jpn J Cancer Res* 2002; 93(10):1123-8.
94. Alo PL, Visca P, Botti C, et al. Immunohistochemical expression of human erythrocyte glucose transporter and fatty acid synthase in infiltrating breast carcinomas and adjacent typical/atypical hyperplastic or normal breast tissue. *Am J Clin Pathol* 2001; 116(1):129-34.
95. Avril N, Menzel M, Dose J, et al. Glucose metabolism of breast cancer assessed by 18F-FDG PET: histologic and immunohistochemical tissue analysis. *J Nucl Med* 2001; 42(1):9-16.
96. Binder C, Binder L, Marx D, Schauer A and Hiddemann W. Deregulated simultaneous expression of multiple glucose transporter isoforms in malignant cells and tissues. *Anticancer Res* 1997; 17(6D):4299-304.
97. Younes M, Brown RW, Mody DR, Fernandez L and Laucirica R. GLUT1 expression in human breast carcinoma: correlation with known prognostic markers. *Anticancer Res* 1995; 15(6B):2895-8.
98. Brown RS and Wahl RL. Overexpression of Glut-1 glucose transporter in human breast cancer. An immunohistochemical study. *Cancer* 1993; 72(10):2979-85.
99. Huang S, Ouyang N, Lin L, et al. HGF-induced PKCzeta activation increases functional CXCR4 expression in human breast cancer cells. *PLoS One* 2012; 7(1):e29124.
100. Jin F, Brockmeier U, Otterbach F and Metzen E. New Insight into the SDF-1/CXCR4 Axis in a Breast Carcinoma Model: Hypoxia-Induced Endothelial SDF-1 and Tumor Cell CXCR4 Are Required for Tumor Cell Intravasation. *Mol Cancer Res* 2012; 10(8):1021-31.
101. Sacanna E, Ibrahim T, Gaudio M, et al. The role of CXCR4 in the prediction of bone metastases from breast cancer: a pilot study. *Oncology* 2011; 80(3-4):225-31.
102. Bohn OL, Nasir I, Brufsky A, et al. Biomarker profile in breast carcinomas presenting with bone metastasis. *Int J Clin Exp Pathol* 2009; 3(2):139-46.
103. Kobayashi T, Tsuda H, Moriya T, et al. Expression pattern of stromal cell-derived factor-1 chemokine in invasive breast cancer is correlated with estrogen receptor status and patient prognosis. *Breast Cancer Res Treat* 2010; 123(3):733-45.
104. Liu Y, Ji R, Li J, et al. Correlation effect of EGFR and CXCR4 and CCR7 chemokine receptors in predicting breast cancer metastasis and prognosis. *J Exp Clin Cancer Res* 2010; 29:16.
105. Andre F, Xia W, Conforti R, et al. CXCR4 expression in early breast cancer and risk of distant recurrence. *Oncologist* 2009; 14(12):1182-8.
106. Cabioglu N, Sahin AA, Morandi P, et al. Chemokine receptors in advanced breast cancer: differential expression in metastatic disease sites with diagnostic and therapeutic implications. *Ann Oncol* 2009; 20(6):1013-9.
107. Hassan S, Ferrario C, Saragovi U, et al. The influence of tumor-host interactions in the stromal cell-derived factor-1/CXCR4 ligand/receptor axis in determining metastatic risk in breast cancer. *Am J Pathol* 2009; 175(1):66-73.
108. Kim J-O, Suh K-S, Lee D-H, et al. Expression of CXCR4 and SDF-1 $\alpha$  in Primary Breast Cancers and Metastatic Lymph Nodes. *J Breast Cancer* 2009; 12(4):249-56.

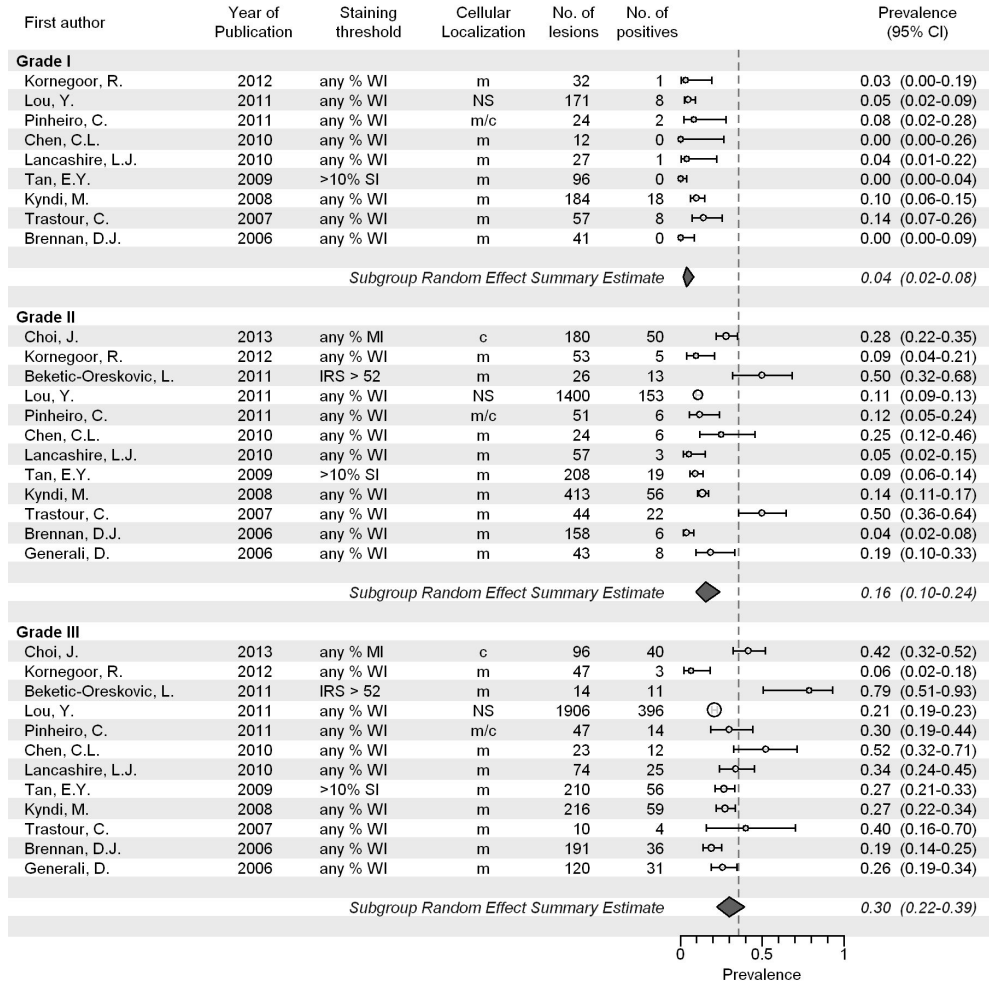


109. Liu F, Lang R, Wei J, *et al.* Increased expression of SDF-1/CXCR4 is associated with lymph node metastasis of invasive micropapillary carcinoma of the breast. *Histopathology* 2009; 54(6):741-50.
110. Yasuoka H, Kodama R, Tsujimoto M, *et al.* Neuropilin-2 expression in breast cancer: correlation with lymph node metastasis, poor prognosis, and regulation of CXCR4 expression. *BMC Cancer* 2009; 9:220.
111. Zhou W, Jiang Z, Liu N, *et al.* Down-regulation of CXCL12 mRNA expression by promoter hypermethylation and its association with metastatic progression in human breast carcinomas. *J Cancer Res Clin Oncol* 2009; 135(1):91-102.
112. Blot E, Laberge-Le Couteux S, Jamali H, *et al.* CXCR4 membrane expression in node-negative breast cancer. *Breast J* 2008; 14(3):268-74.
113. Fujii T, Kawahara A, Basaki Y, *et al.* Expression of HER2 and estrogen receptor alpha depends upon nuclear localization of Y-box binding protein-1 in human breast cancers. *Cancer Res* 2008; 68(5):1504-12.
114. Woo SU, Bae JW, Kim CH, Lee JB and Koo BW. A significant correlation between nuclear CXCR4 expression and axillary lymph node metastasis in hormonal receptor negative breast cancer. *Ann Surg Oncol* 2008; 15(1):281-5.
115. Hao L, Zhang C, Qiu Y, *et al.* Recombination of CXCR4, VEGF, and MMP-9 predicting lymph node metastasis in human breast cancer. *Cancer Lett* 2007; 253(1):34-42.
116. Tsoli E, Tsantoulis PK, Papalambros A, *et al.* Simultaneous evaluation of maspin and CXCR4 in patients with breast cancer. *J Clin Pathol* 2007; 60(3):261-6.
117. Andre F, Cabioglu N, Assi H, *et al.* Expression of chemokine receptors predicts the site of metastatic relapse in patients with axillary node positive primary breast cancer. *Ann Oncol* 2006; 17(6):945-51.
118. Kim R, Arihiro K, Emi M, Tanabe K and Osaki A. Potential role of HER-2; in primary breast tumor with bone metastasis. *Oncol Rep* 2006; 15(6):1477-84.
119. Salvucci O, Bouchard A, Baccarelli A, *et al.* The role of CXCR4 receptor expression in breast cancer: a large tissue microarray study. *Breast Cancer Res Treat* 2006; 97(3):275-83.
120. Shim H, Lau SK, Devi S, *et al.* Lower expression of CXCR4 in lymph node metastases than in primary breast cancers: potential regulation by ligand-dependent degradation and HIF-1alpha. *Biochem Biophys Res Commun* 2006; 346(1):252-8.
121. Su YC, Wu MT, Huang CJ, *et al.* Expression of CXCR4 is associated with axillary lymph node status in patients with early breast cancer. *Breast* 2006; 15(4):533-9.
122. Cabioglu N, Yazici MS, Arun B, *et al.* CCR7 and CXCR4 as novel biomarkers predicting axillary lymph node metastasis in T1 breast cancer. *Clin Cancer Res* 2005; 11(16):5686-93.
123. Cabioglu N, Sahin A, Doucet M, *et al.* Chemokine receptor CXCR4 expression in breast cancer as a potential predictive marker of isolated tumor cells in bone marrow. *Clin Exp Metastasis* 2005; 22(1):39-46.
124. Li YM, Pan Y, Wei Y, *et al.* Upregulation of CXCR4 is essential for HER2-mediated tumor metastasis. *Cancer Cell* 2004; 6(5):459-69.
125. Schmid BC, Rudas M, Reznicek GA, Leodolter S and Zeillinger R. CXCR4 is expressed in ductal carcinoma in situ of the breast and in atypical ductal hyperplasia. *Breast Cancer Res Treat* 2004; 84(3):247-50.
126. Kato M, Kitayama J, Kazama S and Nagawa H. Expression pattern of CXC chemokine receptor-4 is correlated with lymph node metastasis in human invasive ductal carcinoma. *Breast Cancer Res* 2003; 5(5):R144-50.
127. Gallardo A, Lerma E, Escuin D, *et al.* Increased signalling of EGFR and IGF1R, and deregulation of PTEN/PI3K/Akt pathway are related with trastuzumab resistance in HER2 breast carcinomas. *Br J Cancer* 2012; 106(8):1367-73.
128. Iqbal J, Thike AA, Cheok PY, Tse GM and Tan PH. Insulin growth factor receptor-1 expression and loss of PTEN protein predict early recurrence in triple-negative breast cancer. *Histopathology* 2012.
129. Kurebayashi J, Kanomata N, Shimo T, *et al.* Marked lymphovascular invasion, progesterone receptor negativity, and high Ki67 labeling index predict poor outcome in breast cancer patients treated with endocrine therapy alone. *Breast Cancer* 2012.
130. Taromaru GC, VM DEO, Silva MA, *et al.* Interaction between cyclooxygenase-2 and insulin-like growth factor in breast cancer: A new field for prevention and treatment. *Oncol Lett* 2012; 3(3):682-8.
131. Yerushalmi R, Gelmon KA, Leung S, *et al.* Insulin-like growth factor receptor (IGF-1R) in breast cancer subtypes. *Breast Cancer Res Treat* 2012; 132(1):131-42.
132. Bhargava R, Beriwal S, McManus K and Dabbs DJ. Insulin-like growth factor receptor-1 (IGF-1R) expression in normal breast, proliferative breast lesions, and breast carcinoma. *Appl Immunohistochem Mol Morphol* 2011; 19(3):218-25.
133. Drury SC, Detre S, Leary A, *et al.* Changes in breast cancer biomarkers in the IGF1R/PI3K pathway in recurrent breast cancer after tamoxifen treatment. *Endocr Relat Cancer* 2011; 18(5):565-77.
134. Fu P, Ibusuki M, Yamamoto Y, *et al.* Insulin-like growth factor-1 receptor gene expression is associated with survival in breast cancer: a comprehensive analysis of gene copy number, mRNA and protein expression. *Breast Cancer Res Treat* 2011; 130(1):307-17.

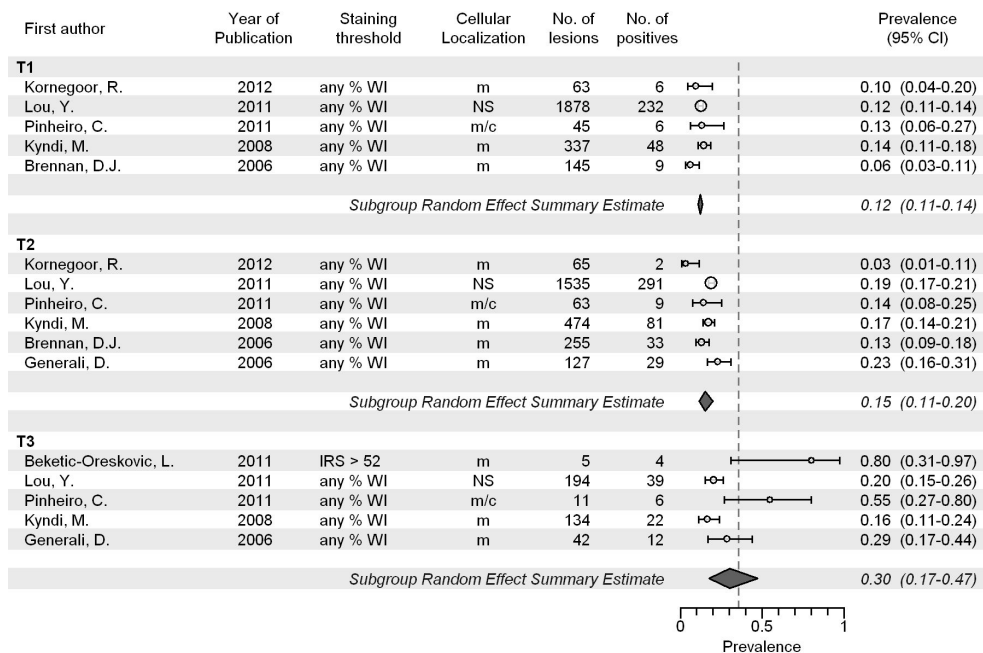
135. Fu P, Ibusuki M, Yamamoto Y, *et al.* Quantitative determination of insulin-like growth factor 1 receptor mRNA in formalin-fixed paraffin-embedded tissues of invasive breast cancer. *Breast Cancer* 2011.
136. Hartog H, Horlings HM, van der Veegt B, *et al.* Divergent effects of insulin-like growth factor-1 receptor expression on prognosis of estrogen receptor positive versus triple negative invasive ductal breast carcinoma. *Breast Cancer Res Treat* 2011; 129(3):725-36.
137. Peiro G, Adrover E, Sanchez-Tejada L, *et al.* Increased insulin-like growth factor-1 receptor mRNA expression predicts poor survival in immunophenotypes of early breast carcinoma. *Mod Pathol* 2011; 24(2):201-8.
138. Tamimi RM, Colditz GA, Wang Y, *et al.* Expression of IGF1R in normal breast tissue and subsequent risk of breast cancer. *Breast Cancer Res Treat* 2011; 128(1):243-50.
139. Kim JH, Cho YH, Park YL, Sohn JH and Kim HS. Prognostic significance of insulin growth factor-I receptor and insulin growth factor binding protein-3 expression in primary breast cancer. *Oncol Rep* 2010; 23(4):989-95.
140. Sircoulomb F, Bekhouche I, Finetti P, *et al.* Genome profiling of ERBB2-amplified breast cancers. *BMC Cancer* 2010; 10:539.
141. Taunk NK, Goyal S, Moran MS, *et al.* Prognostic significance of IGF-1R expression in patients treated with breast-conserving surgery and radiation therapy. *Radiother Oncol* 2010; 96(2):204-8.
142. Chen C, Zhou Z, Sheehan CE, *et al.* Overexpression of WWP1 is associated with the estrogen receptor and insulin-like growth factor receptor 1 in breast carcinoma. *Int J Cancer* 2009; 124(12):2829-36.
143. Henriksen KL, Rasmussen BB, Lykkesfeldt AE, *et al.* An ER activity profile including ER, PR, Bcl-2 and IGF-1R may have potential as selection criterion for letrozole or tamoxifen treatment of patients with advanced breast cancer. *Acta Oncol* 2009; 48(4):522-31.
144. Law JH, Habibi G, Hu K, *et al.* Phosphorylated insulin-like growth factor-i/insulin receptor is present in all breast cancer subtypes and is related to poor survival. *Cancer Res* 2008; 68(24):10238-46.
145. Sutandyo N, Suzanna E, Haryono SJ and Reksodiputro AH. Signaling pathways in early onset sporadic breast cancer of patients in Indonesia. *Acta Med Indones* 2008; 40(3):139-45.
146. Zoubir M, Mathieu MC, Mazouni C, *et al.* Modulation of ER phosphorylation on serine 118 by endocrine therapy: a new surrogate marker for efficacy. *Ann Oncol* 2008; 19(8):1402-6.
147. Hudelist G, Wagner T, Rosner M, *et al.* Intratumoral IGF-I protein expression is selectively upregulated in breast cancer patients with BRCA1/2 mutations. *Endocr Relat Cancer* 2007; 14(4):1053-62.
148. Lerma E, Peiro G, Ramon T, *et al.* Immunohistochemical heterogeneity of breast carcinomas negative for estrogen receptors, progesterone receptors and Her2/neu (basal-like breast carcinomas). *Mod Pathol* 2007; 20(11):1200-7.
149. Mulligan AM, O'Malley FP, Ennis M, Fantus IG and Goodwin PJ. Insulin receptor is an independent predictor of a favorable outcome in early stage breast cancer. *Breast Cancer Res Treat* 2007; 106(1):39-47.
150. Chong YM, Williams SL, Elkak A, Sharma AK and Mokbel K. Insulin-like growth factor 1 (IGF-1) and its receptor mRNA levels in breast cancer and adjacent non-neoplastic tissue. *Anticancer Res* 2006; 26(1A):167-73.
151. Kostler WJ, Hudelist G, Rabitsch W, *et al.* Insulin-like growth factor-1 receptor (IGF-1R) expression does not predict for resistance to trastuzumab-based treatment in patients with Her-2/neu overexpressing metastatic breast cancer. *J Cancer Res Clin Oncol* 2006; 132(1):9-18.
152. Ueda S, Tsuda H, Sato K, *et al.* Alternative tyrosine phosphorylation of signaling kinases according to hormone receptor status in breast cancer overexpressing the insulin-like growth factor receptor type 1. *Cancer Sci* 2006; 97(7):597-604.
153. Nielsen TO, Andrews HN, Cheang M, *et al.* Expression of the insulin-like growth factor I receptor and urokinase plasminogen activator in breast cancer is associated with poor survival: potential for intervention with 17-allylamino geldanamycin. *Cancer Res* 2004; 64(1):286-91.
154. Shimizu C, Hasegawa T, Tani Y, *et al.* Expression of insulin-like growth factor 1 receptor in primary breast cancer: immunohistochemical analysis. *Hum Pathol* 2004; 35(12):1537-42.
155. Koda M, Sulkowski S, Garofalo C, *et al.* Expression of the insulin-like growth factor-I receptor in primary breast cancer and lymph node metastases: correlations with estrogen receptors alpha and beta. *Horm Metab Res* 2003; 35(11-12):794-801.
156. Ouban A, Muraca P, Yeatman T and Coppola D. Expression and distribution of insulin-like growth factor-1 receptor in human carcinomas. *Hum Pathol* 2003; 34(8):803-8.
157. Happerfield LC, Miles DW, Barnes DM, *et al.* The localization of the insulin-like growth factor receptor 1 (IGFR-1) in benign and malignant breast tissue. *J Pathol* 1997; 183(4):412-7.
158. Turner BC, Haffty BG, Narayanan L, *et al.* Insulin-like growth factor-I receptor overexpression mediates cellular radioresistance and local breast cancer recurrence after lumpectomy and radiation. *Cancer Res* 1997; 57(15):3079-83.

# Supplemental data

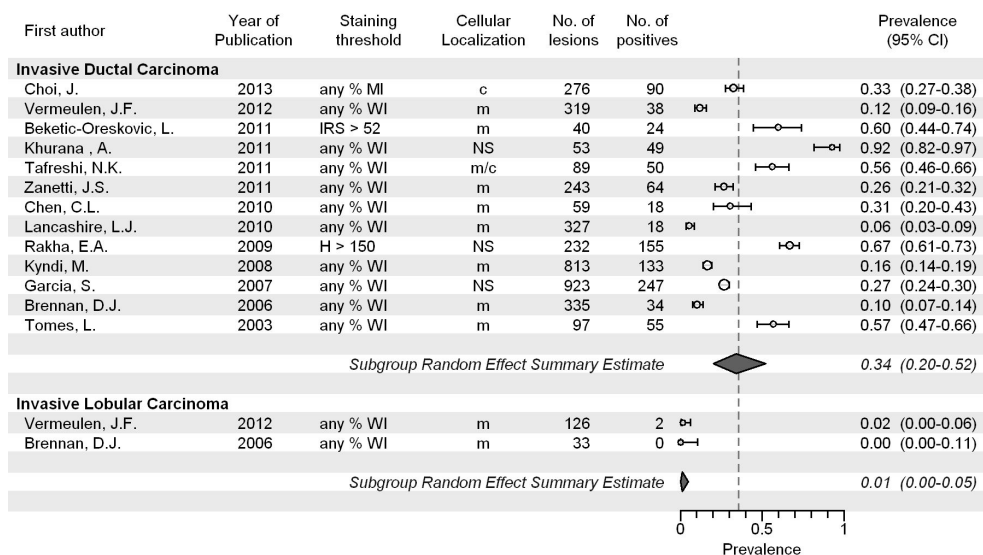
**Figure S1.** Prevalence of CAIX expression in relation to histological grade.



Dashed line represents overall random effect summary prevalence estimate. Abbreviations: Staining threshold: weak intensity (WI), moderate intensity (MI), strong intensity (SI), immunoreactive score (IRS), H-score (H); Localization: cytoplasm (c), membrane (m); confidence interval (CI); not stated (NS)

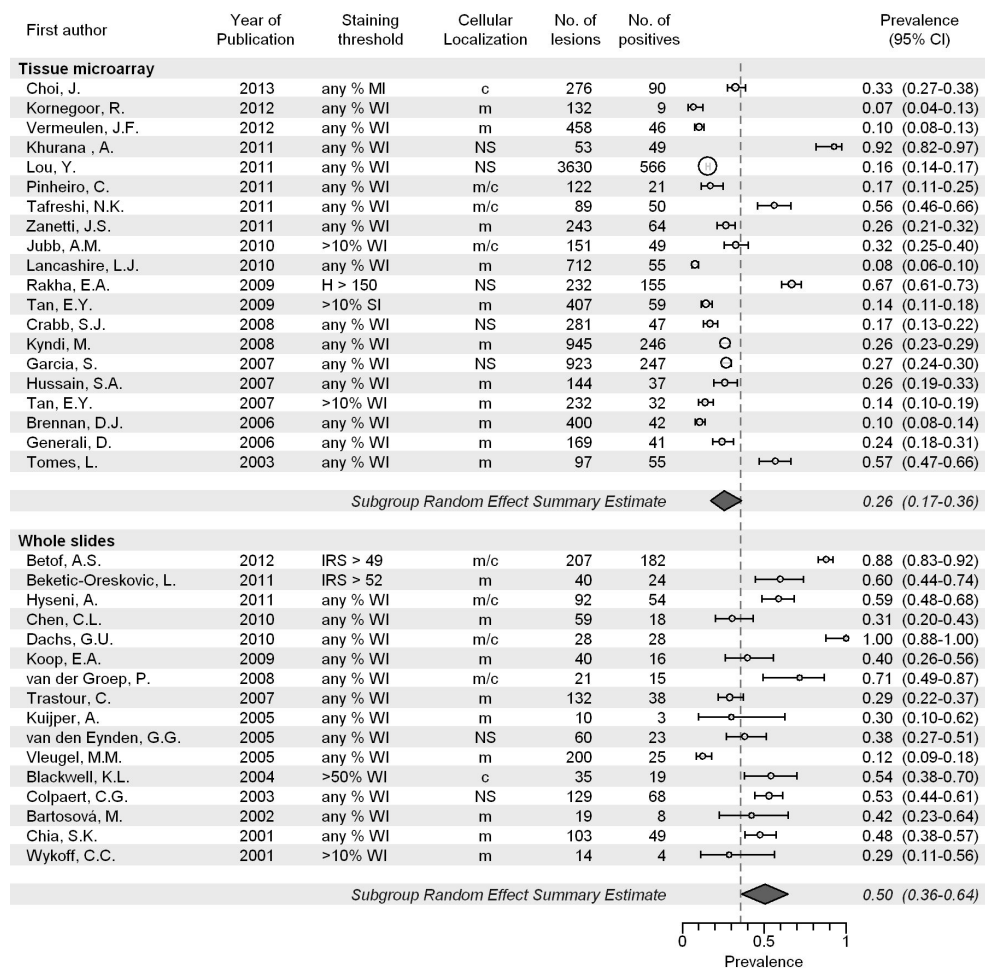
**Figure S2.** Prevalence of CAIX expression in relation to tumor size.

Dashed line represents overall random effect summary prevalence estimate. Abbreviations: Staining threshold: weak intensity (WI), moderate intensity (MI), strong intensity (SI), immunoreactive score (IRS), H-score (H); Localization: cytoplasm (c), membrane (m); confidence interval (CI); not stated (NS)

**Figure S3.** Prevalence of CAIX expression in relation to histological type.

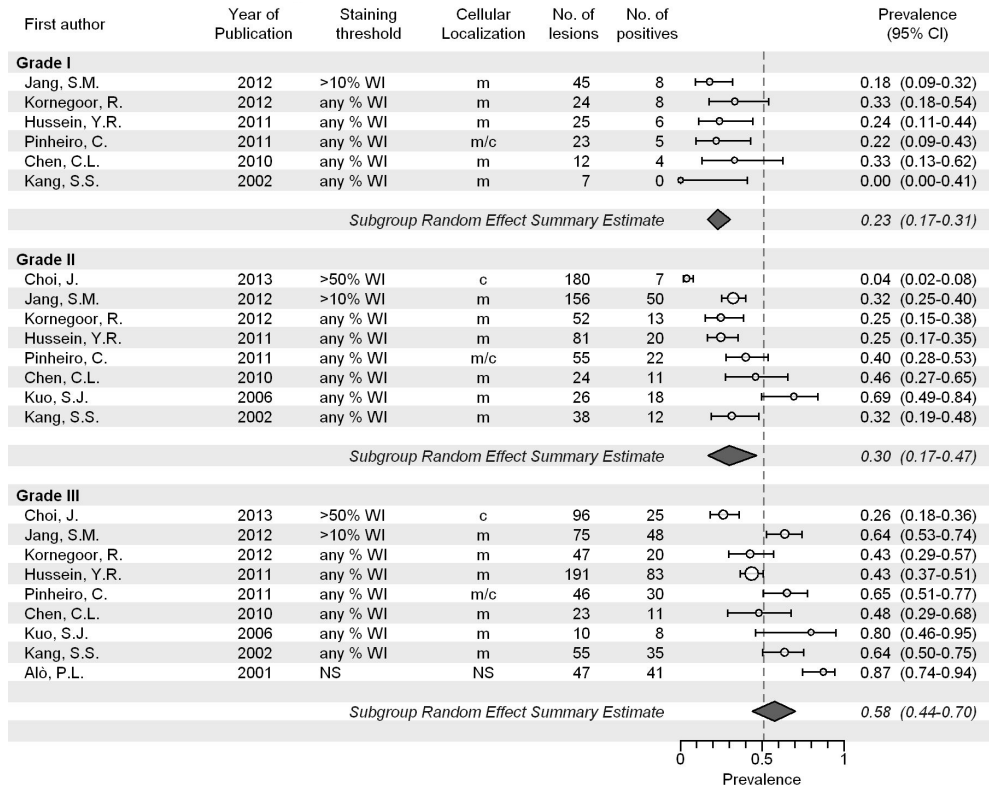
Dashed line represents overall random effect summary prevalence estimate. Abbreviations: Staining threshold: weak intensity (WI), moderate intensity (MI), strong intensity (SI), immunoreactive score (IRS), H-score (H); Localization: cytoplasm (c), membrane (m); confidence interval (CI); not stated (NS)

**Figure S4.** Prevalence of CAIX expression in relation to specimen handling.



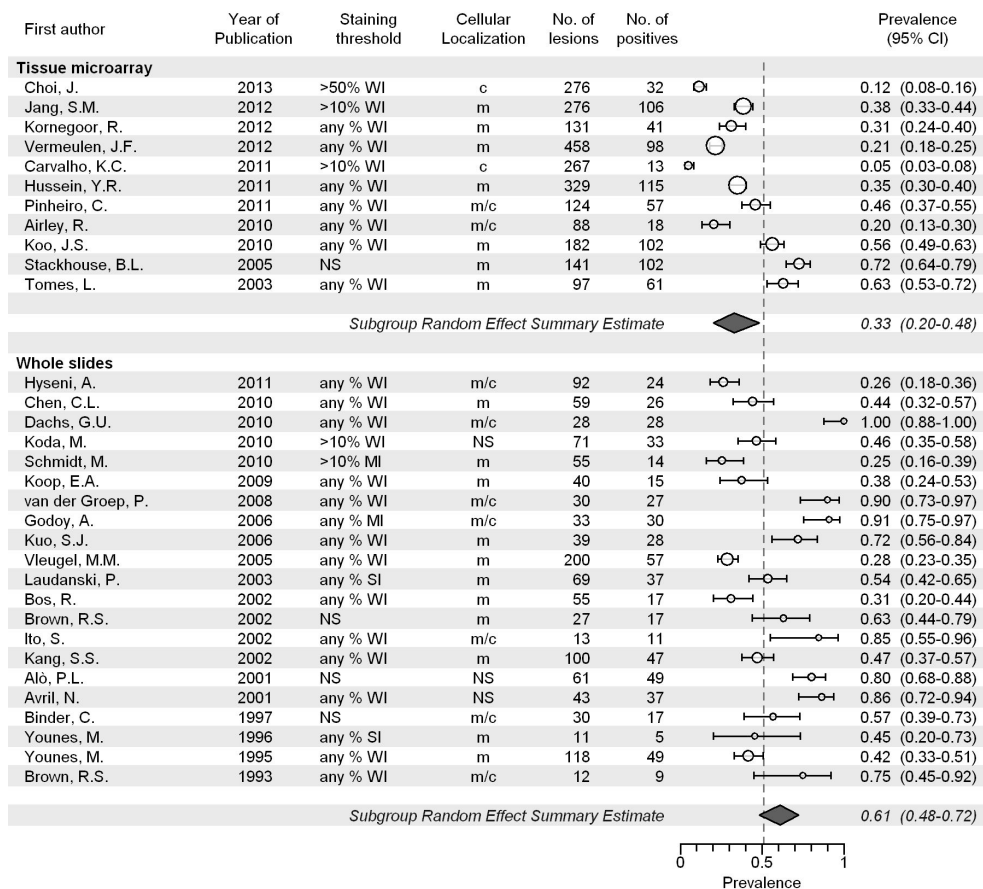
Dashed line represents overall random effect summary prevalence estimate. Abbreviations: Staining threshold: weak intensity (WI), moderate intensity (MI), strong intensity (SI), immunoreactive score (IRS), H-score (H); Localization: cytoplasm (c), membrane (m); confidence interval (CI); not stated (NS)

**Figure S5.** Prevalence of GLUT1 expression in relation to histological grade.



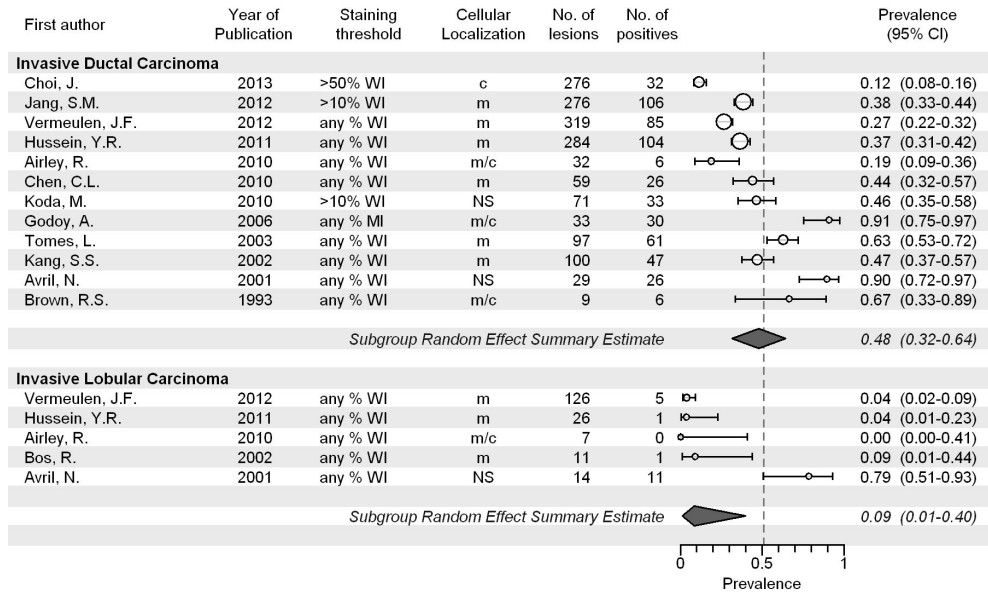
Dashed line represents overall random effect summary prevalence estimate. Abbreviations: Staining threshold: weak intensity (WI), moderate intensity (MI), strong intensity (SI); Localization: cytoplasm (c), membrane (m); confidence interval (CI); not stated (NS)

**Figure S6.** Prevalence of GLUT1 expression in relation to specimen handling.



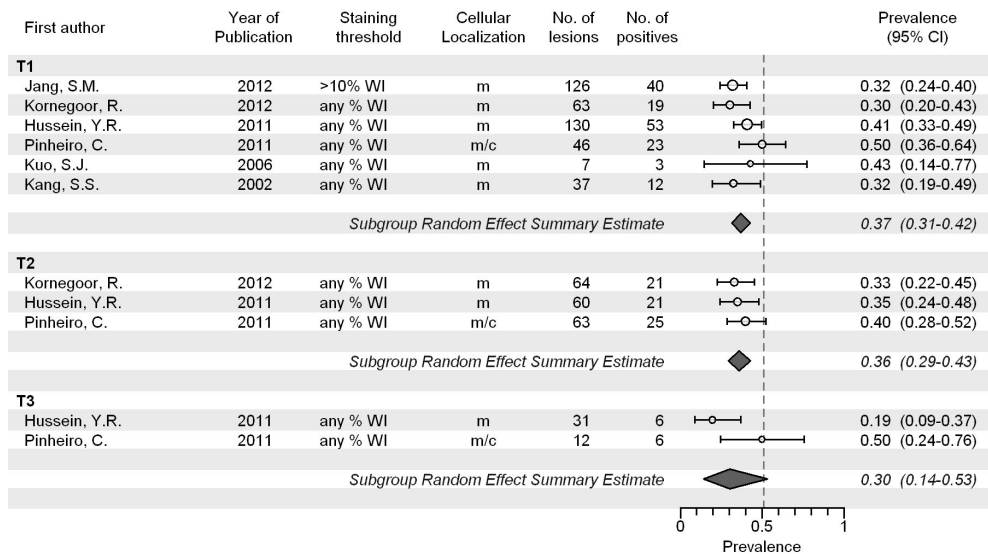
Dashed line represents overall random effect summary prevalence estimate. Abbreviations: Staining threshold: weak intensity (WI), moderate intensity (MI), strong intensity (SI); Localization: cytoplasm (c), membrane (m); confidence interval (CI); not stated (NS)

**Figure S7.** Prevalence of GLUT1 expression in relation to histological type.



Dashed line represents overall random effect summary prevalence estimate. Abbreviations: Staining threshold: weak intensity (WI), moderate intensity (MI), strong intensity (SI); Localization: cytoplasm (c), membrane (m); confidence interval (CI); not stated (NS)

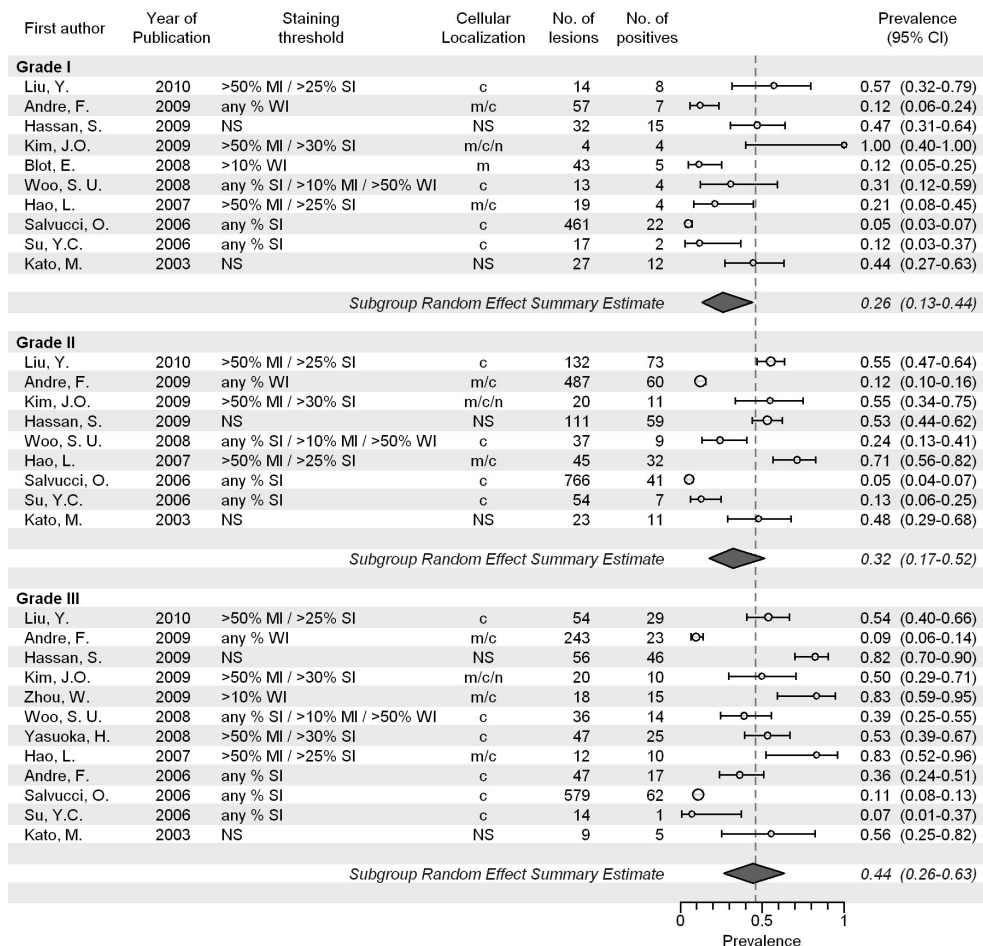
**Figure S8.** Prevalence of GLUT1 expression in relation to tumor size.



Dashed line represents overall random effect summary prevalence estimate. Abbreviations: Staining threshold: weak intensity (WI), moderate intensity (MI), strong intensity (SI); Localization: cytoplasm (c), membrane (m); confidence interval (CI); not stated (NS)

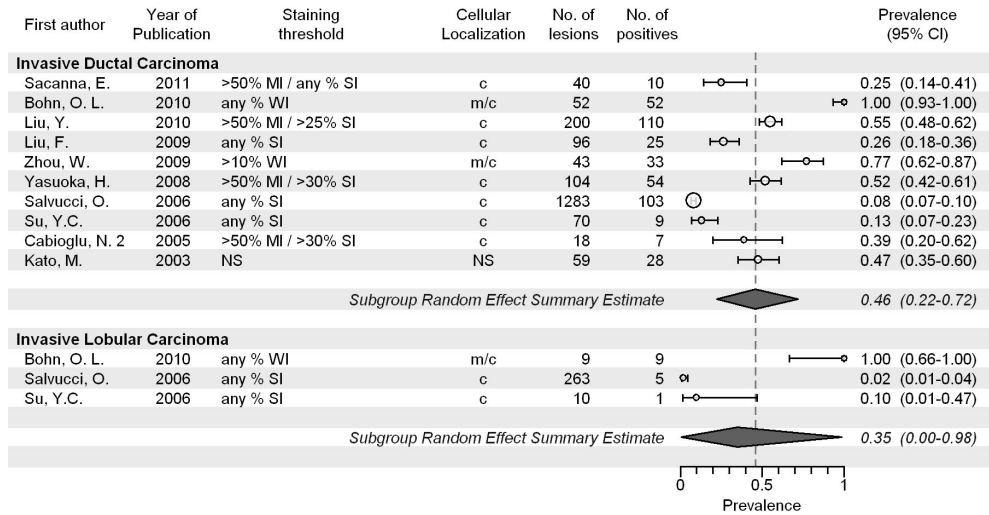


**Figure S9.** Prevalence of CXCR4 expression in relation to histological grade.



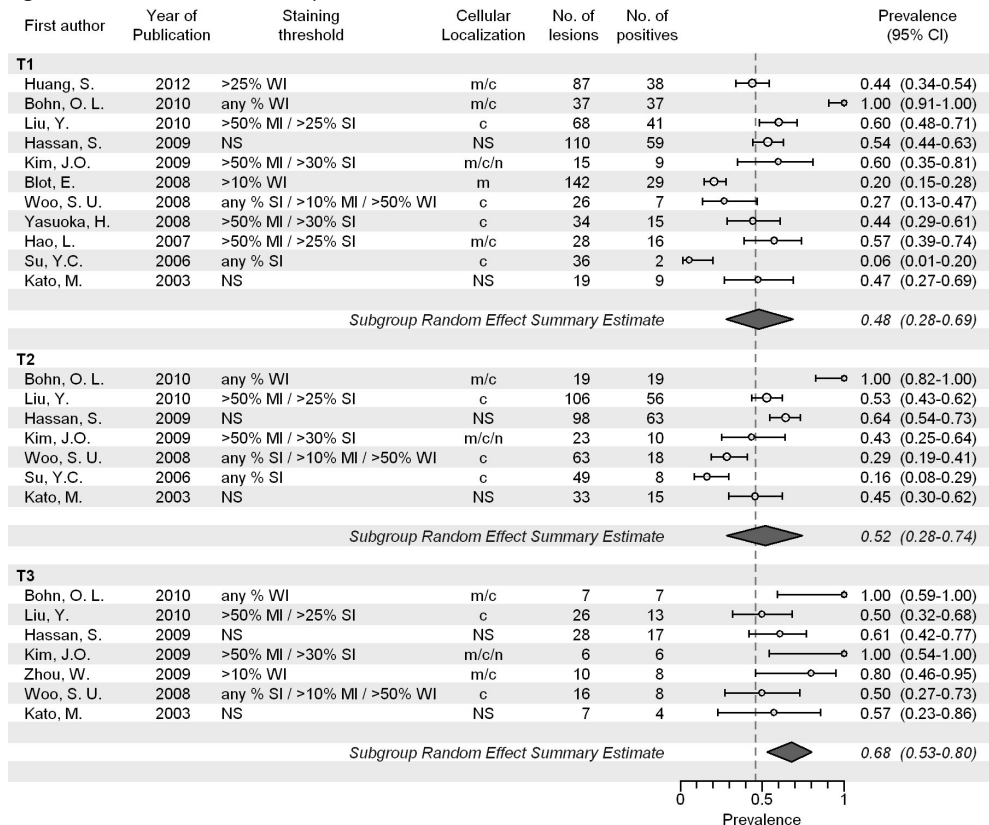
Dashed line represents overall random effect summary prevalence estimate. Abbreviations: Staining threshold: weak intensity (WI), moderate intensity (MI), strong intensity (SI); Localization: cytoplasm (c), membrane (m), nuclear (n); confidence interval (CI); not stated (NS)

**Figure S10.** Prevalence of CXCR4 expression in relation to histological type.



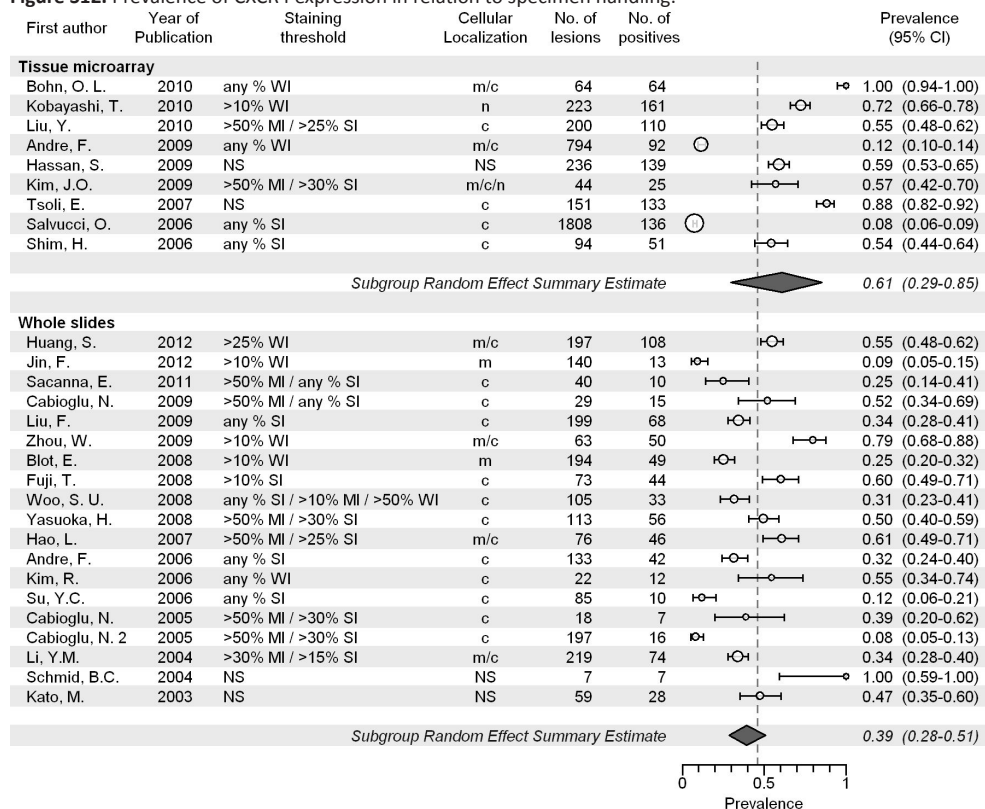
Dashed line represents overall random effect summary prevalence estimate. Abbreviations: Staining threshold: weak intensity (WI), moderate intensity (MI), strong intensity (SI); Localization: cytoplasm (c), membrane (m), nuclear (n); confidence interval (CI); not stated (NS)

**Figure S11.** Prevalence of CXCR4 expression in relation to tumor size.



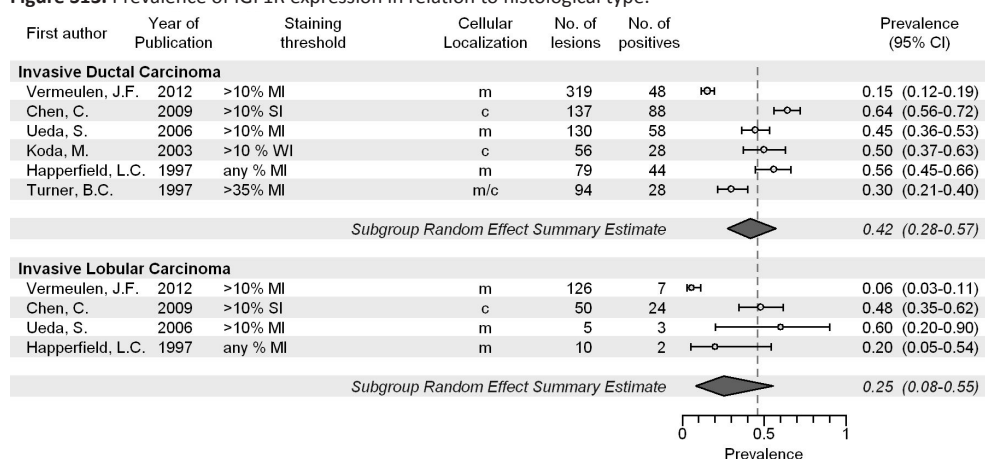
Dashed line represents overall random effect summary prevalence estimate. Abbreviations: Staining threshold: weak intensity (WI), moderate intensity (MI), strong intensity (SI); Localization: cytoplasm (c), membrane (m), nuclear (n); confidence interval (CI); not stated (NS)

**Figure S12.** Prevalence of CXCR4 expression in relation to specimen handling.

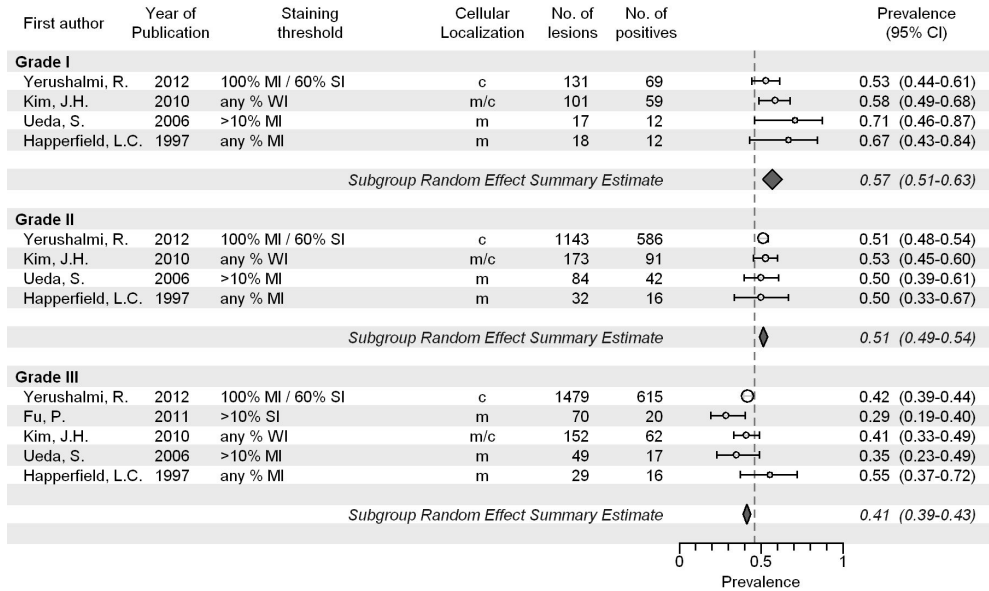


Dashed line represents overall random effect summary prevalence estimate. Abbreviations: Staining threshold: weak intensity (WI), moderate intensity (MI), strong intensity (SI); Localization: cytoplasm (c), membrane (m), nuclear (n); confidence interval (CI); not stated (NS)

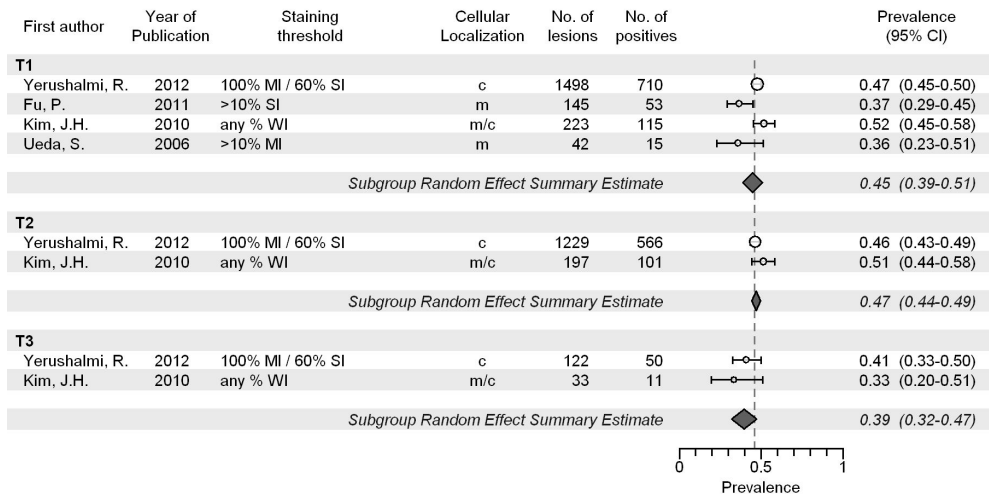
**Figure S13.** Prevalence of IGF1R expression in relation to histological type.



Dashed line represents overall random effect summary prevalence estimate. Abbreviations: Staining threshold: weak intensity (WI), moderate intensity (MI), strong intensity (SI); Localization: cytoplasm (c), membrane (m); confidence interval (CI); not stated (NS)

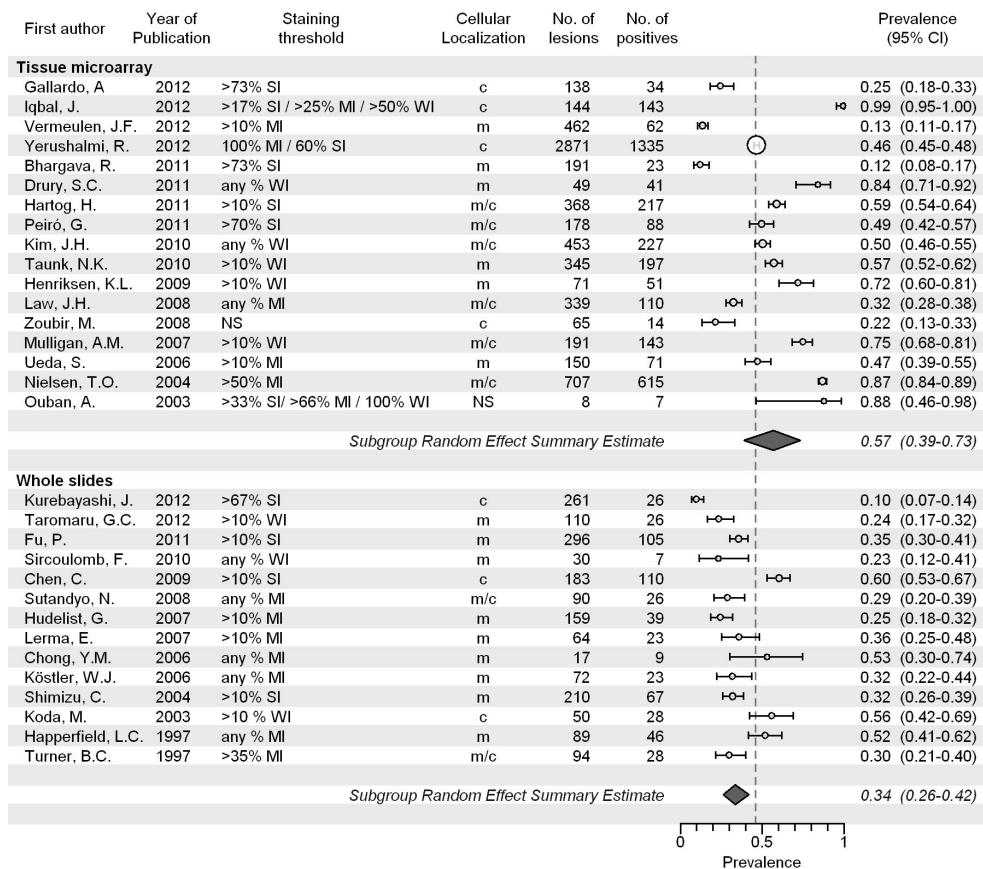
**Figure S14.** Prevalence of IGF1R expression in relation to histological grade.

Dashed line represents overall random effect summary prevalence estimate. Abbreviations: Staining threshold: weak intensity (WI), moderate intensity (MI), strong intensity (SI); Localization: cytoplasm (c), membrane (m); confidence interval (CI); not stated (NS)

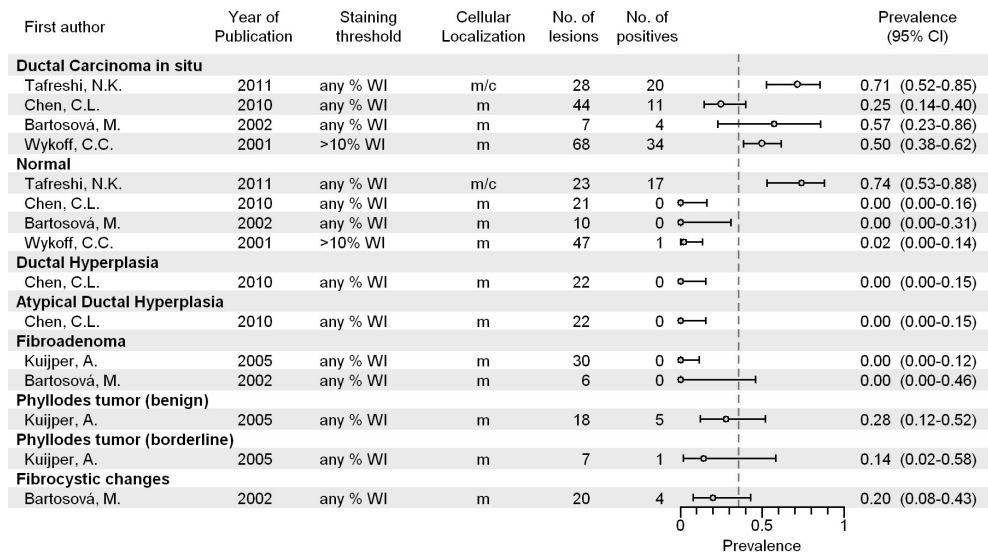
**Figure S15.** Prevalence of IGF1R expression in relation to tumor size.

Dashed line represents overall random effect summary prevalence estimate. Abbreviations: Staining threshold: weak intensity (WI), moderate intensity (MI), strong intensity (SI); Localization: cytoplasm (c), membrane (m); confidence interval (CI); not stated (NS)

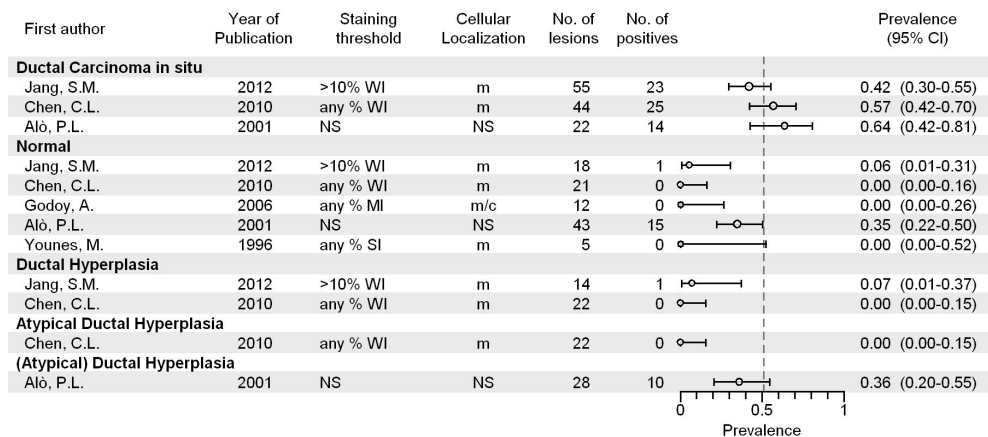
**Figure S16.** Prevalence of IGF1R expression in relation to specimen handling.



Dashed line represents overall random effect summary prevalence estimate. Abbreviations: Staining threshold: weak intensity (WI), moderate intensity (MI), strong intensity (SI); Localization: cytoplasm (c), membrane (m); confidence interval (CI); not stated (NS)

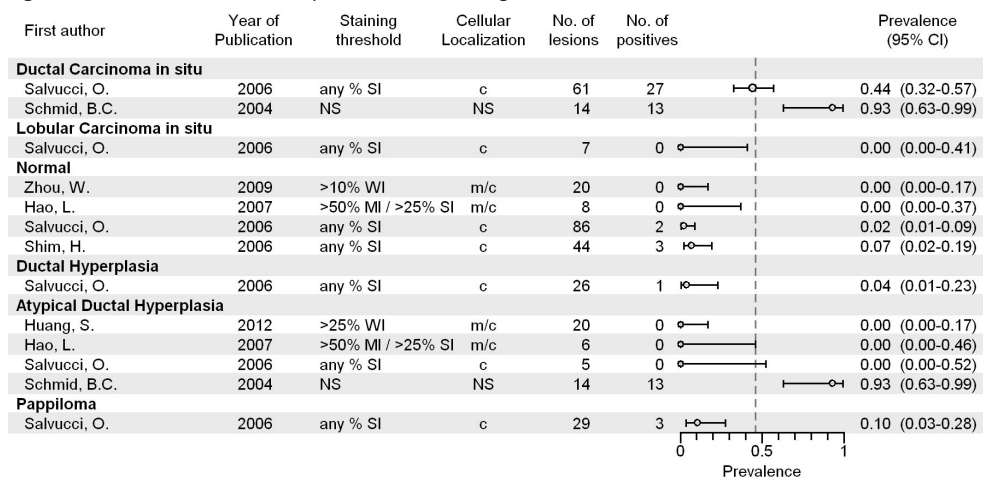
**Figure S17.** Prevalence of CAIX expression in DCIS, benign lesions and normal tissue.

Dashed line represents overall random effect summary prevalence estimate for invasive cancer. Abbreviations: Staining threshold: weak intensity (WI), moderate intensity (MI), strong intensity (SI); Localization: cytoplasm (c), membrane (m); confidence interval (CI); not stated (NS)

**Figure S18.** Prevalence of GLUT1 expression in DCIS, benign lesions and normal tissue.

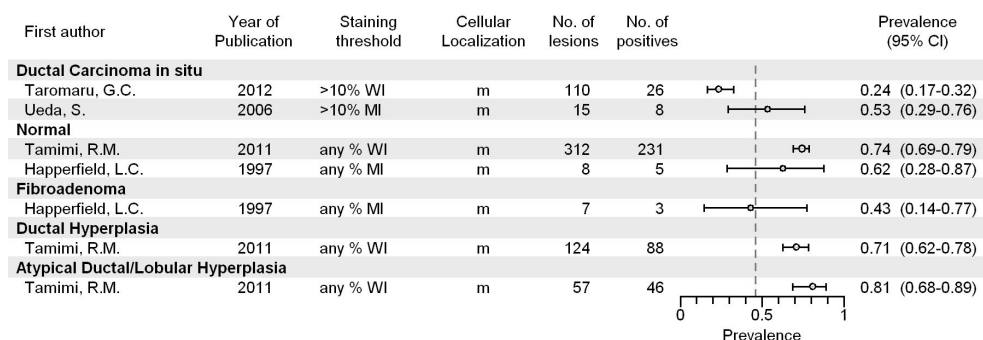
Dashed line represents overall random effect summary prevalence estimate for invasive cancer. Abbreviations: Staining threshold: weak intensity (WI), moderate intensity (MI), strong intensity (SI); Localization: cytoplasm (c), membrane (m); confidence interval (CI); not stated (NS)

**Figure S19.** Prevalence of CXCR4 expression in DCIS, benign lesions and normal tissue.



Dashed line represents overall random effect summary prevalence estimate for invasive cancer. Abbreviations: Staining threshold: weak intensity (WI), moderate intensity (MI), strong intensity (SI); Localization: cytoplasm (c), membrane (m); confidence interval (CI); not stated (NS)

**Figure S20.** Prevalence of IGF1R expression in DCIS, benign lesions and normal tissue.



Dashed line represents overall random effect summary prevalence estimate for invasive cancer. Abbreviations: Staining threshold: weak intensity (WI), moderate intensity (MI), strong intensity (SI); Localization: cytoplasm (c), membrane (m); confidence interval (CI); not stated (NS)

Table S1. Baseline characteristics of selected studies.

Reference	Year, Country of patient inclusion	Study population	Age		Tumor size*		Histological grade		LN <sup>†</sup>	Histology				IHC assessment		Results																
			No. of invasive cancers (+Other)	Important selection criteria	Median (range or SD)	Pl	%	Pl		%	Normal	Benign	In situ	IDC	ILC		Other	Antibody (manufacturer)	Prevalence (95% CI) %													
<b>CAIX</b>																																
Bentz, A.S. [56] 2012, USA (ns)	-	207	-	48 (24-79)	ns	1 2 3	ns	ns	86	o	o	o	o	o	o	M75 (na)	88 (83-92)															
																		2013, South Korea (2000-2001)	276	IDC	49 <sup>a</sup> (11)	ns	I II III	I II III	45	o	o	o	o	o	ns (Abcam)	33 (27-38)
Tafreshi, N.K. [57] 2012, USA (+51) (ns)	89	IDC	ns	ns	ns	I II III	I II III	49	o	o	o	o	o	o	ns (Abcam)	56 (46-66)																
																	2012, The Netherlands (1997-2007)	458	-	60 <sup>a</sup> (28-88)	I II III	I II III	48	o	o	o	o	o	o	Ab15086 (Abcam)	10 (8-13)	
																																Belcic-Oreskovic, L. [58] 2011, Croatia (1999-2005)
Fox, S.B. [42] 2011, Italy (1997-2001)	166	T2-4, N0-1	ns	ns	I II III	I II III	43	o	o	o	o	o	o	o	M75 (na)	25 (19-32)																
																	2011, The Netherlands (ns)	92	-	56 (ns)	I II III	I II III	ns	o	o	o	o	o	o	ns (Abcam)	59 (48-68)	
																																2011, USA (199X-2003)
Lou, Y. [60] 2011, USA (ns)	3630	-	ns	ns	I II III	I II III	44	o	o	o	o	o	o	o	M75 (na)	16 (14-17)																
																	2011, Portugal (ns)	122	-	ns	ns	I II III	I II III	50	o	o	o	o	o	o	Ab15086 (Abcam)	17 (11-25)
Zanetti, J.S. [61] 2011, Brazil (1994-2004)	243	IDC	55 (25-85)	ns	I II III	I II III	53	o	o	o	o	o	o	o	ns (Abcam)	26 (21-32)																
																	2010, Taiwan (ns)	59 (+109)	IDC	ns	ns	I II III	I II III	50	o	o	o	o	o	o	ns (Santa Cruz)	31 (20-43)
Jubb, A.M. [62] 2010, UK (1989-1998)	151	-	57 <sup>a</sup> (27-80)	ns	I II III	I II III	43	o	o	o	o	o	o	o	M75 (na)	32 (25-40)																



Lancashire, L.J. [63] 2010, UK (1986-2000)	712	-	ns	small large		I II III		43	o o o o o o o o	Ab15086 (Abcam)	8 (6-10)
Koop, E.A. [37] 2009, The Netherlands (2004-2006)	40	-	ns	1 2/3		I/II III		58	o o o o o o o o	ns (Abcam)	40 (26-56)
Rakha, E.A. [64] 2009, UK (1987-1998)	232	TN1, IDC, Stage T1-2	50 (25-70)	ns		I II III		40	o o o o o o o o	ns (Abcam)	67 (61-73)
Tan, E.X. [65] 2009, UK (ns)	407	-	55 (24-87)	22 (ns)		I II III		46	o o o o o o o o	M75 (na)	14 (11-18)
Crabb, S.J. [66] 2008, Canada (1986-1992)	281	Clinically LN+	ns	1 2 3		I II III		100	o o o o o o o o	M75 (na)	17 (13-22)
van der Groep, P. [38] 2008, The Netherlands (ns)	21	BRCA1+ or BRCA1+ family	ns	1 2 3		I II III		ns	o o o o o o o o	ns (Abcam)	71 (49-87)
Kyndt, M. [67] 2008, Denmark (1982-1989)	945	-	ns	1 2 3		I II III		6	o o o o o o o o	M75 (na)	26 (23-29)
Garcia, S. [68] 2007, France (1995-2002)	923	IDC	54* (31-84)	23 (7-45)		I II III		50	o o o o o o o o	Ab15086 (Abcam)	27 (24-30)
Hussain, S.A. [69] 2007, UK (ns)	144	-	62 (29-94)	1 2/3		I II III		39	o o o o o o o o	M75 (na)	26 (19-33)
Tan, E.X. [70] 2007, UK (ns)	232	-	57 (29-90)	20 (2-230)		I II III		43	o o o o o o o o	M75 (na)	14 (10-19)
Trastour, C. [71] 2007, France (1993-1993)	132	-	62 (28-87)	15 (2-100)		I II III		36	o o o o o o o o	MN75 (Bayer)	29 (22-37)
Brennan, D.J. [72] 2006, Sweden (1984-1991)	400	Premenopausal patients / <50 yr, stage II	44 (25-57)	1 2 3		I II III		73	o o o o o o o o	M75 (na)	10 (8-14)
Generali, D. [73] 2006, Italy (1997-2002)	169	T2-4 NO-1	ns	1 2 3		I II III		43	o o o o o o o o	M75 (na)	24 (18-31)
Generali, D. [48] 2006, Italy (1997-2002)	169	T2-4 NO-1	ns	1 2 3		I II III		43	o o o o o o o o	M75 (na)	24 (18-31)
Vlugel, M.M. [49] 2005, The Netherlands (1982-1994)	183	M0, no palpable supra-/intra- cervicular LN	ns	ns		ns		35	o o o o o o o o	M75 (na)	12 (9-18)
van den Eynden, G.G. [74] 2005, Belgium (ns)	60	Clinically LN+	59* (25-84)	1 2 3		I II III		100	o o o o o o o o	NB100-417A (Novus)	38 (27-51)
Kuiper, A. [75] 2005, The Netherlands (ns)	10 (+55)	Phylloides tumors and fibroadenomas	34* (11)	16 (6)		ns		ns	o o o o o o o o	M75 (na)	30 (10-62)
Vlugel, M.M. [39] 2005, The Netherlands (1982-1994)	200	-	ns	1 2 3		I II III		39	o o o o o o o o	M75 (na)	12 (9-18)

Reference	Study population		Patient and tumor characteristics				Histology					IHC assessment		Results	
	Year, Country of patient inclusion	No. of invasive cancers (tother)	Important selection criteria	Age (range or SD)	Tumor size*	LN*	Normal	Benign	In situ	IDC	ILC	Other	TMA	Antibody (manufacturer)	Prevalence (95% CI) %
CAIX (continued)															
Blackwell, K.L. [76] 2004, USA (1988-1995)	35	-	ns	ns	32 (15-84)	ns								M75 (na)	54 (38-70)
Cooper, C. [40] 2004, Canada (ns)	51	ERα+	ns	ns			I	II	III					M75 (na)	na
Colpaert, C.G. [77] 2003, Belgium (ns)	129	including IBC	54* (25-83)	18 (8)		66								M75 (na)	53 (44-61)
Tomes, L. [41] 2003, Canada (ns)	97	IDC	ns			48	I	II	III					M75 (na)	57 (47-66)
Bartosova, M. [78] 2002, Slovakia (1998-1999)	19 (+43)	-	50* (19-82)	ns		ns								M75 (na)	42 (23-64)
Chia, S.K. [79] 2004, UK (1989-1994)	103	-	59 (28-82)	1 2/3		56	I	II	III					M75 (na)	48 (38-57)
Wykoff, C.C. [13] 2001, UK (1997-1999)	14 (+115)	-	ns	na		ns								M75 (na)	29 (11-56)
GLUT1															
Choi, J. [31] 2012, South Korea (2000-2001)	276	IDC	49* (11)	ns		45	I	II	III					SPM498 (Abcam)	12 (8-16)
Jang, S.M. [80] 2012, South Korea (2000-2009)	276 (+87)	IDC	50* (ns)	1 2/3		ns								Ab40084 (Abcam)	38 (33-44)
Kornegoor, R. [32] 2012, The Netherlands (1986-2010)	131	Males only	66* (32-89)	1 2/3		54	I/II	III						ns (DAKO)	31 (24-40)
Vermeulen, J.F. [23] 2012, The Netherlands (1997-2007)	458	-	60* (28-88)	1 2 3		48	I	II	III					A3536 (DAKO)	21 (18-25)
Carvalho, K.C. [81] 2011, Brazil (ns)	267	-	ns	ns		ns								ns (DAKO)	5 (3-8)
Hussain, Y.R. [82] 2011, USA (2004-2006)	329	-	57* (26-94)	1 2 3		46	I	II	III					E308 (DAKO)	35 (30-40)
Hyseml, A. [33] 2011, The Netherlands (ns)	92	-	56 (ns)	20 (ns)		ns								ns (DAKO)	26 (18-36)
Pinheiro, C. [34] 2011, Portugal (ns)	124	-	ns	1 2 3		50	I	II	III					Ab15309 (Abcam)	46 (37-55)
Airley, R. [83] 2010, USA (ns)	88	-	58* (27-81)	ns		ns								ns (Alpha Diagnostics Int.)	20 (13-30)

<b>Chen, C.L.</b> [35] 2010, Taiwan (ns)	59 (+109)	IDC	ns	1/2		50	• • • • •	ns (DAKO)	44 (32-57)
<b>Dachs, G.U.</b> [36] 2010, New Zealand (2003-2007)	28	-	61* (14)	22 (13)		50	• • • • •	ns (Abcam)	100 (88-100)
<b>Koda, M.</b> [84] 2010, Poland (ns)	71	IDC	54* (30-82)	1 2		49	• • • • •	A3536 (DAKO)	46 (35-58)
<b>Koo, J.S.</b> [85] 2010, South Korea (2000-2001)	182	IDC	49* (11)	ns		43	• • • • •	SPM498 (Abcam)	56 (49-63)
<b>Schmidt, M.</b> [86] 2010, Germany (ns)	55	-	53* (27-96)	ns		49	• • • • •	ns (US Biologicals)	25 (16-39)
<b>Koop, E.A.</b> [37] 2009, The Netherlands (2004-2006)	40	-	ns	1 2/3		58	• • • • •	ns (DAKO)	38 (24-53)
<b>van der Groep, P.</b> [38] 2008, The Netherlands (ns)	30	BRCAl+ or BRCAl+ family	ns	1 2 3		ns	• • • • •	ns (DAKO)	90 (73-97)
<b>Godoy, A.</b> [87] 2006, Chile (ns)	33 (+12)	-	ns	ns		ns	• • • • •	ns (Alpha Diagnostics Int.)	91 (75-97)
<b>Kuo, S.J.</b> [88] 2006, Taiwan (1999-2001)	39	-	ns (29-82)	1 2/3		54	• • • • •	ns (DAKO)	72 (56-84)
<b>Stackhouse, B.L.</b> [89] 2005, USA (1991-1996)	141	-	ns	1 2 3		49	• • • • •	ns (Research Diagnostics)	72 (64-79)
<b>Viuegel, M.M.</b> [39] 2005, The Netherlands (1982-1994)	200	-	ns	1 2 3		39	• • • • •	A3536 (DAKO)	28 (23-35)
<b>Cooper, C.</b> [40] 2004, Canada (ns)	51	ER+	ns	ns		ns	• • • • •	ns (Chemicon)	na
<b>Laudanski, P.</b> [90] 2004, Poland (ns)	69	-	54* (31-74)	1 2		46	• • • • •	ns (DAKO)	54 (42-65)
<b>Tomes, L.</b> [41] 2003, Canada (ns)	97	IDC	ns	1 2 3		48	• • • • •	ns (Chemicon Int.)	63 (53-72)
<b>Bos, R.</b> [91] 2005, The Netherlands (1996-2000)	55	-	60* (34-85)	1 2 3		43	• • • • •	ns (DAKO)	31 (20-44)
<b>Brown, R.S.</b> [92] 2002, USA (1992-2000)	27	-	49* (32-78)	22 (8-100)		ns	• • • • •	ns (Chemicon Int.)	63 (44-79)
<b>Ito, S.</b> [29] 2002, Japan (ns)	13	-	ns	ns		ns	• • • • •	ns (Santa Cruz)	85 (55-96)
<b>Kang, S.S.</b> [93] 2002, South Korea (1996-1997)	100	IDC	48* (23-74)	1 2/3		47	• • • • •	ns (DAKO)	47 (37-57)
<b>Aiò, P.L.</b> [94] 2001, Italy (1995-1999)	61 (+66)	-	ns	ns		ns	• • • • •	ns (ns)	80 (68-88)



Liu, F. [109] 2009, China (2004-2007)	199	IDC or micropapillary carcinoma	53* (29-83)	1 2 3			70	o o o o o o o	o	MAB172 (R&D systems)	34 (28-41)
Yasuoka, H. [110] 2009, Japan (1981-1992)	113	Negative family history	51 (24-87)	1 2/3			52	o o o o o o o	o	ns (Abcam)	50 (40-59)
Zhou, W. [111] 2009, China (2004-2006)	63 (+20)	Stage sIIA	53* (32-80)	1 2 3			46	o o o o o o o	o	MAB172 (R&D systems)	79 (68-88)
Blot, E. [112] 2008, France (1991-1991)	194	-	57* (26-84)	1 2/3			56	o o o o o o o	o	12G5 (R&D systems)	25 (20-32)
Fujii, T. [113] 2008, Japan (1993-1999)	73	-	56* (11)	1 2/3			46	o o o o o o o	o	ns (Prosci Inc.)	60 (49-71)
Woo, S. [114] 2008, South Korea (1997-2002)	105	No metastatic disease	50 (28-78)	1 2 3			52	o o o o o o o	o	MAB172 (R&D systems)	31 (23-41)
Yasuoka, H. [46] 2008, Japan (1981-1992)	113	Negative family history	51 (24-87)	1 2/3			52	o o o o o o o	o	ns (Abcam)	50 (40-59)
Hao, L. [115] 2007, China (2002-2005)	76 (+14)	-	50 (ns)	1 2/3			54	o o o o o o o	o	MAB172 (R&D systems)	61 (49-71)
Tsoli, E. [116] 2007, UK (1999-2001)	151	-	63 (29-94)	ns			38	o o o o o o o	o	MAB171 (R&D systems)	88 (82-92)
Andre, F. [117] 2006, France (1972-1979)	133	LN+	50 (29-64)	25 (10-90)			100	o o o o o o o	o	MAB172 (R&D systems)	32 (24-40)
Kim, R. [118] 2006, Japan (1980-2001)	22	Bone metastases	55 (23-79)	ns			69	o o o o o o o	o	ns (Abcam)	55 (34-74)
Salvucci, O. [119] 2006, Switzerland (1985-2001)	1808 (+214)	-	62 (26-101)	ns			48	o o o o o o o	o	MAB172 (R&D systems)	8 (6-9)
Shim, H. [120] 2006, USA (ns)	94 (+44)	-	ns	1/2 3			21	o o o o o o o	o	TNI4003 (ns)	54 (44-64)
Su, Y.C. [121] 2006, Taiwan (1998-2004)	85	pT1-2, clinically LN-	44* (ns)	1 2 3			31	o o o o o o o	o	MAB172 (R&D systems)	12 (6-20)
Cabioglu, N. [122] 2005a, USA (ns)	197	pT1	ns	1 2 3			50	o o o o o o o	o	MAB173 (R&D systems)	8 (5-13)
Cabioglu, N. [123] 2005b, Turkey (2000-2001)	18	Clinically LN-	45 (38-76)	1 2/3			67	o o o o o o o	o	MAB173 (R&D systems)	39 (20-61)
Li, Y.M. [124] 2004, USA (ns)	219	-	ns	ns			ns	o o o o o o o	o	MAB170 (R&D systems)	34 (28-40)
Schmid, B.C. [125] 2004, Austria (2000-2001)	7 (+28)	pT1-2	ns	1/2 3			ns	o o o o o o o	o	12G5 (R&D systems)	100 (59-100)
Kato, M. [126] 2003, Japan (1990-1996)	59	IDC	53* (9)	1 2 3			49	o o o o o o o	o	ns (BD)	47 (35-60)

Reference	Study population		Patient and tumor characteristics				Histology				IHC assessment		Results Prevalence (95% CI) %		
	Year, Country of patient inclusion Inclusion period	No. of invasive cancers (other)	Age Median (range or SD)	Tumor size* p	LN <sup>†</sup> %	Normal	Benign	In situ	Invasive	IDC	ILC	Other		TMA	Antibody (manufacturer)
<b>IGF1R</b>															
Gallardo, A. [127] 2012, Spain (ns)	138	HER2+	55 (31-92)	25 (10-200)		I II III								24-31 (Neomarkers)	25 (18-32)
Isabel J. [128] 2012, Singapore (ns)	144	TN	53 (28-88)	2/3		I II III								Clone 3027 (Cell Signaling)	99 (96-100)
Kurebayashi, J. [129] 2012, Japan (1999-2003)	261	-	59 (ns)	2/3		I II III								24-31 (Millipore)	10 (7-14)
Taromanu, G.C. [130] 2012, Brazil (2002-2008)	110 (+110)	IDC with DCIS	55 (26-90)	ns		ns								24-31 (Pleasanton)	24 (17-32)
Yerushalmi, R. [131] 2012, Canada (1986-1992)	2871	-	ns			I II III								5c-7L3 (Santa Cruz)	46 (45-48)
Vermeulen, J.F. [23] 2012, The Netherlands (1997-2007)	462	-	60* (28-88)	2 3		I II III								NB110-87052 (Novus)	13 (11-17)
Bhargava, R. [132] 2011, USA (ns)	191	-	ns	ns		ns								G11 (Ventana)	12 (8-17)
Drury, S.C. [133] 2011, UK (1981-2004)	49	invasive recurrence	55 (28-81)	20 (3-70)		I II III								G11 (Ventana)	84 (71-91)
Fu, P. [134] 2011, Japan (2001-2009)	296	-	59 (21-93)	1 2/3		I/II <sup>b</sup> III								Clone 3027 (Cell Signaling)	35 (30-41)
Fu, P. [135] 2011, Japan (2001-2009)	77	-	ns	2/3		I/II <sup>b</sup> III								3027 (Cell Signaling)	40 (30-51)
Hartog, H. [136] 2011, The Netherlands (1996-2005)	368	-	59 (27-91)	1 2 3		I II III								24-31 (Calbiochem)	59 (54-64)
Peiró, G. [137] 2011, Spain (1990-2001)	178	LN-, stage I-II	52* (23-88)	1 2 3		I II III								ns (Neomarkers)	49 (42-57)
Tamimi, R.M. [138] 2011, USA (1976-1996)	0 (+312)	-	46* (9)	na		na								24-31 (Lab Vision)	-
Kim, J.H. [139] 2010, South Korea (2000-2006)	453	-	46 (23-84)	1 2 3		I II III								ns (Cell Signaling)	50 (46-55)
Sircoulomb, F. [140] 2010, France (1987-2007)	30	HER2+	ns	1 2 3		I II III								G11 (Ventana)	23 (12-41)
Taunk, N.K. [141] 2010, USA (1975-2003)	345	-	ns	1 2 3		ns								T8C8 (Abcam)	57 (52-62)
Chen, C. [142] 2009, US (1983-1998)	183	-	58* (26-89)	ns		ns								5c-462 (Santa Cruz)	60 (53-67)







# Three

## **Immunophenotyping invasive breast cancer: paving the road for molecular imaging**

Jeroen F. Vermeulen<sup>1</sup>, Aram S.A. van Brussel<sup>1</sup>, Petra van der Groep<sup>1,2</sup>,  
Folkert H.M. Morsink<sup>1</sup>, Peter Bult<sup>3</sup>, Elsken van der Wall<sup>2</sup>, Paul J. van Diest<sup>1</sup>

<sup>1</sup> Department of Pathology, University Medical Center Utrecht, Utrecht, The Netherlands,

<sup>2</sup> Division of Internal Medicine and Dermatology, University Medical Center Utrecht, Utrecht, The Netherlands,

<sup>3</sup> Department of Pathology, Radboud University Nijmegen Medical Centre, Nijmegen, The Netherlands

***BMC Cancer 2012; 12(1): 240***

## Abstract

**Background:** Mammographic population screening in The Netherlands has increased the number of breast cancer patients with small and non-palpable breast tumors. Nevertheless, mammography is not ultimately sensitive and specific for distinct subtypes. Molecular imaging with targeted tracers might increase specificity and sensitivity of detection. Because development of new tracers is labor-intensive and costly, we searched for the smallest panel of tumor membrane markers that would allow detection of the wide spectrum of invasive breast cancers.

**Methods:** Tissue microarrays containing 483 invasive breast cancers were stained by immunohistochemistry for a selected set of membrane proteins known to be expressed in breast cancer.

**Results:** The combination of highly tumor-specific markers glucose transporter 1 (GLUT1), epidermal growth factor receptor (EGFR), insulin-like growth factor-1 receptor (IGF1-R), human epidermal growth factor receptor 2 (HER2), hepatocyte growth factor receptor (MET), and carbonic anhydrase 9 (CAIX) 'detected' 45.5% of tumors, especially basal/ triple negative and HER2-driven ductal cancers. Addition of markers with a 2-fold tumor-to-normal ratio increased the detection rate to 98%. Including only markers with a >3-fold tumor-to-normal ratio (CD44v6) resulted in an 80% detection rate. The detection rate of the panel containing both tumor-specific and less tumor-specific markers was not dependent on age, tumor grade, tumor size, or lymph node status.

**Conclusions:** In search of the minimal panel of targeted probes needed for the highest possible detection rate, we showed that 80% of all breast cancers express at least one of a panel of membrane markers (CD44v6, GLUT1, EGFR, HER2, and IGF1-R) that may therefore be suitable for molecular imaging strategies. This study thereby serves as a starting point for further development of a set of antibody-based optical tracers with a high breast cancer detection rate.

## Introduction

In The Netherlands, the lifetime risk to develop breast cancer increased in the last decades from 1 in 10 in 1989 to 1 in 7 in 2003 [1]. In parallel, the annual number of newly diagnosed cases of breast cancer rose to over 13,000 in 2008 [2]. This makes breast cancer the most commonly diagnosed female cancer in The Netherlands. Despite this increase in incidence, the number of deaths due to breast cancer has remained stable in the last decades, with annually around 3,300 deaths in The Netherlands in the period 1989-2008 [3]. Early detection by mammographic population screening has likely contributed to this, leading to diagnosis of smaller, often non-palpable breast cancers and ductal carcinoma *in situ* (DCIS) lesions [4, 5]. Nevertheless, mammography is not optimally sensitive and specific, especially in younger patients and patients with dense breasts [6-11]. Ultrasonography and magnetic resonance imaging (MRI) have been shown to contribute to early detection of breast cancer, as has positron emission tomography (PET) imaging, but these three imaging devices also have their limitations [12].

Molecular optical imaging with near-infrared fluorescent (NIRF) probes holds promise here [13]. First, the spectral properties (emission wavelengths between 700-900 nm) of the fluorescent tracers result in low background (auto)fluorescence [14]. Second, the detection can be highly sensitive and specific and third, it enables to detect tumors up to centimeters deep in tissue [15]. Fourth, no protective measures are required since no ionizing radiation is emitted [16], and fifth, NIRF probes can be conjugated to highly specific targeted molecules such as antibodies, antibody fragments, peptides, or protease activatable substrates to increase the specificity of the signal in the tumor as reviewed by Pleijhuis et al [17].

Several molecular targets have been suggested to be suitable for optical detection of breast cancer such as the epidermal growth factor receptor (EGFR) [18], vascular endothelial growth factor (VEGF) [13, 19], and human epidermal growth factor receptor 2 (HER2) [20, 21]. In addition, hypoxia up-regulated surface antigens like glucose transporter 1 (GLUT1) and carbonic anhydrase 9 (CAIX) are expressed in about half of invasive breast cancers [22] and also in DCIS [23] and therefore might be valuable targets. Since NIRF antibodies will not be easily internalized, intracellular molecular targets relevant for optical detection of breast cancer have so far been ignored.

However, no single molecular target is expressed in all invasive breast cancers and at the same time provides adequate signal-to-noise ratio to the normal breast. For screening

purposes a panel of probes, i.e. antibodies or antibody fragments will likely be necessary. Because development of such antibody-based probes is labor-intensive and costly, we set out to screen for expression of a selected set of candidate targets on tissue microarrays containing 483 cases of human invasive breast cancer, in search of the minimum antibody panel that would be suitable for detection of most breast cancers in vivo by molecular imaging.

**Table 1.** Clinicopathological characteristics of 483 invasive breast cancer patients studied for expression of selected membrane markers.

Feature	Grouping	N or value	%
Age (years)	Mean	60	
	Range	28-88	
Histological type	IDC	319	66.0
	ILC	126	26.1
	Others	38	7.9
Tumor size	pT1	206	42.7
	pT2	219	45.3
	pT3	49	10.1
	Not available	9	1.9
Histological grade	1	89	18.4
	2	169	35.0
	3	219	45.4
	Not available	6	1.2
Lymph node status	Negative *	225	46.6
	Positive **	232	48.0
	Not available	26	5.4

\*: negative = N0 or N0(i+); \*\*: positive =  $\geq$ N1mi (according to TNM 7<sup>th</sup> edition, 2010)

## Methods

### *Patients*

The study population was derived from the archives of the Departments of Pathology of the University Medical Center Utrecht, Utrecht and the Radboud University Nijmegen Medical Centre, Nijmegen, The Netherlands. These comprised 483 cases of invasive breast cancer (operated between 1997 and 2007), of which 340 cases were part of a consecutive series (operated between 2003-2007). The series was enriched with a small consecutive series of lobular breast cancers and a consecutive series of 23 cases with a BRCA germline mutation as previously described [24].

Histological grade was assessed according to the Nottingham scheme [25], and mitotic activity index (MAI) was assessed as before [26]. Other clinicopathological characteristics are shown in Table 1. From representative donor paraffin blocks of the primary tumors, tissue microarrays were constructed by transferring tissue cylinders of 0.6 mm (3 cylinders per tumor) from the tumor area, determined by a pathologist based on haematoxylin-eosin stained slides, using a tissue arrayer (Beecher Instruments, Sun Prairie, WI, USA) as described before [27]. Normal breast tissue was obtained from patients that underwent mastoplasmy (and thus had no tumor at all). In case of matched tumor and normal tissue, we analyzed normal tissue in paraffin blocks that did not contain any tumor and thus were far away from the tumor. The use of anonymous or coded left over material for scientific purposes is part of the standard treatment contract with patients in The Netherlands [28]. Ethical approval was not required.

### *Immunohistochemistry*

Immunohistochemistry was carried out on 4µm thick sections for a panel of potential membrane bound targets for molecular imaging, that are known to be expressed in a frequency of >10% in breast cancer. These were partly highly tumor specific, meaning that they have no or low intensity staining of the normal breast tissue (GLUT1, EGFR, insulin-like growth factor-1 receptor (IGF-1R), HER2, CAIX, hepatocyte growth factor receptor (MET)). We also included less tumor-specific, meaning that are known to have moderate or high intensity staining of the normal breast tissue (Mucin 1 (MUC1), CD44v6, Mammaglobin, transferrin receptor (TfR), carbonic anhydrase 12 (CAXII)), since cancers have usually increased cellularity compared to the normal breast and could thereby also provide adequate signal-to-noise in tumors compared to the normal breast.

After deparaffination and rehydration, endogenous peroxidase activity was blocked for 15 min in a buffer solution pH5.8 containing 0.3% hydrogen peroxide. After antigen retrieval, i.e. boiling for 20 min in 10mM citrate pH6.0 (for progesterone receptor (PR),

CD44v6, GLUT1, CAIX, MET, Tfr, and CAXII), Tris/EDTA pH9.0 (estrogen receptor  $\alpha$  (ER $\alpha$ ), HER2, IGF1-R, MUC1, and Mammaglobin) or Prot K (0.15mg/ml) for 5 min at room temperature (EGFR), a cooling off period of 30 min preceded the primary antibody incubation. CD44v6 (clone VFF18, BMS125, Bender MedSystems, Austria) 1:500; ER $\alpha$  (clone ID5, DAKO, Glostrup Denmark) 1:200; PR (clone PgR636, DAKO) 1:100; HER2 (SP3, Neomarkers, Duiven, The Netherlands) 1:100; GLUT1 (A3536, DAKO) 1:200; CAIX (ab15086, Abcam, Cambridge, UK) 1:1,000; IGF1-R (NB110-87052, Novus Biologicals, Cambridge, UK) 1:400; Tfr (13-6800, Invitrogen, Breda, The Netherlands) 1:300; MUC1 (EMA, M1613 clone E29, DAKO) 1:400; Mammaglobin (clone 304-1A5, DAKO) 1:100; CAXII (HPA008773, Sigma Aldrich, Zwijndrecht, The Netherlands) 1:200 were incubated for 1h at room temperature. Primary antibodies against EGFR (clone 31G7, Zymed, Invitrogen) 1:30; MET (18-2257, Zymed, Invitrogen) 1:100 were incubated overnight at 4°C. All primary antibodies were diluted in PBS containing 1% BSA.

The signal was amplified using Brightvision poly-HRP anti-mouse, rabbit, rat (DPVO-HRP, Immunologic, Duiven, The Netherlands) or the Novolink kit (Leica, Rijswijk, The Netherlands) (in the case of EGFR) and developed with diaminobenzidine, followed by counterstaining with haematoxylin, dehydration in alcohol and mounting.

#### *Scoring of immunohistochemistry*

All stainings were compared to normal breast tissue and scored as positive when a clear membranous staining was seen and when the expression in the tumor was clearly higher than in the normal breast tissue. All stainings were scored using the DAKO/HER2 scoring system for membranous staining. Scores 2+ and 3+ were considered as positive except for HER2 where only a score of 3+ was considered positive. Due to the strong intra-tumor heterogeneity of Mammaglobin expression, scoring was performed by estimating the percentage of positive tumor cells, considering cancers with more than 35% of the membrane stained tumor cells as positive. All scoring was done by a single experienced pathologist (PJVd) who was blinded to patient characteristics and results of other stainings. To take tumor-heterogeneity between the tumor cores into account, the average score per tumor was calculated and used for analyses. Only in case of GLUT1 and CAIX, the tumor was classified as positive when a single core showed positivity. In this study a maximum of 3 missing stainings per patient was allowed, these stainings were considered as negative in the analyses. This potentially results in underestimation of the percentage positivity of a marker.

Based on ER $\alpha$ , PR, and HER2 immunohistochemistry, tumors were classified as luminal (ER $\alpha$  and/or PR positive), HER2-driven (ER $\alpha$ -, PR-, HER2+), triple negative (ER $\alpha$ -, PR-, HER2-) or basal (ER $\alpha$ -, PR-, HER2-, EGFR+), the immunohistochemical surrogate [29] of the original Sorlie/Perou classification [30].

### *Immunofluorescence for quantification of protein expression in tumor and normal breast tissue*

Several of the evaluated molecular membrane targets (CD44v6, MUC1, Tfr, Mammaglobin, and CAXII) are known to be expressed to some extent in the normal breast epithelium. In order for these targets to be useful for breast cancer screening by optical imaging, the signal to background ratio needs to be high enough to be discriminative. We therefore performed immunofluorescence with these antibodies to allow quantification of expression ratios between normal breast and cancer tissue of four randomly selected patients by image analysis.

Immunofluorescence was performed as described above for immunohistochemistry, except that the primary antibodies were detected by incubation with goat-anti-mouse/rabbit Alexa Fluor 555 (1:1,000, Invitrogen) for 1h at room temperature, followed by 4,6-Diamidine-2-phenylindole dihydrochloride (DAPI) counterstaining and mounting with Immumount (Thermo Scientific, Etten-Leur, The Netherlands).

Representative images of normal breast tissue and breast cancer from the same patient were taken using identical settings at 20x magnification using a Leica DMI4000b inverted bright-field / fluorescence microscope.

### *Image analysis of tumor expression versus normal breast tissue*

Conventional immunohistochemical slides were digitalized for image analysis using a digital slide scanner (Aperio Technologies Inc., Vista, CA, USA). Of each patient four representative areas of normal and tumor tissue were selected and the average membrane intensity was calculated with the IHC membrane algorithm (Aperio, v8.001). As the signal-to-noise ratio *in vivo* is determined by the difference in expression between cancer and normal cells as well as by cellularity, the number of cells in the selected area was obtained from the algorithm. Tumor-to-normal ratio was calculated as (membrane intensity\*cellularity/area) of the tumor / (membrane intensity\*cellularity/area) of normal tissue. Tumor-to-normal ratios of the fluorescently labeled antibodies were calculated with ImageJ using the median intensity scores. Values are expressed as the average tumor-to-normal ratio  $\pm$  SEM.

Based on experience in radiology with the blood-pool agent indocyanine green in studies assuming a leaky vessel model [31, 32], and from studies using NIRF labeled trastuzumab/bevacizumab in mouse models [33], a tumor-to-normal ratio larger than 3 was considered to be sufficient for optical imaging.

### *Statistics*

Statistical analysis was performed using IBM SPSS Statistics version 18.0 (SPSS Inc., Chicago, IL, USA). Associations between categorical variables were examined using the Pearson's Chi-square test. P-values <0.05 were considered to be statistically significant.

## Results

To investigate the most promising combination of markers suitable for imaging, we studied the expression of a panel of membrane markers in our study population that comprised 319 (66.0%) invasive ductal, 126 (26.1%) invasive lobular, and 38 (7.9%) invasive breast cancers with other histology. Other clinicopathological characteristics are shown in Table 1.

Representative pictures of immunohistochemistry for the highly tumor-specific molecular membrane targets are shown in Figure 1A. The most widely expressed tumor-specific protein in our cohort was GLUT1, positive in 20.3% of the cancers, followed by EGFR (17.4%), IGF-1R (12.8%), HER2 (10.4%), CAIX (9.5%), and MET (8.9%). The less tumor-specific targets MUC1 (90.7%), CD44v6 (63.8%), Mammaglobin (16.8%), Tfr (14.5%), and CAXII (8.7%) were in general more frequently expressed than the tumor-specific targets (Table 2). Representative pictures of immunohistochemistry for the less tumor-specific molecular membrane targets are shown in Figure 1B.

**Table 2.** Frequency of expression by immunohistochemistry of tumor-specific and less tumor-specific membrane markers in breast cancers.

Target	Positive		Negative		Missing	
	N	%	N	%	N	%
HER2	50	10.4	432	89.4	1	0.2
EGFR	84	17.4	395	81.8	4	0.8
MET	43	8.9	423	87.6	17	3.5
IGF1-R	62	12.8	400	82.8	21	4.3
GLUT1	98	20.3	360	74.5	25	5.2
CAIX	46	9.5	412	85.3	25	5.2
TFR	70	14.5	402	83.2	11	2.3
CD44v6	308	63.8	160	33.1	15	3.1
CAXII	42	8.7	426	88.2	15	3.1
Mammaglobin	81	16.8	382	79.1	20	4.1
MUC1	438	90.7	26	5.4	19	3.9

### *Detection rate of combinations of highly tumor-specific molecular targets in relation to grade, molecular and histological type*

Because the frequency of expression (further denoted 'detection rate') of individual highly tumor-specific markers did not exceed 20.3% of the cases, we examined several combinations of markers by sequential addition of markers to the expression of GLUT1, the most widely expressed highly tumor-specific marker. GLUT1 in combination with EGFR resulted in 30.0% positive cases, GLUT1/IGF1-R in 28.8%, GLUT1/HER2 in 27.7%, GLUT1/MET in 25.2%, and GLUT1/CAIX in 22.3% positive cases. The panel GLUT1, EGFR, HER2, IGF1-R, MET, and CAIX resulted in 45.5% positive cases, although the contribution of CAIX and MET was minimal (Figure 2A).



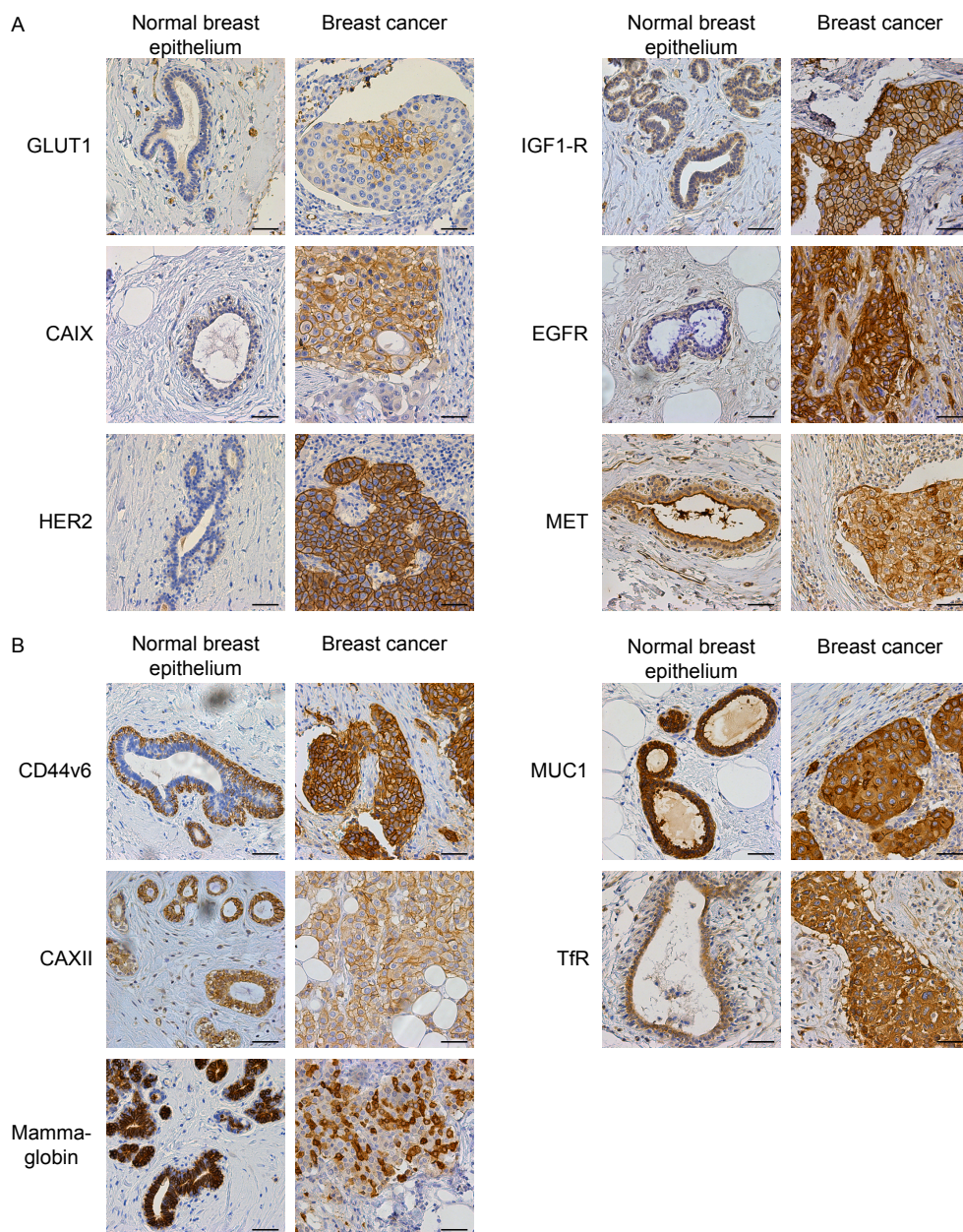


**Figure 1. Membrane marker expression in normal breast epithelium and breast cancer.** Images of representative breast cancer cases with the corresponding normal breast epithelium that were scored as positive. (A) Expression of tumor-specific markers with low or no expression in normal breast epithelium. (B) Expression of membrane markers that are also expressed in normal breast tissue. The intensity in the normal breast epithelium was classified as moderate or high. Scale bar equals 50 $\mu$ m.

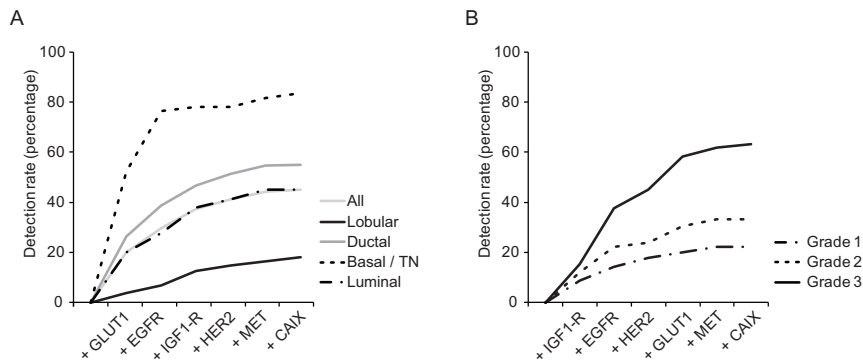


**Figure 2. Detection rate of tumor-specific membrane markers for detection of breast cancer.** Detection rate was calculated by the fraction of positive cases over the total population, taking into account that cancers can express multiple markers. (A) Detection rate of highly tumor-specific membrane markers for detecting luminal, HER2-driven, basal/TN ductal breast cancers, and lobular breast cancers. (B) Detection rate of tumor-specific membrane markers in relation to histological grade.

Clear differences were found between histological subtypes of breast cancer (Table 3). Lobular carcinomas hardly expressed any of the tumor-specific membrane targets present in the panel compared to ductal carcinomas (detection rate 18.3% vs. 55.5%,  $p < 0.001$ ). Within the group of lobular carcinomas, pleomorphic lobular carcinomas expressed more membrane targets than classical lobular carcinomas (detection rate 26.8% vs. 8.6%,  $p = 0.034$ ). Within the group of ductal carcinomas, the basal/triple negative (TN) and HER2-driven ductal cancers expressed more frequently hypoxia markers or growth factor receptors than luminal-type ductal cancers (detection rate 84.2% vs. 45.0%,  $p < 0.001$ ) (Table 4). Therefore the panel EGFR, MET, HER2, GLUT1, CAIX, and IGF1-R detected 84.2% of the basal/TN ductal breast cancers compared to 45.0% of the luminal-type, and 18.3% of the lobular breast cancer cases (Figure 2A, Tables 3 and 4).

**Table 3.** Expression of a panel of membrane markers in various histological types of breast cancer.

Target	Ductal (N = 319)		Lobular (N = 126)		Other (N = 38)	
	N	%	N	%	N	%
HER2	43	13.5	4	3.2	3	7.9
EGFR	71	22.3	4	3.2	9	23.7
MET	34	10.7	4	3.2	5	13.2
IGF1-R	48	15.0	7	5.6	7	18.4
GLUT1	85	26.6	5	4.0	8	21.1
CAIX	38	11.9	2	1.6	6	15.8
TfR	53	16.6	10	7.9	7	18.4
CD44v6	197	61.8	82	65.1	29	76.3
CAXII	30	9.4	12	9.5	1	2.6
Mammaglobin	44	13.8	34	27.0	3	7.9
MUC1	218	88.1	119	94.4	38	100

Because the markers included in our panel are associated with an aggressive phenotype and poor prognosis, we evaluated the detection rate of our panel in relation to grade (Figure 2B). Low grade (grade 1) tumors had a detection rate of 22.5% for this panel, in contrast to 33.7% of grade 2 and 63.9% of grade 3 tumors ( $p < 0.001$ ). This indicates that the panel with tumor-specific antigens is less sensitive for detecting luminal-type, lobular, and low grade/well-differentiated tumors when applied for imaging strategies.

**Table 4.** Expression of membrane markers in molecular subtypes of ductal breast cancer.

Target	Luminal (N = 242)		HER2-driven (N = 20)		Basal/TN (N = 57)	
	N	%	N	%	N	%
HER2	23	9.5	20	100	0	0.0
EGFR	25	10.3	11	55	35	61.4
MET	21	8.7	4	20	9	15.8
IGF1-R	41	16.9	2	10	5	8.8
GLUT1	49	20.2	6	30	30	52.6
CAIX	11	4.5	4	20	23	40.4
TfR	33	13.6	5	25	40	70.2
CD44v6	148	61.8	9	45	15	26.3
CAXII	28	11.6	1	5	1	1.8
Mammaglobin	39	16.1	4	20	1	1.8
MUC1	213	88.0	20	100	48	84.2

*Molecular targets that are expressed in normal breast tissue have sufficient signal-to-noise to detect lobular and luminal-type breast cancer*

Since lobular and luminal-types of breast cancer appeared to hardly express tumor-specific antigens, antigens that are less tumor-specific are required for their detection. Like with tumor-specific markers, variation between histological and molecular subtypes was observed for TfR, Mammaglobin, and CAXII. Luminal-type ductal cancers and lobular cancers expressed significantly more CAXII (10.5% vs. 2.3%,  $p = 0.017$ ) and Mammaglobin (19.9% vs. 5.9%,  $p = 0.002$ ) compared to HER2-driven and basal/TN ductal cancers (Tables 3 and 4). TfR expression in lobular and luminal type ductal cancers was significantly lower than in HER2-driven and basal/TN cancers (11.9% vs. 27.9%,  $p < 0.001$ ). For MUC1 and CD44v6, no differences in expression were found between lobular and ductal cancer (Tables 3 and 4).

Due to the expression of less tumor-specific antigens in the normal breast epithelium (Figure 1B), the signal-to-noise ratio (or tumor-to-normal) needs to be sufficiently discriminating to be applicable for imaging strategies. We determined therefore the tumor-to-normal ratio in a quantitative manner by image analysis of digital slides, considering a 3-fold tumor-to-normal ratio as sufficient. Image quantification using conventional IHC showed that the intensity of the staining was dependent on the cellularity of the tumor as expected. This resulted in tumor-to-normal ratios of  $4.8 \pm 0.56$ ,  $2.3 \pm 0.27$ ,  $1.2 \pm 0.10$ ,  $4.6 \pm 0.62$ , and  $2.4 \pm 0.88$  for CD44v6, MUC1, Mammaglobin, CAXII, and TfR, respectively.

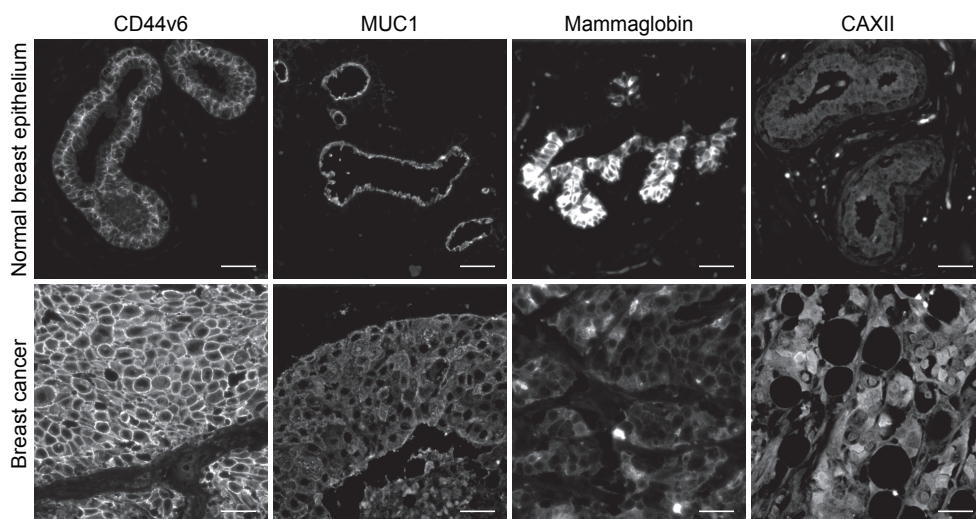


**Figure 3. Quantitation of expression levels of less tumor specific markers using immunofluorescence.** Expression levels of less tumor-specific membrane markers (CD44v6, MUC1, Mammaglobin, and CAXII) as determined by immunofluorescence resulted in staining patterns in normal breast epithelium and positive tumors comparable to conventional immunohistochemistry. Scale bar equals 25 $\mu$ m.

Since conventional immunohistochemistry is not necessarily quantitative, we also performed immunofluorescence using directly fluorescently labeled antibodies. The results were comparable with conventional immunohistochemistry (Figure 3) resulting in tumor-to-normal ratios of  $3.93 \pm 0.14$ ,  $2.74 \pm 0.46$ ,  $1.54 \pm 0.11$ , and  $1.66 \pm 0.07$  for CD44v6, MUC1, Mammaglobin, and CAXII, respectively. TfR expression was not detectable using immunofluorescence. Thereby, CD44v6 was the only less tumor-specific marker consistently meeting the required 3-fold tumor-to-normal ratio.

*Detection rate of combined highly and less tumor-specific molecular targets*

Including TfR, Mammaglobin, and MUC1 to the panel of highly tumor-specific markers: GLUT1, MET, EGFR, IGF1-R, CAIX, and HER2 increased the detection rate from 45.5% to 49.8% (TfR), 56.4% (Mammaglobin), and 98.1% (MUC1), respectively. However, of these markers, only CD44v6 reached a sufficiently high tumor-to-normal ratio (see above), so adding CD44v6 to the panel of highly specific markers therefore realistically increased the overall detection rate to 80.1%. When CD44v6 was included, removal of CAIX or MET from the panel had no influence on the detection rate.

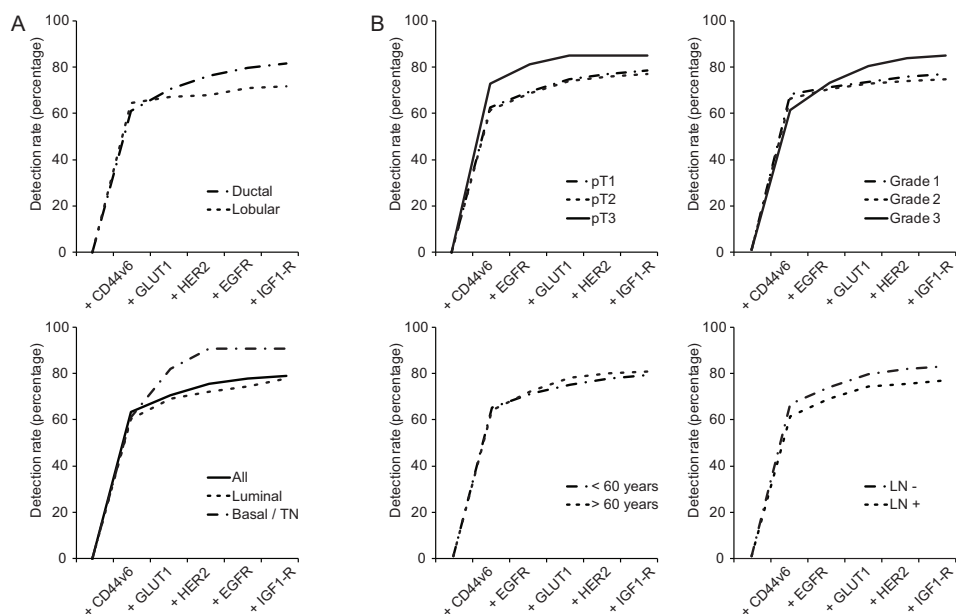


**Figure 4. Optimal combination of membrane markers for detection of breast cancer with respect to clinicopathological characteristics.** Detection rate was calculated by the fraction of positive cases over the total population, taking into account that cancers can express multiple markers. (A) The contribution of each tumor-specific and less tumor-specific membrane marker in the optimal panel for detection of breast cancer. (B) The detection rate of the panel with respect to several clinicopathological features.

Especially the luminal-type ductal and lobular breast cancers were better detected by including CD44v6. Upon addition of CD44v6, the detection rate rose from 45.5% to 78.9% for luminal-type cancers, from 18.3% to 72.2% for the lobular breast cancers, and from 84.2% to 90.0% for basal/TN ductal breast cancers (Figure 4A). Moreover, the detection rate of the panel was not dependent on grade (76.4%, 74.0%, and 84.5% for grade 1, grade 2, and grade 3 tumors, respectively), tumor size (79.1%, 77.6%, and 85.7% for pT1, pT2, and pT3, respectively), lymph node status (76.2% for lymph node negative, and 82.7% for lymph node positive cases), or age (78.8% for patients <60 years and 80.1% for patients >60 years) (Figure 4B).

Therefore, the optimal combination of membrane-expressed proteins to target by molecular imaging seemed to consist of CD44v6, GLUT1, EGFR, HER2, and IGF1-R by which about 80% of invasive breast cancers are predicted to be detectable.

## Discussion

The aim of this study was to identify the minimum panel of membrane markers that might be suitable for detection of invasive breast cancer by molecular imaging. In order to determine this combination, we stained TMAs consisting of 483 clinical specimens of invasive breast cancer by immunohistochemistry. Based on the expression profiles in normal breast tissue, we defined highly tumor-specific (no or low staining of normal breast tissue) and less tumor-specific (moderate or high staining of normal breast tissue) membrane targets. We found that the expression of highly tumor-specific targets (HER2, EGFR, GLUT1, CAIX, IGF1-R, and MET) is quite dependent on the tumor histology and molecular subtype: ductal cancers and in particular the basal/TN and HER2-driven subtypes express more frequently highly tumor-specific membrane targets than lobular cancers.

Because the individual tumor-specific markers are clearly not sensitive enough, application of a tumor-specific panel of tracers is required to detect all types of breast cancer. A panel of tumor-specific markers (GLUT1, EGFR, HER2, IGF1-R, MET, and CAIX) was in the present study able to 'detect' 45.5% of all cancers and 55.6% of ductal cancers. For lobular cancers and low grade tumors, the panel was not very suitable because of detection rates of 18.3% and 22.5%, respectively. Addition of less tumor-specific markers theoretically increased the detection rate to 98.1% using MUC1, but of the less tumor specific markers only CD44v6 met the desired 3-fold tumor-to-normal tissue ratio measured by image analysis. When adding CD44v6 to the panel, 80.1% of all cancers could be 'detected' with at least one marker in a panel consisting of HER2, GLUT1, EGFR, IGF1-R, and CD44v6. CAIX and MET had no additional effect on the sensitivity of the panel once CD44v6 had been included. Our estimation of positivity of breast cancers for our panel may have been conservative since we have been very stringent in calling expression positive, explaining why our rates of expression for GLUT1, CAIX, EGFR, MET, TfR, CAXII, and Mammaglobin are on the lower side compared to the literature [22, 34-43]. Tumors with 1+ membrane staining were consistently considered negative as we expect that this level of staining provides insufficient signal-to-noise, but only *in vivo* studies can confirm this. Moreover, quantification of expression levels based on image analysis of immunohistochemical stainings may be hampered by the non-linear amplification of the signal during immunohistochemistry. For that reason we applied immunofluorescence of directly labeled antibodies for more reliable quantitation of protein expression. Tumor-to-normal ratios above 3 were only obtained when tumors are scored as DAKO 2+ or 3+ membranous staining. This justifies the predefined thresholds for calling tumors positive. Furthermore, cytoplasmic staining was ignored as imaging antibodies will not be easily internalized and will have to bind to

receptors on the outside of the cancer cells. Lastly, using TMAs may have resulted in slight underestimation of GLUT1 and CAIX expression, because the expression is usually limited to hypoxic areas within the tumor [44, 45].

Adding further candidate tumor markers may enable us to improve the results of our panel of membrane related markers. For instance, biomarkers that are specifically expressed in the stroma of breast cancers like growth factors (e.g. VEGF) may be valuable.

This study provides information on the expression levels of membrane bound targets for imaging using paraffin embedded material of invasive breast cancers. To be suitable for breast cancer detection or screening, multiple steps have to be taken before tracer development and testing in (pre)clinical trials results in treatment of patients. However, the present study elucidates which targets might be most suitable based on the expression in cancer vs. normal breast tissue. One of the current challenges is specific detection of lobular breast cancers and DCIS, because these lesions are difficult to detect by mammography. Although, DCIS was beyond the scope of the current paper, for detection of lobular breast cancer CD44v6 is potentially quite useful.

Next to expression of target proteins, tumor perfusion and penetration of the tracer into the tumor could influence the signal for imaging. Further, affinity after labeling and half-life of the tracer in the human body determine the tumor-to-background ratio and thus the applicability of a tracer in a clinical setting. Based on preclinical studies using NIRF labeled trastuzumab and bevacizumab, the maximal tumor-to-background ratio was obtained 6 days post injection [33]. Optimizing this by reducing the half-life of the tracer would be beneficial for clinical practice.

The present study underlines that no single membrane marker probe is likely to detect all breast cancers by molecular imaging, and that a panel of at least five probes may be required. So far, experience is limited to molecular imaging with maximally two different tracers at once. Barrett et al [46] showed that two antibodies allowed to identify differences in tumor expression of HER2 and EGFR *in vivo*. When aiming to be just discriminative between tumor and normal, a panel of markers can be injected with the same probe attached to simplify imaging. Feasibility and toxicity of injecting a panel of markers require further *in vivo* experiments in mouse models.

## Conclusions

We studied which tumor membrane markers are most discriminating between invasive breast cancer and normal breast tissue in order to identify the minimal number of targeted probes needed for the highest possible breast cancer detection rate. We showed that 80% of all breast cancers express at least one of a panel of markers (CD44v6, GLUT1, EGFR, HER2, and IGF1-R) that therefore may be suitable for molecular imaging strategies. The present study thereby serves as a starting point for further development of a set of antibody-based optical tracers with high potential for detecting breast cancer.

## Acknowledgements

This work was supported by an unrestricted research grant of AEGON Inc. and by the MAMmary carcinoma MOlecular imaging for diagnostics and THERapeutics (MAMMOTH) project of the Dutch Center for Translational Molecular Medicine.



## References

1. Paap E, Broeders MJ, van Schoor G, Otten JD and Verbeek AL. Large increase in a Dutch woman's lifetime risk of developing breast cancer. *Eur J Cancer* 2008; 44(11):1485-7.
2. Integraal KankerCentrum Nederland. Incidentie van invasieve tumoren naar geslacht en lokalisatie per incidentiejaar (1989-2008). [www.ikcnet.nl/page.php?id=2902&nav\\_id=114](http://www.ikcnet.nl/page.php?id=2902&nav_id=114). Accessed: 28 May 2011.
3. Integraal KankerCentrum Nederland. Sterfte aan kanker naar geslacht en lokalisatie en jaar van overlijden (1989-2008). [www.ikcnet.nl/uploaded/docs/Landelijk/cijfers/incidentie%202008/B1\\_NL.xls](http://www.ikcnet.nl/uploaded/docs/Landelijk/cijfers/incidentie%202008/B1_NL.xls). Accessed: 28 May 2011.
4. Medina-Franco H, Abarca-Perez L, Garcia-Alvarez MN, *et al.* Radioguided occult lesion localization (ROLL) versus wire-guided lumpectomy for non-palpable breast lesions: a randomized prospective evaluation. *J Surg Oncol* 2008; 97(2):108-11.
5. Singletary SE. Surgical margins in patients with early-stage breast cancer treated with breast conservation therapy. *Am J Surg* 2002; 184(5):383-93.
6. Brown ML, Houn F, Sickles EA and Kessler LG. Screening mammography in community practice: positive predictive value of abnormal findings and yield of follow-up diagnostic procedures. *Am J Roentgenol* 1995; 165(6):1373-7.
7. Elmore JG, Armstrong K, Lehman CD and Fletcher SW. Screening for breast cancer. *JAMA* 2005; 293(10):1245-56.
8. Kerlikowske K, Grady D, Barclay J, *et al.* Positive predictive value of screening mammography by age and family history of breast cancer. *JAMA* 1993; 270(20):2444-50.
9. Lidbrink E, Elfving J, Frisell J and Jonsson E. Neglected aspects of false positive findings of mammography in breast cancer screening: analysis of false positive cases from the Stockholm trial. *BMJ* 1996; 312(7026):273-6.
10. Moadel RM. Breast cancer imaging devices. *Semin Nucl Med* 2011; 41(3):229-41.
11. Brewer NT, Salz T and Lillie SE. Systematic review: the long-term effects of false-positive mammograms. *Ann Intern Med* 2007; 146(7):502-10.
12. Bos R, van der Hoeven JJ, van der Wall E, *et al.* Biologic correlates of (18)fluorodeoxyglucose uptake in human breast cancer measured by positron emission tomography. *J Clin Oncol* 2002; 20(2):379-87.
13. Oude Munnink TH, Nagengast WB, Brouwers AH, *et al.* Molecular imaging of breast cancer. *Breast* 2009; 18 Suppl 3:S66-73.
14. Frangioni JV. In vivo near-infrared fluorescence imaging. *Curr Opin Chem Biol* 2003; 7(5):626-34.
15. Frangioni JV. New technologies for human cancer imaging. *J Clin Oncol* 2008; 26(24):4012-21.
16. Ntziachristos V. Fluorescence molecular imaging. *Ann Rev Biomed Eng* 2006; 8:1-33.
17. Pleijhuis RG, Graafland M, de Vries J, *et al.* Obtaining adequate surgical margins in breast-conserving therapy for patients with early-stage breast cancer: current modalities and future directions. *Ann Surg Oncol* 2009; 16(10):2717-30.
18. Sampath L, Kwon S, Ke S, *et al.* Dual-labeled trastuzumab-based imaging agent for the detection of human epidermal growth factor receptor 2 overexpression in breast cancer. *J Nucl Med* 2007; 48(9):1501-10.
19. Viacava P, Naccarato AG, Bocci G, *et al.* Angiogenesis and VEGF expression in pre-invasive lesions of the human breast. *J Pathol* 2004; 204(2):140-6.
20. Gee MS, Upadhyay R, Bergquist H, *et al.* Human breast cancer tumor models: molecular imaging of drug susceptibility and dosing during HER2/neu-targeted therapy. *Radiology* 2008; 248(3):925-35.
21. Lee SB, Hassan M, Fisher R, *et al.* Affibody molecules for in vivo characterization of HER2-positive tumors by near-infrared imaging. *Clin Cancer Res* 2008; 14(12):3840-9.
22. Bos R, van der Groep P, Greijer AE, *et al.* Levels of hypoxia-inducible factor-1alpha independently predict prognosis in patients with lymph node negative breast carcinoma. *Cancer* 2003; 97(6):1573-81.
23. Bos R, Zhong H, Hanrahan CF, *et al.* Levels of hypoxia-inducible factor-1 alpha during breast carcinogenesis. *J Natl Cancer Inst* 2001; 93(4):309-14.

24. van der Groep P, Bouter A, van der Zanden R, *et al.* Re: Germline BRCA1 mutations and a basal epithelial phenotype in breast cancer. *J Natl Cancer Inst* 2004; 96(9):712-3; author reply 4.
25. Elston CW and Ellis IO. Pathological prognostic factors in breast cancer. I. The value of histological grade in breast cancer: experience from a large study with long-term follow-up. *Histopathology* 1991; 19(5):403-10.
26. van der Groep P, Bouter A, van der Zanden R, *et al.* Distinction between hereditary and sporadic breast cancer on the basis of clinicopathological data. *J Clin Pathol* 2006; 59(6):611-7.
27. Packeisen J, Korsching E, Herbst H, Boecker W and Buerger H. Demystified...tissue microarray technology. *Mol Pathol* 2003; 56(4):198-204.
28. van Diest PJ. No consent should be needed for using leftover body material for scientific purposes. *For. BMJ* 2002; 325(7365):648-51.
29. Kornegoor R, Verschuur-Maes AH, Buerger H, *et al.* Molecular subtyping of male breast cancer by immunohistochemistry. *Mod Pathol* 2012; 25(3):398-404.
30. Sorlie T, Perou CM, Tibshirani R, *et al.* Gene expression patterns of breast carcinomas distinguish tumor subclasses with clinical implications. *Proc Natl Acad Sci U S A* 2001; 98(19):10869-74.
31. Corlu A, Choe R, Durduran T, *et al.* Three-dimensional in vivo fluorescence diffuse optical tomography of breast cancer in humans. *Opt Express* 2007; 15(11):6696-716.
32. van de Ven S, Wiethoff A, Nielsen T, *et al.* A novel fluorescent imaging agent for diffuse optical tomography of the breast: first clinical experience in patients. *Mol Imaging Biol* 2010; 12(3):343-8.
33. Terwisscha van Scheltinga AG, van Dam GM, Nagengast WB, *et al.* Intraoperative near-infrared fluorescence tumor imaging with vascular endothelial growth factor and human epidermal growth factor receptor 2 targeting antibodies. *J Nucl Med* 2011; 52(11):1778-85.
34. Afify A, McNeil MA, Braggin J, Bailey H and Paulino AF. Expression of CD44s, CD44v6, and hyaluronan across the spectrum of normal-hyperplasia-carcinoma in breast. *Appl Immunohistochem Mol Morphol* 2008; 16(2):121-7.
35. Bhargava R, Beriwal S and Dabbs DJ. Mammaglobin vs GCDPF-15: an immunohistologic validation survey for sensitivity and specificity. *Am J Clin Pathol* 2007; 127(1):103-13.
36. Carracedo A, Egervari K, Salido M, *et al.* FISH and immunohistochemical status of the hepatocyte growth factor receptor (c-Met) in 184 invasive breast tumors. *Breast Cancer Res* 2009; 11(2):402.
37. Habashy HO, Powe DG, Staka CM, *et al.* Transferrin receptor (CD71) is a marker of poor prognosis in breast cancer and can predict response to tamoxifen. *Breast Cancer Res Treat* 2010; 119(2):283-93.
38. Klijn JG, Berns PM, Schmitz PI and Foekens JA. The clinical significance of epidermal growth factor receptor (EGF-R) in human breast cancer: a review on 5232 patients. *Endocr Rev* 1992; 13(1):3-17.
39. Lacunza E, Baudis M, Colussi AG, *et al.* MUC1 oncogene amplification correlates with protein overexpression in invasive breast carcinoma cells. *Cancer Genet Cytogenet* 2010; 201(2):102-10.
40. Sasaki E, Tsunoda N, Hatanaka Y, *et al.* Breast-specific expression of MGB1/mammaglobin: an examination of 480 tumors from various organs and clinicopathological analysis of MGB1-positive breast cancers. *Mod Pathol* 2007; 20(2):208-14.
41. Tafreshi NK, Enkemann SA, Bui MM, *et al.* A mammaglobin-A targeting agent for noninvasive detection of breast cancer metastasis in lymph nodes. *Cancer Res* 2011; 71(3):1050-9.
42. Watson PH, Chia SK, Wykoff CC, *et al.* Carbonic anhydrase XII is a marker of good prognosis in invasive breast carcinoma. *Br J Cancer* 2003; 88(7):1065-70.
43. Wykoff CC, Beasley N, Watson PH, *et al.* Expression of the hypoxia-inducible and tumor-associated carbonic anhydrases in ductal carcinoma in situ of the breast. *Am J Pathol* 2001; 158(3):1011-9.
44. van Diest PJ, Vleugel MM, van der Groep P and van der Wall E. VEGF-D and HIF-1alpha in breast cancer. *J Clin Pathol* 2005; 58(3):335; author reply 6.
45. van Diest PJ, Vleugel MM and van der Wall E. Expression of HIF-1alpha in human tumours. *J Clin Pathol* 2005; 58(3):335-6.
46. Barrett T, Koyama Y, Hama Y, *et al.* In vivo diagnosis of epidermal growth factor receptor expression using molecular imaging with a cocktail of optically labeled monoclonal antibodies. *Clin Cancer Res* 2007; 13(22 Pt 1):6639-48.

# Four

## **Differential expression of growth factor receptors and membrane-bound tumor markers for imaging in male and female breast cancer**

Jeroen F. Vermeulen<sup>1</sup>, Robert Kornegoor<sup>1</sup>, Elsken van der Wall<sup>2</sup>,  
Petra van der Groep<sup>1,2</sup>, Paul J. van Diest<sup>1</sup>

<sup>1</sup> Department of Pathology, University Medical Center Utrecht, Utrecht, The Netherlands,

<sup>2</sup> Division of Internal Medicine and Dermatology, University Medical Center Utrecht, Utrecht,  
The Netherlands

***Submitted***

## Abstract

**Introduction:** Male breast cancer accounts for 0.5-1% of all breast cancers and is generally diagnosed at higher stage than female breast cancer and therefore might benefit from earlier detection and targeted therapy. Except for HER2 and EGFR, little is known about expression of growth factor receptors in male breast cancer. We therefore investigated expression profiles of growth factor receptors and membrane-bound tumor markers in male breast cancer and gynecomastia, in comparison with female breast cancer.

**Methods:** Tissue microarrays containing 133 male breast cancer and 32 gynecomastia cases were stained by immunohistochemistry for a panel of membrane-bound targets and compared with data on 266 female breast cancers.

**Results:** Growth factor receptors were variably expressed in 4.5% (MET) up to 38.5% (IGF1-R) of male breast cancers. Compared to female breast cancer, IGF1-R and carbonic anhydrase 12 (CAXII) were more frequently and CD44v6, MET and FGFR2 less frequently expressed in male breast cancer. Expression of EGFR, HER2, CAIX, and GLUT1 was not significantly different between male and female breast cancer. Further, 48.1% of male breast cancers expressed at least one and 18.0% expressed multiple growth factor receptors. Since individual membrane receptors are expressed in only half of male breast cancers, a panel of membrane markers will be required for molecular imaging strategies to reach sensitivity. A potential panel of markers for molecular imaging, consisting of EGFR, IGF1-R, FGFR2, CD44v6, CAXII, GLUT1, and CD44v6 was positive in 77.0% of male breast cancers, and thereby the sensitivity was comparable to female breast cancers.

**Conclusions:** Expression patterns of growth factor receptors and hypoxia membrane proteins in male breast cancer are different from female breast cancer. For molecular imaging strategies, a putative panel consisting of markers for EGFR, IGF1-R, FGFR2, GLUT1, CAXII, and CD44v6 was positive in 77.0% of cases and might be considered for development of molecular tracers for male breast cancer.

## Introduction

Breast cancer in males is a rare disease, accounting for 0.5-1% of all breast cancer cases [1, 2]. Male breast cancer patients generally present at higher age than female breast cancer patients and at a higher stage including more frequently lymph node metastases [1, 3, 4]. Furthermore, molecular subtypes of male breast cancer are differently distributed than in female breast cancer, the most predominant subtype in male being Luminal A followed by Luminal B. HER2-driven subtypes have not been observed [5-7]. Conflicting data exist whether triple negative/basal-like breast cancers occur in male breast cancer, but at least it is infrequent [6-8].

With regard to potential druggable targets, knowledge on the expression of individual tumor markers is limited and variable. Estrogen Receptor  $\alpha$  (ER $\alpha$ ) and progesterone receptor (PR) expression in male breast is present in around 90% of patients [4], which makes them eligible for adjuvant therapy using tamoxifen and aromatase inhibitors. HER2 expression in male ranges between 0-45% of cases in different studies [5-7, 9-11], but current consensus in recent studies shows that HER2 expression in male breast cancer is seen in no more than 3-7% of cases. The epidermal growth factor receptor (EGFR) is the only other growth factor receptor for which expression data is available in male breast cancer, suggesting that EGFR is expressed in 12-76% of cases [6, 7, 9, 11, 12].

Nowadays, antibody-based molecular therapies have been developed for e.g. HER2 [13, 14] and EGFR [15, 16] and molecular therapies for other growth factor receptors are still investigational. In addition to being therapeutic targets, growth factor receptors might be useful for molecular imaging [17-19]. Molecular imaging using optical near-infrared fluorescent probes has advantages compared to mammography alone, because probes can be conjugated to antibodies, antibody fragments or peptides which increases the specificity of the signal [20]. Further, near-infrared fluorescently labeled antibodies can be used for image-guided surgery, thereby enhancing radical resection of breast cancer and lymph node metastases [21-23]. We recently described that in addition to growth factor receptors, hypoxia upregulated proteins (carbonic anhydrase IX (CAIX) and XII (CAXII), and GLUT1) and CD44 variants might be useful for molecular imaging of female breast cancer [24]. Because fluorescently labeled antibodies and antibody-fragments are not easily internalized, ER $\alpha$  and PR are not considered for optical imaging strategies. Selection of potential antibody-based agents for detection and therapy of male breast cancer is labor intensive and costly. Furthermore, the expression of membrane markers in male breast cancer is unknown.

Since male breast cancer patients have more frequently lymph node metastases, molecular imaging may be of benefit for males to assess stage of disease and monitor disease progression or response to therapy. In the present study, we therefore investigated by immunohistochemistry the expression of growth factor receptors and membrane markers in male breast cancer and compared the results with those we observed in female breast cancer and gynecomastia, in order to find a panel of potential markers for therapy and molecular imaging of male breast cancer.

**Table 1.** Clinicopathological characteristics of male and female breast cancer.

Feature	Grouping	Male N (%)	Female N (%)	p-value
Age (years)	Mean	66	59	<b>&lt;0.001</b>
	Range	32-89	28-88	
Histological type	IDC	121 (91.0)	211 (79.3)	<b>0.008</b>
	ILC	3 (2.3)	25 (9.4)	
	Others	9 (6.7)	30 (11.3)	
Tumor size	pT1	73 (54.9)	130 (48.9)	<b>0.030</b>
	pT2	54 (40.6)	113 (42.5)	
	pT3	2 (1.5)	21 (7.9)	
	Not available	4 (3.0)	2 (0.7)	
Histological grade	1	32 (24.1)	45 (16.9)	0.094
	2	54 (40.6)	100 (37.6)	
	3	47 (35.3)	121 (45.5)	
Lymph node status	Negative *	51 (38.3)	119 (44.7)	0.797
	Positive **	60 (45.2)	132 (49.6)	
	Not available	22 (16.5)	15 (5.7)	
Mitotic index #	≤ 12	76 (57.1)	132 (49.6)	0.156
	≥ 13	57 (42.9)	134 (50.4)	
ERα †	Negative	8 (6.0)	53 (19.9)	<b>&lt;0.001</b>
	Positive	125 (94.0)	213 (80.1)	
PR †	Negative	43 (32.3)	89 (33.5)	0.802
	Positive	90 (67.7)	177 (66.5)	

#: per 2 mm<sup>2</sup>; \*: negative = NO or NO(i+); \*\*: positive = ≥N1mi (according to TNM 7<sup>th</sup> edition, 2010);

†: positive = ≥10% nuclear staining

## Materials and methods

### *Patients*

The origin and composition of the male breast cancer study population was described before [7]. Female breast cancer cases from 2003-2007 were derived from the archive of the Department of Pathology University Medical Center Utrecht, Utrecht, The Netherlands as described before [25]. The study population comprised 133 cases of male and 266 cases of female invasive breast cancer. For all cases haematoxylin and eosin (HE) slides were reviewed by two experienced observers (PJvD, RK) to confirm the diagnosis and to characterize the tumor. Histological grade was assessed according to the modified Bloom and Richardson score [26], and mitotic activity index (MAI) was assessed as described before [27]. Clinicopathological characteristics of all male and female breast cancer cases are shown in Table 1.

In addition, 32 gynecomastia cases from 2000-2010 were retrieved from the archives of the Department of Pathology of the University Medical Center Utrecht. Original HE slides were reviewed by two observers (PJvD, RK) to confirm the diagnosis, and to subtype gynecomastia (florid, intermediate, fibrous) as described before [28]. Tissue microarrays were constructed as described by Kornegoor et al. [7, 28]. Use of anonymous or coded left over material for scientific purposes is part of the standard treatment contract with patients in The Netherlands [29]. Ethical approval was not required.

### *Immunohistochemistry*

Immunohistochemistry was carried out on 4µm thick sections for a panel of growth factor receptors. After deparaffination and rehydration, endogenous peroxidase activity was blocked for 15 min in a buffer solution pH5.8 containing 0.3% hydrogen peroxide. After antigen retrieval, i.e. boiling for 20 min in 10mM citrate pH6.0 (for progesterone receptor (PR), Hepatocyte growth factor receptor (MET), Fibroblast growth factor receptor 2 (FGFR2), CD44v6, CAXII, carbonic anhydrase 9 (CAIX), and GLUT1), or Tris/EDTA pH9.0 (estrogen receptor  $\alpha$  (ER $\alpha$ ), HER2, and Insulin-like Growth Factor-1 receptor (IGF1-R)) or Prot K (0.15mg/ml) for 5 min at room temperature (EGFR), a cooling off period of 30 min preceded the primary antibody incubation. ER $\alpha$  (clone ID5, DAKO, Glostrup Denmark) 1:200; PR (clone PgR636, DAKO) 1:100; HER2 (SP3, Neomarkers, Duiven, The Netherlands) 1:100; IGF1-R (NB110-87052, Novus Biologicals, Cambridge, UK) 1:400; FGFR2 (M01, clone 1G3, Abnova, Heidelberg, Germany) 1:800; CD44v6 (clone VFF18, BMS125, Bender MedSystems, Austria) 1:500; GLUT1 (A3536, DAKO) 1:200; CAXII (HPA008773, Sigma Aldrich, Zwijndrecht, The Netherlands) 1:200; CAIX (ab15086, Abcam, Cambridge, UK) 1:1,000 were incubated for 1h at room temperature. Primary antibodies against EGFR (clone 31G7, Zymed, Invitrogen)

1:30; MET (18-2257, Zymed, Invitrogen) 1:100 were incubated overnight at 4°C. All primary antibodies were diluted in PBS containing 1% BSA.

The signal was amplified using Brightvision poly-HRP anti-mouse, rabbit, rat (DPVO-HRP, Immunologic, Duiven, The Netherlands) or the Novolink kit (Leica, Rijswijk, The Netherlands) (in the case of EGFR) and developed with diaminobenzidine, followed by counterstaining with haematoxylin, dehydration in alcohol and mounting.

#### *Scoring of immunohistochemistry*

All stainings were compared to normal breast tissue (obtained from female patients that underwent mastoplasmy) and scored as positive when a clear membrane staining (2+ or 3+) was observed, except for HER2 where only a score of 3+ was considered positive. All scoring was done by JFV, RK and PJvD who were blinded to patient characteristics and results of other stainings. Expression data for the female breast cancers and for the hypoxia proteins in male breast cancer were derived from our previous studies [24, 30].

#### *Statistics*

Statistical analysis was performed using IBM SPSS Statistics version 18.0 (SPSS Inc., Chicago, IL, USA). Associations between categorical variables were examined using the Pearson's Chi-square test and associations between continuous variables using Student's T-test. Logistic regression was used to correct for differences in ER $\alpha$  expression, tumor size (pT1 vs. pT2/3), age (<60 years vs.  $\geq$ 60 years), and histological type (ductal vs. lobular/ other histological type) between male and female breast cancers. P-values <0.05 were considered to be statistically significant.



## Results

In our study population of 133 cases of male breast cancer, we found 4 cases (3.0%) expressing HER2, 15 cases (11.4%) EGFR, 6 cases (4.5%) MET, 16 cases (12.1%) FGFR2, and 50 cases (38.5%) IGF1-R (Table 2). CD44v6, CAIX, CAXII, and GLUT1 were expressed in 44 cases (33.3%), 9 cases (6.8%), 36 cases (27.1%), and 41 cases (31.3%) of male breast cancers, respectively.

### *Membrane protein expression in male breast cancer compared to female breast cancer*

Compared to female breast cancer, IGF1-R was more frequently expressed in male breast cancer ( $p < 0.001$ ), while MET and FGFR2 were less frequently expressed (both  $p < 0.001$ ; Table 2) in male breast cancer. Expression of EGFR and HER2 was not significantly different between male and female breast cancer. Moreover, expression of any growth factor receptor was present in 64 cases (48.1%) of male breast cancer and in 147 cases (55.3%) of female breast cancer ( $p = 0.178$ ). Further, expression rate of CD44v6 was significantly lower ( $p < 0.001$ ) and of CAXII significantly higher ( $p = 0.001$ ) in male compared to female breast cancer. However, expression rates of the hypoxia markers CAIX and GLUT1 were not significantly different between male and female breast cancer ( $p = 0.865$  and  $p = 0.164$ , respectively) (Table 2).

We found that co-expression of growth factor receptors was equally frequent in male (18.0%) and female (20.7%) breast cancer ( $p = 0.178$ ). As shown in Table 3, co-expression of IGF1-R with other growth factor receptors was comparable between male (15.7%) and female breast cancer (13.6%) ( $p = 0.187$ ). Furthermore, co-expression of EGFR with HER2 was similar in male (2.3%) and female (3.0%) breast cancer ( $p = 0.665$ ), while co-expression rates for MET with EGFR and MET with FGFR2 were higher in female than in male breast cancer (4.5% vs. 0.0%,  $p = 0.013$ ) and (5.6% vs. 0.8%,  $p = 0.019$ ), respectively. Simultaneous expression of more than 3 growth factor receptors was found in 2.3% of male and 4.1% of female breast cancer cases ( $p = 0.336$ ).

**Table 2.** Expression of membrane markers in male and female invasive breast cancer.

Feature	Male	Female	p-value	Logistic regression *	
	N (%)	N (%)		OR	95% CI
IGF1-R					
Negative	80 (61.5)	219 (84.6)			
Positive	50 (38.5)	40 (15.4)	<b>&lt;0.001</b>	3.317	1.948-5.647
HER2					
Negative	129 (97.0)	246 (92.5)			
Positive	4 (3.0)	20 (7.5)	0.316	0.555	0.175-1.754
EGFR					
Negative	117 (88.6)	226 (85.6)			
Positive	15 (11.4)	38 (14.4)	0.329	1.494	0.667-3.347
MET					
Negative	126 (95.5)	206 (78.0)			
Positive	6 (4.5)	58 (22.0)	<b>&lt;0.001</b>	0.194	0.079-0.473
FGFR2					
Negative	116 (87.9)	195 (76.5)			
Positive	16 (12.1)	60 (23.5)	<b>0.001</b>	0.331	0.174-0.628
CD44v6					
Negative	88 (66.7)	93 (35.2)			
Positive	44 (33.3)	171 (64.8)	<b>&lt;0.001</b>	0.269	0.168-0.432
GLUT1					
Negative	90 (68.7)	175 (72.6)			
Positive	41 (31.3)	66 (27.4)	0.164	1.439	0.862-2.401
CAIX					
Negative	123 (93.2)	215 (88.5)			
Positive	9 (6.8)	28 (11.5)	0.865	0.924	0.372-2.297
CAXII					
Negative	97 (72.9)	238 (90.8)			
Positive	36 (27.1)	24 (9.2)	<b>0.001</b>	2.753	1.501-5.049

\* Correction for age, histology, ER $\alpha$  expression, and tumor size; Confidence Interval (CI), Odds Ratio (OR).

OR >1 indicates higher expression in male.

**Table 3.** Co-expression of growth factor receptors in male and female breast cancer.

Expression of:	Co-expression with:			
	FGFR2 N (%)	MET N (%)	EGFR N (%)	HER2 N (%)
IGF1-R				
male	8 (6.0)	3 (2.3)	8 (6.0)	2 (1.5)
female	13 (4.9)	13 (4.9)	6 (2.3)	5 (1.9)
HER2				
male	1 (0.8)	1 (0.8)	3 (2.3)	
female	5 (1.8)	8 (3.0)	8 (3.0)	
EGFR				
male	3 (2.3)	0 (0.0)		
female	3 (1.1)	12 (4.5)		
MET				
male	1 (0.8)			
female	15 (5.6)			

### *Clinicopathological correlations of membrane marker expression*

Like in female breast cancer, expression of HER2 in male breast cancer correlated with high histological grade ( $p=0.023$ ) and tumor-size ( $p<0.001$ ). In contrast to female breast cancer, expression of EGFR, GLUT1, and CAIX in male breast cancer did not correlate with any clinicopathological feature. Expression of IGF1-R, MET, FGFR2, and CD44v6 was not correlated to clinicopathological features in both male and female breast cancer. Nevertheless, expression of HER2, MET, EGFR, GLUT1, and CAIX was, as expected, significantly associated with loss of ER $\alpha$  and PR expression in female breast cancer ( $p<0.001$ ,  $p=0.027$ ,  $p<0.001$ ,  $p<0.001$ ,  $p<0.001$  respectively), whereas FGFR2 and CAXII were associated with ER $\alpha$  and PR expression ( $p=0.003$  and  $p=0.016$ ; Table 4). In male breast cancer, only expression of EGFR was significantly associated with loss of ER $\alpha$  and PR expression, probably due to a limited number of ER $\alpha$  and PR negative male breast cancer cases.

### *Towards a panel of potential membrane markers for molecular imaging*

From the previous results it became clear all growth factor receptors are too infrequently expressed in male breast cancer to serve as individual targets for molecular imaging strategies, meaning that a panel of growth factor receptors supplemented with membrane-bound tumor markers is required to obtain a sufficient detection rate like in female breast cancer [24]. Our previously proposed panel consisting of CD44v6, EGFR, HER2, IGF1-R, and GLUT1 for imaging of female breast cancer was significantly less sensitive for imaging of male breast cancer (female breast cancer 79.3% vs. male breast cancer 69.1%,  $p=0.025$ ; Figure 1A). Inclusion of FGFR2 increased the difference in detection rate between male and female breast cancer (detection rate of female breast cancer 85.0% vs. male breast cancer 72.9%,  $p=0.004$ ). However, inclusion of CAXII resulted in the optimal the detection rate possible for male breast cancer (76.7%, Figure 1B). Because the panel of membrane markers mainly consists of growth factor receptors and hypoxia markers, we investigated whether high grade male breast cancers are more frequently detected than low grade cancers. The sensitivity of a combination of growth factor receptors, supplemented with hypoxia markers and CD44v6 was independent of histological grade, tumor size, lymph node status, or age (Figure 1C).

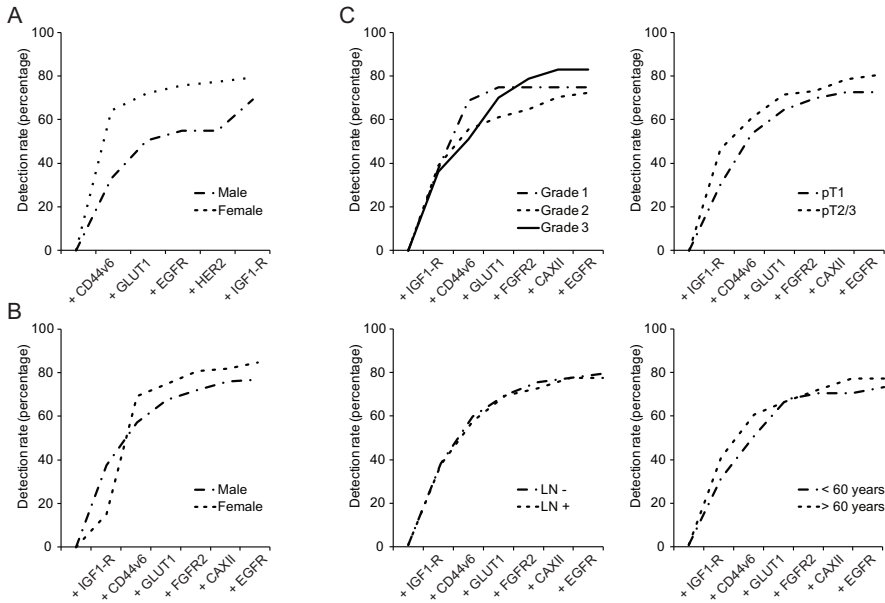


**Figure 1. Potential detection rate of a panel of membrane markers for molecular imaging.** Detection rate was calculated by the fraction of positive cases over the total population, taking into account that cancers can express multiple markers. (A) Detection rate of the previously described panel in male and female breast cancer. (B) The optimal combination of markers to detect male breast cancer. (C) The detection rate of the panel in relation to clinicopathological features of male breast cancer.

### *Specificity of a panel of potential membrane markers in male breast cancer*

Since male breast cancer is often diagnosed together with gynecomastia, although gynecomastia is not an obligate precursor of male breast cancer [28], we examined whether the expression of the selected membrane markers was specific for male breast cancer. We found that expression patterns in gynecomastia were largely comparable with normal female breast tissue; i.e. no expression of HER2, EGFR, MET, GLUT1 and CAIX was detectable. However, we observed FGFR2 expression in 3 cases (9.4%), IGF1-R expression in 1 case (3.1%), and a clear membranous staining of CAXII in 2 cases (6.3%). Gynecomastia was positive for CD44v6 (predominant staining of the myoepithelium) in all cases like normal female breast epithelium, which is probably not influencing the sensitivity of detection as we previously stated [24]. No difference in expression between the subtypes of gynecomastia was observed.

In summary, the expression of growth factor receptors in male and female breast cancer differs. However for molecular imaging strategies, the most optimal panel of potential membrane proteins for imaging of male breast cancer was similar to female breast cancer. Therefore a panel composed of IGF1-R, CD44v6, GLUT1, CAXII, FGFR2, and EGFR might be suitable for molecular imaging of male breast cancer.

**Table 4.** Membrane marker expression in relation to hormone receptor expression.

Feature	Male			Female		
	ERα/PR positive	ERα/PR negative	p-value	ERα/PR positive	ERα/PR negative	p-value
	N (%)	N (%)		N (%)	N (%)	
IGF1-R						
Negative	76 (60.8)	4 (80.0)	0.387	177 (83.5)	42 (89.4)	0.314
Positive	49 (39.2)	1 (20.0)		35 (16.5)	5 (10.6)	
HER2						
Negative	124 (96.9)	5 (100.0)	0.688	207 (95.0)	39 (81.3)	<b>&lt;0.001</b>
Positive	4 (3.1)	0 (0.0)		11 (5.0)	9 (18.8)	
EGFR						
Negative	114 (89.8)	3 (60.0)	<b>0.040</b>	208 (96.3)	18 (37.5)	<b>&lt;0.001</b>
Positive	13 (10.2)	2 (40.0)		8 (3.7)	30 (62.5)	
MET						
Negative	121 (95.3)	5 (100.0)	0.619	175 (80.6)	31 (66.0)	<b>0.027</b>
Positive	6 (4.7)	0 (0.0)		42 (19.4)	16 (34.0)	
FGFR2						
Negative	111 (87.4)	5 (100.0)	0.397	152 (72.7)	43 (93.5)	<b>0.003</b>
Positive	16 (12.6)	0 (0.0)		57 (27.3)	3 (6.5)	
GLUT1						
Negative	85 (67.5)	5 (100.0)	0.124	155 (79.1)	19 (43.2)	<b>&lt;0.001</b>
Positive	41 (32.5)	0 (0.0)		41 (20.9)	25 (56.8)	
CAIX						
Negative	118 (92.9)	5 (100.0)	0.537	189 (95.5)	25 (56.8)	<b>&lt;0.001</b>
Positive	9 (7.1)	0 (0.0)		9 (4.5)	19 (43.2)	
CAXII						
Negative	92 (71.9)	5 (100.0)	0.165	190 (88.8)	47 (100.0)	<b>0.016</b>
Positive	36 (28.1)	0 (0.0)		24 (11.2)	0 (0.0)	
CD44v6						
Negative	83 (65.4)	5 (100.0)	0.107	77 (35.8)	16 (33.3)	0.745
Positive	44 (34.6)	0 (0.0)		138 (64.2)	32 (66.7)	

## Discussion

The aim of this study was to identify the expression patterns of growth factor receptors in male breast cancer, and to determine whether growth factor receptors are suitable candidates for imaging strategies in male breast cancer patients. In addition, these markers could be potential candidates for targeted therapy in the near future next to hormonal therapy using tamoxifen and aromatase inhibitors. In order to determine the expression patterns we stained tissue microarrays containing 133 clinical specimens of male breast cancer by immunohistochemistry and compared it with 266 clinical specimens of female breast cancers and 32 cases of gynecomastia.

We found that expression of IGF1-R was present in 38.5%, FGFR2 in 12.1%, EGFR in 11.4%, HER2 in 3.0%, and MET in 4.5% of male breast cancers. Compared to female breast cancer, IGF1-R expression was higher and MET and FGFR2 expression lower in male breast cancer. In total, half of male breast cancers expressed one of the selected receptors. Furthermore, we found that 18.0% of male breast cancer patients expressed more than one growth factor receptor. The most predominant combination was IGF1-R with EGFR or FGFR2 expression. The expression rates of HER2 and EGFR in male breast cancer were comparable with recent findings [5-7, 10], but for IGF1-R and MET expression other data in the male breast cancer literature is unavailable. Since MET expression is more prevalent in non-luminal female breast cancer, it seemed likely that MET expression in male breast cancer would be low (4.5%), because only 6% of male breast cancers was non-luminal type. IGF1-R expression was found in almost 40% of male breast cancers, suggesting that IGF1-R might be the driving growth factor receptor in male breast cancer. As described by the study of Peyrat et al [31] and Stoll [32], IGF1-R expression is related to ER $\alpha$  positivity, since almost all male breast cancers are ER $\alpha$  positive, high IGF1-R expression was expected. Further, FGFR2 expression in female breast cancer was highly correlated with ER $\alpha$ , PR expression and low grade [33], and with cancers in patients with a BRCA2 mutation [34]. Given that BRCA2 mutations are more frequent in male breast cancer [35, 36], FGFR2 levels were expected to be higher in male than in female breast cancer. However, in our study population FGFR2 expression in male breast cancer was two-fold lower than in female breast cancer.

When only growth factor receptors are used for molecular imaging, the sensitivity would be low (48.1%), however the specificity (as compared to gynecomastia) would be high. Due to low sensitivity, expression patterns of hypoxia markers and CD44v6 were studied in male breast cancer. We found that the ER $\alpha$  and hypoxia associated marker CAXII was more frequently expressed in male compared to female breast cancer. This could not be explained

by ER $\alpha$  expression or a different regulation of the hypoxia response, because expression of CAIX and GLUT1 was not significantly different in male and female breast cancer [37, 38]. Therefore, gender specific differences e.g. hormonal balances probably play a role. Finally, we found that the expression of CD44v6 was significantly lower in male breast cancer than in female breast cancer, although no differential expression was seen between normal female breast tissue and gynecomastia, as judged by extensive staining of the myoepithelial cells. The underlying mechanism and clinical consequences of low CD44v6 in male breast cancer remains to be elucidated.

In conclusion, we found that expression of individual growth factor receptors (IGF1-R, FGFR2, and MET) and CD44v6, CAXII in male breast cancer is different compared to female breast cancer. However, when used as a panel of markers for molecular imaging strategies, the potential detection rate is similar for male and female breast cancer. This implies that membrane targets for molecular imaging of female breast cancer can also be used for detecting male breast cancer. The feasibility of molecular imaging (and therapy) of male breast cancer requires further study, but the present study thereby serves as a starting point for development of a set of antibody-based therapeutics and molecular tracers for male breast cancer.

## Acknowledgements

This work was supported by an unrestricted research grant of AEGON Inc. and by the MAMmary carcinoma MOlecular imaging for diagnostics and THERapeutics (MAMMOTH) project of the Dutch Center for Translational Molecular Medicine.

## References

1. Miao H, Verkooijen HM, Chia KS, *et al.* Incidence and outcome of male breast cancer: an international population-based study. *J Clin Oncol* 2011; 29(33):4381-6.
2. Anderson WF, Jatoi I, Tse J and Rosenberg PS. Male breast cancer: a population-based comparison with female breast cancer. *J Clin Oncol* 2010; 28(2):232-9.
3. Fentiman IS, Fourquet A and Hortobagyi GN. Male breast cancer. *Lancet* 2006; 367(9510):595-604.
4. Giordano SH, Cohen DS, Buzdar AU, Perkins G and Hortobagyi GN. Breast carcinoma in men: a population-based study. *Cancer* 2004; 101(1):51-7.
5. Shaaban AM, Ball GR, Brannan RA, *et al.* A comparative biomarker study of 514 matched cases of male and female breast cancer reveals gender-specific biological differences. *Breast Cancer Res Treat* 2012; 133(3):949-58.
6. Ge Y, Sneige N, Eltorky MA, *et al.* Immunohistochemical characterization of subtypes of male breast carcinoma. *Breast Cancer Res* 2009; 11(3):R28.
7. Kornegoor R, Verschuur-Maes AH, Buerger H, *et al.* Molecular subtyping of male breast cancer by immunohistochemistry. *Mod Pathol* 2012; 25(3):398-404.
8. Ciocca V, Bombonati A, Gatalica Z, *et al.* Cytokeratin profiles of male breast cancers. *Histopathology* 2006; 49(4):365-70.
9. Moore J, Friedman MI, Gansler T, *et al.* Prognostic indicators in male breast carcinoma. *Breast J* 1998; 4(4):261-9.
10. Foerster R, Foerster FG, Wulff V, *et al.* Matched-pair analysis of patients with female and male breast cancer: a comparative analysis. *BMC Cancer* 2011; 11:335.
11. Willsher PC, Leach IH, Ellis IO, *et al.* Male breast cancer: pathological and immunohistochemical features. *Anticancer Res* 1997; 17(3C):2335-8.
12. Fox SB, Rogers S, Day CA and Underwood JC. Oestrogen receptor and epidermal growth factor receptor expression in male breast carcinoma. *J Pathol* 1992; 166(1):13-8.
13. Pivot X, Bedairia N, Thiery-Vuillemin A, Espie M and Marty M. Combining molecular targeted therapies: clinical experience. *Anticancer Drugs* 2011; 22(8):701-10.
14. Valachis A, Mauri D, Polyzos NP, *et al.* Trastuzumab combined to neoadjuvant chemotherapy in patients with HER2-positive breast cancer: a systematic review and meta-analysis. *Breast* 2011; 20(6):485-90.
15. Garrett CR and Eng C. Cetuximab in the treatment of patients with colorectal cancer. *Expert Opin Biol Ther* 2011; 11(7):937-49.
16. Brockstein BE. Management of recurrent head and neck cancer: recent progress and future directions. *Drugs* 2011; 71(12):1551-9.
17. Sampath L, Kwon S, Ke S, *et al.* Dual-labeled trastuzumab-based imaging agent for the detection of human epidermal growth factor receptor 2 overexpression in breast cancer. *J Nucl Med* 2007; 48(9):1501-10.
18. Lee SB, Hassan M, Fisher R, *et al.* Affibody molecules for in vivo characterization of HER2-positive tumors by near-infrared imaging. *Clin Cancer Res* 2008; 14(12):3840-9.
19. Gee MS, Upadhyay R, Bergquist H, *et al.* Human breast cancer tumor models: molecular imaging of drug susceptibility and dosing during HER2/neu-targeted therapy. *Radiology* 2008; 248(3):925-35.
20. Pleijhuis RG, Graafland M, de Vries J, *et al.* Obtaining adequate surgical margins in breast-conserving therapy for patients with early-stage breast cancer: current modalities and future directions. *Ann Surg Oncol* 2009; 16(10):2717-30.
21. Pleijhuis RG, Langhout GC, Helfrich W, *et al.* Near-infrared fluorescence (NIRF) imaging in breast-conserving surgery: assessing intraoperative techniques in tissue-simulating breast phantoms. *Eur J Surg Oncol* 2011; 37(1):32-9.
22. Hirche C, Murawa D, Mohr Z, Kneif S and Hunerbein M. ICG fluorescence-guided sentinel node biopsy for axillary nodal staging in breast cancer. *Breast Cancer Res Treat* 2010; 121(2):373-8.



23. Crane LM, Themelis G, Arts HJ, *et al.* Intraoperative near-infrared fluorescence imaging for sentinel lymph node detection in vulvar cancer: first clinical results. *Gynecol Oncol* 2011; 120(2):291-5.
24. Vermeulen JF, van Brussel AS, van der Groep P, *et al.* Immunophenotyping invasive breast cancer: paving the road for molecular imaging. *BMC Cancer* 2012; 12(1):240.
25. Vermeulen JF, van de Ven RA, Ercan C, *et al.* Nuclear kaiso expression is associated with high grade and triple-negative invasive breast cancer. *PLoS One* 2012; 7(5):e37864.
26. Elston CW and Ellis IO. Pathological prognostic factors in breast cancer. I. The value of histological grade in breast cancer: experience from a large study with long-term follow-up. *Histopathology* 1991; 19(5):403-10.
27. van der Groep P, Bouter A, van der Zanden R, *et al.* Distinction between hereditary and sporadic breast cancer on the basis of clinicopathological data. *J Clin Pathol* 2006; 59(6):611-7.
28. Kornegoor R, Verschuur-Maes AH, Buerger H and van Diest PJ. The 3-layered Ductal Epithelium in Gynecomastia. *Am J Surg Pathol* 2012; 36(5):762-8.
29. van Diest PJ. No consent should be needed for using leftover body material for scientific purposes. For. *BMJ* 2002; 325(7365):648-51.
30. Kornegoor R, Verschuur-Maes AH, Buerger H, *et al.* Fibrotic focus and hypoxia in male breast cancer. *Mod Pathol* 2012; 25(10):1397-404.
31. Peyrat JP, Bonneterre J, Beuscart R, Djiane J and Demaille A. Insulin-like growth factor 1 receptors in human breast cancer and their relation to estradiol and progesterone receptors. *Cancer Res* 1988; 48(22):6429-33.
32. Stoll BA. Oestrogen/insulin-like growth factor-I receptor interaction in early breast cancer: clinical implications. *Ann Oncol* 2002; 13(2):191-6.
33. Garcia-Closas M, Hall P, Nevanlinna H, *et al.* Heterogeneity of breast cancer associations with five susceptibility loci by clinical and pathological characteristics. *PLoS Genet* 2008; 4(4):e1000054.
34. Bane AL, Pinnaduwa D, Colby S, *et al.* Expression profiling of familial breast cancers demonstrates higher expression of FGFR2 in BRCA2-associated tumors. *Breast Cancer Res Treat* 2009; 117(1):183-91.
35. Gethins M. Breast cancer in men. *J Natl Cancer Inst* 2012; 104(6):436-8.
36. Evans DG, Susnerwala I, Dawson J, *et al.* Risk of breast cancer in male BRCA2 carriers. *J Med Genet* 2010; 47(10):710-1.
37. Barnett DH, Sheng S, Charn TH, *et al.* Estrogen receptor regulation of carbonic anhydrase XII through a distal enhancer in breast cancer. *Cancer Res* 2008; 68(9):3505-15.
38. Wykoff CC, Beasley N, Watson PH, *et al.* Expression of the hypoxia-inducible and tumor-associated carbonic anhydrases in ductal carcinoma in situ of the breast. *Am J Pathol* 2001; 158(3):1011-9.



# Five

## **Expression of membrane markers for molecular imaging of ductal carcinoma in situ of the breast**

Jeroen F. Vermeulen<sup>1</sup>, Elsken van der Wall<sup>2</sup>,  
Arjen J. Witkamp<sup>3</sup>, Paul J. van Diest<sup>1</sup>

<sup>1</sup> Department of Pathology, University Medical Center Utrecht, Utrecht, The Netherlands,

<sup>2</sup> Division of Internal Medicine and Dermatology, University Medical Center Utrecht, Utrecht, The Netherlands,

<sup>3</sup> Department of Surgery, University Medical Center Utrecht, Utrecht, The Netherlands

***Submitted***

## Abstract

**Introduction:** Achieving radicality during breast conserving surgery for pure DCIS and invasive cancer surrounded by DCIS is challenging. However, molecular imaging holds promise here, when applied as a tool for image-guided surgery of DCIS.

**Methods:** Tissue microarrays containing 24 pure DCIS and 63 DCIS with adjacent invasive breast cancer cases were stained by immunohistochemistry for a panel of membrane-bound targets.

**Results:** GLUT1 expression was present in 60.9%, IGF1-R in 55.2% HER2 in 28.7%, MET in 18.4%, EGFR in 16.1%, CD44v6 in 69.0%, carbonic anhydrase XII (CAXII) in 24.1%, and Mammaglobin in 14.9% of DCIS cases. No expression differences between pure DCIS and DCIS with adjacent cancer were observed. Further, HER2 and EGFR expression were correlated with high grade DCIS ( $p=0.001$ ) in contrast to CAXII ( $p=0.027$ ) that was more frequent in low grade DCIS. A putative panel of markers for molecular imaging consisting of HER2, CD44v6, EGFR, GLUT1 and IGF1-R had a sensitivity of 96.3% for DCIS and 84.2% for adjacent breast cancer. When invasive breast cancer was positive using the panel, 1.8% of DCIS cases was not.

**Conclusions:** Expression of membrane targets in DCIS is generally higher than in adjacent invasive breast cancer, but single membrane proteins are still too infrequently expressed to serve as a single imaging target for detection of DCIS. However, a panel of markers consisting of IGF1-R, CD44v6, GLUT1, and HER2 was positive in 95% of DCIS lesions, and addition of EGFR to this panel resulted in a potentially comparable sensitivity for DCIS and adjacent invasive breast cancer. This implies that detection of DCIS and adjacent invasive breast cancer during breast conserving surgery should be possible with a panel of molecular imaging tracers targeting CD44v6, GLUT1, HER2, IGF1-R, and EGFR.

## Introduction

Ductal carcinoma *in situ* (DCIS) is a persistent problem during breast surgery. Pure DCIS is increasingly the sole target of surgery, and about 60% of invasive breast cancers detected by mammography have a DCIS component [1]. Radical dissection of DCIS is hampered because DCIS lesions are often surrounding the invasive cancer, are usually non-palpable during breast conserving surgery, and DCIS is rarely completely visible by mammography, ultrasonography or MRI. Since DCIS may lead to invasive recurrence, imaging methods to visualize DCIS during surgery to facilitate radical resection would be very useful.

Molecular optical imaging with near-infrared fluorescent (NIRF) tracers holds promise here [2, 3]. Recent advancements demonstrated that molecular imaging (with NIRF-tracers) is not restricted to screening and can be applied for image-guided surgery using the signal of NIRF-tracers. In ovarian cancer, metastatic lesions of <1 mm were easily detected and removed using folate-fluorescein isothiocyanate [4], and sentinel node dissection could be performed using indocyanine green in breast cancer [5, 6]. Furthermore, phantom experiments in a model for breast cancer showed that radical resection of ‘tumors’ was feasible based on the signal of NIRF tracers [7]. Compared to indocyanine green, molecular imaging using antibody-based tracers has increased the specificity of molecular imaging probes [8], but the number of relevant targets for optical imaging will be limited to membrane proteins, since NIRF-labeled antibodies will not be easily internalized.

Currently, knowledge about expression of membrane markers in DCIS is well established for EGFR and HER2. Previous reports have shown that expression of HER2 in DCIS is higher than in invasive breast cancer, approximately 30-50% [9-12]. Several studies reported EGFR to be more frequently expressed than HER2, between 82-94% [11, 13], while others report 0-22% positivity [12, 14]. Data on expression of other membrane proteins markers like insulin-like growth factor 1 receptor (IGF1-R) is limited [12] or in the case of hepatocyte growth factor receptor (MET) inconsistent, positive in 10-41% of DCIS cases [15, 16]. Based on our previous study in invasive breast cancer [17], other markers might also be suitable for detection of DCIS. The hypoxia-regulated targets GLUT1, Carbonic anhydrase IX and XII (CAIX and CAXII, respectively) were previously reported to be highly expressed in DCIS [18-21] and could serve as potent markers for detecting DCIS using molecular imaging.

In the present study we therefore examined by immunohistochemistry the expression of growth factor receptors, hypoxia and other abundant membrane markers in DCIS in order to find a panel of markers for detection of DCIS by molecular imaging.

# Methods

## *Patients*

The study population was derived from the archives of the Department of Pathology of the University Medical Center Utrecht, Utrecht, The Netherlands. These comprised 87 cases of ductal carcinoma *in situ* (DCIS) operated between 2000 and 2007 of which 24 cases contained only DCIS and 63 DCIS with invasive breast cancer. DCIS was graded according to Holland et al. [22], and histological grade of invasive cancers was assessed according to the Nottingham scheme [23]. From representative donor paraffin blocks containing DCIS, tissue microarrays were constructed by transferring tissue cylinders of 0.6 mm (3 cylinders per patient, each containing a single DCIS lesion), as determined by a pathologist based on haematoxylin-eosin stained slides, using a tissue arrayer (Beecher Instruments, Sun Prairie, WI, USA) as described before [24]. Tissue microarrays of the adjacent invasive breast cancers were constructed using the same procedure. Clinicopathological characteristics are shown in Table 1. The use of anonymous or coded left over material for scientific purposes is part of the standard treatment contract with patients in The Netherlands [25]. Ethical approval was therefore not required.

## *Immunohistochemistry*

Immunohistochemistry was carried out as described before [17] on 4µm thick sections for a panel of membrane targets. All stainings were scored as positive when a clear membranous staining was seen using the DAKO/HER2 scoring system for membranous staining. Scores 2+ and 3+ were considered as positive except for HER2 where only a score of 3+ was considered positive. All scoring was done by two independent observers (JFV and PJvD) as before [26] who were blinded to patient characteristics and results of other stainings.

## *Statistics*

Statistical analysis was performed using IBM SPSS Statistics version 18.0 (SPSS Inc., Chicago, IL, USA). Associations between categorical variables were examined using the Pearson's Chi-square test. P-values <0.05 were considered to be statistically significant.

**Table 1.** Clinicopathological characteristics of 87 patients with DCIS with or without invasive breast cancer studied for expression of selected membrane markers.

Feature	Grouping	pure DCIS		DCIS + invasive	
		N	%	N	%
Total		24	27.5	63	72.5
Age (years)	Mean	57		54	
	Range	24-74		37-83	
Grade DCIS	1	3	12.5	9	14.2
	2	10	41.7	23	36.5
	3	11	45.8	28	44.5
	Not available	0	0	3	4.8
Histological type	IDC			58	92.0
	ILC			3	4.8
	Others			2	3.2
Tumor size	pT1			36	57.1
	pT2			18	28.6
	pT3			6	9.5
	Not available			3	4.8
Histological grade	1			11	17.5
	2			24	38.0
	3			26	41.3
	Not available			2	3.2
Lymph node status	Negative *			19	30.2
	Positive **			28	44.4
	Not available			16	25.4

\*: negative = N0 or N0(i+); \*\*: positive =  $\geq$ N1mi (according to TNM 7<sup>th</sup> edition, 2010)

## Results

### *Expression of membrane targets in DCIS*

Membrane targets were classified as tumor-specific or as less tumor-specific based on the staining of normal breast epithelium as previously reported [17]. In our dataset of 87 DCIS cases, the most abundantly expressed tumor-specific marker was GLUT1 in 53 (60.9%) cases followed by IGF1-R in 48 (55.2%), HER2 in 25 (28.7%), MET in 16 (18.4%), and EGFR in 14 (16.1%) cases. Compared to invasive breast cancer (as described in [17]) all tumor-specific markers were more frequently expressed in DCIS. The less tumor-specific targets CD44v6, CAXII, and Mammaglobin were expressed in 60 (69.0%), 21 (24.1%), and 13 (14.9%) of DCIS cases, respectively. The expression of CD44v6 and Mammaglobin in DCIS was comparable with invasive breast cancer, but CAXII was 3 times more frequently expressed in DCIS than in invasive breast cancer. Because in 63 cases (72.5%) DCIS lesions were located adjacent to invasive breast cancer, we examined whether membrane marker expression was different between pure DCIS and DCIS adjacent to breast cancer. As shown in Table 2, except for EGFR ( $p=0.049$ ), no significant differences in expression rate were found between pure DCIS and DCIS adjacent to synchronous breast cancer.

**Table 2.** Expression of membrane markers in DCIS with or without adjacent breast cancer.

Feature	pure DCIS N (%)	DCIS + invasive N (%)	p-value
IGF1-R			
Positive	15 (68.2)	33 (56.9)	0.358
Negative	7 (31.8)	25 (43.1)	
HER2			
Positive	5 (21.7)	20 (32.8)	0.323
Negative	18 (78.3)	41 (67.2)	
EGFR			
Positive	7 (30.4)	7 (12.1)	<b>0.049</b>
Negative	16 (69.6)	51 (87.9)	
MET			
Positive	5 (21.7)	11 (18.3)	0.725
Negative	18 (78.3)	49 (81.73)	
CD44v6			
Positive	18 (78.3)	42 (72.4)	0.588
Negative	5 (21.7)	16 (27.6)	
GLUT1			
Positive	13 (56.5)	40 (69.0)	0.288
Negative	10 (43.5)	18 (31.0)	
CAXII			
Positive	5 (21.7)	16 (28.6)	0.523
Negative	18 (78.3)	40 (71.4)	
Mammaglobin			
Positive	4 (18.2)	9 (16.1)	0.822
Negative	18 (81.8)	47 (83.9)	



Furthermore, expression of HER2 and EGFR was correlated with high grade DCIS ( $p < 0.001$  and  $p = 0.001$ , respectively), whereas expression of CAXII was more frequently observed in low grade DCIS ( $p = 0.014$ ), as shown in Table 3. Although MET expression was less frequent in grade 1 DCIS compared to grade 2 or 3, this was not statistically significant. Expression of the other membrane markers in DCIS did not correlate with grade.

**Table 3.** Expression of membrane markers in DCIS in relation to grade of DCIS.

Feature	DCIS grade			p-value
	1 N (%)	2 N (%)	3 N (%)	
IGF1-R				
Positive	9 (75.0)	20 (64.5)	19 (52.8)	
Negative	3 (25.0)	11 (35.5)	17 (47.2)	0.339
HER2				
Positive	0 (0.0)	4 (12.9)	19 (48.7)	
Negative	12 (100)	27 (87.1)	20 (51.3)	<b>&lt;0.001</b>
EGFR				
Positive	0 (0.0)	1 (3.3)	13 (34.2)	
Negative	12 (100)	29 (96.7)	25 (65.8)	<b>0.001</b>
MET				
Positive	1 (8.3)	6 (20.0)	9 (23.1)	
Negative	11 (91.7)	24 (80.0)	30 (76.9)	0.533
GLUT1				
Positive	7 (58.3)	21 (70.0)	25 (65.8)	
Negative	5 (41.7)	9 (30.0)	13 (34.2)	0.768
CD44v6				
Positive	7 (58.3)	26 (83.9)	27 (73.0)	
Negative	5 (41.7)	5 (16.1)	10 (27.0)	0.206
CAXII				
Positive	4 (36.4)	12 (41.4)	5 (13.2)	
Negative	7 (63.6)	17 (58.6)	33 (86.8)	<b>0.027</b>
Mammaglobin				
Positive	1 (9.1)	5 (17.2)	7 (18.9)	
Negative	10 (90.9)	24 (82.8)	30 (81.1)	0.745

#### *Sensitivity of a panel of molecular markers for imaging of DCIS*

From the presented results, it became clear that expression of single membrane markers in DCIS is too infrequent to be suitable as a general target for molecular imaging. Only a panel of membrane-bound markers would be capable to obtain sufficient sensitivity (or detection rate) for imaging of DCIS by molecular imaging strategies. The panel of tumor-specific markers, consisting of GLUT1, EGFR, HER2, and IGF1-R, was positive in 90.2% of DCIS cases. Addition of MET did not increase the sensitivity. When less tumor-specific markers were included, only CD44v6 increased the sensitivity to 96.3% of DCIS cases.

The panel of membrane markers had a similar sensitivity for pure DCIS and DCIS with synchronous breast cancer, 96.6% vs. 95% respectively (Figure 1A). Inclusion of CD44v6 resulted that the sensitivity was not dependent on grade of the DCIS (Figure 1B). However, 92% of grade 3 invasive breast cancers was positive compared to 80% for grade 1/2 breast cancers for the panel of markers, which was in line with our previous results [17].

*Expression of membrane markers in DCIS compared to synchronous breast cancer*

As shown in Table 4, expression of the less tumor-specific markers Mammaglobin and CD44v6 was similar in DCIS and invasive breast cancer in 71.4% and 63.1% of cases, respectively. Lack of EGFR, MET, HER2 expression in both invasive breast cancer and DCIS was observed in 81.0%, 77.6%, and 66.7% of cases, respectively. However, in 30 cases (52.6%) the invasive breast cancer was negative for IGF1-R whereas the DCIS was positive. Similar results were obtained for GLUT1 and CAXII: in 62.5% of GLUT1 positive DCIS there was no expression in the invasive breast cancer, and for CAXII this was always the case. A panel of GLUT1, EGFR, CD44v6, IGF1-R, and HER2 was in 84.2% of cases positive for both DCIS and invasive breast cancer. Only in 1.8% of cases the DCIS and in 14.0% of cases the invasive cancer was negative for the markers in the panel.

**Table 4.** Comparison of expression of membrane markers in DCIS and adjacent invasive cancer.

Invasive cancer	DCIS	
	Positive N (%)	Negative N (%)
IGF1-R		
Positive	2 (3.5)	4 (7.0)
Negative	30 (52.6)	21 (36.9)
HER2		
Positive	13 (21.7)	0 (0.0)
Negative	7 (11.6)	40 (66.7)
EGFR		
Positive	3 (5.2)	4 (6.9)
Negative	4 (6.9)	47 (81.0)
MET		
Positive	2 (3.4)	3 (5.2)
Negative	8 (13.8)	45 (77.6)
CD44v6		
Positive	29 (50.8)	9 (15.8)
Negative	12 (21.1)	7 (12.3)
GLUT1		
Positive	15 (25.9)	4 (6.9)
Negative	25 (43.1)	14 (24.1)
CAXII		
Positive	0 (0.0)	2 (3.6)
Negative	16 (28.6)	38 (67.8)
Mammaglobin		
Positive	3 (5.3)	10 (17.9)
Negative	6 (10.7)	37 (66.1)

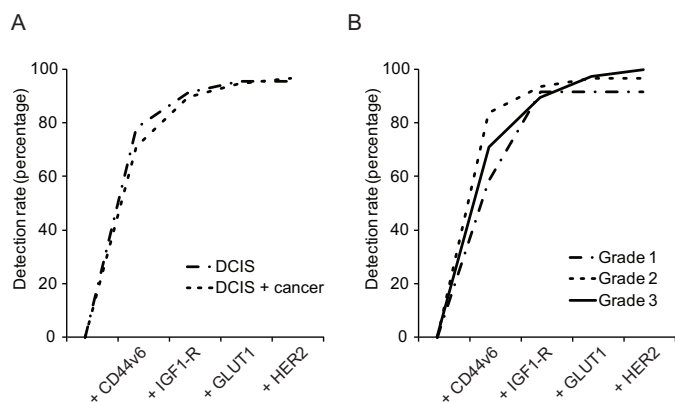


**Figure 1. Sensitivity of a panel of membrane markers for molecular imaging of DCIS.** Cumulative detection rate with addition of each marker was calculated by the fraction of positive cases over the total population, taking into account that DCIS can express multiple markers. (A) Detection rate of DCIS with and without adjacent invasive breast cancer using a previously described panel of membrane-bound markers for imaging of invasive breast cancer. (B) The detection rate of the panel in relation to clinicopathological features of DCIS.

## Discussion

The aim of this study was to identify a panel of membrane bound targets for molecular imaging of DCIS. To this end, we stained tissue microarrays containing 87 DCIS cases by immunohistochemistry of which 63 cases had adjacent invasive breast cancer.

The most frequently expressed tumor-specific marker was GLUT1 in 60.9% of DCIS cases, followed by IGF1-R in 55.2% HER2 in 28.7%, MET in 18.4%, EGFR in 16.1% of DCIS cases. The less tumor-specific markers CD44v6, CAXII, and Mammaglobin were expressed in 69.0%, 24.1% and 14.9% of DCIS cases, respectively. Compared with invasive breast cancer, expression of markers was higher in DCIS, and there was no difference in marker expression between pure DCIS and DCIS with adjacent invasive breast cancer. Therefore, the selected targets do not seem to be suitable for discriminating DCIS with and without a progression risk towards invasive breast cancer. Compared with previous studies describing HER2 and EGFR expression in DCIS [9-14], our results are on the lower end of what has been described, potentially due to the applied strict cut-offs for positivity or to only scoring membranous staining.

Because none of the markers was ultimately sensitive in detecting DCIS when used as single targets for molecular imaging, a combination of markers is needed to arrive at a clinically desirable detection sensitivity. A panel consisting of CD44v6, GLUT1, HER2, and IGF1-R was positive in 96% of DCIS lesions, which is higher than we previously achieved in invasive breast cancer [17]. This means that development of molecular tracers for optimal imaging of DCIS should be directed towards these targets. In cases with synchronous invasive breast cancer and DCIS, large differences in GLUT1, CAXII and IGF1-R expression were found. This might be explained by the focal expression of GLUT1 in invasive breast cancer that can be easily missed during construction of a TMA. In case of IGF1-R and CAXII, other studies showed that IGF1-R and CAXII expression was correlated to expression of ER $\alpha$  [14, 27]. Nevertheless, patients in our cohort with luminal-type breast cancer expressed rarely IGF1-R or CAXII, while expression of IGF1-R and CAXII in DCIS was not differently distributed among the molecular types of breast cancer.

In conclusion, we found that expression of membrane targets in DCIS is generally higher than in adjacent invasive breast cancer. Like for invasive breast cancer, single membrane proteins are still too infrequently expressed to serve as a single imaging target for detection of DCIS, and thus a panel of markers is required. A panel consisting of IGF1-R, CD44v6, GLUT1, HER2, was positive in 96% of DCIS lesions. Addition of EGFR to this panel resulted in a comparable sensitivity for DCIS and adjacent invasive breast cancer. This implies that detection of DCIS and adjacent invasive breast cancer during breast conserving surgery should be possible with molecular imaging tracers targeting CD44v6, GLUT1, HER2, IGF1-R and EGFR.

## Acknowledgements

This work was supported by an unrestricted research grant of AEGON Inc. and by the MAMmary carcinoma MOlecular imaging for diagnostics and THERapeutics (MAMMOTH) project of the Dutch Center for Translational Molecular Medicine.

## References

1. Wong H, Lau S, Leung R, *et al.* Coexisting ductal carcinoma in situ independently predicts lower tumor aggressiveness in node-positive luminal breast cancer. *Med Oncol* 2011.
2. Frangioni JV. In vivo near-infrared fluorescence imaging. *Curr Opin Chem Biol* 2003; 7(5):626-34.
3. Frangioni JV. New technologies for human cancer imaging. *J Clin Oncol* 2008; 26(24):4012-21.
4. van Dam GM, Themelis G, Crane LM, *et al.* Intraoperative tumor-specific fluorescence imaging in ovarian cancer by folate receptor-alpha targeting: first in-human results. *Nat Med* 2011; 17(10):1315-9.
5. Hirche C, Murawa D, Mohr Z, Kneif S and Hunerbein M. ICG fluorescence-guided sentinel node biopsy for axillary nodal staging in breast cancer. *Breast Cancer Res Treat* 2010; 121(2):373-8.
6. Murawa D, Hirche C, Dresel S and Hunerbein M. Sentinel lymph node biopsy in breast cancer guided by indocyanine green fluorescence. *Br J Surg* 2009; 96(11):1289-94.
7. Pleijhuis RG, Langhout GC, Helfrich W, *et al.* Near-infrared fluorescence (NIRF) imaging in breast-conserving surgery: assessing intraoperative techniques in tissue-simulating breast phantoms. *Eur J Surg Oncol* 2011; 37(1):32-9.
8. Pleijhuis RG, Graafland M, de Vries J, *et al.* Obtaining adequate surgical margins in breast-conserving therapy for patients with early-stage breast cancer: current modalities and future directions. *Ann Surg Oncol* 2009; 16(10):2717-30.
9. Park K, Han S, Kim HJ, Kim J and Shin E. HER2 status in pure ductal carcinoma in situ and in the intraductal and invasive components of invasive ductal carcinoma determined by fluorescence in situ hybridization and immunohistochemistry. *Histopathology* 2006; 48(6):702-7.
10. Tamimi RM, Baer HJ, Marotti J, *et al.* Comparison of molecular phenotypes of ductal carcinoma in situ and invasive breast cancer. *Breast Cancer Res* 2008; 10(4):R67.
11. Bryan BB, Schnitt SJ and Collins LC. Ductal carcinoma in situ with basal-like phenotype: a possible precursor to invasive basal-like breast cancer. *Mod Pathol* 2006; 19(5):617-21.
12. Meijnen P, Peterse JL, Antonini N, Rutgers EJ and van de Vijver MJ. Immunohistochemical categorisation of ductal carcinoma in situ of the breast. *Br J Cancer* 2008; 98(1):137-42.
13. Dabbs DJ, Chivukula M, Carter G and Bhargava R. Basal phenotype of ductal carcinoma in situ: recognition and immunohistologic profile. *Mod Pathol* 2006; 19(11):1506-11.
14. Clark SE, Warwick J, Carpenter R, *et al.* Molecular subtyping of DCIS: heterogeneity of breast cancer reflected in pre-invasive disease. *Br J Cancer* 2011; 104(1):120-7.
15. Logullo AF, Nonogaki S, Pasini FS, *et al.* Concomitant expression of epithelial-mesenchymal transition biomarkers in breast ductal carcinoma: association with progression. *Oncol Rep* 2010; 23(2):313-20.
16. Lindemann K, Resau J, Nahrig J, *et al.* Differential expression of c-Met, its ligand HGF/SF and HER2/neu in DCIS and adjacent normal breast tissue. *Histopathology* 2007; 51(1):54-62.
17. Happerfield LC, Miles DW, Barnes DM, *et al.* The localization of the insulin-like growth factor receptor 1 (IGFR-1) in benign and malignant breast tissue. *J Pathol* 1997; 183(4):412-7.
18. Wykoff CC, Beasley N, Watson PH, *et al.* Expression of the hypoxia-inducible and tumor-associated carbonic anhydrases in ductal carcinoma in situ of the breast. *Am J Pathol* 2001; 158(3):1011-9.
19. Bos R, Zhong H, Hanrahan CF, *et al.* Levels of hypoxia-inducible factor-1 alpha during breast carcinogenesis. *J Natl Cancer Inst* 2001; 93(4):309-14.
20. Chen CL, Chu JS, Su WC, Huang SC and Lee WY. Hypoxia and metabolic phenotypes during breast carcinogenesis: expression of HIF-1alpha, GLUT1, and CAIX. *Virchows Arch* 2010; 457(1):53-61.
21. Schmidt M, Voelker HU, Kapp M, *et al.* Glycolytic phenotype in breast cancer: activation of Akt, up-regulation of GLUT1, TKTL1 and down-regulation of M2PK. *J Cancer Res Clin Oncol* 2010; 136(2):219-25.
22. Holland R, Peterse JL, Millis RR, *et al.* Ductal carcinoma in situ: a proposal for a new classification. *Semin Diagn Pathol* 1994; 11(3):167-80.
23. Elston CW and Ellis IO. Pathological prognostic factors in breast cancer. I. The value of histological grade in breast cancer: experience from a large study with long-term follow-up. *Histopathology* 1991; 19(5):403-10.
24. Packeisen J, Korsching E, Herbst H, Boecker W and Buerger H. Demystified...tissue microarray technology. *Mol Pathol* 2003; 56(4):198-204.
25. van Diest PJ. No consent should be needed for using leftover body material for scientific purposes. *For BMJ* 2002; 325(7365):648-51.
26. Vermeulen JF, van Brussel AS, van der Groep P, *et al.* Immunophenotyping invasive breast cancer: paving the road for molecular imaging. *BMC Cancer* 2012; 12(1):240.
27. Barnett DH, Sheng S, Charn TH, *et al.* Estrogen receptor regulation of carbonic anhydrase XII through a distal enhancer in breast cancer. *Cancer Res* 2008; 68(9):3505-15.

# Six

## **Near-infrared fluorescence molecular imaging of ductal carcinoma in situ with CD44v6-specific antibodies in mice: a preclinical study**

Jeroen F. Vermeulen<sup>1</sup>, Aram S.A. van Brussel<sup>1\*</sup>, Arthur Adams<sup>2\*</sup>, Willem P.Th.M. Mali<sup>2</sup>, Elsken van der Wall<sup>3</sup>, Paul J. van Diest<sup>1</sup>, Patrick W.B. Derksen<sup>1</sup>

<sup>1</sup> Department of Pathology, University Medical Center Utrecht, Utrecht, The Netherlands,

<sup>2</sup> Department of Radiology, University Medical Center Utrecht, Utrecht, The Netherlands,

<sup>3</sup> Division of Internal Medicine and Dermatology, University Medical Center Utrecht, Utrecht, The Netherlands

\* These authors contributed equally to this study

***Submitted***

## Abstract

**Introduction:** Development of a molecular imaging technique using tracers specific for ductal carcinoma *in situ* (DCIS) is required to improve visualization and localization of DCIS during surgery. As CD44v6 is frequently expressed in DCIS, we used near-infrared fluorescently labeled CD44v6-targeting antibodies for detection of DCIS.

**Methods:** Mice bearing orthotopically transplanted CD44v6-positive MCF10DCIS DCIS-like tumors and CD44v6-negative MDA-MB-231 control tumors, were intravenously injected with IRDye800CW conjugated to CD44v6-specific antibodies or control IgGs. Non-invasive imaging was performed for eight days post-injection, followed by intra-operative imaging. Antibody accumulation and intra-tumor distribution were examined.

**Results:** Maximum accumulation of CD44v6-specific antibodies was obtained 24h post-injection. Maximum tumor-to-background ratio for MCF10DCIS tumors was  $4.5 \pm 0.2$ , compared to  $1.4 \pm 0.1$  (control tumors,  $p=0.006$ ), and  $1.7 \pm 0.1$  (control IgG,  $p=0.014$ ), eight days post-injection. *Ex vivo*, tumor-to-background ratios were comparable to those obtained by intra-operative imaging.

**Conclusions:** We show applicability of non-invasive and intra-operative optical imaging of DCIS-like lesions *in vivo* using CD44v6-specific antibodies.



## Introduction

Molecular imaging of cell surface markers, e.g. growth factor receptors, hypoxia markers and adhesion molecules, has become an important field for imaging of cancer for diagnosis, assessment of therapy response, or for tumor delineation during surgical resection [1-4]. Achieving radical excision during breast conserving surgery for ductal carcinoma *in situ* (DCIS), and diffusely growing or small (T1) breast cancers is challenging, since these lesions are often not palpable. Molecular imaging with near-infrared fluorescent (NIRF) tracers holds promise when applied as a tool for image-guided surgery. First, detection of lesions can be highly sensitive and specific by using targeted tracers. Second, due to its physical properties NIRF can penetrate several millimeters in tissue, allowing non-invasive visualization of tumors [5]. Third, no ionizing radiation is used, limiting the need for protective measures. Fourth, the spectral properties (emission wavelengths between 700-900 nm) of the fluorescent tracers result in low background (auto)fluorescence [6].

Previously, we examined the expression of membrane markers in breast cancer to identify the most sensitive and specific molecular markers for optical imaging. The expression rate of tumor-specific markers did not exceed 20% of all breast cancers, whereas tumor markers expressed by normal breast epithelium (i.e. with a lower tumor specificity), were expressed in the majority of breast cancers. CD44v6 was expressed in 64% of breast cancers and thereby the most frequently expressed marker achieving a 3-fold tumor-to-normal ratio (that was predefined as sufficient for molecular imaging). Therefore, CD44v6 was considered the most promising tumor marker for molecular imaging of breast cancer [7].

The glycoprotein CD44 is a hyaluronic acid-binding adhesion molecule that facilitates binding of epithelial cells to the extracellular matrix (ECM). Due to alternative splicing CD44 is expressed as multiple isoforms that structurally and functionally differ as a result of changes in the extracellular stem region of the receptor [8, 9]. The standard CD44 variant (CD44s) is widely expressed in epithelial tissues and has been used to mark stem cells, but the expression of these variants is mainly restricted to neoplastic lesions [8-10]. Although the most widely studied variant of CD44, CD44v6, is abundantly expressed in invasive cancers, benign tumors do not express the v6 isoform [10-13]. Despite the high expression in invasive cancer, the relation between aggressiveness, invasiveness and CD44v6 expression is not clear [14]. A possible role for CD44v6 in tumor progression may lie in its function as co-receptor and scaffolding platform. Since CD44v6 contains a heparin sulfate side chain able to bind and present glycosylated growth factors to their cognate receptors, it thereby potentiates receptor tyrosine kinase signaling [15-19].

In studies investigating radioactively-labeled antibodies targeting CD44v6 for detection of head and neck cancer, it was shown that administration was safe and allowed specific tumor detection [20, 21]. Furthermore, imaging of breast cancer with CD44v6 antibodies was only described by one group for detection of T1 cancers with SPECT and showed that 66% of breast cancers could be correctly assigned [22].

To study the applicability of NIRF-labeled antibodies for non-invasive and intra-operative optical imaging of DCIS *in vivo*, we examined NIRF-labeled CD44v6-specific antibodies in a transplantation-based model of DCIS. Our data indicate that detection of pre-invasive lesions with NIRF-labeled antibodies is feasible and not hampered by limited vascularization.

## Methods

### *Cell culture, virus generation and cell transduction*

MCF10DCIS.com cells (further referred to as MCF10DCIS) were obtained from Asterand Inc. (Detroit, MI, USA), and cultured according to supplier's guidelines. MDA-MB-231/Luc<sup>+</sup> [23] (gift of G. van der Pluijm, Leiden University Medical Center, Leiden, The Netherlands) were cultured in DMEM containing 10% FCS supplemented with 100 IU/ml penicillin, and 100 µg/ml streptomycin. Both cell lines were confirmed negative for ERα, PR and HER2. CD44v6 and E-cadherin were expressed in MCF10DCIS only. All cell lines were validated by STR-analysis and routinely checked for *Mycoplasma* infection. All lines were consistently *Mycoplasma* free.

To generate luciferase expressing MCF10DCIS cells, pLV-CMV-Luc2-IRES-GFP vector (gift from A. Martens, UMC Utrecht, The Netherlands) was introduced by lentiviral transduction as described before [24]. Transduction efficiency was 100% (determined by expression of GFP) after two rounds of infection.

### *Antibody production, fluorescent labeling and binding affinity measurements after labeling*

The sequences of the variable domain of the heavy and light chains of humanized VFF18, directed against CD44v6, were obtained from the patent WO2008/060367. DNA of the variable domain fragments was synthesized by Geneart (LifeTechnologies, Bleiswijk, The Netherlands). Variable domains were cloned into human IgG expression constructs and produced by U-protein Express (Utrecht, The Netherlands). IgG purification was performed by chromatography on Proteinase A columns and eluted with sodium citrate (pH 3.6) followed by desalting and buffer exchange to PBS using the automated AKTA express purifier (GE Healthcare, Hoevelaken, The Netherlands). Protein concentration was determined using a Nanodrop spectrophotometer (Thermo Fischer Scientific, Breda, The Netherlands) and purity was confirmed by Coomassie stain of a SDS-PAGE gel. Human IgG from serum was obtained from Sigma-Aldrich (I4506, Zwijndrecht, The Netherlands) and served as a negative control (further referred to as control IgG). Labeling of IgG antibodies was performed as described before [25]. The NIRF dye IRDye800CW, purchased as an N-hydroxysuccinimide (NHS) ester (LI-COR Biosciences, Lincoln, NE, USA), was incubated in a 4-fold molar excess of dye to IgG for 2h at room temperature. After conjugation, free dye was removed using Zebra Spin desalting columns (Thermo Fisher Scientific). Dye to protein ratio was determined with:  $IR/protein = (A_{774} / \epsilon_{IRDye\ 800CW}) / (A_{280} - (0.03 \times A_{774}) / \epsilon_{protein})$ , where the molar extinction coefficient of IRDye800CW is 240,000 M<sup>-1</sup> cm<sup>-1</sup> and the molar extinction coefficient for IgG is 210,000 M<sup>-1</sup> cm<sup>-1</sup>.

For affinity measurements 15,000 MDA-MB-231 and MCF10DCIS cells were seeded in 96-well plates (Thermo Fischer Scientific) and allowed to adhere overnight. Next, medium was aspirated, cells were blocked with 4% Marvel (skimmed milk powder) in PBS, and cells were incubated for 2h at 4°C with IRDye800CW-labeled IgG in 2% Marvel in PBS in the dark. Cells were washed three times with PBS, and bound IgG was detected using an Odyssey Imaging System (LI-COR) at 800nm. The dissociation constant (Kd) was derived from the concentration of IgG at which half the intensity of Bmax was found. Graphpad Prism 5 software (Non linear regression - one site specific binding) was used for computational analyses.

### *Mouse studies*

Five-week old female SCID Beige (C.B-17/lcrHsd-Prkdc<sup>scid</sup>Lyst<sup>bg</sup>) immunodeficient mice (Harlan Laboratories, Horst, The Netherlands) were orthotopically transplanted as described before [24], with some modifications. Approximately  $4 \times 10^4$  luciferase-expressing MCF10DCIS and  $1 \times 10^5$  luciferase expressing MDA-MB-231 cells were injected using a 10 $\mu$ l Hamilton syringe in the 4<sup>th</sup> (inguinal) and 3<sup>rd</sup> (thoracic) mammary fat pad, respectively. Tumor growth was monitored on a weekly basis using bioluminescence imaging (Photon-Imager, BiospaceLabs, Paris, France). Upon development of palpable tumors (typically 2-3 mm diameter), mice were intravenously injected in the tail vein with 100  $\mu$ g fluorescently labeled IgG.

All animal experiments were approved by the Utrecht University Animal Experimental Committee (DEC-Utrecht no. 2011.III.03.027).

### *Imaging and image analysis*

Probe distribution was visualized and quantified based on the fluorescent signal from the labeled CD44v6 and control IgGs. A real-time intra-operative multispectral fluorescence imaging system, developed by the group of Ntziachristos et al, was used for the measurements [26]. In summary, the system consists of a charge-coupled digital (CCD) iXon3 DU888 camera (Andor Technology, Belfast, UK) cooled at -80°C for sensitive fluorescence signal detection, and a continuous wave laser with an excitation wavelength of 750 nm for optimal excitation of IRDye800CW. The following imaging parameters were used: distance between object and lens 30-32 cm, zoom 43%, focus 0%, iris 93%. The exposure time for each image was set at 150 ms and gain at 1000. The field of view for each image was 125 x 125 mm, corresponding to a resolution of 0.25 mm per pixel. Static images were acquired every 30 minutes in the first two hours post-injection and subsequently 3h, 4h and 8h post-injection. After the first day images were acquired daily until 8 days post-injection. After image acquisition, a region of interest (ROI) was drawn around each tumor, and the average signal intensity was determined. For each time point, the same size of the ROI was

used. Also, an equal sized ROI was drawn in a representative region without tumor tissue to determine background fluorescence levels and to be able to calculate tumor to background ratios. All values are displayed as mean  $\pm$  SEM.

#### *Biodistribution of IRDye800Cw labeled antibodies*

One week post-injection of the CD44v6 or control IgGs, mice were sacrificed, organs were collected, weighted and snap frozen in liquid nitrogen and stored at  $-80^{\circ}\text{C}$ . Tissues and tumors were homogenized in RIPA buffer supplemented with protease inhibitors using a Tissuelyser II system (Qiagen, Venlo, The Netherlands). A dilution series of homogenized organs was made in order to measure the intensity in the linear range at 800 nm with the Odyssey Imager (Licor). The quantity of IRDye800CW was determined by intra- and extrapolation of the fluorescent value from a calibration curve that consisted of serial dilutions of the injected probe as described before [25,27].

#### *Immunohistochemistry*

Immediately after resection, the tumors were fixed in neutral buffered formalin, paraffin embedded and stored in the dark. Immunohistochemistry was performed on  $4\mu\text{m}$  thick sequential sections. Following deparaffination and rehydration, endogenous peroxidase activity was blocked for 15 min in buffer solution containing 0.3% hydrogen peroxide. The different antigen retrieval methods used were as follows: boiling for 20 min in 10mM citrate pH6.0 (CD44v6), Tris/EDTA pH9.0 (p63), or pepsin (1mg/ml) for 15 min at  $37^{\circ}\text{C}$  (human IgG). A cooling period of 30 minutes preceded the primary antibody incubation: p63 (clone 4A4, Neomarkers) 1:400, human IgG specific for gamma chains (A0423, DAKO, Glostrup, Denmark) 1:500, or CD44v6 (clone VFF18, BMS125, Bender MedSystems, Vienna, Austria) 1:500. The signal was amplified using Brightvision poly-HRP anti-mouse, rabbit, rat (DPVO-HRP, Immunologic, Duiven, The Netherlands), and developed with diaminobenzidine, followed by counterstaining with haematoxylin, dehydration in alcohol, and mounting. Appropriate negative and positive controls were used throughout. For detection of IRDye800CW, tumor slides were deparaffinized, mounted with Immu-mount (Thermo Fisher Scientific), and scanned using the Odyssey Imaging System.

#### *Statistics*

Statistical analysis was performed using IBM SPSS Statistics version 18.0 (SPSS Inc., Chicago, IL, USA). Comparison of tumor to background levels of injected probes was performed using Mann-Whitney U test. Wilcoxon Signed-Ranks test was performed to compare the fluorescent intensity of non-invasive with intra-operative imaging. P-values  $<0.05$  were considered to be statistically significant.

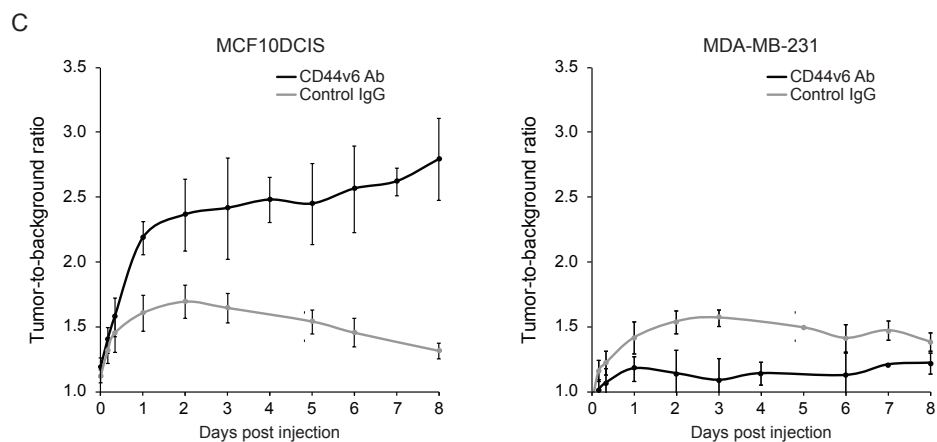
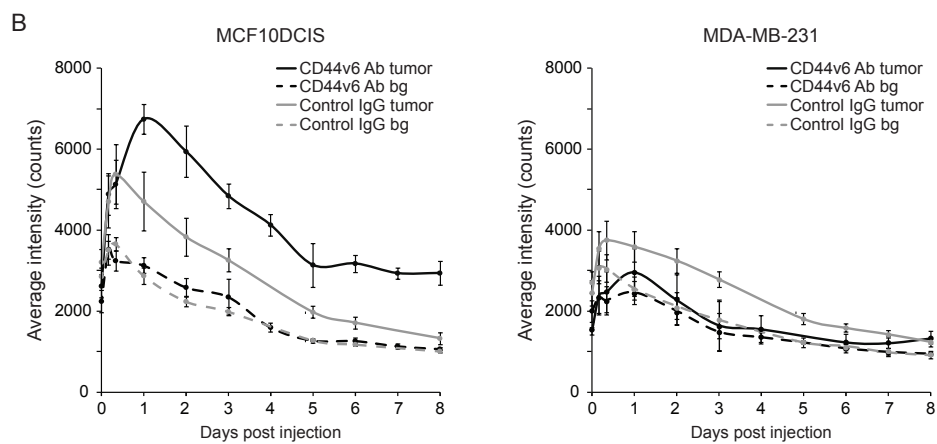
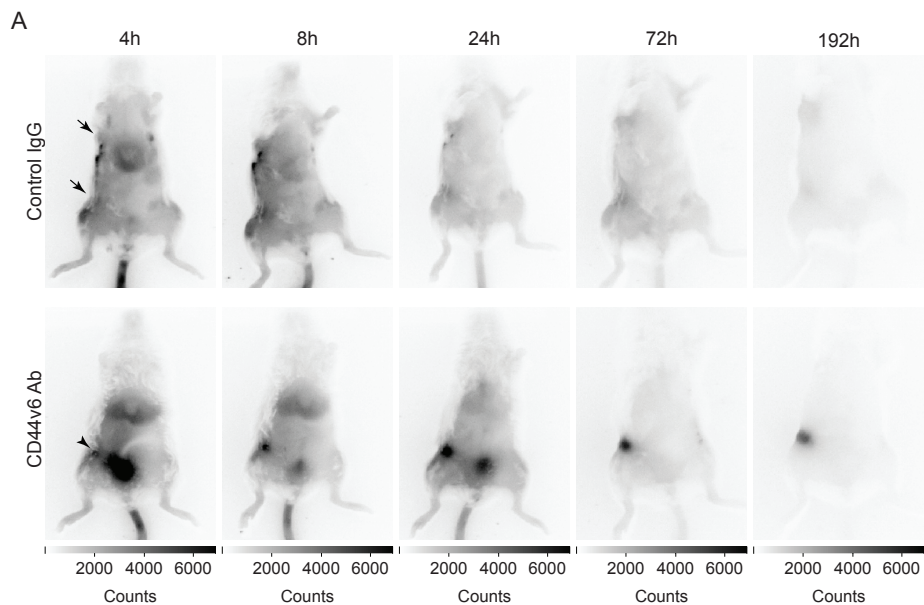
## Results

### *Characterization of CD44v6 antibodies for non-invasive imaging of breast cancer*

The potential of CD44v6-specific antibodies (further referred to as CD44v6 Ab) as tracer for optical imaging was examined in a model for pre-invasive breast cancer. Labeling efficiency, expressed as IRDye800CW-to-protein ratio, was 1.43 and 1.57 for CD44v6 Ab and human serum IgG (further referred to as control IgG), respectively. After purification, 5.6% free dye remained present, which was comparable to previous studies [25]. The apparent affinity (Kd) of labeled CD44v6 Ab was 10 nM and 17  $\mu$ M on MCF10DCIS (CD44v6 positive) and MDA-MB-231 (CD44v6 negative) cells, respectively. Control IgG had an apparent affinity of approximately 40 nM (MCF10DCIS), and 90 nM (MDA-MB-231), but with maximum binding (Bmax) 13 times smaller than CD44v6 Ab on MCF10DCIS cells.

Mice bearing MCF10DCIS and MDA-MB-231 tumors (used as a CD44v6 negative control) were intravenously injected with IRDye800CW-conjugated CD44v6 Ab or control IgG. Accumulation of CD44v6 Ab in the MCF10DCIS tumor became detectable 4h post-injection, whereas control IgG did not (Figure 1A). A clear signal of the MCF10DCIS tumor was obtained from three days onwards, due to accumulation of the tracer in the tumor and decreased background signal from circulating tracer. In contrast, accumulation of free IRDye800CW, was not observed (data not shown), while levels of the control IgG were similar in MCF10DCIS versus MDA-MB-231 tumors (Figure 1A). The maximal fluorescence intensity in the MCF10DCIS tumor was reached after 8h (control IgG) and 24h (CD44v6 Ab), and decreased to background levels in eight days (control IgG) or stabilized after five days (CD44v6 Ab), (Figure 1B). These differences are most likely caused by dissimilar pharmacokinetics of the antibodies used. Fluorescence intensity of control IgG and CD44v6 Ab in the MDA-MB-231 control tumor was lower than the MCF10DCIS tumor, while the background levels and the decrease in fluorescent signal was comparable (Figure 1B). As a result, tumor-to-background ratio for CD44v6 Ab increased from  $2.41 \pm 0.39$  three days post-injection to  $2.78 \pm 0.31$  eight days post-injection and tended to increase further in MCF10DCIS (Figure 1C). In contrast, tumor-to-background ratio of control IgG declined to  $1.31 \pm 0.06$  eight days post-injection and was significantly lower than CD44v6 Ab ( $p=0.004$ ) in the MCF10DCIS tumor.

**Figure 1. Non-invasive optical molecular imaging of breast cancers.** (A) Representative SCID Beige mice bearing orthotopically transplanted MCF10DCIS (inguinal) and MDA-MB-231 (thoracic) tumors. Mice were intravenously injected in the tail vein with CD44v6 Ab or control IgG. At 4h post-injection, tumor accumulation of CD44v6 Ab was observed in the MCF10DCIS tumors (arrowhead), whereas no accumulation of control IgG was observed in MCF10DCIS or MDA-MB-231 tumors (arrows). (B) Fluorescence intensity of MCF10DCIS tumors (left panel) or MDA-MB-231 tumors (right panel) and background of mice injected with CD44v6 Ab or control IgG over time. Data are displayed as mean  $\pm$  SEM (n=6). (bg = background). (C) Tumor-to-background ratio of CD44v6 Ab and control IgG in MCF10DCIS and MDA-MB-231 tumors. Data are displayed as mean  $\pm$  SEM (n=6).



The tumor-to-background ratio of CD44v6 Ab in the MDA-MB-231 tumor was comparable to control IgG ( $1.41 \pm 0.11$ ,  $p=0.201$ ) and significantly lower than in the MCF10DCIS tumor ( $p=0.011$ ).

Because the antibody levels eight days post-injection were relatively low and positioning of the mice and localization of the tumor could influence the accuracy of the fluorescent signal levels obtained (and thus the tumor-to-background ratio), we determined the coefficient of variation of the optical imaging technique. Four mice were imaged four times each, with readjustment of the imaging device, repositioning of the mice, and re-assessing the volume and location of the ROI. The coefficient of variation was 6.1%, supporting the reproducibility of the optical imaging technique.

#### *Performance of the intra-operative camera system for non-invasive imaging*

Since the camera system used is intended for intra-operative image-guided surgery rather than for non-invasive imaging and quantification of tracer accumulation, we examined whether the performance differed between these applications. Non-invasive imaging was performed on day 8, directly followed by intra-operative imaging, using identical imaging parameters. Specific accumulation of the CD44v6 Ab was observed in the MCF10DCIS tumor (Figure 2A). As expected we neither detected accumulation of the CD44v6 Ab in the MDA-MB-231 tumor, nor was control IgG observed in the MCF10DCIS tumor. Tumor intensity of MCF10DCIS and MDA-MB-231 tumors compared to the surrounding tissue (skin and abdomen) was higher, independent of the injected IgG (Figure 2A and B), most likely due to probe retention caused by enhanced tumor vascularization. MCF10DCIS tumor signals were significantly higher in CD44v6 Ab injected mice intra-operatively, compared to the MDA-MB-231 tumors in the same mouse and compared to the MCF10DCIS tumors in mice injected with control IgG ( $p=0.014$  and  $p=0.006$ , respectively; Figure 2B). Accordingly, the resulting tumor-to-background ratios were significantly higher for CD44v6 Ab in MCF10DCIS vs. MDA-MB-231 ( $4.5 \pm 0.18$  vs.  $1.4 \pm 0.11$ ,  $p=0.006$ ) and for CD44v6 Ab vs. control IgG in the MCF10DCIS tumor ( $4.5 \pm 0.18$  vs.  $1.7 \pm 0.05$ ,  $p=0.014$ ), indicating specific accumulation of CD44v6 Ab in the MCF10DCIS tumors (Figure 2C).

To test the performance of the imaging system, we quantified all MCF10DCIS tumors using non-invasive and intra-operative imaging after CD44v6 Ab treatment. Compared to intra-operative imaging, fluorescence intensity of MCF10DCIS lesions with non-invasive imaging were significantly lower in CD44v6 Ab injected (5083 vs. 2900 counts,  $p=0.043$ ), and in IgG injected mice (2135 vs. 1537 counts,  $p=0.028$ ). In conclusion, NIRF intra-operative imaging yields a superior tumor-to-background ratio compared to non-invasive imaging.



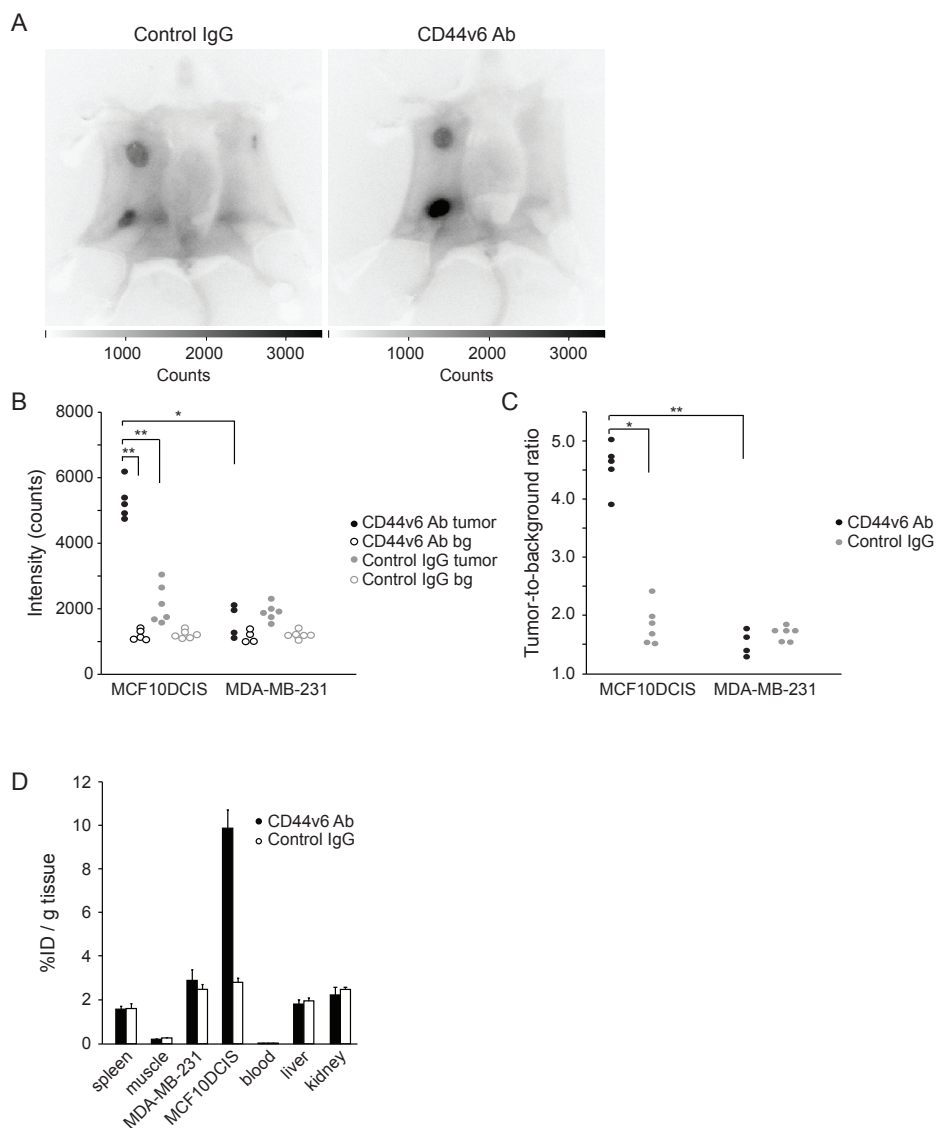


**Figure 2. Intra-operative imaging of breast cancers.** (A) Representative fluorescence images of mice bearing MDA-MB-231 tumors and MCF10DCIS tumors 8 days post-injection with control IgG and CD44v6 Ab. Clear accumulation of CD44v6 Ab was observed in the MCF10DCIS tumor compared to control IgG. Higher signals in both tumors compared to the background were found, independent of injected antibody due to enhanced perfusion and retention of the tumor. (B) Fluorescence intensity of MCF10DCIS, MDA-MB-231 tumors and the corresponding background (bg) in individual mice. (\* =  $p < 0.05$ ; \*\* =  $p < 0.01$ ). (C) Tumor-to-background ratio of CD44v6 Ab and control IgG in MCF10DCIS and MDA-MB-231 tumors displayed for individual mice (\* =  $p < 0.05$ ; \*\* =  $p < 0.01$ ). (D) Biodistribution of CD44v6 Ab and control IgG 8 days post-injection. Tissue levels are expressed as percentage injected dose per gram tissue (%ID/g) as mean  $\pm$  SEM ( $n=6$ ).

### *Biodistribution of NIRF-labeled antibodies*

To quantitate the tumor uptake of CD44v6 Ab and control IgG, liver, kidneys, blood, spleen and muscle of individual mice were collected directly after intra-operative imaging. Eight days post-injection, the levels of CD44v6 Ab and control IgG in blood were very low (2‰ of the injected dose (ID) per gram tissue) (Figure 2D). The level of CD44v6 Ab and control IgG in muscle was low (approximately 0.2% ID/g tissue), while  $9.9\% \pm 0.8\%$  ID/g of the CD44v6 Ab, and  $2.8\% \pm 0.2\%$  ID/g tissue of the control IgG was present in the MCF10DCIS tumor. The percentage of the injected dose per gram tissue of the CD44v6 Ab or the control IgG in the MDA-MB-231 tumor ( $2.9\% \pm 0.5\%$  ID/g vs.  $2.5\% \pm 0.3\%$  ID/g, respectively) was slightly higher compared to spleen, kidney, and liver. Furthermore, no difference was found between the injected dose per gram tissue of control IgG in the MDA-MB-231 and MCF10DCIS tumor (Figure 2D). In conclusion, our data indicate that NIRF signals measured with intra-operative imaging (8 days post-injection) reflect the actual levels of NIRF tracer in the tumors and can be used as a surrogate measure for biodistribution.

### *Heterogeneous CD44v6 antibody uptake in pre-invasive breast cancer lesions*

As shown in Figure 3A, no accumulation of control IgG was observed in both MDA-MB-231 and MCF10DCIS tumors, while CD44v6 Ab specifically accumulated in the MCF10DCIS lesion, which is in line with the imaging results. Similar to human DCIS, p63 staining of the myoepithelial cells surrounding the MCF10DCIS lesion confirmed the non-invasive phenotype of the MCF10DCIS lesion. Staining for the injected tracers by immunohistochemistry revealed a clear difference in tumor distribution; low levels of control IgG were present in the stroma surrounding the tumor cells (Figure 3B), while CD44v6 Ab was exclusively bound to the epithelial cells of the MCF10DCIS lesion and correlated with CD44v6 expression. Furthermore, staining suggested that tumor penetration of CD44v6 Ab was limited to the first two cell layers aligning blood vessels or stroma (arrow, Figure 3B). These results show that tumor penetration of antibodies is limited and resulted in heterogeneous tumor distribution. Further, detection of DCIS-like lesions using NIRF tracers was not hampered by the non-invasive phenotype of the DCIS, suggesting that molecular imaging is suitable for detection of DCIS *in vivo*.

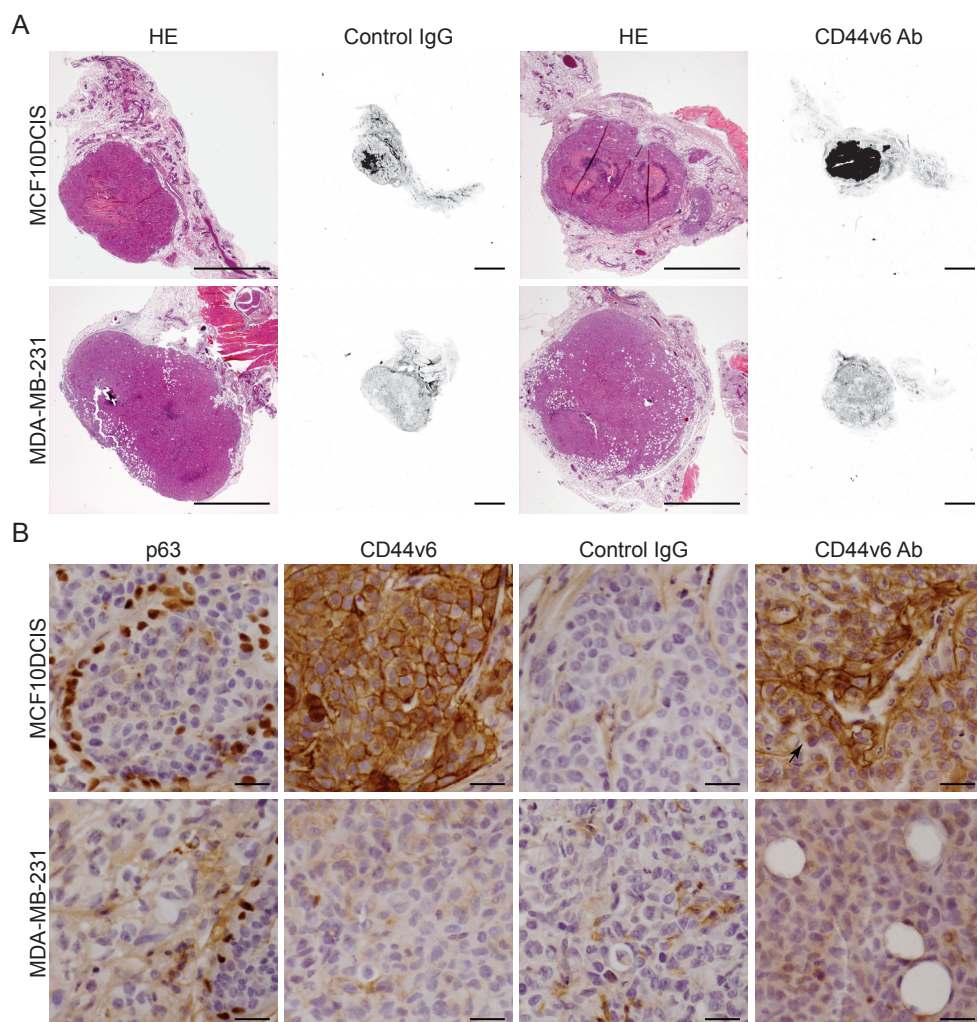


**Figure 3. Tumor-specific accumulation of fluorescent tracers in breast cancer.** (A) Representative sections of MDA-MB-231 tumors and MCF10DCIS tumor of mice injected with control IgG or CD44v6 Ab. Haematoxylin and eosin (HE) stained sections show the non-invasive character of the MCF10DCIS tumor maintaining the preexisting ductal structures intact, whereas the MDA-MB-231 tumors are invading in the mammary fat pad. Accumulation of IRDye800CW-labeled antibodies was detected for CD44v6 Ab in the MCF10DCIS tumor (fluorescence in control IgG was caused by necrosis for unknown reasons). Scale bar equals 2 mm. (B) Immunohistochemical characterization of breast cancers and evaluation of intra-tumor distribution of injected antibodies. The non-invasive (DCIS) phenotype of MCF10DCIS lesions was shown by p63 staining of the myoepithelial cells surrounding the MCF10DCIS lesion, which was absent in the MDA-MB-231 tumor. CD44v6 was homogeneously expressed in the MCF10DCIS lesion, which correlated with tumor accumulation of injected CD44v6 Ab. In addition, no accumulation of control IgG was observed in the MCF10DCIS and MDA-MB-231 lesions, whereas CD44v6 Ab accumulation in MCF10DCIS lesions was mainly restricted to the first two cell layers aligning blood vessels or stroma (arrow). Scale bar equals 50  $\mu$ m.

## Discussion

There is increasing interest in molecular imaging of breast cancer. Multiple membrane markers, e.g. growth factor receptors and hypoxia-upregulated membrane markers, are currently investigated as candidates for molecular imaging of breast cancer [4]. We showed previously that CD44v6 might be required as tumor marker to achieve sufficient sensitivity for molecular imaging, since growth factor receptors and hypoxia-upregulated membrane markers alone are too infrequently expressed in breast cancer [7].

In the present study we show that optical imaging with IRDye800CW-labeled humanized antibodies directed to CD44v6 is feasible in a model of pre-invasive breast cancer. We could assess the specific uptake of the tracer *in vivo* and demonstrate application of this tracer for intra-operative surgery purposes. Tumor accumulation of IRDye800CW-labeled CD44v6 antibodies in our study ( $9.9\% \pm 0.8\%$  ID/g) was comparable to studies using radio-labeled CD44v6 antibodies, which reported a tumor accumulation of 12.9%-15.4% ID/g in human or 15.3% ID/g using A431 xenografts in mice [21, 28]. This indicates that biodistribution of IRDye800CW-labeled CD44v6-specific antibodies is comparable to radio-labeled CD44v6 antibodies, which was also recently shown for EGFR-specific antibodies [27]. In comparison with previous studies using Bevacizumab and Trastuzumab as tracers for optical imaging of breast cancer (tumor-to-background ratio's of  $1.93 \pm 0.40$  and  $2.92 \pm 0.29$  respectively) [29], the tumor-to-background ratios of CD44v6 Ab were higher after 6-8 days. Whether these differences were caused by differences in pharmacokinetics or related to target expression remains unclear. Furthermore, using a control IgG we were able to determine the contribution of perfusion/non-specific accumulation to the tumor-to-background ratio, which attributed as much as 50% to the tumor-to-background ratio in the first two days.

In the present study, non-invasive imaging underestimated fluorescence signal intensities of the tumors by approximately 50%, which might be caused by absorption of fluorescence signal by the skin and the subcutaneous and mammary fat. This directly affected the minimal tumor size we could detect, i.e. DCIS lesions of approximately 3 mm were detectable *in vivo*, while sub-millimeter DCIS lesions could be detected with intra-operative imaging. Therefore, non-invasive imaging of breast cancer may significantly underestimate the tumor size, tumor uptake and/or tumor-to-background ratios of injected tracers. More importantly, it might even falsify the conclusions drawn regarding the suitability of a tracer for molecular imaging. Given these potential disadvantages of optical imaging, detection of small breast cancer and *in situ* lesions in patients (e.g. when molecular imaging is applied for screening purposes) might become problematic due to limited excitation power of the laser, localization of the breast tumor, absorption by breast tissue/tumor, and size of the breast. Upcoming clinical trials with IRDye800CW conjugated antibodies will demonstrate the value

of molecular optical imaging for screening purposes.

We showed previously that within normal breast epithelium myoepithelial cells express low levels of CD44v6. Therefore the choice of CD44v6 as imaging target might result in increased background signal from normal breast epithelium and thereby diminished sensitivity and specificity for detection of breast cancer or DCIS lesions. In our preclinical model, the normal (mouse) mammary epithelium did not express CD44v6, and thus did not influence the specificity and sensitivity of detection. Although the uptake of the normal human breast tissue was comparable to that of tumors, Koppe et al. showed that while SPECT imaging of T1-tumors using CD44v6 antibodies had sufficient sensitivity to detect the majority of breast cancers due to increased cellularity of the tumor tissue, the limited resolution of the camera was likely hampering the detection of the cancer in the remaining patients. In addition, when less than 20% of tumor cells were positive for CD44v6, SPECT imaging was not able to detect the lesion [22]. For optical imaging methods the influence of heterogeneous target expression on the tumor detection is not described, but our unpublished data reveal a similar pattern using optical imaging.

Another parameter attenuating imaging sensitivity was intra-tumor distribution of the tracers. We found that diffusion of IgGs from tumor-associated blood vessels was limited to the aligning first 2-3 cell layers of the lesion, probably due to size-limited diffusion. Tumor accumulation, expressed as injected dose per gram tissue of CD44v6 Ab after eight days, was not different from previous studies performed with Erbitux after 24h [25]. This suggests that maximum tumor accumulation is achieved one day post-injection, and that increased tumor-to-background ratios are solely achieved by clearance of circulating antibodies. Increasing tumor accumulation by size reduction of the tracers could enhance the sensitivity of optical imaging for small breast cancers and DCIS. In case of EGFR, improved tumor uptake and intra-tumor distribution was achieved by using VHHs (15kDa antibody fragments consisting of only the Vh domain of the heavy-chain-only antibodies from camelids). In the study of Oliveira et al. VHH-based tracers showed a maximum uptake after 2h resulting in homogeneous distribution, suggesting a better tumor penetration [25]. For detection of DCIS and other poorly vascularized lesions, application of VHHs and other small tumor-specific tracers for optical imaging might be the preferred option for optical imaging.

## Conclusion

Using CD44v6-specific antibodies we show that near-infrared optical molecular imaging has sufficient sensitivity for non-invasive and intra-operative imaging of DCIS lesions *in vivo*. This opens the way to clinical image-guided surgery trials in humans. In parallel, further improvements may be achieved by better tumor penetration through size reduction of tracers.

## Acknowledgements

We would like to thank G. van der Pluijm for providing the luciferase-expressing MDA-MB-231 cells, A. Martens for the pLV-CMV-LUC2-IRES-GFP vector. M. van Amersfoort is acknowledged for expert technical assistance with the mouse experiments. We are also indebted to the UMC Utrecht biobank for their support. This work was supported by an unrestricted research grant of AEGON Inc. and by the MAMmary carcinoma MOlecular imaging for diagnostics and THERapeutics (MAMMOTH) project of the Dutch Center for Translational Molecular Medicine.

## References

1. Stillebroer AB, Zegers CM, Boerman OC, *et al.* Dosimetric analysis of <sup>177</sup>Lu-cG250 radioimmunotherapy in renal cell carcinoma patients: correlation with myelotoxicity and pretherapeutic absorbed dose predictions based on <sup>111</sup>In-cG250 imaging. *J Nucl Med* 2012; 53(1):82-9.
2. Hirche C, Murawa D, Mohr Z, Kneif S and Hunerbein M. ICG fluorescence-guided sentinel node biopsy for axillary nodal staging in breast cancer. *Breast Cancer Res Treat* 2010; 121(2):373-8.
3. Murawa D, Hirche C, Dresel S and Hunerbein M. Sentinel lymph node biopsy in breast cancer guided by indocyanine green fluorescence. *Br J Surg* 2009; 96(11):1289-94.
4. Oude Munnink TH, Nagengast WB, Brouwers AH, *et al.* Molecular imaging of breast cancer. *Breast* 2009; 18 Suppl 3:S66-73.
5. Frangioni JV. New technologies for human cancer imaging. *J Clin Oncol* 2008; 26(24):4012-21.
6. Frangioni JV. In vivo near-infrared fluorescence imaging. *Curr Opin Chem Biol* 2003; 7(5):626-34.
7. Vermeulen JF, van Brussel AS, van der Groep P, *et al.* Immunophenotyping invasive breast cancer: paving the road for molecular imaging. *BMC Cancer* 2012; 12(1):240.
8. Fox SB, Fawcett J, Jackson DG, *et al.* Normal human tissues, in addition to some tumors, express multiple different CD44 isoforms. *Cancer Res* 1994; 54(16):4539-46.
9. Ponta H, Wainwright D and Herrlich P. The CD44 protein family. *Int J Biochem Cell Biol* 1998; 30(3):299-305.
10. Afify A, McNeil MA, Braggin J, Bailey H and Paulino AF. Expression of CD44s, CD44v6, and hyaluronan across the spectrum of normal-hyperplasia-carcinoma in breast. *Appl Immunohistochem Mol Morphol* 2008; 16(2):121-7.
11. Foekens JA, Dall P, Klijn JG, *et al.* Prognostic value of CD44 variant expression in primary breast cancer. *Int J Cancer* 1999; 84(3):209-15.
12. Schumacher U, Horny HP, Horst HA, Herrlich P and Kaiserling E. A CD44 variant exon 6 epitope as a prognostic indicator in breast cancer. *Eur J Surg Oncol* 1996; 22(3):259-61.
13. Morris SF, O'Hanlon DM, McLaughlin R, *et al.* The prognostic significance of CD44s and CD44v6 expression in stage two breast carcinoma: an immunohistochemical study. *Eur J Surg Oncol* 2001; 27(6):527-31.
14. Heider KH, Kuthan H, Stehle G and Munzert G. CD44v6: a target for antibody-based cancer therapy. *Cancer Immunol Immunother* 2004; 53(7):567-79.
15. Orian-Rousseau V, Chen L, Sleeman JP, Herrlich P and Ponta H. CD44 is required for two consecutive steps in HGF/c-Met signaling. *Genes Dev* 2002; 16(23):3074-86.
16. Wobus M, Kuns R, Sheyn I, *et al.* Endometrial carcinoma cells are nonpermissive for CD44-erbB2 interactions. *Appl Immunohistochem Mol Morphol* 2002; 10(3):242-6.
17. Kaufmann M, Heider KH, Sinn HP, *et al.* CD44 isoforms in prognosis of breast cancer. *Lancet* 1995; 346(8973):502.
18. Marhaba R and Zoller M. CD44 in cancer progression: adhesion, migration and growth regulation. *J Mol Histol* 2004; 35(3):211-31.
19. van der Voort R, Taher TE, Wielenga VJ, *et al.* Heparan sulfate-modified CD44 promotes hepatocyte growth factor/scatter factor-induced signal transduction through the receptor tyrosine kinase c-Met. *J Biol Chem* 1999; 274(10):6499-506.
20. Postema EJ, Borjesson PK, Buijs WC, *et al.* Dosimetric analysis of radioimmunotherapy with <sup>186</sup>Re-labeled bivatuzumab in patients with head and neck cancer. *J Nucl Med* 2003; 44(10):1690-9.
21. Colnot DR, Roos JC, de Bree R, *et al.* Safety, biodistribution, pharmacokinetics, and immunogenicity of <sup>99m</sup>Tc-labeled humanized monoclonal antibody BIWA 4 (bivatuzumab) in patients with squamous cell carcinoma of the head and neck. *Cancer Immunol Immunother* 2003; 52(9):576-82.
22. Koppe M, Schaijk F, Roos J, *et al.* Safety, pharmacokinetics, immunogenicity, and biodistribution of (<sup>186</sup>Re)-labeled humanized monoclonal antibody BIWA 4 (Bivatuzumab) in patients with early-stage breast cancer. *Cancer Biother Radiopharm* 2004; 19(6):720-9.

23. Wetterwald A, van der Pluijm G, Que I, *et al.* Optical imaging of cancer metastasis to bone marrow: a mouse model of minimal residual disease. *Am J Pathol* 2002; 160(3):1143-53.
24. Schackmann RC, van Amersfoort M, Haarhuis JH, *et al.* Cytosolic p120-catenin regulates growth of metastatic lobular carcinoma through Rock1-mediated anoikis resistance. *J Clin Invest* 2011; 121(8):3176-88.
25. Oliveira S, van Dongen GA, Stigter-van Walsum M, *et al.* Rapid Visualization of Human Tumor Xenografts through Optical Imaging with a Near-infrared Fluorescent Anti-Epidermal Growth Factor Receptor Nanobody. *Mol Imaging* 2011.
26. Themelis G, Yoo JS, Soh KS, Schulz R and Ntziachristos V. Real-time intraoperative fluorescence imaging system using light-absorption correction. *J Biomed Opt* 2009; 14(6):064012.
27. Oliveira S, Cohen R, Stigter-van Walsum M, *et al.* A novel method to quantify IRDye800CW fluorescent antibody probes *ex vivo* in tissue distribution studies. *EJNMMI Res* 2012; 2(1):50.
28. Heider KH, Sproll M, Susani S, *et al.* Characterization of a high-affinity monoclonal antibody specific for CD44v6 as candidate for immunotherapy of squamous cell carcinomas. *Cancer Immunol Immunother* 1996; 43(4):245-53.
29. Terwisscha van Scheltinga AG, van Dam GM, Nagengast WB, *et al.* Intraoperative near-infrared fluorescence tumor imaging with vascular endothelial growth factor and human epidermal growth factor receptor 2 targeting antibodies. *J Nucl Med* 2011; 52(11):1778-85.





# Part 2



# Seven

## **Nuclear Kaiso expression is associated with high grade and triple-negative invasive breast cancer**

Jeroen F. Vermeulen<sup>1\*</sup>, Robert A.H. van de Ven<sup>1\*</sup>, Cigdem Ercan<sup>1</sup>, Petra van der Groep<sup>1,2</sup>, Elsken van der Wall<sup>2</sup>, Peter Bult<sup>3</sup>, Matthias Christgen<sup>4</sup>, Ulrich Lehmann<sup>4</sup>, Juliet Daniel<sup>5</sup>, Paul J. van Diest<sup>1</sup>, Patrick W.B. Derksen<sup>1</sup>

<sup>1</sup> Department of Pathology, University Medical Center Utrecht, Utrecht, The Netherlands,

<sup>2</sup> Division of Internal Medicine and Dermatology, University Medical Center Utrecht, Utrecht, The Netherlands,

<sup>3</sup> Department of Pathology, Radboud University Nijmegen Medical Centre, Nijmegen, The Netherlands,

<sup>4</sup> Institute of Pathology, Hannover Medical School, Hannover, Germany,

<sup>5</sup> Department of Biology, McMaster University, Hamilton, ON, Canada

\*These authors contributed equally to this study

***PLOS One 2012; 7(5): e37864***

## Abstract

Kaiso is a BTB/POZ transcription factor that is ubiquitously expressed in multiple cell types and functions as a transcriptional repressor and activator. Little is known about Kaiso expression and localization in breast cancer. Here, we have related pathological features and molecular subtypes to Kaiso expression in 477 cases of human invasive breast cancer. Nuclear Kaiso was predominantly found in invasive ductal carcinoma (IDC) ( $p=0.007$ ), while cytoplasmic Kaiso expression was linked to invasive lobular carcinoma (ILC) ( $p=0.006$ ). Although cytoplasmic Kaiso did not correlate to clinicopathological features, we found a significant correlation between nuclear Kaiso, high histological grade ( $p=0.023$ ), ER $\alpha$  negativity ( $p=0.001$ ), and the HER2-driven and basal/triple-negative breast cancers ( $p=0.018$ ). Interestingly, nuclear Kaiso was also abundant in BRCA1-associated breast cancer ( $p<0.001$ ) and invasive breast cancer overexpressing EGFR ( $p=0.019$ ). We observed a correlation between nuclear Kaiso and membrane-localized E-cadherin and p120-catenin (p120) ( $p<0.01$ ). In contrast, cytoplasmic p120 strongly correlated with loss of E-cadherin and low nuclear Kaiso ( $p=0.005$ ). We could confirm these findings in human ILC cells and cell lines derived from conditional mouse models of ILC. Moreover, we present functional data that substantiate a mechanism whereby E-cadherin controls p120-mediated relief of Kaiso-dependent gene repression. In conclusion, our data indicate that nuclear Kaiso is common in clinically aggressive ductal breast cancer, while cytoplasmic Kaiso and a p120-mediated relief of Kaiso-dependent transcriptional repression characterize ILC.

## Introduction

Kaiso was initially identified as a binding partner of the adherens junction (AJ) complex member p120-catenin (p120) [1]. Kaiso is a member of the BTB/POZ-ZF (Broad complex, Tramtrak, Bric à brac/Pox virus and zinc finger) family of transcription factors [2] consisting of approximately 60 BTB/POZ-ZF members that include the cancer-associated B cell lymphoma 6 (*BCL6*), lymphoma-related factor (*TRAF3*), and hypermethylated in cancer (*HIC1*) genes (reviewed in [3]). Kaiso (also known as zinc finger- and BTB domain-containing protein 33; ZBTB33) interacts with its target gene promoters via two distinct mechanisms: via sequence-specific Kaiso binding sites (KBS) consisting of the consensus sequence CTGCNA, or via methylated CpG dinucleotides [4-7]. Although Kaiso can act as a transcriptional activator [8], it mainly acts as a transcriptional repressor by binding to the promoters of its target genes. This interaction can be inhibited by p120 binding to a region flanking Kaiso's ZF motifs [1], and results in expression of distinct target genes [9,10]. Kaiso has been shown to directly repress canonical Wnt targets via TCF/LEF family members [11,12]. These target genes include the matrix metalloprotease *Matrilysin (aka MMP7)*, *CCND1*, *Siamois*, *Fos* and *Myc* [4,12]. In addition, Kaiso can regulate expression of Wnt11, a regulator of directed cell movement and morphogenesis [10].

While there is data demonstrating a role for Kaiso in early vertebrate development [12,13], data implicating Kaiso-mediated regulation of gene transcription in cancer are scarce. Kaiso expression and sub-cellular localization seems dynamic and highly dependent on tumor type and micro-environmental conditions [14,15]. Interestingly, *Kaiso*-null mice show resistance to intestinal cancer characterized by a delayed onset of tumor development, decreased tumor size, and prolonged survival when crossed with *APC<sup>MIN/+</sup>* mice [16].

Loss of E-cadherin and subsequent disruption of AJ function is strongly linked to breast cancer development and progression (reviewed in [17]). Using tissue-specific and conditional mouse models, we have established a causal relationship between early inactivation of E-cadherin and formation of invasive lobular carcinoma (ILC) [18,19]. While  $\beta$ -catenin is rapidly degraded upon loss of E-cadherin [20,21], p120 translocates and resides in the cytosol [22], where it regulates anchorage-independent tumor growth and metastasis through Mrip-dependent activation of the Rock pathway [20]. In addition, cytoplasmic p120 has been implicated in the acquisition of motility and invasiveness in E-cadherin negative breast cancer [23,24]. The structure of p120 reveals a number of domains including a protein-protein interaction Armadillo (Arm) domain consisting of 10 Armadillo repeats. This domain mediates not only the interaction with cadherins but also p120 binding to the transcriptional repressor Kaiso, probably in a mutually exclusive manner [1].

Given the importance of p120 in the pathobiology of breast cancer, and its regulation of Kaiso-mediated transcriptional repression, we performed a comprehensive analysis of Kaiso expression and localization to pathological features and molecular subtypes in 477 cases of invasive breast cancer.

## Materials and Methods

### *Patients*

The study population was derived from the archives of the Departments of Pathology of the University Medical Center Utrecht, Utrecht and the Radboud University Nijmegen Medical Centre, Nijmegen, The Netherlands. These comprised 477 cases of invasive breast cancer, including cases with a *BRCA1* germ-line mutation as previously described [25]. Histological grade was assessed according to the Nottingham scheme, and mitotic activity index (MAI) was assessed as before [26]. From representative donor paraffin blocks of the primary tumors, tissue microarrays were constructed by transferring tissue cylinders of 0.6 mm (3 cylinders per tumor) from the tumor area, determined by a pathologist based on haematoxylin-eosin stained slides, using a tissue arrayer (Beecher Instruments, Sun Prairie, WI, USA) as described before [27]. The use of anonymous or coded left over material for scientific purposes is part of the standard treatment contract with patients in The Netherlands [28]. Ethical approval was not required.

### *Immunohistochemistry*

Immunohistochemistry was carried out on 4µm thick sections. After deparaffination and rehydration, endogenous peroxidase activity was blocked for 15 min in a 46mM citric acid-100mM sodiumphosphate buffer solution pH5.8 containing 0.3% hydrogen peroxide. After antigen retrieval, i.e. boiling for 20 min in 10mM citrate pH6.0 (Kaiso, p120, PR), Tris/EDTA pH9.0 (E-cadherin, ERα, HER2), or Prot K (0.15mg/ml, DAKO, Glostrup Denmark) for 5 min at room temperature (EGFR), a cooling period of 30 min preceded the primary antibody incubation. Kaiso (clone 6F, Upstate, Billerica, MA, USA)[29] 1:100; E-cadherin (clone 4A2C7, Zymed, Invitrogen, Breda, The Netherlands) 1:200; ERα (clone ID5, DAKO) 1:80; PR (clone PgR636, DAKO) 1:25; HER2 (SP3, Neomarkers, Duiven, The Netherlands) 1:100 were diluted in PBS containing 1% BSA and incubated for 1h at room temperature. Primary antibodies against p120 (cat 610134, BD Transduction Labs, San Diego, CA, USA) 1:500 and EGFR (clone 31G7, Zymed, Invitrogen) 1:30 were diluted in PBS containing 1% BSA and incubated overnight at 4°C. The signal was amplified using Powervision poly-HRP anti-mouse, rabbit, rat (DPVO-HRP, Immunologic, Duiven, The Netherlands) or the Novolink kit (Leica, Rijswijk, The Netherlands) (in the case of EGFR) and developed with diaminobenzidine, followed by counterstaining with haematoxylin, dehydration in alcohol, and mounting. Appropriate negative and positive controls were used throughout.

### *Scoring of immunohistochemistry*

All scoring was done blinded to patient characteristics and results of other staining by two independent observers. E-cadherin and EGFR stainings were scored using the DAKO/HER2 scoring system for membranous staining. Membranous scores 1+, 2+, and 3+ were considered positive, except for HER2 where only a score of 3+ was considered positive. Kaiso staining was scored based on localization and by counting the positive tumor nuclei, considering samples with more than 5% positive tumor nuclei as positive. Using thresholds of 1 or 10% for scoring nuclear accumulation as positive did not change the results. p120 staining was scored based on the localization as membranous or cytoplasmic.

Based on ER $\alpha$ , PR, and HER2 immunohistochemistry, tumors were classified as luminal (ER $\alpha$  and/or PR positive), HER2-driven (ER $\alpha$ -, PR-, HER2+), or basal-like/triple negative (ER $\alpha$ -, PR-, HER2- with or without EGFR expression), the immunohistochemical surrogate [30] of the original Sorlie/Perou classification [31].

### *Statistics*

Statistical analysis was performed using IBM SPSS Statistics version 18.0 (SPSS Inc., Chicago, IL, USA). Associations between categorical variables were examined using the Pearson's Chi-square test and associations between continuous variables using the Student's T-test. P-values <0.05 were considered to be statistically significant.

### *Cell culture*

Origin and culture of the mouse cell lines Trp53 $\Delta/\Delta$ -3, Trp53 $\Delta/\Delta$ -4 and mILC-1 were described before [20]. ILC cell line IPH-926 was cultured as described [32]. Human breast cancer cell line MCF10a was obtained from ATCC (validated by STR profiling), and cultured in DMEM/F12 (Invitrogen) supplemented with 10mg/l insulin, 20 $\mu$ g/l EGF, 100 $\mu$ g/l cholera toxin, and 500  $\mu$ g/l hydrocortisone (Sigma, Zwijndrecht, The Netherlands). All media contained 10% fetal calf serum, 100 IU/ml penicillin, and 100  $\mu$ g/ml streptomycin. All cell lines were maintained at 37°C in a 5% CO<sub>2</sub> humidified atmosphere.

### *Immunofluorescence*

Cells were cultured on coverslips and fixed in methanol for 10 minutes, permeabilized using 0.3% Triton-X100/PBS and subsequently blocked using 4% BSA (Roche, Woerden, The Netherlands). Cover slips were incubated with mouse anti Kaiso 1:500 (clone 6F) in 4% BSA for 1 hour at room temperature. Subsequently, cells were incubated in 4% BSA with goat-anti-mouse Alexa Fluor 488 (1:600; Molecular Probes, Breda, The Netherlands) for 1 hour. Next, cells were incubated with TRITC-conjugated mouse anti-p120 1:300 (clone 98/pp120, BD Biosciences) overnight at 4°C. Cover slips were mounted using Vectashield mounting medium (Vector Laboratories, Burlingame, CA, USA). Samples were analyzed by confocal laser microscopy.



### Luciferase reporter assay

Cells were cultured in 6-wells culture plates and grown to 40-50% confluency. Next, cells were transfected with either 600ng of the Kaiso-specific reporter (pGL3-4XKBS), a mutated Kaiso reporter (pGL3-4XKBS CAmut) or empty vector (pGL3-Control) and co-transfected with 5ng Renilla (pRL-CMV, Promega, Leiden, The Netherlands) for normalization of transfection efficiency, using Lipofectamine 2000 (Invitrogen) according to manufacturers instructions. In addition, cells were transfected with 400ng effector plasmid consisting either of pC2-p120 isoform 1a, pcDNA3.1-Kaiso or empty vector (pcDNA3.1). The transfection mixture was added to the cells and incubated for 2.5 hours. Followed by replacement of the transfection mixture by complete medium.

Two days post-transfection cells were washed twice with PBS, lysed by scraping in 200µl Passive Lysis Buffer (Promega) and subjected to a freeze-thaw cycle. Cellular debris was spun down at 5,000 g at 4°C for 5 minutes and supernatants were collected. Bioluminescence was measured in 50µl sample with Dual Luciferase Reporter assay system (Promega) on a Lumat LB9507 Luminometer (Berthold Technologies, Vilvoorde, Belgium) according manufacturers instructions.

**Table 1.** Clinicopathological characteristics of 477 invasive breast cancer patients studied for the expression of Kaiso.

Feature	Grouping	N or value	%
Age (years)	Mean	60	
	Range	28-88	
Histological type	IDC	312	65.4
	ILC	130	27.3
	Other	35	7.3
Tumor size	pT1	207	43.4
	pT2	213	44.7
	pT3	50	10.5
	Not available	7	1.4
Histological grade	1	85	17.8
	2	165	34.6
	3	208	43.6
	Not available	19	4.0
MAI #	≤ 12	241	50.5
	≥ 13	236	49.5
Lymph node status	Negative*	229	48.0
	Positive**	223	46.8
	Not available	25	5.2

# : per 2mm<sup>2</sup>; \*: negative = NO or NO(i+); \*\*: positive = ≥N1mi (according to TNM 7<sup>th</sup> edition, 2010)

## Results

### *Kaiso expression in normal breast epithelium and invasive breast cancer*

In normal breast tissue, localization of Kaiso was observed in the cytosol of both luminal and myoepithelial cells (Figure 1). We detected nuclear Kaiso expression mainly in the luminal epithelial cells, which was heterogeneous while the number of cells showing nuclear Kaiso varied between ductal structures (5-35% of the cells; Figure 1).

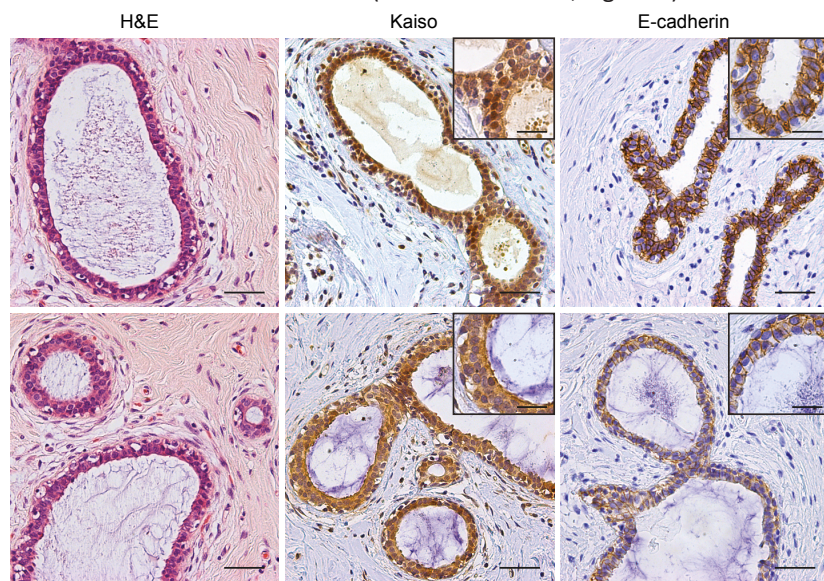


**Figure 1. Kaiso expression in normal breast epithelium.** Sections were stained using immunohistochemistry for Kaiso (middle panel) or E-cadherin (right panel). Kaiso expression in normal breast epithelium is heterogeneous; high nuclear expression (top row) versus only cytoplasmic expression (bottom row) is found with equal frequency. Left panels show a haematoxylin and eosin (H&E) staining. Scale bar equals 50 $\mu$ m, in inserts 25 $\mu$ m.

Next, we set out to analyze Kaiso expression in invasive breast cancer. We used a study population comprised of 312 (65.4%) IDC, 130 (27.3%) ILC, and 35 (7.3%) invasive breast cancer cases with other histology (Table 1). First, we scored absence or presence of cytoplasmic expression of Kaiso, since this variable has recently been linked to poor prognosis in non-small cell lung cancer (NSCLC) [33]. Although cytoplasmic expression of Kaiso was significantly different between the histological sub-types of breast cancer ( $p=0.006$ ), it was not associated with other clinicopathological features (Table 2 and Figure 2). Given that Kaiso functions as a transcriptional repressor, we scored nuclear expression in our breast cancer cohort. Since using thresholds of 1%, 5% or 10% for scoring of nuclear accumulation resulted in identical outcome and statistical significance (data not shown), we used 5% nuclear localization as a positive cut-off percentage. IDC expressed nuclear Kaiso more often than ILC ( $p=0.007$ ; Table 3; Figure 2), while exclusive cytoplasmic expression of Kaiso was a

common feature of ILC. In addition, no significant difference was found between classical and pleomorphic lobular cancers ( $p=0.237$ ) (data not shown). For the other clinicopathological features, we observed that high-grade tumors and cancers with a MAI  $\geq 13$ , had significantly more nuclear Kaiso than low-grade tumors ( $p=0.023$  and  $p=0.003$ , respectively), while no significant differences were found for lymph node status and tumor size (Table 3).

**Table 2.** Correlation of cytoplasmic Kaiso with clinicopathological features in breast cancer.

Feature	N	Cytoplasmic Kaiso expression		p-value
		Negative N (%)	Positive N (%)	
Histological type				
IDC	312	45 (14.4)	267 (85.6)	
ILC	130	5 (3.8)	125 (96.2)	
Other	35	5 (14.3)	30 (85.7)	<b>0.006</b>
Histological grade				
1	85	12 (14.1)	73 (85.9)	
2	163	16 (9.8)	147 (90.2)	
3	207	25 (12.1)	182 (87.9)	0.585
Tumor size				
pT1	205	22 (10.7)	183 (89.3)	
pT2	213	29 (13.6)	184 (86.4)	
pT3	49	3 (6.1)	46 (93.9)	0.296
MAI (per 2mm <sup>2</sup> )				
$\leq 12$	238	29 (12.2)	209 (87.8)	
$\geq 13$	236	26 (11.0)	210 (89.0)	0.691
Lymph node status				
Negative	229	28(12.2)	201(87.8)	
Positive	223	25 (11.2)	198 (88.8)	0.737

**Table 3.** Correlation of nuclear Kaiso with clinicopathological features in breast cancer.

Feature	N	Nuclear Kaiso expression		p-value
		Low (<5%) N (%)	High ( $\geq 5\%$ ) N (%)	
Histological type				
IDC	312	211 (67.6)	101 (32.4)	
ILC	130	107 (82.3)	23 (17.7)	
Other	35	25 (71.4)	10 (28.6)	<b>0.007</b>
Histological grade				
1	85	67 (78.8)	18 (21.2)	
2	165	125 (75.8)	40 (24.2)	
3	208	136 (65.4)	72 (34.6)	<b>0.023</b>
Tumor size				
pT1	207	154 (74.4)	53 (25.6)	
pT2	213	149 (70.0)	64 (30.0)	
pT3	50	37 (74.0)	13 (26.0)	0.573
MAI (per 2mm <sup>2</sup> )				
$\leq 12$	241	188 (78.0)	53 (22.0)	
$\geq 13$	236	155 (65.7)	81 (34.3)	<b>0.003</b>
Lymph node status				
Negative	229	168 (73.4)	61(26.6)	
Positive	223	158 (70.9)	65 (29.1)	0.552

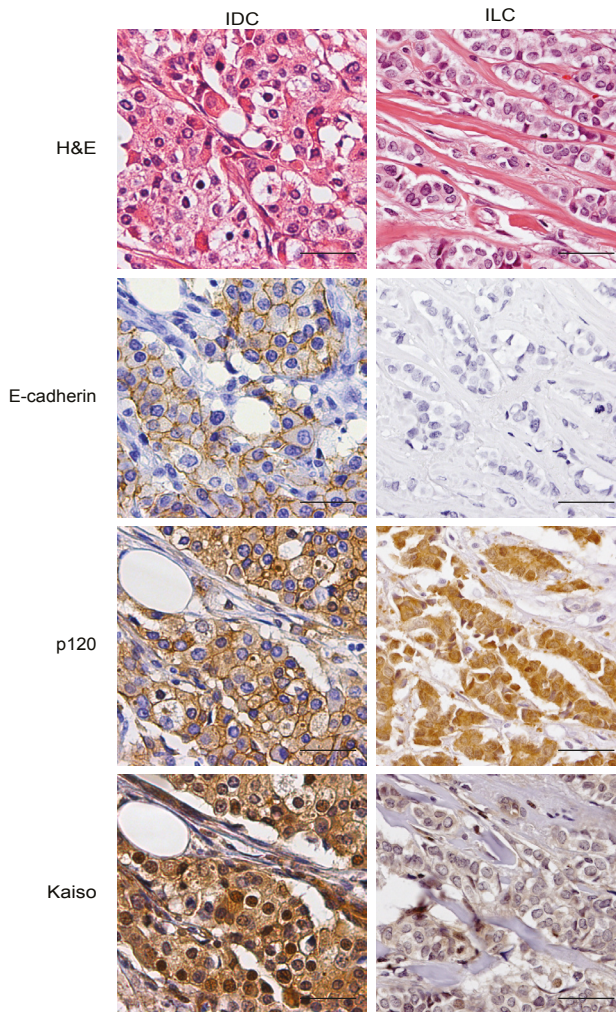


**Figure 2. E-cadherin and p120 membrane localization correlates with nuclear Kaiso expression.** IDC (left panels) and ILC (right panels) were stained for E-cadherin, p120, and Kaiso using immunohistochemistry. Note the association between membrane-localized E-cadherin and p120, and high nuclear Kaiso in IDC. In contrast, ILC is characterized by loss of E-cadherin, and expression of cytoplasmic p120, which correlates with absence of nuclear Kaiso. Scale bar equals 50 $\mu$ m.

### *Nuclear Kaiso expression and molecular subtypes of breast cancer*

Since Kaiso is implicated in transcriptional repression of specific target genes, and our data indicated that nuclear Kaiso correlated with histology and grading in our invasive breast cancer cohort, we performed a cross-comparison between nuclear Kaiso expression and the molecular subtypes of breast cancer. Nuclear Kaiso was significantly enriched in the basal/triple negative and HER2-driven invasive breast cancer than luminal-type invasive breast cancer ( $p=0.018$ ; Table 4). While we did not find differences in nuclear Kaiso expression in the context of PR and HER2 ( $p=0.104$  and  $p=0.246$ , respectively), an inverse correlation

between nuclear Kaiso and ER $\alpha$  expression was detected ( $p=0.001$ ) (Table 4). Moreover, *BRCA1*-associated breast cancers showed a significantly higher number of tumors expressing nuclear-localized Kaiso than sporadic carcinomas (71.4% versus 29.3%, respectively;  $p<0.001$ , Table 4).

**Table 4.** Correlation of nuclear Kaiso with the molecular subtypes of breast cancer.

Feature	N	Nuclear Kaiso expression		p-value
		Low (<5%) N (%)	High ( $\geq$ 5%) N (%)	
Perou / Sorlie classification				
Luminal	386	288 (74.6)	98 (25.4)	
HER2-driven	19	13 (68.4)	6 (31.6)	
Basal/Triple Negative	72	42 (58.3)	30 (42.7)	<b>0.018</b>
ER $\alpha$				
Positive	378	285(76.0)	93 (24.0)	
Negative	99	58 (58.6)	41 (41.4)	<b>0.001</b>
PR				
Positive	276	206 (74.6)	70 (25.4)	
Negative	199	135 (67.8)	64 (32.2)	0.104
HER2				
Positive	45	29 (64.4)	16 (35.6)	
Negative	431	313 (72.6)	118 (27.4)	0.246
BRCA1				
Mutation carrier	21	6 (28.6)	15 (71.4)	
Sporadic	324	229 (70.7)	95 (29.3)	<b>0.001</b>
EGFR				
Positive	80	49 (61.3)	31 (38.7)	
Negative	395	293 (74.2)	102 (25.8)	<b>0.019</b>

#### *Localization of Kaiso, EGFR and the adherens junction in breast cancer*

Expression of EGFR has been linked to prognosis in basal/triple-negative breast cancer [34,35]. Because EGFR partly co-localizes with the AJ [36], and EGF stimulation can modulate AJ function through phosphorylation of Src, p120 and PKC $\delta$  [37,38], we determined whether EGFR expression correlated with levels of membranous E-cadherin and nuclear Kaiso. Indeed, a strong association between EGFR and E-cadherin ( $p<0.001$ ) was observed, which coincided with a higher prevalence of nuclear Kaiso expression in EGFR-expressing invasive breast cancer ( $p=0.019$ ; Table 4).

Kaiso was identified as a p120-binding partner in a yeast two-hybrid screen, using p120 as bait [1]. Since then, several studies indicated that p120 controls relief of Kaiso-mediated transcriptional repression through binding and shuttling from and to the cytosol [9,10]. Interestingly, this feature can be antagonized by E-cadherin expression, a key determinant in the differential diagnosis between IDC and ILC [39]. While approximately 90% of ILC cases show loss of E-cadherin expression, the majority of IDC cases have retained E-cadherin on the membrane [40-42]. Our data indicated that IDC and ILC show significant differences in

cytoplasmic and nuclear Kaiso localization (Figure 2, Tables 3 and 4). The presence of AJs, *i.e.* membranous localization of E-cadherin and p120, strongly correlated with high nuclear Kaiso ( $p=0.008$  and  $p=0.001$ , respectively; Table 5). Moreover, nuclear Kaiso inversely correlated with cytoplasmic p120 ( $p=0.005$ ), thus supporting the notion that loss of E-cadherin and subsequent translocation of p120 to the cytosol may control Kaiso localization.

**Table 5.** Correlation between functional adherens junctions and nuclear Kaiso expression.

Feature	N	Nuclear Kaiso expression		p-value
		Low (<5%) N (%)	High ( $\geq 5\%$ ) N (%)	
E-cadherin				
Positive	327	220 (67.3)	107 (32.7)	
Negative	121	97 (80.2)	24 (19.8)	<b>0.008</b>
p120				
Membranous	320	214(66.9)	106 (33.1)	
Cytoplasmic	139	114 (82.0)	25 (18.0)	<b>0.001</b>

To substantiate these findings, we analyzed expression of Kaiso in MCF10a, a breast cancer cell line that expressed membranous E-cadherin and p120. Furthermore, since our data indicated that nuclear Kaiso and ILC were inversely correlated, we also used immunofluorescence to examine Kaiso localization in a recently generated and characterized bona fide human ILC cell line; IPH-926 [32]. Although Kaiso expression was observed in E-cadherin-expressing as well as in E-cadherin-mutant cells, nuclear Kaiso was enriched in MCF10a cells, whereas IPH-926 virtually lacked nuclear Kaiso (Figure 3A). In addition, we employed cell lines derived from conditional mouse models in which E-cadherin and/or p53 were somatically inactivated [19]. In agreement with our findings in human cell lines, we could detect nuclear Kaiso in an E-cadherin expressing and p53-deficient mammary carcinoma cell line (Trp53 $\Delta/\Delta$ -3), whereas mouse ILC (mILC) cells mainly lacked nuclear Kaiso (Figure 3B). Evidence that p120 could direct nuclear localization of Kaiso was obtained by overexpressing p120 in Trp53 $\Delta/\Delta$ -4 cells, which resulted in high cytoplasmic p120 and a reduction in nuclear Kaiso (Figure 3C). To determine the effect of p120 overexpression on Kaiso-dependent transcriptional repression, we performed reporter assays using a Kaiso reporter system (containing 4 tandem-repeats of the consensus Kaiso Binding Sequence; 4XKBS reporter). In line with our expression data, we observed that Kaiso-dependent transcriptional repression was significantly higher in Trp53 $\Delta/\Delta$ -4 than in mILC-1 cells ( $p=0.015$ ; Figure 3D). Furthermore, transcriptional repression of the 4XKBS reporter was attenuated by exogenous Kaiso expression in mILC-1 cells (Figure 3D). Finally, we observed that overexpression of p120 in Trp53 $\Delta/\Delta$ -4 cells resulted in decreased Kaiso-dependent transcriptional repression (Figure 3C and 3D), consistent with a decrease in nuclear Kaiso expression. These results support our findings in primary breast cancer samples and indicate that p120 controls localization of Kaiso and subsequent de-repression of Kaiso-dependent transcription in breast cancer.

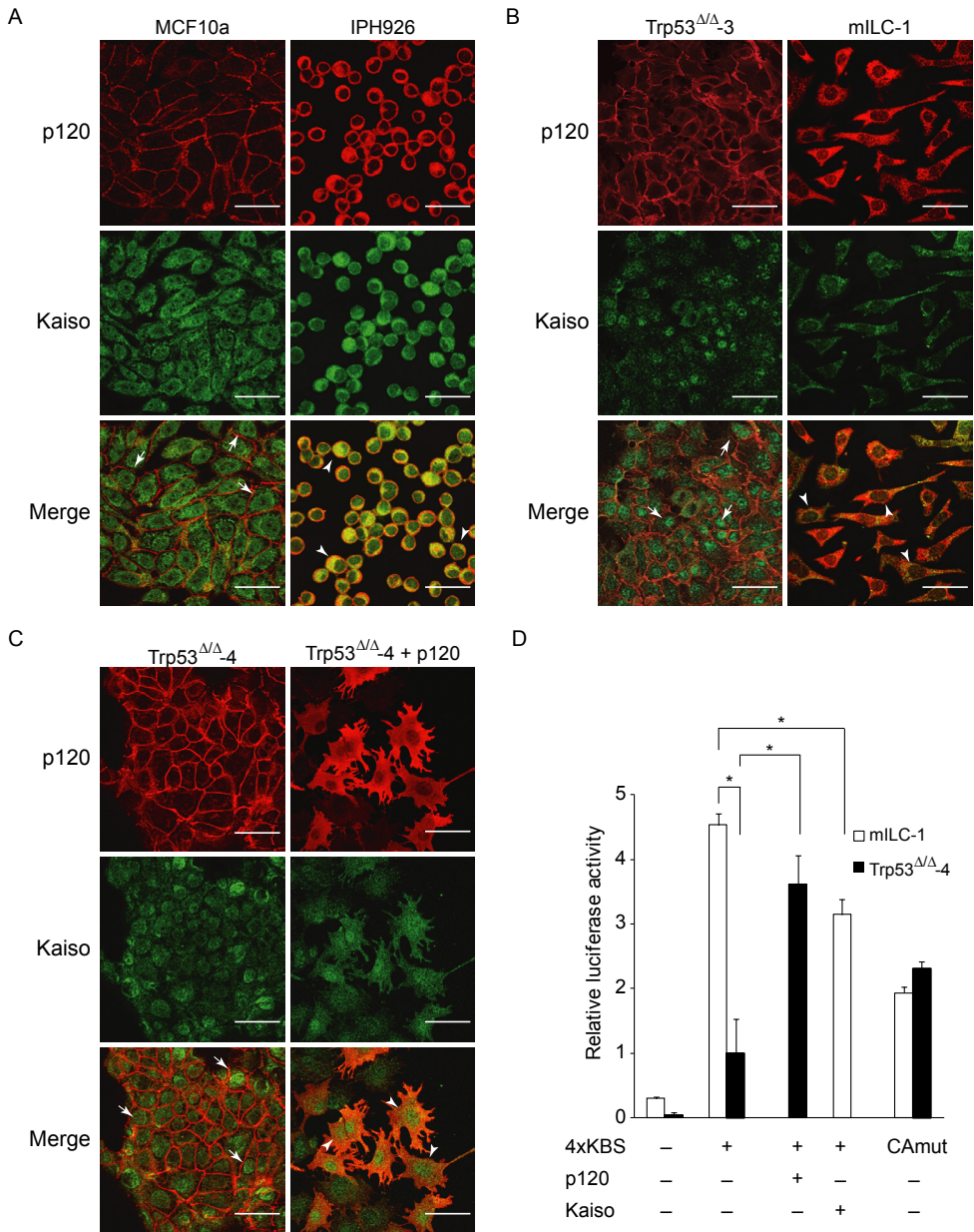


**Figure 3. p120 and Kaiso localization in breast cancer cell lines.** Human (A) and mouse (B) E-cadherin-expressing (left panels) and E-cadherin-deficient (right panels) breast cancer cell lines were stained for p120 (top panels) and Kaiso (middle panels). Bottom panels depict the merge of Kaiso (green) and p120 (red). Note the nuclear accumulation in MCF10a and Trp53<sup>ΔΔ</sup>-3 (arrows) versus cytoplasmic Kaiso expression in human and mouse ILC (arrowheads; IPH-926 and mILC-1). (C) Overexpression of p120 in Trp53<sup>ΔΔ</sup>-4 cells resulted in decreased nuclear accumulation of Kaiso (arrowheads) compared to untransfected Trp53<sup>ΔΔ</sup>-4, which shows predominantly nuclear Kaiso (arrows). Scale bar equals 20μm. (D) Kaiso-dependent reporter assay using the 4XKBS reporter in mILC-1 and Trp53<sup>ΔΔ</sup>-4 cells. Upon overexpression of p120 in Trp53<sup>ΔΔ</sup>-4 cells, Kaiso-dependent gene repression is attenuated, whereas exogenous expression of Kaiso in mILC-1 increased gene repression. (\* = p<0.05)

## Discussion

In addition to the established role of BTB-POZ-ZF transcription factors in vertebrate development, increasing evidence emerges that these factors can function as oncogenes or tumor suppressors [43]. For instance, the BTB/POZ promyelocytic leukemia zinc finger (PLZF) has been identified as a translocation partner of the retinoic receptor alpha (RAR $\alpha$ ). In this setting, PLZF confers oncogenic potential through fusion to the hormone-binding domain of RAR $\alpha$ , subsequent binding to its target sites and local recruitment of histone deacetylases [44]. Another well-studied BTB-POZ oncogene is BCL6, a protein that exerts its pro-tumorigenic functions by repression of target genes necessary for terminal B cell differentiation [45,46]. In contrast, *HIC1* is a candidate tumor suppressor that is often found mutated or hypermethylated in human cancer [47]. However, unlike PLZF, BCL-6 and HIC1, it remains unclear whether Kaiso mislocalization or absence could drive malignancy.

Kaiso could function as an oncogene or as a tumor suppressor as it has been implicated in both transcriptional activation and repression [4,8,13]. In colon cancer, Kaiso may regulate methylation-dependent inhibition of tumor suppressors such as *CDKN2A* by binding to its methylated promoter. As a consequence, tumor cells are resistant to cell cycle arrest and chemotherapy-mediated cell death [48]. Interestingly, genetic Kaiso ablation results in a delay in intestinal tumorigenesis in the context of *APC*<sup>MIN/+</sup> mice [16], which suggests that Kaiso may indeed contribute to intestinal tumor progression through silencing of tumor suppressors. Conversely, Kaiso has been strongly implicated in regulation of Wnt signaling-related target genes [4,11,12,49,50]. Given its bi-modal nature of  $\beta$ -catenin-dependent regulation of Wnt signaling [51] and the overlap between TCF/LEF regulated genes and Kaiso targets, the effects of Kaiso on tumor development may be highly dependent on cell type and their dependency on (canonical) Wnt signals. In lung cancer, cytoplasmic Kaiso was correlated with poor prognosis [33]. Here it was proposed that the invasive phenotype of NSCLC might be regulated by nuclear export of Kaiso, which was mediated by phosphorylation of p120 isoform 3 [52]. Lung and other epithelial tissue differ substantially from breast with respect to cadherin expression and p120 function. For instance, condition p120 knockout in the skin, gastro-intestinal tract or oral cavity is tolerated and induces hyperplasia or tumor formation [53-56]. In contrast, p120 knock-out in the mammary gland is not tolerated and leads to apoptosis and subsequent cell clearance (our unpublished results), indicating that p120 family members may play tissue-specific redundant roles, as has been suggested for  $\delta$ -catenin in NSCLC [57].



In this study we have performed to the best of our knowledge, the first comprehensive analysis of Kaiso expression in breast cancer, using a tissue micro array (TMA)-based collection of 477 invasive breast cancer cases. Previous studies had already indicated that localization of Kaiso may be highly variable depending on tumor type and environmental context [14]. Our data indicate that nuclear Kaiso expression correlates with the pathological and phenotypical traits of specific breast cancer sub-types that are linked to poor prognosis, *i.e.* high grade, and basal/triple-negative breast cancer. These tumors were also associated with high EGFR expression, which is associated with worse prognosis for basal/triple-negative breast cancers [34,35]. Our observation that BRCA1-associated hereditary breast cancers often showed high nuclear Kaiso, is in line with the finding that nuclear Kaiso is in general associated with high grade, basal-like and EGFR positive breast cancers. Since our data does not indicate differential E-cadherin expression and localization between sporadic and BRCA1-related invasive breast cancer, this cannot explain the increase in nuclear Kaiso localization. Future research will have to determine if and how other (p120-unrelated) events such as promoter methylation of specific genes may recruit Kaiso to the nucleus and initiate subsequent epigenetic silencing in BRCA1-related invasive breast cancer. We have furthermore shown that nuclear Kaiso correlated with the presence of membrane-localized E-cadherin and p120, a finding that is in line with the reported regulation of Kaiso by p120 [58]. In this scenario, p120 relieves transcriptional repression by Kaiso and as such may control shuttling of the p120/Kaiso complex to the cytosol [9]. Because most IDC retain a membrane-localized E-cadherin/p120 complex, our data confirmed this concept by showing that nuclear Kaiso correlated with tumors expressing E-cadherin. Also, since the basal-like and ER $\alpha$  negative high grade tumors mainly reside in the E-cadherin-expressing IDC cohort, it supports the notion that p120 may regulate Kaiso distribution in breast cancer. The mechanism of this needs to be further elucidated.

ILC is characterized by loss of the AJ complex through early mutational inactivation of E-cadherin and subsequent translocation of p120 to the cytosol. If p120 was a major factor controlling Kaiso distribution, one would expect that the absence of nuclear Kaiso associated with ILC. Our data indeed conforms to this hypothesis by showing that exclusive cytoplasmic Kaiso expression is strongly correlated with the lobular phenotype. Together, these findings suggest that genes may be differentially regulated in IDC versus ILC as a result of differential Kaiso localization. This notion may therefore partly explain the differences in expression profiles that have been reported when comparing IDC and ILC [59,60].

Recent data have indicated that phosphorylation of p120 can increase its binding to Kaiso and induce inhibition of canonical Wnt signaling [11]. It is well established that ILC expresses cytoplasmic p120 and does not activate canonical Wnt signals [20,21,61].

Although it is unclear if this mechanism controls expression of Kaiso targets in ILC, it clearly emphasizes the possible ramifications of Kaiso and its regulation by p120 in breast cancer. Moreover, we have recently shown that cytoplasmic translocation of p120 controls ILC tumor growth and metastasis through Mrip-dependent regulation of Rock1 signaling, while IDC does not appear to be contingent on these signals for anchorage-independence [20]. We envisage that differential cadherin-catenin localization in IDC and ILC and the signals that emanate from p120 may not only explain the lobular phenotype, but probably also control regulation of transcriptional regulation and cellular biochemistry. Although Kaiso's target genes in breast cancer are unknown, our findings suggest that Kaiso may function as an oncogene in IDC through inhibition of tumor suppressor gene expression whereas in ILC, Kaiso might harbor tumor suppressor functions by p120-mediated relieve of transcriptional repression of oncogenic target genes. As such, it may have significant impact on the development of personalized cancer care since it suggests that the main breast cancer types may depend on diametrical mechanisms for tumor progression.

## Acknowledgements

This work was supported by the UMC Utrecht Cancer Center, grants from The Netherlands Organization for Scientific Research (NWO-VIDI 917.96.318), the Dutch Cancer Society (KWF-UU 2011-5230), Pink Ribbon, and an unrestricted educational research grant from AEGON Inc.

## References

1. Daniel JM, Reynolds AB. The catenin p120(ctn) interacts with Kaiso, a novel BTB/POZ domain zinc finger transcription factor. *Mol Cell Biol* 1999; 19(5):3614-23.
2. Daniel JM. Dancing in and out of the nucleus: p120(ctn) and the transcription factor Kaiso. *Biochim Biophys Acta* 2007; 1773(1):59-68.
3. van Roy FM, McCrean PD. A role for Kaiso-p120ctn complexes in cancer? *Nat Rev Cancer* 2005; 5(12):956-64.
4. Daniel JM, Spring CM, Crawford HC, Reynolds AB, Baig A. The p120(ctn)-binding partner Kaiso is a bi-modal DNA-binding protein that recognizes both a sequence-specific consensus and methylated CpG dinucleotides. *Nucleic Acids Res* 2002; 30(13):2911-9.
5. Prokhortchouk A, Hendrich B, Jorgensen H, et al. The p120 catenin partner Kaiso is a DNA methylation-dependent transcriptional repressor. *Genes Dev* 2001; 15(13):1613-8.
6. Ruzov A, Hackett JA, Prokhortchouk A, et al. The interaction of xKaiso with xTcf3: a revised model for integration of epigenetic and Wnt signalling pathways. *Development* 2009; 136(5):723-7.
7. Ruzov A, Savitskaya E, Hackett JA, et al. The non-methylated DNA-binding function of Kaiso is not required in early *Xenopus laevis* development. *Development* 2009; 136(5):729-38.
8. Rodova M, Kelly KF, VanSaun M, Daniel JM, Werle MJ. Regulation of the rapsyn promoter by kaiso and delta-catenin. *Mol Cell Biol* 2004; 24(16):7188-96.
9. Kelly KF, Spring CM, Otchere AA, Daniel JM. NLS-dependent nuclear localization of p120ctn is necessary to relieve Kaiso-mediated transcriptional repression. *J Cell Sci* 2004; 117(Pt 13):2675-86.
10. Kim SW, Park JI, Spring CM, et al. Non-canonical Wnt signals are modulated by the Kaiso transcriptional repressor and p120-catenin. *Nat Cell Biol* 2004; 6(12):1212-20.
11. Del Valle-Perez B, Casagolda D, Lugalde E, et al. Wnt controls the transcriptional activity of Kaiso through CK1epsilon-dependent phosphorylation of p120-catenin. *J Cell Sci* 2011; 124(Pt 13):2298-309.
12. Park JI, Kim SW, Lyons JP, et al. Kaiso/p120-catenin and TCF/beta-catenin complexes coordinately regulate canonical Wnt gene targets. *Dev Cell* 2005; 8(6):843-54.
13. Ruzov A, Dunican DS, Prokhortchouk A, et al. Kaiso is a genome-wide repressor of transcription that is essential for amphibian development. *Development* 2004; 131(24):6185-94.
14. Soubry A, van Hengel J, Parthoens E, et al. Expression and nuclear location of the transcriptional repressor Kaiso is regulated by the tumor microenvironment. *Cancer Res* 2005; 65(6):2224-33.
15. Donaldson NS, Nordgaard CL, Pierre CC, et al. Kaiso regulates Znf131-mediated transcriptional activation. *Exp Cell Res* 2010; 316(10):1692-705.
16. Prokhortchouk A, Sansom O, Selfridge J, et al. Kaiso-deficient mice show resistance to intestinal cancer. *Mol Cell Biol* 2006; 26(1):199-208.
17. Berx G, van Roy F. Involvement of members of the cadherin superfamily in cancer. *Cold Spring Harb Perspect Biol* 2009; 1(6):a003129.
18. Derksen PW, Braumuller TM, van der Burg E, et al. Mammary-specific inactivation of E-cadherin and p53 impairs functional gland development and leads to pleomorphic invasive lobular carcinoma in mice. *Dis Model Mech* 2011; 4(3):347-58.
19. Derksen PW, Liu X, Saridin F, et al. Somatic inactivation of E-cadherin and p53 in mice leads to metastatic lobular mammary carcinoma through induction of anoikis resistance and angiogenesis. *Cancer Cell* 2006; 10(5):437-49.
20. Schackmann RC, van Amersfoort M, Haarhuis JH, et al. Cytosolic p120-catenin regulates growth of metastatic lobular carcinoma through Rock1-mediated anoikis resistance. *J Clin Invest* 2011; 121(8):3176-88.
21. van de Wetering M, Barker N, Harkes IC, et al. Mutant E-cadherin breast cancer cells do not display constitutive Wnt signaling. *Cancer Res* 2001; 61(1):278-84.
22. Dabbs DJ, Bhargava R, Chivukula M. Lobular versus ductal breast neoplasms: the diagnostic utility of p120 catenin. *Am J Surg Pathol* 2007; 31(3):427-37.

23. Sarrio D, Perez-Mies B, Hardisson D, et al. Cytoplasmic localization of p120ctn and E-cadherin loss characterize lobular breast carcinoma from preinvasive to metastatic lesions. *Oncogene* 2004; 23(19):3272-83.
24. Shibata T, Kokubu A, Sekine S, Kanai Y, Hirohashi S. Cytoplasmic p120ctn regulates the invasive phenotypes of E-cadherin-deficient breast cancer. *Am J Pathol* 2004; 164(6):2269-78.
25. van der Groep P, Bouter A, van der Zanden R, et al. Re: Germline BRCA1 mutations and a basal epithelial phenotype in breast cancer. *J Natl Cancer Inst* 2004; 96(9):712-3; author reply 4.
26. van der Groep P, Bouter A, van der Zanden R, et al. Distinction between hereditary and sporadic breast cancer on the basis of clinicopathological data. *J Clin Pathol* 2006; 59(6):611-7.
27. Packeisen J, Korsching E, Herbst H, Boecker W, Buerger H. Demystified...tissue microarray technology. *Mol Pathol* 2003; 56(4):198-204.
28. van Diest PJ. No consent should be needed for using leftover body material for scientific purposes. *For BMJ* 2002; 325(7365):648-51.
29. Daniel JM, Ireton RC, Reynolds AB. Monoclonal antibodies to Kaiso: a novel transcription factor and p120ctn-binding protein. *Hybridoma* 2001; 20(3):159-66.
30. Kornegoor R, Verschuur-Maes AH, Buerger H, et al. Molecular subtyping of male breast cancer by immunohistochemistry. *Mod Pathol* 2012; 25(3):398-404.
31. Sorlie T, Perou CM, Tibshirani R, et al. Gene expression patterns of breast carcinomas distinguish tumor subclasses with clinical implications. *Proc Natl Acad Sci U S A* 2001; 98(19):10869-74.
32. Christgen M, Bruchhardt H, Hadamitzky C, et al. Comprehensive genetic and functional characterization of IPH-926: a novel CDH1-null tumour cell line from human lobular breast cancer. *J Pathol* 2009; 217(5):620-32.
33. Dai SD, Wang Y, Miao Y, et al. Cytoplasmic Kaiso is associated with poor prognosis in non-small cell lung cancer. *BMC Cancer* 2009; 9:178.
34. Siziopikou KP, Cobleigh M. The basal subtype of breast carcinomas may represent the group of breast tumors that could benefit from EGFR-targeted therapies. *Breast* 2007; 16(1):104-7.
35. Livasy CA, Karaca G, Nanda R, et al. Phenotypic evaluation of the basal-like subtype of invasive breast carcinoma. *Mod Pathol* 2006; 19(2):264-71.
36. Takahashi K, Suzuki K, Tsukatani Y. Induction of tyrosine phosphorylation and association of beta-catenin with EGF receptor upon tryptic digestion of quiescent cells at confluence. *Oncogene* 1997; 15(1):71-8.
37. Mariner DJ, Davis MA, Reynolds AB. EGFR signaling to p120-catenin through phosphorylation at Y228. *J Cell Sci* 2004; 117(Pt 8):1339-50.
38. Singh R, Lei P, Andreadis ST. PKC-delta binds to E-cadherin and mediates EGF-induced cell scattering. *Exp Cell Res* 2009; 315(17):2899-913.
39. van Hengel J, Vanhoenacker P, Staes K, van Roy F. Nuclear localization of the p120(ctn) Armadillo-like catenin is counteracted by a nuclear export signal and by E-cadherin expression. *Proc Natl Acad Sci U S A* 1999; 96(14):7980-5.
40. Schonborn I, Zschiesche W, Behrens J, Herrenknecht K, Birchmeier W. Expression of E-cadherin/catenin complexes in breast cancer. *Int J Oncol* 1997; 11(6):1327-34.
41. Qureshi HS, Linden MD, Divine G, Raju UB. E-cadherin status in breast cancer correlates with histologic type but does not correlate with established prognostic parameters. *Am J Clin Pathol* 2006; 125(3):377-85.
42. Gonzalez-Angulo AM, Sahin A, Krishnamurthy S, et al. Biologic markers in axillary node-negative breast cancer: differential expression in invasive ductal carcinoma versus invasive lobular carcinoma. *Clin Breast Cancer* 2006; 7(5):396-400.
43. Kelly KF, Daniel JM. POZ for effect--POZ-ZF transcription factors in cancer and development. *Trends Cell Biol* 2006; 16(11):578-87.
44. Costoya JA, Pandolfi PP. The role of promyelocytic leukemia zinc finger and promyelocytic leukemia in leukemogenesis and development. *Curr Opin Hematol* 2001; 8(4):212-7.

45. Reljic R, Wagner SD, Peakman LJ, Fearon DT. Suppression of signal transducer and activator of transcription 3-dependent B lymphocyte terminal differentiation by BCL-6. *J Exp Med* 2000; 192(12):1841-8.
46. Wagner SD, Ahearne M, Ferrigno PK. The role of BCL6 in lymphomas and routes to therapy. *Br J Haematol* 2011; 152(1):3-12.
47. Chen WY, Zeng X, Carter MG, et al. Heterozygous disruption of *Hic1* predisposes mice to a gender-dependent spectrum of malignant tumors. *Nat Genet* 2003; 33(2):197-202.
48. Lopes EC, Valls E, Figueroa ME, et al. Kaiso contributes to DNA methylation-dependent silencing of tumor suppressor genes in colon cancer cell lines. *Cancer Res* 2008; 68(18):7258-63.
49. Park JI, Ji H, Jun S, et al. Frdod links Dishevelled to the p120-catenin/Kaiso pathway: distinct catenin subfamilies promote Wnt signals. *Dev Cell* 2006; 11(5):683-95.
50. Peek RM, Ogden SR, Wroblewski LE, et al. p120 and Kaiso Regulate Helicobacter pylori-induced Expression of Matrix Metalloproteinase-7. *Mol Bio Cell* 2008; 19(10):4110-21.
51. Iioka H, Doerner SK, Tamai K. Kaiso is a bimodal modulator for Wnt/beta-catenin signaling. *FEBS Lett* 2009; 583(4):627-32.
52. Zhang PX, Wang Y, Liu Y, et al. p120-catenin isoform 3 regulates subcellular localization of Kaiso and promotes invasion in lung cancer cells via a phosphorylation-dependent mechanism. *Int J Oncol* 2011; 38(6):1625-35.
53. Perez-Moreno M, Davis MA, Wong E, et al. p120-catenin mediates inflammatory responses in the skin. *Cell* 2006; 124(3):631-44.
54. Stairs DB, Bayne LJ, Rhoades B, et al. Deletion of p120-catenin results in a tumor microenvironment with inflammation and cancer that establishes it as a tumor suppressor gene. *Cancer Cell* 2011; 19(4):470-83.
55. Smalley-Freed WG, Efimov A, Short SP, et al. Adenoma formation following limited ablation of p120-catenin in the mouse intestine. *PLoS one* 2011; 6(5):e19880.
56. Davis MA, Reynolds AB. Blocked acinar development, E-cadherin reduction, and intraepithelial neoplasia upon ablation of p120-catenin in the mouse salivary gland. *Dev Cell* 2006; 10(1):21-31.
57. Dai SD, Wang Y, Zhang JY, et al. Upregulation of delta-catenin is associated with poor prognosis and enhances transcriptional activity through Kaiso in non-small-cell lung cancer. *Cancer Sci* 2011; 102(1):95-103.
58. Kelly KF, Otchere AA, Graham M, Daniel JM. Nuclear import of the BTB/POZ transcriptional regulator Kaiso. *J Cell Sci* 2004; 117(Pt 25):6143-52.
59. Korkola JE, DeVries S, Fridlyand J, et al. Differentiation of lobular versus ductal breast carcinomas by expression microarray analysis. *Cancer Res* 2003; 63(21):7167-75.
60. Zhao H, Langerod A, Ji Y, et al. Different gene expression patterns in invasive lobular and ductal carcinomas of the breast. *Mol Biol Cell* 2004; 15(6):2523-36.
61. de Leeuw WJ, Berx G, Vos CB, et al. Simultaneous loss of E-cadherin and catenins in invasive lobular breast cancer and lobular carcinoma in situ. *J Pathol* 1997; 183(4):404-11.



# Eight

## **FER kinase promotes breast cancer growth and metastasis through inhibition of cell adhesion and anchorage dependence**

Iordanka A. Ivanova<sup>1</sup>, Jeroen F. Vermeulen<sup>1</sup>, Cigdem Ercan<sup>1</sup>,  
Julia M. Houthuijzen<sup>1</sup>, Farah Al Saig<sup>1</sup>, Eva J. Vlug<sup>1</sup>, Elsken van der Wall<sup>2</sup>,  
Paul J. van Diest<sup>1</sup>, Marc Vooijs<sup>1,3</sup>, Patrick W.B. Derksen<sup>1</sup>

<sup>1</sup> Department of Pathology, University Medical Center Utrecht, Utrecht, The Netherlands,

<sup>2</sup> Division of Internal Medicine and Dermatology, University Medical Center Utrecht, Utrecht, The Netherlands,

<sup>3</sup> Department of Radiation Oncology, Maastricht University Medical Center+, Maastricht, The Netherlands

***Submitted***

## Abstract

**Introduction:** The Feline Sarcoma (FES) and FES-related kinase (FER) proteins are the two members of a family of non-receptor tyrosine kinases, which have been implicated in cell adhesion and the regulation of the actin cytoskeleton. Since metastatic breast cancer cells are characterized by aberrant adhesive and migratory properties, we studied whether FER is involved in breast cancer development and progression.

**Methods:** We used human breast cancer cells to determine the contribution of FER to cell adhesion, migration and invasion. Further, a mouse xenograft breast cancer model was used to investigate the role of FER in tumor growth and metastasis. Finally, we examined FER expression in 485 cases of invasive breast carcinoma by immunohistochemistry.

**Results:** RNAi-mediated downregulation of FER in metastatic cells inhibited invasion and migration through increased  $\alpha_6$  and  $\beta_1$  integrin-dependent cell adhesion. Conversely, overexpression of FER in non-metastatic breast cancer cells induced lamellipodia formation and increased cell migration. In agreement with the pro-metastatic role of FER *in vitro*, we found that inducible FER downregulation inhibited tumor growth and the formation of distant metastases. High FER expression was significantly associated with tumor size, grade and mitotic activity. We found that basal/triple negative tumors have higher FER levels as compared to luminal carcinomas. High FER expression correlated with a significantly worse prognosis based on overall survival. Further, multivariate analysis revealed that high FER expression is an independent prognostic factor.

**Conclusions:** Our data indicate that FER regulates tumor growth and metastasis of invasive breast cancer.



## Introduction

Breast cancer is the second most commonly occurring cancer worldwide with 1.38 million new cases diagnosed in 2008, and the leading cause of cancer mortality in women [1]. Advancements in diagnostics and treatment have increased breast cancer survival rates, but still approximately one third of patients will develop distant metastases and eventually die of the disease [2]. Targeted therapies have improved survival in patients with HER2-positive metastatic disease [3]. However, further insight into the molecular processes underlying metastasis is needed to identify new potential drug targets.

The feline sarcoma (FES) and FES-related (FER) proteins are the only two members of a unique family of non-receptor tyrosine kinases. They are distinguished from other tyrosine kinases by an N-terminal FES/FER/CIP4 homology (FCH) domain, which is also found in Rho GTPase activating proteins (RhoGAPs) and adaptor proteins involved in regulation of cytoskeletal rearrangements, cell polarity, vesicular trafficking and endocytosis [4].

FER is ubiquitously expressed and its subcellular localization is cytoplasmic [5, 6]. Upon activation by growth factors FER can associate with and phosphorylate the adherens junction (AJ) molecule p120-catenin (p120) and actin binding protein cortactin [7, 8]. FER indirectly associates with N-cadherin via p120 and is necessary for maintaining AJ stability [9, 10]. However, others have reported that FER overexpression may lead to AJ dissolution and loss of focal adhesions (FAs) [11]. FER can shuttle between N-cadherin-containing AJs and  $\beta_1$  integrin FA complexes, thus coordinately regulating cell-cell and cell-extracellular matrix (ECM) adhesion [12]. FER-mediated cortactin phosphorylation is associated with fibroblast migration [13]. Additionally, FER has been shown to regulate migration in several other cell types [14-16].

Several lines of evidence support a role of FER in malignant progression. FER regulates cell cycle progression in prostate and breast cancer, as well as in AML cells [17, 18]. Further, FER is highly expressed in prostate cancer as compared to normal prostate epithelium and regulates prostate cancer cell proliferation by activating STAT3 [19, 20]. Increased FER expression is associated with hepatocellular carcinoma (HCC) metastasis and FER downregulation inhibits invasion of metastatic HCC cells [21]. Also, recent data indicate that FER can mediate resistance to the anti-cancer agent quinacrine via activation of NF- $\kappa$ B, which could have therapeutic implications [22].

These observations prompted us to investigate the role of FER in breast cancer progression. Here we show that FER regulates breast cancer cell adhesion, migration and anoikis resistance and is necessary for tumor growth and metastasis formation. Moreover, FER expression is high in poorly differentiated breast carcinomas and independently predicts decreased patient survival.

## Methods

### *Cell culture and transfections*

MCF10A, MCF10CA1a, MCF10CA1a.cl1 and MCF10CA1d.cl1 cells [23] were obtained from the Barbara Ann Karmanos Cancer Institute (Detroit, MI, USA). All other cell lines, except MDA-MB-453, ZR-75-30, CAMA-1, SKBR3, MDA-MB-330 (ATCC), SUM44PE (Asterand, Inc.) and MDA-MB-231/Luc<sup>+</sup> [24], were from Cell Lines Service (Eppelheim, Germany). Cell lines from non-commercial sources were authenticated by STR profiling. Cell culture conditions are described in the Supplementary Methods.

*Silencer* Negative Control #1 (AM4611) and *Silencer* Validated siRNAs targeting FER kinase (AM51323; siRNA ID# 657 and 658) were purchased from Ambion. MDA-MB-231 cells were transfected with 80 nM siRNA using Lipofectamine 2000 transfection reagent (11668500; Invitrogen).

### *Constructs, virus generation and cell transduction*

The cloning strategy used to generate lenti viral vectors encoding wild-type (WT) and kinase dead (D742R) [25] FER (D742D FER) is described in the Supplementary Methods. Inducible shRNA-expressing lenti virus construct generation, lenti virus production and transduction have been described previously [26]. Oligonucleotide sequences are shown in the Supplementary Methods.

### *Immunoblotting*

Cell lysates were prepared and analyzed as described [27].

### *Immunofluorescence analysis*

Specimens for immunofluorescence microscopy were prepared as described [28]. Primary antibodies used were: rat anti-human CD49f (555734, BD Pharmingen) 1:300, rat anti-integrin  $\beta_1$  (A1B2, Developmental Studies Hybridoma Bank, The University of Iowa, Iowa City, USA) 1:200, rabbit anti-paxillin pY<sup>118</sup> (44-722; Invitrogen) 1:500. Secondary antibodies were: Alexa Fluor 488 goat anti-rat IgG (A11006) and Alexa Fluor 555 goat anti-rabbit IgG (A21429, Invitrogen) 1:1,000. F-actin was visualized with Alexa Fluor 633-conjugated phalloidin (A22284; Invitrogen) 1:200. Confocal analysis was conducted with a Plan-Apochromat 63x/1.40 Oil DIC M27 objective mounted on an inverted Carl Zeiss LSM 700 Laser Scanning Microscope. Images were acquired and analyzed with ZEN 2010 software (Carl Zeiss International).

### *Adhesion assay*

Adhesion assays were performed as described [29] with some modifications. Wells of 96 well tissue culture plates were coated with collagen I (8  $\mu\text{g}/\text{cm}^2$ ), fibronectin (3  $\mu\text{g}/\text{cm}^2$ ) or laminin (10  $\mu\text{g}/\text{cm}^2$ ) overnight at 4°C.

### *Integrin expression measurement*

Cells were prepared for flow cytometry as described [29]. The following primary antibodies and dilutions were used: mouse anti- $\alpha_2$  integrin (clone 10G11; 1:100), mouse anti- $\alpha_3$  integrin (clone J143; 1:2), mouse anti- $\alpha_v$  integrin (clone 13C2; 1:10), rat anti- $\beta_1$  integrin (clone A11B2; 1:200), rat anti- $\alpha_5$  integrin (clone M16; 1:1,000), rat anti- $\alpha_6$  integrin (555734, BD Pharmingen; 1:100). The secondary antibodies and dilutions used were: Alexa Fluor 488 goat anti-mouse IgG (A11001, Invitrogen; 1:500), Alexa Fluor 488 goat anti-rat IgG (A11006, Invitrogen, 1:500). Integrin expression was measured with a FACSCalibur flow cytometer (Becton Dickinson) using CellQuest Pro software.

### *Migration assay*

The 96-well Oris Cell Migration Kit (CMAU101; Platypus Technologies) was used for cell migration assays. Wells were coated with 8  $\mu\text{g}/\text{cm}^2$  collagen I (C3867; Sigma) for 2 h at room temperature. Following two washes in PBS silicone stoppers were inserted in the wells to create “exclusion zones”. Cells were plated in triplicate wells (15,000 cells/well) and incubated at 37°C overnight. The medium was replaced with serum-free DMEM/2.5% BSA and cells were incubated for 8 h at 37°C prior to removing the silicone stoppers to start the assay by allowing cells to migrate into the exclusion zone. Cells were incubated for 24 h at 37°C, fixed with 3.7% formaldehyde and stained with 0.05% crystal violet. Migration was quantified by taking low magnification images of each well, measuring the remaining area of the exclusion zone using Adobe Photoshop CS3 Extended and comparing it to the exclusion zone area in reference wells (no migration).

### *Matrigel outgrowth assay*

BD Matrigel Basement Membrane Matrix (356234; BD Biosciences) was diluted 1:1 with normal growth medium and 40  $\mu\text{l}$ /well were added to 96-well, flat bottom, optical plastic plates (3720; Costar). Plates were incubated at 37°C for 15 min to allow the Matrigel to solidify. MDA-MB-231 cells were seeded at a density of 3,000 cells/well in 200  $\mu\text{l}$  of normal growth medium and cultured for 4 days at 37°C. Cultures were fixed with 3.7% formaldehyde/PBS for 30-40 min, followed by permeabilization with 0.1% Triton-X/PBS for 20 min at room temperature. Confocal analysis was conducted with a long working distance LD Plan-Neofluar 40x/0.6 Korr M27 objective mounted on an inverted Carl Zeiss LSM 700 Laser Scanning Microscope. Images were acquired and analyzed with ZEN 2010 software

(Carl Zeiss International).

#### *Anoikis assay*

MDA-MB-231 cells were seeded in Ultra Low Attachment 24-well plates (3473; Costar) at 100,000 cells/well in duplicate and cultured in DMEM containing 1% FCS at 37°C for 72 hours. The percentage of anoikis resistant cells was determined as described [26].

#### *Mouse studies*

Female *RAG2<sup>-/-</sup>;IL-2R $\gamma$ <sup>-/-</sup>* immunodeficient mice [30] were a kind gift from The Netherlands Cancer Institute, Amsterdam, The Netherlands. Orthotopic transplantations and bioluminescence imaging were performed as described [26], with some modifications. Approximately  $1 \times 10^6$  luciferase-expressing MDA-MB-231 cells were injected using a 50 $\mu$ l Hamilton syringe. Tumor growth was measured using a digital caliper (VWR) on a weekly basis. Upon development of palpable tumors mice were switched from a standard diet to doxycycline-containing chow (S3888; Bio-Serv) for the remainder of the experiment. Mice were sacrificed when tumor volume exceeded 1,000 mm<sup>3</sup> or when bioluminescence imaging revealed metastases.

#### *Clinical samples and immunohistochemistry (IHC)*

The clinical sample set and tissue microarray assembly have been previously described [31]. IHC antigen retrieval methods, antibodies and detection have been described previously [31]. The protocol used to detect FER was as follows: antigen retrieval by boiling for 20 min in 10mM citrate pH 6.0. A cooling period of 30 min, followed by incubation with anti-FER antibody (1:300; clone 5D2, Cell Signaling Technologies) for 1h at room temperature.

#### *Scoring of immunohistochemistry*

All scoring was done by two individual observers blinded to patient characteristics and results of other staining, as described [31]. FER staining was scored based on the intensity of the cytosolic staining, scores of 0 and 1+ were scored as low and 2+ and 3+ were scored as high intensity.

#### *Statistical analysis*

All statistical analyses were performed using IBM SPSS Statistics version 18.0 (SPSS Inc., Chicago, IL, USA). For clinical samples associations between categorical variables were examined using Pearson's Chi-square test. Survival analysis was performed with the Kaplan-Meier method. Multivariate analysis was performed using Cox regression. In the model, tumor size, tumor grade, age, lymph node status, histology, MAI, Sorlie/Perou classification, BRCA mutation status, and FER expression were taken into account.

Differences in tumor volume were evaluated using a two-way mixed model ANOVA with TIME (weeks) as the repeated factor and GROUP (control, FER[680-698] and FER[980-998]) as factor 2. Tukey's test was used for post-hoc analysis. All other data were analyzed with one-way ANOVA. Data are presented as mean  $\pm$  SEM. P-values  $<0.05$  were considered to be statistically significant.

#### *Study approval*

All animal experiments were approved by the Utrecht University Animal Experimental Committee (DEC-Utrecht no. 2010.III.10.120). The use of anonymous or coded left over material for scientific purposes is part of the standard treatment contract with patients in The Netherlands [32]. Ethical approval was not required.

## Results

To establish a working model to study the role of FER in breast cancer we examined FER expression in a panel of 18 breast carcinoma cell lines (Figure 1A). FER was almost undetectable in non-transformed MCF10A cells, and its level was low to moderate in non-invasive cells and cell lines with low metastatic potential. Notably, FER was most highly expressed in MDA-MB-231, a basal-like and metastatic breast cancer cell line.

### *FER regulates breast cancer cell morphology, actin cytoskeleton organization and ECM adhesion*

Because FER has been linked to actin cytoskeleton regulation [8], we analyzed the effect of RNAi-mediated FER inhibition on cellular morphology and actin distribution in MDA-MB-231 cells. Transfection with two independent siRNAs significantly downregulated FER expression as compared to a scrambled, control siRNA (Figure 1B). FER knock-down (KD) in MDA-MB-231 cells induced cell spreading accompanied by the formation of prominent F-actin stress fibers. In addition, we observed FA reorganization (Figure 1C). These data suggest that FER controls actin dynamics, FA distribution and cells spreading, and that FER inhibition may lead to increased cell adhesion. To determine whether this is the case we seeded control and FER KD cells on different ECM substrates and measured their ability to adhere. We found that FER KD significantly increased MDA-MB-231 cell adhesion to collagen I and laminin, while adhesion to fibronectin was increased to a lesser extent by one of the siRNAs tested (Figure 2A).

Integrin receptors regulate cell-ECM adhesion, motility and anchorage-dependent survival. To investigate if the increased cell adhesion we observed upon FER KD was due to changes in integrin levels, we measured cell surface expression of  $\alpha_3$ ,  $\alpha_5$ ,  $\alpha_6$ ,  $\alpha_v$  and  $\beta_1$  integrin subunits in control and FER KD cells. While we did not find significant changes in the expression of  $\alpha_3$ ,  $\alpha_v$  and  $\alpha_5$  integrins, cell surface levels of  $\beta_1$  and  $\alpha_6$  integrins were significantly upregulated in FER KD as compared to control cells (Figure 2B). These results suggest that FER may regulate  $\beta_1$  and  $\alpha_6$  integrin subcellular distribution.

To investigate the effect of FER downregulation on  $\beta_1$  and  $\alpha_6$  integrin localization control and FER KD cells were seeded on different ECM substrata and analyzed by immunofluorescence microscopy. Both  $\alpha_6$  and  $\beta_1$  integrins co-localized with phosphorylated paxillin in FAs of FER KD cells (Figure 3). Further, we observed accumulation of  $\alpha_6$  integrin on the cell membrane and in endosomal vesicles upon FER inhibition (Supplementary Figure 1). To determine whether cell spreading and stress fiber formation in FER KD cells are dependent on integrin activation, we treated cells with blocking antibodies prior to plating them on collagen I or laminin.

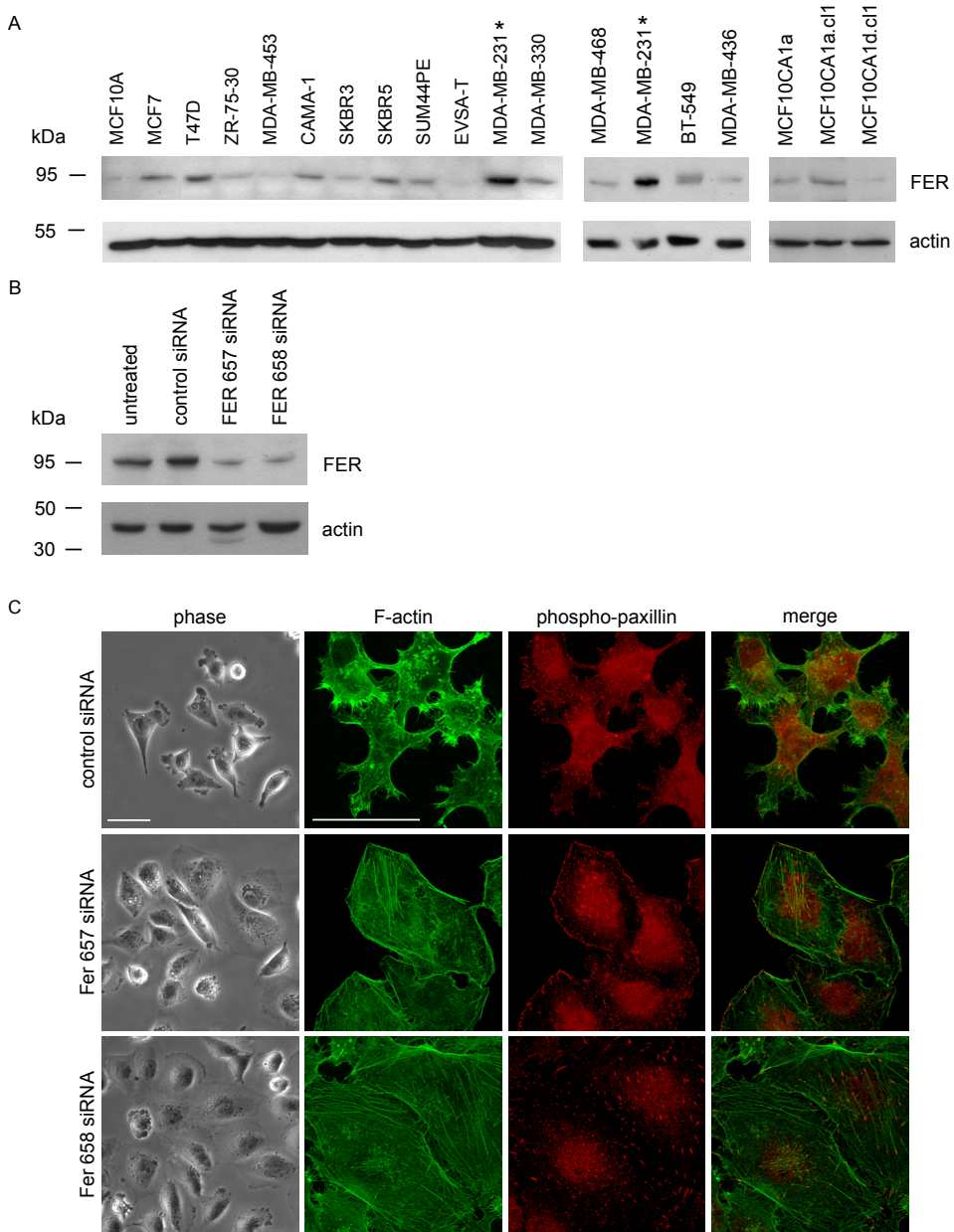


**Figure 1. Inhibition of FER induces cell spreading, actin stress fiber and focal adhesion formation.** (A) Total cell lysates of the indicated breast cancer cell lines were prepared and resolved by SDS-PAGE. FER kinase expression was analyzed by immunoblot. \* indicates that lysates from the same cell line were loaded on different gels. (B) Knock-down (KD) of FER in MDA-MB-231 cells using siRNA transfection. FER expression was analyzed by immunoblot 72 h post-transfection. Actin was used as a loading control. (C) Control and MDA-MB-231 KD cells were plated on collagen I-coated glass coverslips. The morphology of live cells was analyzed by phase contrast microscopy (phase). F-actin (green) and phospho-paxillin (red) distribution was analyzed in fixed cells by immunofluorescence microscopy. Scale bar = 50  $\mu$ m. The results shown are representative of three independent experiments.

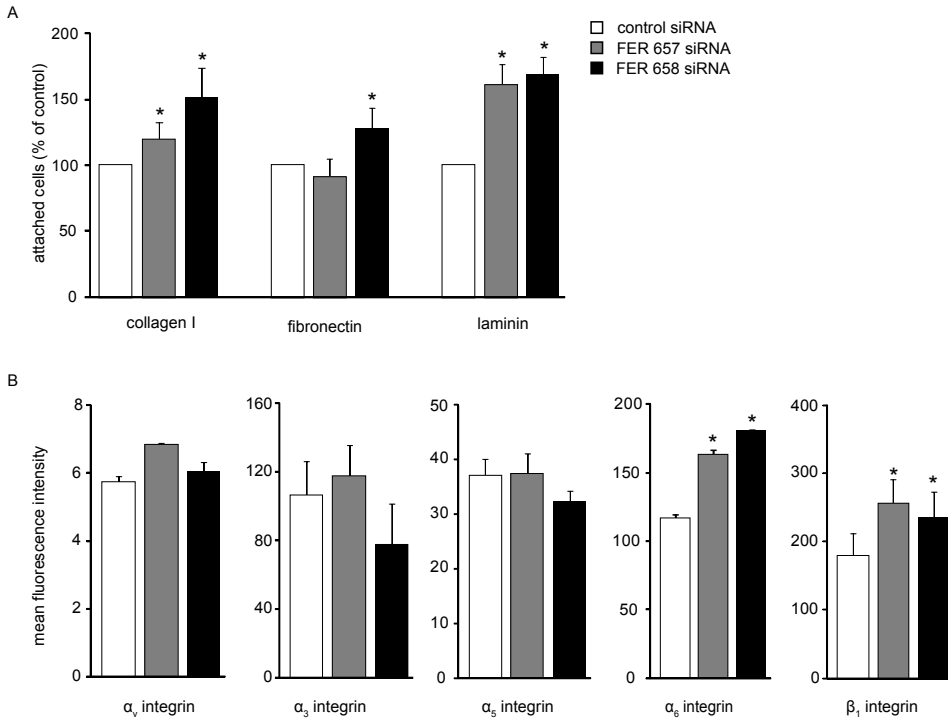
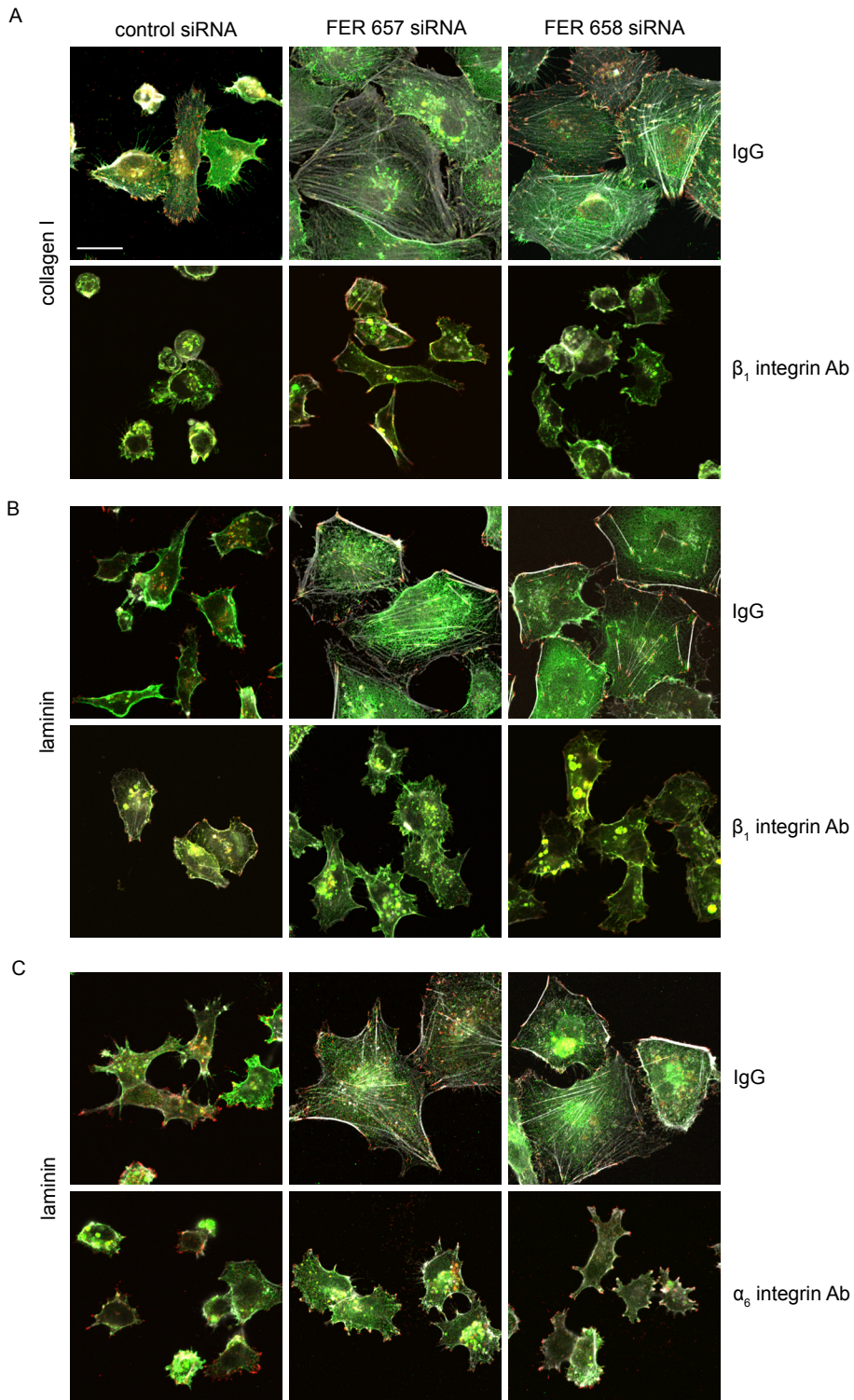


**Figure 2. FER regulates cell-matrix adhesion and integrin expression in breast cancer cells.** (A) MDA-MB-231 FER knock-down (KD) cells were generated by transient transfection with the indicated siRNAs. FER KD cells were plated on 96-well plates coated with collagen I, fibronectin or laminin and the percentage of attached cells was determined. Values represent the relative proportion of attached cells  $\pm$  SEM. \* indicates significantly different proportions of adherent cells, relative to control ( $p < 0.05$ , one-way ANOVA). (B) FER KD cells were trypsinized and surface expression of the indicated integrin subunits was analyzed by FACS. Values represent mean fluorescence units  $\pm$  SEM. \* indicates significantly different integrin levels as compared to control ( $p < 0.05$ , one-way ANOVA). The results shown are representative of three independent experiments.

Cell spreading and stress fiber formation were inhibited upon treatment with a  $\beta_1$  integrin-blocking antibody, indicating that FER KD induced  $\beta_1$  integrin-dependent adhesion to collagen I and laminin (Figure 3A and B). Similar results were observed with an  $\alpha_6$  integrin blocking antibody in cells seeded on laminin (Figure 3C). These results are consistent with the concept that FER inhibition promotes cell adhesion via  $\beta_1$  and  $\alpha_6$  integrin-dependent formation of FAs.

**Figure 3. Focal adhesion and actin stress fiber formation in FER-depleted cells is  $\beta_1$  and  $\alpha_6$  integrin-dependent.** MDA-MB-231 cells were transfected with the indicated siRNAs and cultured for 96 h. Cells were trypsinized and incubated with isotype control (IgG) or integrin-blocking antibodies and re-plated on glass coverslips coated with collagen I (A) or laminin (B and C). Cells were processed for immunofluorescence microscopy using anti- $\beta_1$  or - $\alpha_6$  integrin antibodies (green), anti-phospho-paxillin (red) and Alexa 633-labelled phalloidin (grey) to visualize focal adhesions and F-actin, respectively. Scale bar = 20  $\mu$ m. The results shown are representative of three independent experiments.





### *FER controls breast cancer cell migration, invasion and anoikis-resistance*

The ability of FER to regulate actin dynamics, lamellipodia formation and integrin-dependent adhesion, suggested that it may control cell motility and invasion of breast cancer cells. To determine the effect of FER downregulation on MDA-MB-231 cell migration, we started by using a modified wound healing assay. We employed a doxycycline (dox)-inducible and lentivirus-based shRNA approach to enable inducible knock-down (iKD) of FER in MDA-MB-231 cells (Figure 4A). FER iKD using two independent shRNA sequences significantly inhibited the ability of MDA-MB-231 cells to migrate on a collagen I-coated surface, as compared to control cells (Figure 4B). In a complementary experiment we transduced MCF10A.CA1d, a basal-like breast cancer cell line with low endogenous FER expression, using lenti viruses encoding V5-tagged wild-type (WT) and kinase-deficient (D742R) mutant FER (Supplementary Figure 2A). Overexpression of WT, but not D742R FER, significantly increased lamellipodia formation and migration of MCF10A.CA1d cells (Supplementary Figure 2B and C). In addition, WT FER localized to the leading edges of lamellipodia, whereas D742R FER did not (Supplementary Figure 2C, arrows). These results indicate that regulation of lamellipodia formation and cell migration by FER is dependent on its kinase activity.

The ability of FER to regulate cell motility and lamellipodia formation suggested that it may be involved in breast cancer cell invasion. The invasive *in vivo* behavior of MDA-MB-231 cells can be recapitulated *ex vivo* by culturing the cells on a laminin-rich extracellular matrix substrate (IreCM; Matrigel) in 3D [33]. Control iKD cells formed highly branched, invasive and disorganized colonies when cultured on IreCM (Figure 4C). In contrast, FER iKD resulted in non-invasive cell colonies (Figure 4C), suggesting that FER is necessary for breast cancer cell invasion and migration in IreCM. Thus, our results indicate that downregulation of FER increases integrin-mediated cell adhesion, whilst inhibiting migration and invasion.

Normal epithelial cells require ECM attachment for survival. Detachment from the ECM or inappropriate engagement of integrin receptors results in programmed cell death in a process termed anoikis [34]. Anoikis resistance has been strongly implicated in the formation of distant metastases [35]. Having observed increased integrin-dependent adhesion upon FER KD in breast cancer cells, we reasoned that this could lead to decreased anoikis resistance. To test this hypothesis we cultured control and FER iKD MDA-MB-231 cells in suspension and measured anoikis-resistance. Interestingly, we found a significant decrease in anoikis resistance upon FER iKD using two independent shRNA sequences (Figure 4D). These results suggest that FER may regulate anchorage-independent survival in breast cancer cells.

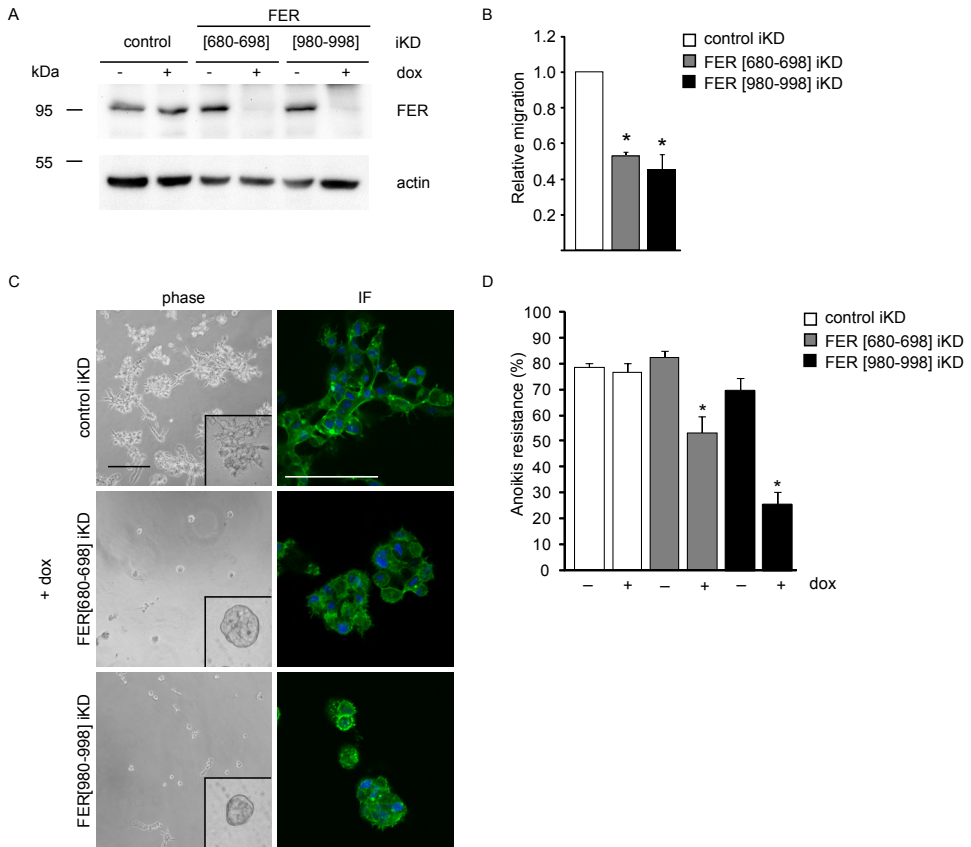


**Figure 4. FER kinase regulates migration, invasion and anoikis resistance in breast cancer cells.** (A) MDA-MB-231 inducible knock-down (iKD) cells were cultured for 96 h in the absence (-) or presence (+) of doxycycline (dox; 2  $\mu$ g/ml) to induce shRNA expression and FER kinase was detected by immunoblot. Actin was used as a loading control. (B) MDA-MB-231 iKD cells treated as in (A) were seeded on collagen I-coated plates and the rate of migration was measured over 24 h using a modified wound-healing assay. Values represent the ratio of the migration rate of untreated *versus* dox-treated cells  $\pm$  SEM. All values were normalized to control. \* indicates significantly different migration rates, relative to control ( $p < 0.05$ , one-way ANOVA). (C) MDA-MB-231 iKD cells treated as in (A) were plated on laminin-rich extracellular matrix substrate (Matrigel) and cultured for 96 h in the presence of dox. Cells were imaged by phase contrast (phase) or immunofluorescence (IF) microscopy using Alexa 488-labelled phalloidin and DAPI to visualise F-actin (green) and DNA (blue), respectively. Images represent a single Z position in the centre of 3D cell structures. Scale bar = 100  $\mu$ m. (D) Adherent cultures of MDA-MB-231 iKD cells were treated as in (A). Cells were trypsinized and cultured in suspension conditions for 72 h in the absence or presence of dox (2  $\mu$ g/ml), followed by labelling with Cy5-conjugated Annexin V (AnnV) and propidium iodide (PI) and FACS analysis. Values represent the percentage of anoikis resistant cells ( $PI^{NEG}/AnnV^{NEG}$ )  $\pm$  SEM. \* indicates a significant difference compared to untreated cells (-dox); ( $p < 0.05$ , one-way ANOVA). The results shown are representative of three independent experiments.

*FER is necessary for breast tumor growth and metastasis formation*

To study the role of FER in breast tumor growth and metastasis, we orthotopically transplanted luciferase-expressing MDA-MB-231 FER iKD cells in *RAG2<sup>-/-</sup>;IL-2Rγ<sup>c/-</sup>* immunodeficient mice [30] and measured tumor growth over time. Since FER KD can inhibit cell cycle progression in several cancer cell lines, including MDA-MB-231 ([17] and Supplementary Figure 3) we transplanted untreated cells, monitored animals until palpable tumors of approximately 50 mm<sup>3</sup> formed in all three groups and then started dox administration to induce FER shRNA expression (Figure 5A, arrow). Expression of both FER shRNAs significantly inhibited tumor growth as compared to the control shRNA (Figure 5A). Furthermore, control tumors were highly invasive, whereas FER iKD resulted in non-invasive tumors with clearly defined borders that were confined to the mammary fat pad (Figure 5B). Next, we used immunohistochemistry (IHC) to detect FER protein in tumor samples. We could confirm that FER expression was downregulated in tumors expressing both FER shRNAs as compared to controls (Figure 5B). In addition, and consistent with the observed tumor volume (Figure 5A), we detected higher FER levels in FER[680-698] iKD than FER[980-998] iKD tumors (Figure 5B). Moreover, we could show using bioluminescence imaging that FER iKD inhibited the development of distant metastases (Figure 5C). Whereas all mice in the control group developed metastases in the spleen, liver, lungs and bones (Figure 5D), mice in the FER[680-698] iKD group developed metastases with decreased frequency and increased latency. In conjunction with the level of FER KD mice in the FER[980-998] iKD group did not develop metastases by 14 weeks of follow-up. The inhibition of metastasis formation was not due to reduced primary tumor growth, as the tumor volumes in these mice were comparable to those in the control group at 7 weeks (Supplementary Figure 4). These results indicate that FER is necessary for breast tumor growth and metastasis formation.

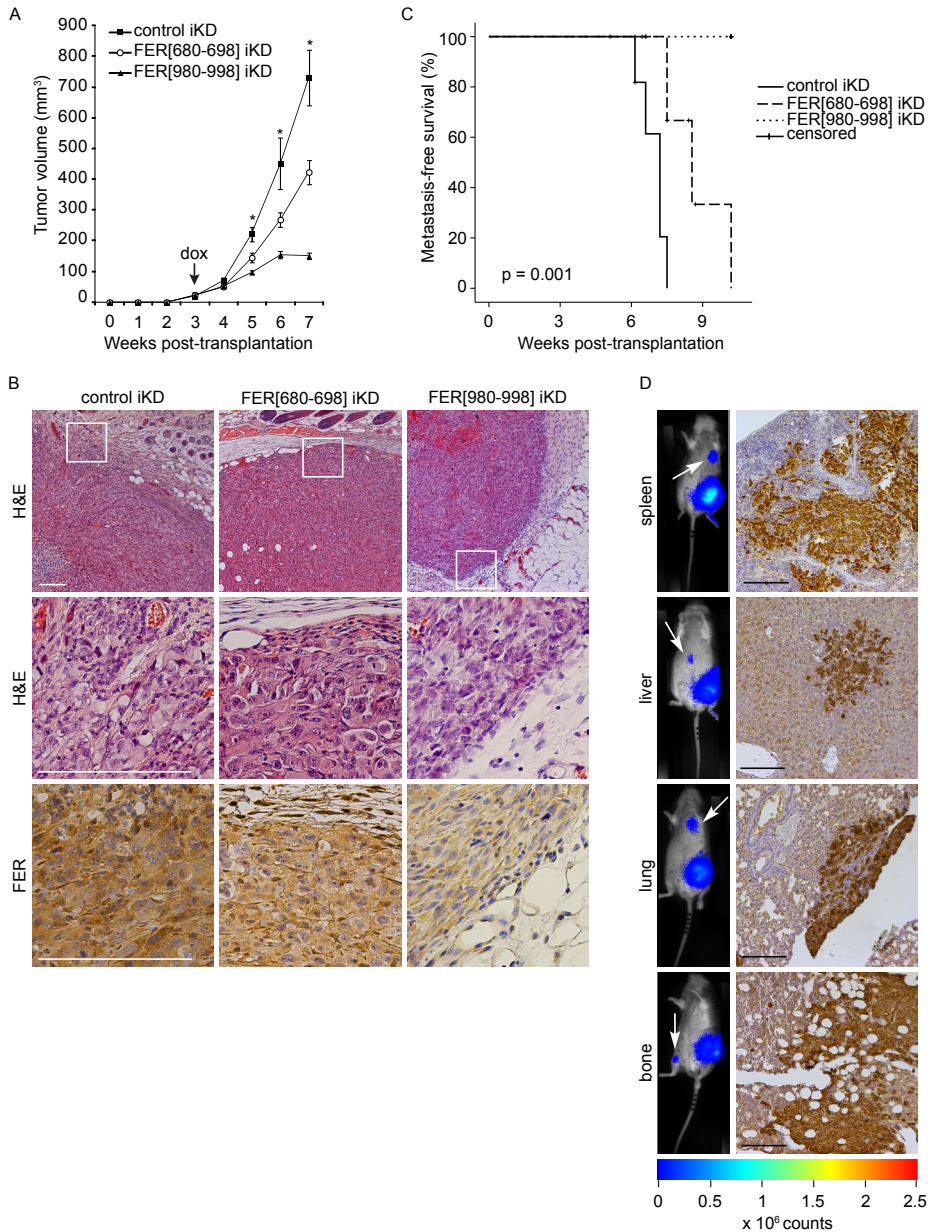


**Figure 5. FER regulates breast tumor growth and metastasis.** (A) Luciferase-expressing MDA-MB-231 inducible knock-down (iKD) cells were orthotopically transplanted into recipient mice. Upon development of palpable tumors mice were switched to a doxycycline-containing diet (dox; arrow) to induce shRNA expression. Values represent the mean tumor volume  $\pm$  SEM. \*  $p < 0.05$   $n = 12$  (control and FER[980-998] iKD),  $n = 13$  (FER[680-698] iKD). (B) Hematoxylin and eosin (H&E) and immunohistochemical (IHC) staining for FER in primary tumors from mice transplanted with the indicated cell lines. Scale bar = 200  $\mu$ m. (C) Kaplan-Meier metastasis-free survival plot. Animals were monitored by bioluminescence and sacrificed when distant metastases developed. (E) Control-iKD cells were transplanted and metastatic spread was assessed using bioluminescence imaging (left; arrow). IHC staining for vimentin was performed to visualize distant metastases of control tumors. Scale bar = 100  $\mu$ m.

*FER expression is associated with aggressive breast cancer and correlates with decreased patient survival*

To extend our experimental findings that implicate FER in breast cancer progression we examined its expression in a tissue microarray or 485 cases of invasive breast carcinoma (Table S1) by IHC. While high FER expression did not correlate with histological breast cancer sub-types, we observed that within the invasive lobular carcinoma group FER levels were significantly higher in pleomorphic ( $p < 0.001$ ) as compared to classical tumors (Figure 6A, Table 1). Overall, high FER expression was significantly associated with tumor size ( $p = 0.003$ ), tumor grade ( $p < 0.001$ ) and mitotic activity ( $p < 0.001$ ; Table 1). Interestingly, basal-type tumors showed higher FER levels than luminal-type carcinomas ( $p = 0.003$ ).

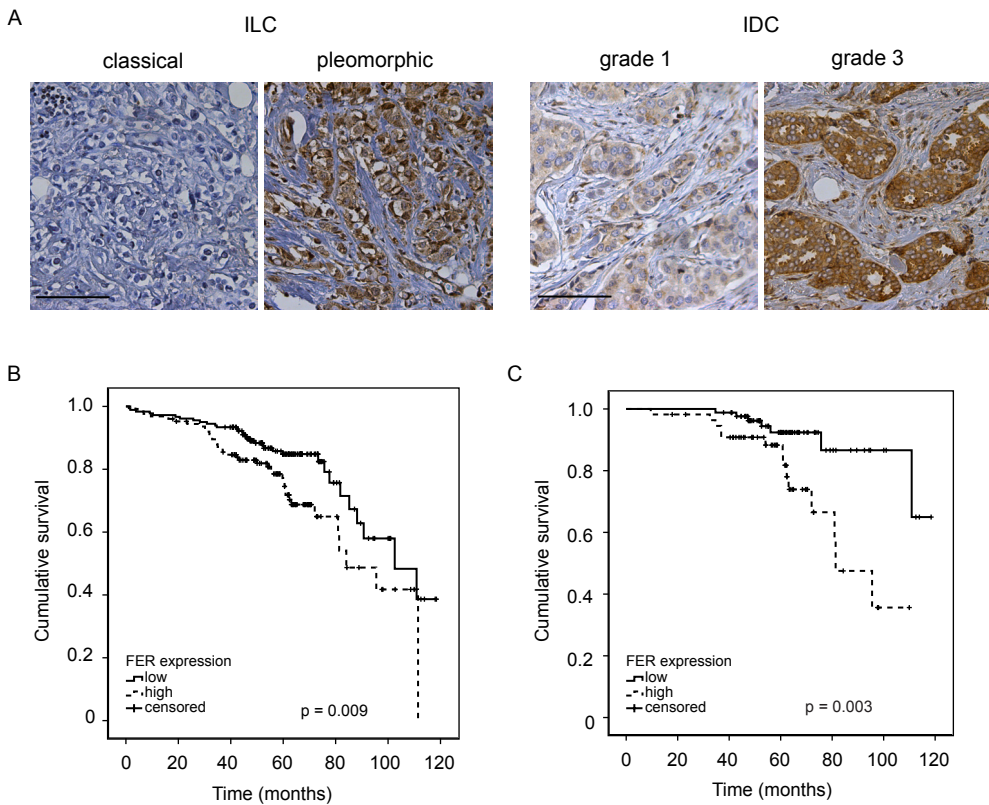


**Figure 6. FER kinase expression correlates with decreased patient survival.** (A) Clinical specimens of invasive lobular carcinoma (ILC) and invasive ductal carcinoma (IDC) were analyzed for FER kinase expression by immunohistochemistry. Note the differential FER expression in classical *versus* pleomorphic ILC, and grade 1 *versus* grade 3 IDC. Scale bar = 100  $\mu$ m. (B) Kaplan-Meier survival curves according to FER expression status ( $n = 293$ ). (C) Kaplan-Meier survival curves of patients with lymph node-negative breast cancer according to FER expression status ( $n = 141$ ).

**Table 1.** Correlation of FER kinase expression with clinicopathological and molecular features of invasive breast cancer.

Feature	N	FER expression		p-value
		Low (0-1+) N (%)	High (2-3+) N (%)	
Histological type				
IDC	320	171 (53.4)	149 (46.6)	
ILC	126	78 (61.9)	48 (38.1)	
Other	39	23 (59.0)	16 (41.0)	0.250
Histological grade				
1	88	63 (71.6)	25 (28.4)	
2	171	110 (64.3)	61 (35.7)	
3	219	94 (42.9)	125 (57.1)	<b>&lt;0.001</b>
MAI (per 2 mm <sup>2</sup> )				
≤ 12	239	164 (68.6)	75 (31.4)	
≥ 13	246	108 (43.9)	138 (56.1)	<b>&lt;0.001</b>
Tumor size				
pT1	208	134 (64.4)	74 (35.6)	
pT2	220	106 (48.2)	114 (51.8)	
pT3	49	29 (59.2)	20 (40.8)	<b>0.003</b>
Lymph node status				
Negative	227	133 (58.6)	94 (41.4)	
Positive	231	127 (55.0)	104 (45.0)	0.435
Invasive lobular carcinomas				
Classical	34	33 (97.1)	1 (2.9)	
Pleomorphic	56	17 (30.4)	39 (69.6)	<b>&lt; 0.001</b>
BRCA1				
Sporadic	459	266 (58.0)	193 (42.0)	
Mutation carrier	24	6 (25.0)	18 (75.0)	<b>0.002</b>
Perou / Sorlie classification				
Luminal	391	234 (59.8)	157 (40.2)	
HER2-driven	22	10 (45.5)	12 (54.5)	
Basal/Triple Negative	72	28 (38.9)	44 (61.1)	<b>0.003</b>
ER $\alpha$				
Negative	104	44 (42.3)	60 (57.7)	
Positive	381	228 (59.8)	153 (40.2)	<b>0.001</b>
PR				
Negative	200	106 (53.0)	94 (47.0)	
Positive	284	165 (58.1)	119 (41.9)	0.266
HER2				
Negative	435	246 (56.6)	189 (43.4)	
Positive	49	25 (51.0)	24 (49.0)	0.460
EGFR				
Negative	393	233 (59.3)	160 (40.7)	
Positive	83	34 (41.0)	49 (59.0)	<b>0.002</b>

Consistently, high FER expression was correlated with EGFR positivity ( $p=0.002$ ) and was inversely correlated with ER $\alpha$  expression ( $p=0.001$ ). These results indicate that FER is predominantly expressed in breast tumors with an aggressive phenotype.

In agreement with the association between FER expression and unfavorable clinicopathological variables, we found that patients with high FER expressing tumors had a significantly worse prognosis based on overall survival ( $p=0.009$ , Figure 6B). The correlation between high FER expression and poor clinical outcome was even more pronounced in the lymph node-negative group of patients ( $p=0.003$ , Figure 6C). Multivariate analysis revealed that high FER expression was a significant independent predictor of decreased overall survival (HR 1.785, 95%CI 1.068-2.982,  $p=0.027$ ), as were lymph node status (HR 2.868, 95%CI 1.675-4.910,  $p<0.001$ ), age (HR 1.050, 95%CI 1.030-1.069,  $p<0.001$ ) and tumor grade (HR 1.578, 95%CI 1.064-2.340,  $p=0.023$ ). Other clinicopathological features were not independent prognostic factors. These clinical findings support the pro-metastatic function of FER, which we have identified *in vitro* and in a mouse model of breast cancer. These data indicate that the ability of FER to potentiate breast cancer cell motility and invasiveness may lead to clinically more aggressive disease and decreased patient survival.



## Discussion

We established that FER is highly expressed in aggressive breast carcinomas and has a negative impact on prognosis. To our knowledge this is the first report that indicates a role of FER in breast cancer. We found a strong correlation between high FER expression and most unfavorable clinicopathological variables, except for lymph node status. However, high FER expression correlated with a poor prognosis in the lymph node-negative group of patients. Approximately 5-10% of patients have metastatic disease at the time of surgery in the absence of lymph node involvement [36] and up to 20% of lymph node-negative patients experience recurrence with distant metastases within 10 years after surgery [37]. Hematogenous tumor cell dissemination in lymph node-negative breast cancer patients is associated with decreased distant disease-free survival [38]. Our results indicate that FER promotes breast cancer cell migration and inhibits anchorage dependence, resulting in increased formation of distant metastases. Others have shown that hematogenous, rather than lymphatic, tumor cell dissemination leads to formation of distant metastases in a breast cancer mouse model [39]. Thus, the correlation between high FER expression and decreased survival in lymph-node negative patients suggests that FER may facilitate hematogenous metastasis.

Metastatic MDA-MB-231 breast cancer cells showed the highest FER protein expression, as compared to other breast cancer cell lines tested. MDA-MB-231 cells are hormone receptor-negative, overexpress EGFR and are classified as basal based on their gene expression profile [40, 41]. Further, they are unique in their capacity to spontaneously metastasize to different organs following orthotopic transplantation in recipient mice. Since we were unable to find a FER expression analogue of MDA-MB-231 cells we attempted to overexpress FER in several breast cancer cell lines. FER overexpression using a virus-based approach resulted in cell death of the non-invasive breast cancer cell lines MCF7 and T47D (data not shown). Likewise, constitutive expression of FER in a non-malignant rat fibroblast cell line (Rat-2) induced cell death [11]. Interestingly, FER overexpression in MCF10. CA1d cells potentiated their invasive characteristics. Since similar results were obtained in malignant prostate (PC3) [20], hepatocellular (Huh7) [42] and pancreatic (RWP1) carcinoma cells [43] we hypothesize that FER overexpression may be a relatively late event in malignant progression.

Inhibition of FER in MDA-MB-231 cells induces changes in cell morphology, including formation of actin stress fibers and FAs, which is consistent with RhoA activation. Indeed, actin stress fibers and FA formation in MDA-MB-231 cells is Rho-associated kinase (ROCK)-dependent and leads to decreased migration and increased anoikis sensitivity [44, 45]. In agreement with our data that loss of FER increases  $\alpha_6$  and  $\beta_1$  integrin expression and

adhesion to collagen I and laminin in breast cancer cells, others have shown that FER can regulate cell adhesion in other cell types. Inhibition of FER activity increased bone marrow-derived mast cell adhesion to fibronectin [14], while FER overexpression in Rat-2 fibroblasts led to cell detachment and anoikis [11]. Further, accumulation of FER in focal adhesion kinase/ $\beta_1$  integrin complexes was associated with decreased cell adhesion in neural retinal cells [12]. Although the exact mechanism whereby FER regulates FA formation is still unclear, these studies suggest that FER activity de-stabilizes FAs, thus inhibiting cell-ECM attachment. Conversely, we have shown that FER inhibition leads to FA formation, increased ECM attachment and reduced cell migration. Apart from decreased p130<sup>cas</sup> phosphorylation upon FER overexpression, the phosphorylation status of other FA molecules was unaltered [11]. It is possible that FER does not directly phosphorylate FA components, but rather regulates the localization of integrin receptors. FER contains an N-terminal FCH domain, which is also found in proteins involved in vesicular transport and endocytosis [4]. Although it has been suggested that FER may be involved in vesicular transport [6], it has not been established whether FER can regulate integrin trafficking. Our data indicated that FER KD induces accumulation of  $\alpha_6$  integrin at the cell membrane, as well as in endosomal vesicles, which suggests that FER may control recycling of  $\alpha_6$  integrin in metastatic breast cancer cells. The association and coordinate trafficking of the fibronectin-binding  $\alpha_5\beta_1$  integrin and EGFR by Rab-coupling protein promotes tumor cell migration and invasion [46]. However, this mechanism may be tumor type-specific as breast cancer cells express primarily collagen- and laminin-binding integrin heterodimers [47].

FER activation downstream of the integrin-ROS pathway is necessary for cortactin phosphorylation and efficient migration in mouse embryonic fibroblasts [13]. FER is also activated by phospholipase D signaling leading to Rac1-dependent and cortactin-mediated lamellipodia formation and increased cell migration [15]. The role of FER in Rho signaling is largely unexplored, but there is some evidence that it can regulate Rac1 by phosphorylating Rho guanine dissociation inhibitor  $\alpha$  (RhoGDI $\alpha$ ) thereby preventing formation of Rac1/RhoGDI $\alpha$  complexes [48]. Also, FER inhibition leads to decreased phosphorylation of Vav2, a direct Rac1 activator [15]. Our data show that the inhibition of lamellipodia formation and migration upon FER KD is accompanied by stress fiber formation, a hallmark of active RhoA. Conversely, we observed that FER overexpression in MCF10.CA1d cells leads to increased lamellipodia formation and migration, which is consistent with Rac1 activation. Since it is assumed that active Rac counterbalances the activity of Rho [49], these results imply that FER KD may lead to indirect activation of Rho through inhibition of Rac. This in turn would inhibit migration and invasion, while promoting cell-ECM adhesion.

In this study we have demonstrated that FER regulates breast tumor growth and metastasis. FER promotes breast cancer growth and metastasis in a cell autonomous

manner through inhibition of adhesion and anchorage dependence. Significantly, we have also shown that FER expression is correlated to prognosis in breast cancer patients. Thus, the development therapeutic strategies based on inhibition of FER signaling may be beneficial in the treatment of metastatic breast cancer.

## Acknowledgements

We would like to thank N. Heisterkamp for providing the pUHG10-3(FER) vector. E. Danen and A. Sonnenberg for anti-integrin antibodies and L. Price for help with the Matrigel assays. Luciferase-expressing MDA-MB-231 cells were a kind gift from G. van der Pluijm. We are grateful to C. Pfauth, T. Westphal and the Netherlands Cancer Institute for providing *RAG2<sup>-/-</sup>;IL2Rγ<sup>-/-</sup>* recipient mice. M. van Amersfoort and D. van der Giezen are acknowledged for expert technical assistance with the mouse experiments and F. Morsink for performing the vimentin IHC staining. We thank S. Huvneers for critically reviewing this manuscript. This research is supported by an unrestricted educational grant from Aegon Inc. I. A. Ivanova is a Research Fellow of the Terry Fox Foundation (Award #700041).

## References

1. Ferlay J, Shin HR, Bray F, *et al.* Estimates of worldwide burden of cancer in 2008: GLOBOCAN 2008. *Int J Cancer* 2010; 127(12):2893-917.
2. Jemal A, Siegel R, Xu J and Ward E. Cancer statistics, 2010. *CA Cancer J Clin* 60(5):277-300.
3. Hudis CA. Trastuzumab--mechanism of action and use in clinical practice. *N Engl J Med* 2007; 357(1):39-51.
4. Greer P. Closing in on the biological functions of Fps/Fes and Fer. *Nat Rev Mol Cell Biol* 2002; 3(4):278-89.
5. Pawson T, Letwin K, Lee T, *et al.* The FER gene is evolutionarily conserved and encodes a widely expressed member of the FPS/FES protein-tyrosine kinase family. *Mol Cell Biol* 1989; 9(12):5722-5.
6. Zirngibl R, Schulze D, Mirski SE, Cole SP and Greer PA. Subcellular localization analysis of the closely related Fps/Fes and Fer protein-tyrosine kinases suggests a distinct role for Fps/Fes in vesicular trafficking. *Exp Cell Res* 2001; 266(1):87-94.
7. Kim L and Wong TW. The cytoplasmic tyrosine kinase FER is associated with the catenin-like substrate pp120 and is activated by growth factors. *Mol Cell Biol* 1995; 15(8):4553-61.
8. Kim L and Wong TW. Growth factor-dependent phosphorylation of the actin-binding protein cortactin is mediated by the cytoplasmic tyrosine kinase FER. *J Biol Chem* 1998; 273(36):23542-8.
9. Xu G, Craig AW, Greer P, *et al.* Continuous association of cadherin with beta-catenin requires the non-receptor tyrosine-kinase Fer. *J Cell Sci* 2004; 117(Pt 15):3207-19.
10. El Sayegh TY, Arora PD, Fan L, *et al.* Phosphorylation of N-cadherin-associated cortactin by Fer kinase regulates N-cadherin mobility and intercellular adhesion strength. *Mol Biol Cell* 2005; 16(12):5514-27.
11. Rosato R, Veltmaat JM, Groffen J and Heisterkamp N. Involvement of the tyrosine kinase fer in cell adhesion. *Mol Cell Biol* 1998; 18(10):5762-70.
12. Arregui C, Pathre P, Lilien J and Balsamo J. The nonreceptor tyrosine kinase fer mediates cross-talk between N-cadherin and beta1-integrins. *J Cell Biol* 2000; 149(6):1263-74.
13. Sangrar W, Gao Y, Scott M, Truesdell P and Greer PA. Fer-mediated cortactin phosphorylation is associated with efficient fibroblast migration and is dependent on reactive oxygen species generation during integrin-mediated cell adhesion. *Mol Cell Biol* 2007; 27(17):6140-52.
14. Craig AW and Greer PA. Fer kinase is required for sustained p38 kinase activation and maximal chemotaxis of activated mast cells. *Mol Cell Biol* 2002; 22(18):6363-74.
15. Itoh T, Hasegawa J, Tsujita K, Kanaho Y and Takenawa T. The tyrosine kinase Fer is a downstream target of the PLD-PA pathway that regulates cell migration. *Sci Signal* 2009; 2(87):ra52.
16. Yoneyama T, Angata K, Bao X, *et al.* Fer kinase regulates cell migration through alpha-dystroglycan glycosylation. *Mol Biol Cell* 2012; 23(5):771-80.
17. Pasder O, Shpungin S, Salem Y, *et al.* Downregulation of Fer induces PP1 activation and cell-cycle arrest in malignant cells. *Oncogene* 2006; 25(30):4194-206.
18. Voisset E, Lopez S, Chaix A, *et al.* FES kinases are required for oncogenic FLT3 signaling. *Leukemia* 24(4):721-8.
19. Allard P, Zoubeidi A, Nguyen LT, *et al.* Links between Fer tyrosine kinase expression levels and prostate cell proliferation. *Mol Cell Endocrinol* 2000; 159(1-2):63-77.
20. Zoubeidi A, Rocha J, Zouanat FZ, *et al.* The Fer tyrosine kinase cooperates with interleukin-6 to activate signal transducer and activator of transcription 3 and promote human prostate cancer cell growth. *Mol Cancer Res* 2009; 7(1):142-55.
21. Li H, Ren Z, Kang X, *et al.* Identification of tyrosine-phosphorylated proteins associated with metastasis and functional analysis of FER in human hepatocellular carcinoma cells. *BMC Cancer* 2009; 9:366.
22. Guo C and Stark GR. FER tyrosine kinase (FER) overexpression mediates resistance to quinacrine through EGF-dependent activation of NF-kappaB. *Proc Natl Acad Sci U S A* 108(19):7968-73.
23. Santner SJ, Dawson PJ, Tait L, *et al.* Malignant MCF10CA1 cell lines derived from premalignant human breast epithelial MCF10AT cells. *Breast Cancer Res Treat* 2001; 65(2):101-10.

24. Wetterwald A, van der Pluijm G, Que I, *et al.* Optical imaging of cancer metastasis to bone marrow: a mouse model of minimal residual disease. *Am J Pathol* 2002; 160(3):1143-53.
25. Craig AW, Zirngibl R, Williams K, Cole LA and Greer PA. Mice devoid of fer protein-tyrosine kinase activity are viable and fertile but display reduced cortactin phosphorylation. *Mol Cell Biol* 2001; 21(2):603-13.
26. Schackmann RC, van Amersfoort M, Haarhuis JH, *et al.* Cytosolic p120-catenin regulates growth of metastatic lobular carcinoma through Rock1-mediated anoikis resistance. *J Clin Invest* 121(8):3176-88.
27. Ivanova IA, D'Souza SJ and Dagnino L. E2F1 stability is regulated by a novel-PKC/p38beta MAP kinase signaling pathway during keratinocyte differentiation. *Oncogene* 2006; 25(3):430-7.
28. Vespa A, D'Souza SJ and Dagnino L. A novel role for integrin-linked kinase in epithelial sheet morphogenesis. *Mol Biol Cell* 2005; 16(9):4084-95.
29. Danen EH, Sonneveld P, Brakebusch C, Fassler R and Sonnenberg A. The fibronectin-binding integrins alpha5beta1 and alphavbeta3 differentially modulate RhoA-GTP loading, organization of cell matrix adhesions, and fibronectin fibrillogenesis. *J Cell Biol* 2002; 159(6):1071-86.
30. Gimeno R, Weijer K, Voordouw A, *et al.* Monitoring the effect of gene silencing by RNA interference in human CD34+ cells injected into newborn RAG2-/- gammac-/- mice: functional inactivation of p53 in developing T cells. *Blood* 2004; 104(13):3886-93.
31. Vermeulen JF, van de Ven RA, Ercan C, *et al.* Nuclear kaiso expression is associated with high grade and triple-negative invasive breast cancer. *PLoS One* 7(5):e37864.
32. van Diest PJ. No consent should be needed for using leftover body material for scientific purposes. *For. BMJ* 2002; 325(7365):648-51.
33. Kenny PA, Lee GY, Myers CA, *et al.* The morphologies of breast cancer cell lines in three-dimensional assays correlate with their profiles of gene expression. *Mol Oncol* 2007; 1(1):84-96.
34. Frisch SM and Francis H. Disruption of epithelial cell-matrix interactions induces apoptosis. *J Cell Biol* 1994; 124(4):619-26.
35. Derksen PW, Liu X, Saridin F, *et al.* Somatic inactivation of E-cadherin and p53 in mice leads to metastatic lobular mammary carcinoma through induction of anoikis resistance and angiogenesis. *Cancer Cell* 2006; 10(5):437-49.
36. Leone BA, Romero A, Rabinovich MG, *et al.* Stage IV breast cancer: clinical course and survival of patients with osseous versus extraosseous metastases at initial diagnosis. The GOCS (Grupo Oncologico Cooperativo del Sur) experience. *Am J Clin Oncol* 1988; 11(6):618-22.
37. Rosen PR, Groshen S, Saigo PE, Kinne DW and Hellman S. A long-term follow-up study of survival in stage I (T1N0M0) and stage II (T1N1M0) breast carcinoma. *J Clin Oncol* 1989; 7(3):355-66.
38. Braun S, Cevatli BS, Assemi C, *et al.* Comparative analysis of micrometastasis to the bone marrow and lymph nodes of node-negative breast cancer patients receiving no adjuvant therapy. *J Clin Oncol* 2001; 19(5):1468-75.
39. Giampieri S, Manning C, Hooper S, *et al.* Localized and reversible TGFbeta signalling switches breast cancer cells from cohesive to single cell motility. *Nat Cell Biol* 2009; 11(11):1287-96.
40. Neve RM, Chin K, Fridlyand J, *et al.* A collection of breast cancer cell lines for the study of functionally distinct cancer subtypes. *Cancer Cell* 2006; 10(6):515-27.
41. Kao J, Salari K, Bocanegra M, *et al.* Molecular profiling of breast cancer cell lines defines relevant tumor models and provides a resource for cancer gene discovery. *PLoS One* 2009; 4(7):e6146.
42. Oh MA, Choi S, Lee MJ, *et al.* Specific tyrosine phosphorylation of focal adhesion kinase mediated by Fer tyrosine kinase in suspended hepatocytes. *Biochim Biophys Acta* 2009; 1793(5):781-91.
43. Piedra J, Miravet S, Castano J, *et al.* p120 Catenin-associated Fer and Fyn tyrosine kinases regulate beta-catenin Tyr-142 phosphorylation and beta-catenin-alpha-catenin Interaction. *Mol Cell Biol* 2003; 23(7):2287-97.
44. Brew CT, Aronchik I, Kosco K, *et al.* Indole-3-carbinol inhibits MDA-MB-231 breast cancer cell motility and induces stress fibers and focal adhesion formation by activation of Rho kinase activity. *Int J Cancer* 2009; 124(10):2294-302.
45. Bharadwaj S, Thanawala R, Bon G, Falcioni R and Prasad GL. Resensitization of breast cancer cells to anoikis by tropomyosin-1: role of Rho kinase-dependent cytoskeleton and adhesion. *Oncogene* 2005; 24(56):8291-303.

46. Caswell PT, Chan M, Lindsay AJ, *et al.* Rab-coupling protein coordinates recycling of alpha5beta1 integrin and EGFR1 to promote cell migration in 3D microenvironments. *J Cell Biol* 2008; 183(1):143-55.
47. Mills GB, Jurisica I, Yarden Y and Norman JC. Genomic amplicons target vesicle recycling in breast cancer. *J Clin Invest* 2009; 119(8):2123-7.
48. Fei F, Kweon SM, Haataja L, *et al.* The Fer tyrosine kinase regulates interactions of Rho GDP-Dissociation Inhibitor alpha with the small GTPase Rac. *BMC Biochem* 2010; 11:48.
49. Sander EE, ten Klooster JP, van Delft S, van der Kammen RA and Collard JG. Rac downregulates Rho activity: reciprocal balance between both GTPases determines cellular morphology and migratory behavior. *J Cell Biol* 1999; 147(5):1009-22.

## Supplementary Data

### Supplementary Methods

#### Cell Culture

MCF10A, MCF10CA1a, MCF10CA1a.cl1 and MCF10CA1d.cl1 cells were cultured in DMEM/F12 supplemented with 10% horse serum, 20 ng/ml EGF, 10 µg/ml insulin, 0.5 µg/ml hydrocortisone, 100 ng/ml cholera toxin, 100 IU/ml penicillin, and 100 µg/ml streptomycin. MCF-7, T47D, MDA-MB-453, CAMA-1, SKBR3, BT-549 and MDA-MB-231 cells were cultured in DMEM, MDA-MB-436 and MDA-MB-468 in DMEM/F12, and ZR-75-30 in RPMI all containing 10% FBS, 100 IU/ml penicillin, and 100 µg/ml streptomycin. SUMPE44 cells were cultured in serum-free Ham's F-12 supplemented with 5 µg/ml insulin and 1µg/ml hydrocortisone.

#### Plasmids

The pUHG10-3(FER) vector (kindly provided by N. Heisterkamp) was used as a template to amplify the full-length human FER cDNA by PCR and subclone it into the pcDNA5/FRT vector (Invitrogen), modified to contain the EF1α instead of CMV promoter. The EF1α-FER cassette was amplified by PCR thereby adding a C-terminal V5 epitope tag to the wild-type FER cDNA and flanking *BstBI/XhoI* restriction sites. EF1α-FER-V5 was then cloned in the *Clal/XhoI* sites of pLV/CMV to generate pLV/EF1α-FER-V5 (WT FER). The QuikChange II XL Site-Directed Mutagenesis Kit (200521; Stratagene) was used to generate kinase dead (D742R) FER (D742D FER).

Control and FER-targeting oligonucleotides were annealed and cloned into the FH1tUTG vector. Oligonucleotide sequences were as follows (targeting sequences are capitalized):

control	sense: 5'-tcccTTCTCCGAACGTGTCACGTtcaagagaACGTGACACGTTCCGAGAAttttc-3'
control	anti-sense: 5'-tcgagaaaaTTCTCCGAACGTGTCACGTtctctttaaACGTGACACGTTCCGAGAA-3'
Fer[680-698]	sense: 5'-tcccGGCTCACCATGATGATTAAttcaagagaTTAATCATCATGGTGAGCCttttc-3'
Fer[680-698]	anti-sense: 5'-tcgagaaaaGGCTCACCATGATGATTAAtctctttaaTTAATCATCATGGTGAGCC-3'
Fer[978-998]	sense: 5'-tcccGTATTATGATATCACACTTCcttcaagagaGGAAGTGTGATATCATAATActtttc-3'
Fer[978-998]	anti-sense: 5'-tcgagaaaaGTATTATGATATCACACTTCcttctttaaGGAAGTGTGATATCATAATAC-3'

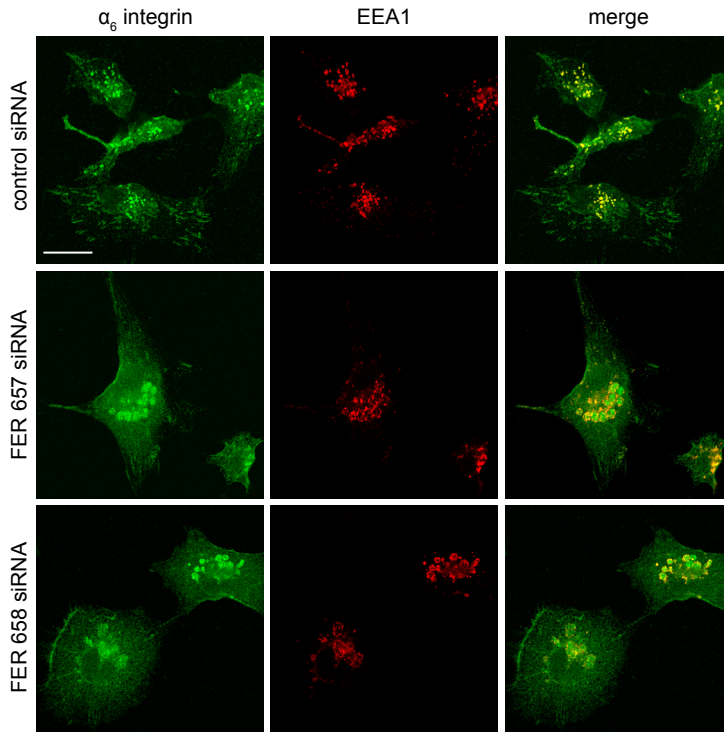
## Supplementary Table

**Table S1.** Clinicopathological characteristics of 485 invasive breast cancer patients studied for the expression of FER kinase.

Feature	Grouping	N or value	%
Age (years)	Mean	60	
	Range	28-88	
Histological type	IDC	320	66.0
	ILC	126	26.0
	Others	39	8.0
Tumor size	pT1	208	42.9
	pT2	220	45.4
	pT3	49	10.1
	Not available	8	1.6
Histological Grade	1	88	18.1
	2	171	35.3
	3	219	45.2
	Not available	7	1.4
MAI <sup>#</sup>	≤ 12	239	49.3
	≥ 13	246	50.7
Lymph node status	Negative*	227	46.8
	Positive**	231	47.6
	Not available	27	5.6

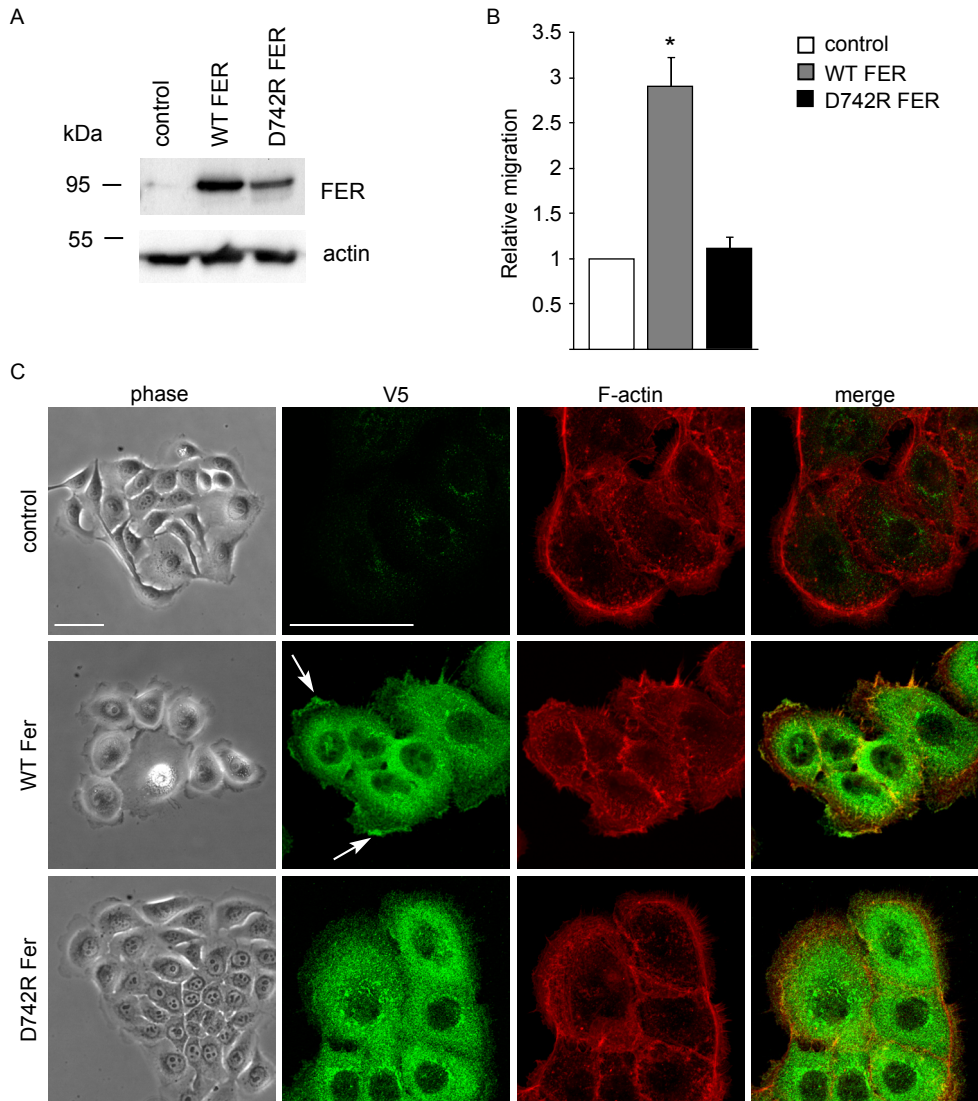
<sup>#</sup>: per 2mm<sup>2</sup>; \*: negative = N0 or N0(+); \*\*:positive = ≥N1mi (according to TNM 7<sup>th</sup> edition, 2010)

## Supplementary Figures

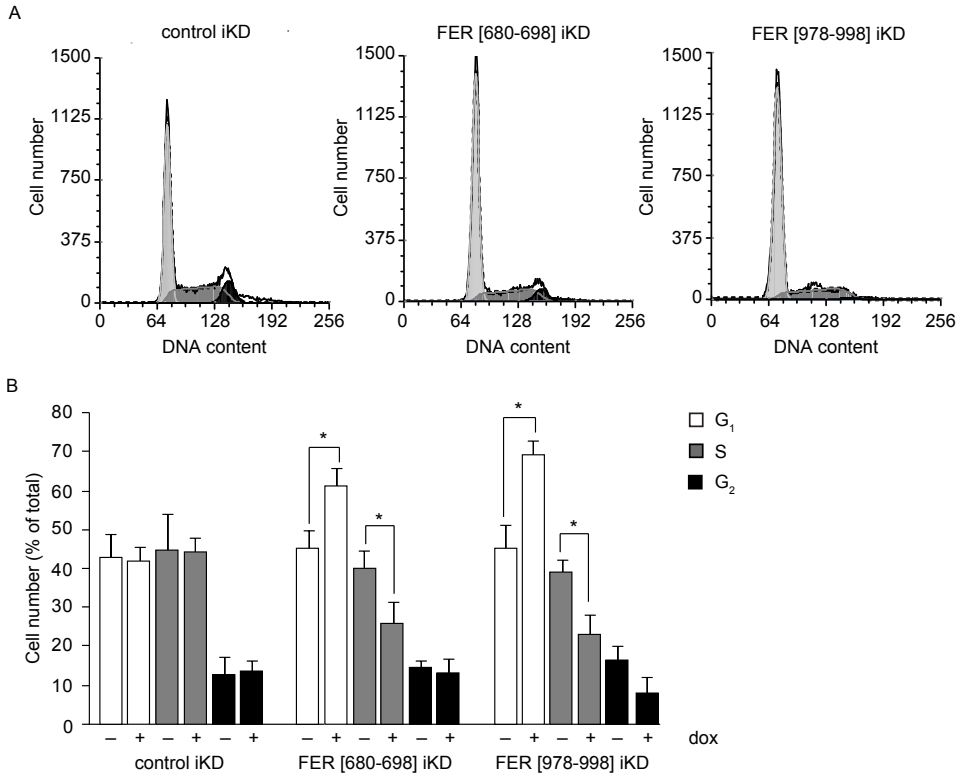


**Supplementary Figure 1. Fer kinase downregulation promotes accumulation of  $\alpha_6$ -integrin in endosomal vesicles.** MDA-MB-231 cells were transfected with the indicated siRNAs and plated on laminin-coated glass coverslips 72 h later. Cells were processed for immunofluorescence microscopy after 24 h using anti- $\alpha_6$  integrin and anti-early endosome antigen 1 (EEA1) antibodies. Scale bar = 20 mm. The results shown are representative of three independent experiments.



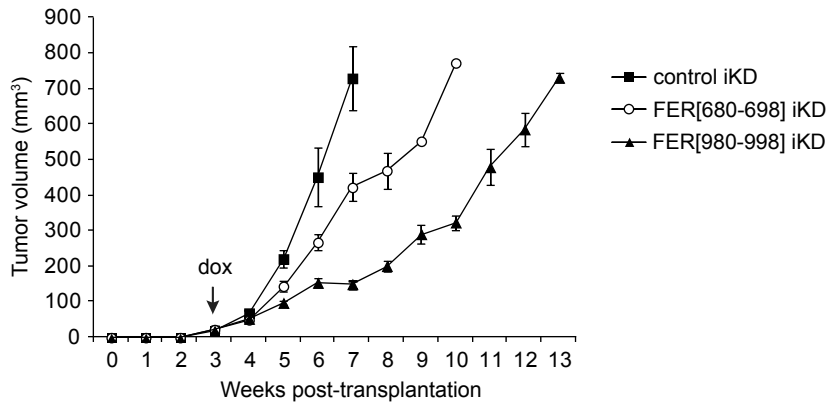


**Supplementary Figure 2. FER regulates lamellipodia formation and migration.** (A) the expression of V5-tagged wild type (WT) and kinase-deficient (D742R) FER in stably transduced MCF10A.CA1d cells was determined by immunoblot using an anti-V5 antibody. Actin was used as a loading control. (B) *FER-induced migration is kinase dependent.* Control, WT and D742R FER-expressing MCF10A.CA1d cells were seeded on collagen I-coated plates. The rate of migration was measured over 24 h using a modified wound-healing assay. Values represent the migration rate normalized to control  $\pm$  SEM. \* indicates significantly different migration rates, relative to control ( $p < 0.05$ , one-way ANOVA). (C) *Lamellipodia formation upon expression of FER.* Control and WT or D742R FER-expressing MCF10A.CA1d cells were plated on collagen I-coated glass coverslips. The morphology of live cells was analyzed by phase contrast microscopy (phase) after 24 h. Cells were then fixed and processed for immunofluorescence microscopy using an anti-V5 antibody to detect exogenously expressed FER-V5 (green) and Alexa 555-conjugated phalloidin to visualize F-actin (red). The arrow indicates accumulation of WT FER at the leading edges of lamellipodia. Scale bar = 50  $\mu$ m.



**Supplementary Figure 3. FER downregulation inhibits cell cycle progression.** MDA-MB-231 inducible knock-down (iKD) cells were cultured for 96 h in the absence (-) or presence (+) of doxycycline (dox; 2  $\mu$ g/ml) to induce shRNA expression. Cells were collected and fixed in 70% ethanol for 1 h on ice, followed by centrifugation (3,000 g, 5 min, room temperature). Pellets were rinsed once with PBS, resuspended in PBS containing 30  $\mu$ g/ml RNaseA and incubated for 30 min at 37°C. DNA was labelled with ToPro-3 (1:20,000; Invitrogen) and samples were analyzed on a FACSCalibur flow cytometer (Becton Dickinson). Cell cycle analysis was performed using FCS Express 4 Flow Cytometry software (De Novo Software).

(A) FACS histograms of iKD cells (+ dox). (B) Quantification of cell cycle distribution of iKD cells. Values represent the relative number of cells  $\pm$  SEM. \*  $p < 0.05$  Two-tailed Student's t test.



**Supplementary Figure 4. Growth kinetics of breast tumors derived MDA-MB-231 inducible knock-down (iKD) cells.** Luciferase-expressing MDA-MB-231 iKD cells were orthotopically transplanted into recipient mice. Upon development of palpable tumors mice were switched to a doxycycline-containing diet (dox; arrow) to induce shRNA expression. Values represent the mean tumor volume  $\pm$  SEM.



# Nine

## **Nuclear SOX4 expression in breast cancer predicts resistance towards adjuvant chemotherapy and radiotherapy**

Stephin J. Vervoort<sup>1,2\*</sup>, Jeroen F. Vermeulen<sup>3\*</sup>, Cathy B. Moelans<sup>3</sup>, Peter Bult<sup>4</sup>, Elsken van der Wall<sup>5</sup>, Paul J. Coffe<sup>1,2</sup>, and Paul J. van Diest<sup>3</sup>

<sup>1</sup>Department of Cell Biology, University Medical Center Utrecht, Utrecht, The Netherlands,

<sup>2</sup>Division of Pediatrics, University Medical Center Utrecht, Utrecht, The Netherlands,

<sup>3</sup>Department of Pathology, University Medical Center Utrecht, Utrecht, The Netherlands,

<sup>4</sup>Department of Pathology, Radboud University Nijmegen Medical Centre, Nijmegen, The Netherlands,

<sup>5</sup>Division of Internal Medicine and Dermatology, University Medical Center Utrecht, Utrecht, The Netherlands

\*These authors contributed equally to this study

***Manuscript in preparation***

## Abstract

**Introduction:** The SRY-related HMG-box transcription factor 4 (SOX4) is abundantly expressed in various cancers and functions as a tumor suppressor or oncogene depending on the cellular context. In breast cancer, SOX4 expression is regulated by TGF- $\beta$  signaling, several microRNAs, and drives tumor metastasis towards lung and bone. It has been shown that expression of SOX4 resulted in acquired therapy resistance towards chemotherapeutics in colorectal cancer cell lines, but this has not been investigated in breast cancer.

**Methods:** We analyzed SOX4 expression by immunohistochemistry in 452 breast cancer samples and investigated the role of SOX4 on survival in relation to adjuvant therapy.

**Results:** High cytoplasmic SOX4 expression correlated with grade ( $p < 0.001$ ) and lymph node metastasis ( $p = 0.036$ ), but not with overall survival. High nuclear SOX4 expression was observed in 18% of breast cancers, especially in pleomorphic lobular breast cancer, and positively correlated with grade in both ductal and lobular breast cancers ( $p = 0.013$  and  $p < 0.001$ ). Nuclear SOX4 expression was a prognostic factor for poor survival ( $p = 0.001$ ) and served as an independent predictor of resistance to chemotherapy and radiotherapy.

**Conclusions:** In breast cancer, nuclear SOX4 is expressed in aggressive ductal and lobular breast cancers, and independently predicts poor survival and resistance to adjuvant chemo- and radiotherapy.

## Introduction

Breast cancer is the most frequently diagnosed malignancy in women, contributing to nearly one third of the diagnosed cancers [1]. In The Netherlands annually over 13,000 women are diagnosed with breast cancer, meaning that one in eight women will develop breast cancer during her life [2, 3]. In Western countries the mortality rate has decreased the last 20 years at least 20% as a result of mammographic population based screening [4, 5] and advances of adjuvant chemotherapy, radiotherapy, hormonal, and targeted therapy [1, 6]. Nevertheless, breast cancer remains the second leading cause of cancer related death in women [1] accounting for 3,500 breast cancer related deaths annually in The Netherlands [7], mainly caused by acquired or intrinsic resistance towards adjuvant systemic therapies.

In the last decade, genome-wide expression profiling has discovered novel genes involved in cancer development, therapy resistance and metastasis formation. These studies have led to the identification of the SRY-related HMG-box transcription factor 4 (SOX4) as a general cancer signature gene, which is highly expressed in the majority of human cancers, suggesting a key role of SOX4 in cancer development and progression [8, 9]. SOX4, which belongs to the SOX-family of transcription factors, was originally identified as an important developmental factor involved in the survival and proliferation of a wide variety of tissues, including the heart, neuronal tissues, and the hematopoietic system [10-12]. As a consequence, SOX4-deficient mice die after 14 days of gestation due to impaired cardiac development and suffer from numerous developmental defects [13, 14]. In contrast, SOX4 expression in adults is restricted to stem cell populations located in the intestine, breast, and hematopoietic system [15-19].

Despite the broad expression in human cancers, SOX4 has been demonstrated to have pleiotropic roles in tumors, acting as a tumor-suppressor or oncogene depending on the cellular context and tumor-type [20-23]. In breast cancer, SOX4 has been proposed to contribute to disease progression by promoting tumor metastasis [24, 25]. In both benign and malignant breast tissues SOX4 expression is controlled by estrogen and progesterone, and is furthermore regulated through the TGF- $\beta$ /SMAD signaling pathway and several microRNAs [24-27]. In xenograph models of breast cancer using MDA-MB-231 cells, SOX4 expression was elevated in lung and bone metastases [24]. Furthermore, the metastatic and invasive capacity of MDA-MB-231 cells was significantly reduced when SOX4 was depleted by shRNAs or microRNA-335. Recently, SOX4 was demonstrated to be an important effector of TGF- $\beta$ -induced epithelial to mesenchymal transition (EMT), a process associated

with tumor metastasis in which cancers of epithelial origin acquire mesenchymal and stem cell characteristics [25]. Accordingly, SOX4 expression was shown to increase the stem cell properties of MCF10A cells and promote tumor growth of RasV12 transformed MCF10A cells *in vivo*. Moreover, in clinical specimens SOX4 expression correlated with tumor grade and triple negative breast cancer [25], suggesting that SOX4 is a hallmark of aggressiveness and plays a fundamental role in breast cancer progression.

In addition to TGF- $\beta$  signaling, SOX4 expression is also potently induced upon treatment of human cancer cell lines with a variety of therapeutic agents including doxorubicin, 5-fluorouracil (5-FU), and oxaliplatin [28]. Similar to its diverse roles in human cancer, therapy-mediated induction of SOX4 may result in distinct effects depending on tumor characteristics. For example, in medulloblastoma, DNA-damage-induced expression of SOX4 has been suggested to promote DNA-repair, resulting in decreased radiosensitivity [29]. Contrarily, in colorectal carcinoma (HCT116 cells) induction of SOX4 expression promoted DNA-damage signaling through SOX4-mediated stabilization of p53 thereby resulting in a p53-dependent reduction in tumorigenesis [30]. Moreover, in 5-FU and oxaliplatin resistant HCT116 cells, SOX4 expression was significantly elevated compared to the parental cells [28]. Taken together, these findings suggest that SOX4 actively contributes to the therapeutic response in human cancer and might act as a marker for therapy-resistance. By virtue of the important role of SOX4 in breast cancer progression and its potential link with efficacy of therapy, we explored the role of SOX4 in therapy resistance and outcome of breast cancer.



## Materials and Methods

### *Patients*

The study population was derived from the archives of the Departments of Pathology of the University Medical Center Utrecht, Utrecht and the Radboud University Nijmegen Medical Centre, Nijmegen, The Netherlands. These comprised 452 cases of invasive breast cancer. Histological grade was assessed according to the modified Bloom and Richardson score [31], and the mitotic activity index (MAI) was assessed as before [32]. Other clinicopathological characteristics are shown in Table S1. From representative donor paraffin blocks of the primary tumors, tissue microarrays were constructed as described by Vermeulen et al [33, 34]. The use of anonymous or coded leftover material for scientific purposes is part of the standard treatment contract with patients in The Netherlands [35]. Ethical approval was therefore not required. Overall survival and treatment data were obtained from the Comprehensive Cancer Center of The Netherlands (Integraal Kankercentrum Nederland). Survival data were available of 295 out of 452 breast cancer cases, with a follow up of 72 months for the ductal and 120 months for the lobular breast cancer cases.

### *Immunohistochemistry*

Immunohistochemistry was carried out on 4µm thick sections. Data on HER2, progesteron receptor (PR), estrogen receptor  $\alpha$  (ER $\alpha$ ), and E-cadherin were derived from Vermeulen et al [33, 34]. After deparaffination and rehydration, endogenous peroxidase activity was blocked for 15 min in a buffer solution pH5.8 containing 0.3% hydrogen peroxide. After antigen retrieval, i.e. boiling for 20 min in 10mM citrate pH6.0, a cooling period of 30 min preceded the primary antibody incubation. Primary antibodies against SOX4 (HPA029901, Sigma Aldrich) 1:50 were diluted in PBS containing 1% BSA and incubated overnight at 4°C. The signal was amplified using the Novolink kit (Leica) and developed with diaminobenzidine, followed by counterstaining with haematoxylin, dehydration in alcohol, and mounting. Appropriate negative and positive controls were used throughout.

### *Scoring of immunohistochemistry*

All scoring was done blinded to patient characteristics and results of other stainings by three independent observers (SJV, JFV, PJVD). E-cadherin and HER2 stainings were scored using the DAKO/HER2 scoring system for membrane staining. Membranous scores 1+, 2+, and 3+ were considered positive. For HER2 only a score of 3+ was considered positive. ER $\alpha$  and PR were scored by estimating the percentage of positive tumor cells, considering cancers with more than 10% positive tumor nuclei as positive. Nuclear and cytoplasmic SOX4 staining intensity was scored as 0-3+, considering samples with 3+ staining intensity as positive. The Perou/Sorlie molecular classification was simulated by ER $\alpha$ / PR/ HER2 as before [36].

## Statistics

Statistical analysis was performed using IBM SPSS Statistics version 18.0 (SPSS Inc., Chicago, IL, USA). Associations between categorical variables were examined using the Pearson's Chi-square test or Fisher's exact test when required. Survival analyses were performed using Kaplan-Meier and differences were analyzed using Log rank test. Multivariate analyses were performed using Cox regression. P-values <0.05 were considered to be statistically significant.

**Table 1.** Correlation of nuclear SOX4 expression with clinicopathological and molecular features of invasive breast cancer.

Feature	N	Nuclear SOX4 expression		p-value
		Low N (%)	High N (%)	
Histological type				
IDC	301	259 (86.0)	42 (14.0)	
ILC	123	88 (71.5)	35 (28.5)	
Other	28	24 (85.7)	4 (14.3)	<b>0.002</b>
Histological grade				
1	80	77 (96.2)	3 (3.8)	
2	160	139 (86.9)	21 (13.1)	
3	195	139 (71.3)	56 (28.7)	<b>&lt;0.001</b>
Tumor size				
pT1	202	177 (87.6)	25 (12.4)	
pT2	197	153 (77.7)	44 (22.3)	
pT3	50	38 (76.0)	12 (24.0)	<b>0.018</b>
MAI (per 2mm <sup>2</sup> )				
≤ 12	230	210 (91.3)	20 (8.7)	
≥ 13	222	161 (72.5)	61 (27.5)	<b>&lt;0.001</b>
Lymph node status				
Positive	212	172 (81.1)	40 (18.9)	
Negative	220	182 (82.7)	38 (17.3)	0.667
Molecular classification				
Luminal	377	311 (82.5)	66 (17.5)	
HER2-driven	17	15 (88.2)	2 (11.8)	
Basal/TN	58	45 (77.6)	13 (22.4)	0.528
ERα				
Positive	372	308 (82.8)	64 (17.2)	
Negative	80	63 (78.8)	17 (21.2)	0.392
PR				
Positive	268	220 (82.1)	48 (17.9)	
Negative	183	150 (82.0)	33 (18.0)	0.973
HER2				
Positive	44	36 (81.8)	8 (18.2)	
Negative	407	334 (82.1)	73 (17.9)	0.968
E-cadherin				
Positive	300	253 (84.3)	47 (15.7)	
Negative	116	83 (71.6)	33 (28.4)	<b>0.003</b>

## Results

### *SOX4 expression in breast cancer correlates with an aggressive phenotype*

SOX4 expression was found to be present at low levels (0 and 1+) in both luminal and myoepithelial cells of normal breast ducts. In our cohort of breast cancers, 191 cases (42.4%) expressed high levels (3+) of cytoplasmic and 81 cases (18%) high levels of nuclear SOX4 (Figure 1), and 308 cases (67.8%) showed high nuclear and/or cytoplasmic SOX4. As shown in Table S2, high cytoplasmic expression was more abundant in invasive ductal carcinoma (IDC) than in invasive lobular carcinoma (ILC) ( $p < 0.001$ ), but no correlations with other clinicopathological features were found. In contrast, nuclear accumulation of SOX4 was correlated with tumor grade, MAI, tumor size, and tumor histology, but not with hormonal receptor status or lymph node status (Table 1). Further, pleomorphic lobular breast cancers expressed nuclear SOX4 more frequently than classical lobular breast cancer ( $p < 0.001$ , Figure 1). Nevertheless, subgroup analysis of IDC and ILC revealed that nuclear SOX4 correlated with tumor grade and MAI in both IDC and ILC (Table S3). In breast cancers with high nuclear and/or cytoplasmic (“total”) SOX4 expression, there was a significant association with lymph node metastasis ( $p = 0.036$ ), high histological grade ( $p < 0.001$ ), and high MAI ( $p < 0.001$ ), but not with ER $\alpha$ , PR, HER2, or molecular classification (Table S2).

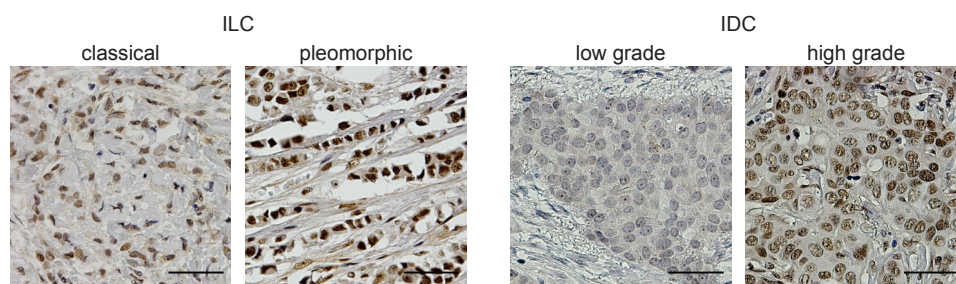


**Figure 1. SOX4 expression in invasive breast cancer.** Images of representative cases of invasive lobular (ILC) and invasive ductal (IDC) breast cancer stained by immunohistochemistry for SOX4. Scale bar equals 25  $\mu$ m.

### *Nuclear SOX4 expression contributes to poor survival of breast cancer patients*

Cytoplasmic ( $p = 0.126$ ) and total SOX4 expression ( $p = 0.841$ ) had no influence on survival, whereas patients with high nuclear SOX4 expression had a worse prognosis than patients with low nuclear SOX4 expression ( $p = 0.001$ ; Figure 2A). This effect of high nuclear SOX4 expression on survival was seen in both IDC and ILC ( $p = 0.047$  and  $p = 0.040$ , respectively; Figure 2B). Multivariate analysis showed that high nuclear SOX4 expression had independent prognostic value next to lymph node status, age, and grade (Table 2). In subgroup analysis, age and lymph node status were determining survival rather than nuclear SOX4 expression in IDC, whereas in ILC nuclear SOX4, age, and lymph node status had independent prognostic value (Table 2).

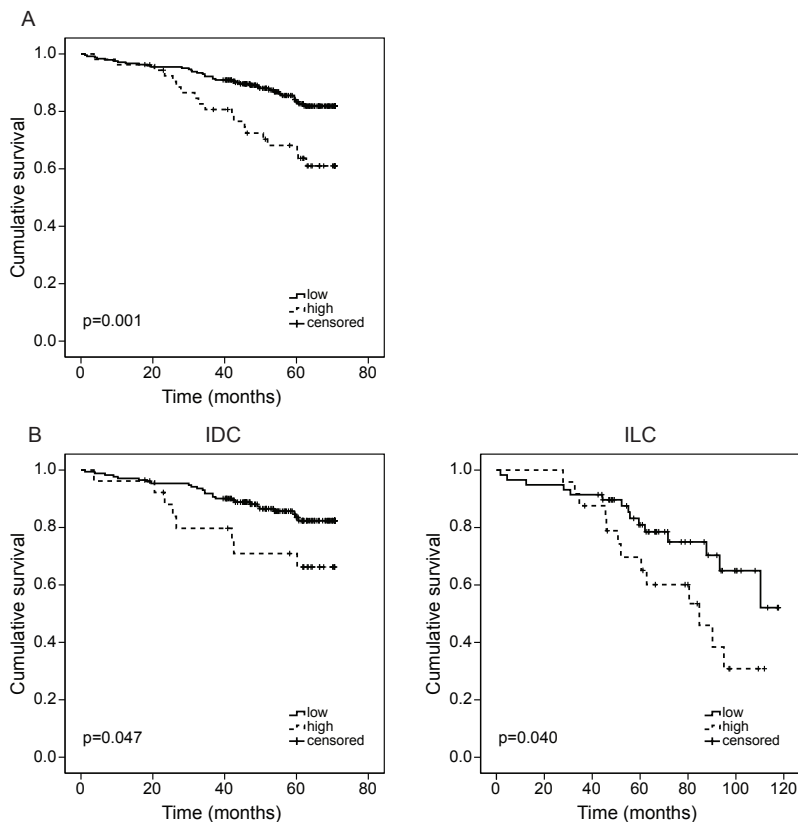


**Figure 2. Overall survival curves for patients with high or low nuclear SOX4 expression.** (A) Overall survival of breast cancer patients stratified for nuclear SOX4 expression. (B) Overall survival of breast cancer patients with IDC or ILC stratified for nuclear SOX4 expression.

#### *Nuclear SOX4 correlates with response to adjuvant radio- and chemotherapy*

In univariate analysis, patients with high nuclear SOX4 expression experienced no benefit from adjuvant chemo- or radiotherapy, showing similar outcome data compared to untreated patients with high nuclear SOX4 expression. ( $p=0.429$  and  $p=0.995$ , respectively). This was in contrast to patients with low nuclear SOX4 that did better on adjuvant therapy ( $p=0.010$  and  $p=0.011$ , respectively), as shown in Figure 3A. This suggests therapy-resistance in patients with high nuclear SOX4 expression. Furthermore, in the univariate analysis, in patients not receiving adjuvant chemo- or radiotherapy, high nuclear SOX4 expression resulted in a worse survival compared to patients with low nuclear SOX4 (Figure 3B); this however could not be confirmed in the multivariate analysis (Table 3). Hormonal therapy in these patients resulted in better survival, although no link between SOX4 expression and hormone receptor expression was found. Within the subgroup of patients receiving adjuvant chemotherapy or radiotherapy, patients with high nuclear SOX4 expression had a

significantly worse survival compared to patients with low nuclear SOX4 expression in univariate analysis (chemotherapy p=0.014 and radiotherapy p<0.001; Figure 3C). Multivariate analysis showed similar results, where high nuclear SOX4 expression was independently correlated with a worse outcome following treatment (Table 3).

**Table 2.** Additional prognostic value of nuclear SOX4 expression to established prognosticators for survival of breast cancer.

Feature	Total data set			IDC			ILC		
	HR	95% CI	p-value	HR	95% CI	p-value	HR	95% CI	p-value
Histological type									
IDC	1.0 (ref)								
ILC	0.637	0.331-1.227	0.177						
Others	0.831	0.197-3.505	0.801						
Histological grade									
1	1.0 (ref)			1.0 (ref)			1.0 (ref)		
2	1.583	0.566-4.429	0.382	1.517	0.381-6.037	0.544	1.773	0.336-9.367	0.500
3	2.815	1.045-7.585	<b>0.041</b>	2.942	0.850-10.180	0.088	1.956	0.381-10.049	0.422
Tumor size									
pT1	1.0 (ref)			1.0 (ref)			1.0 (ref)		
pT2	0.983	0.550-1.759	0.955	1.122	0.538-2.339	0.759	0.387	0.125-1.196	0.099
pT3	1.701	0.833-3.475	0.145	1.988	0.606-6.527	0.257	0.883	0.312-2.500	0.814
Age	1.050	1.029-1.072	<b>&lt;0.001</b>	1.055	1.025-1.085	<b>&lt;0.001</b>	1.065	1.032-1.099	<b>&lt;0.001</b>
Lymph node status									
Negative	1.0 (ref)			1.0 (ref)			1.0 (ref)		
Positive	2.871	1.607-5.130	<b>&lt;0.001</b>	2.606	1.177-5.768	<b>0.018</b>	3.706	1.528-8.989	<b>0.004</b>
Nuclear SOX4									
Low	1.0 (ref)			1.0 (ref)			1.0 (ref)		
High	1.899	1.049-3.437	<b>0.034</b>	1.669	0.693-4.019	0.253	2.605	1.120-6.059	<b>0.026</b>

HR = Hazard rate; CI = Confidence interval

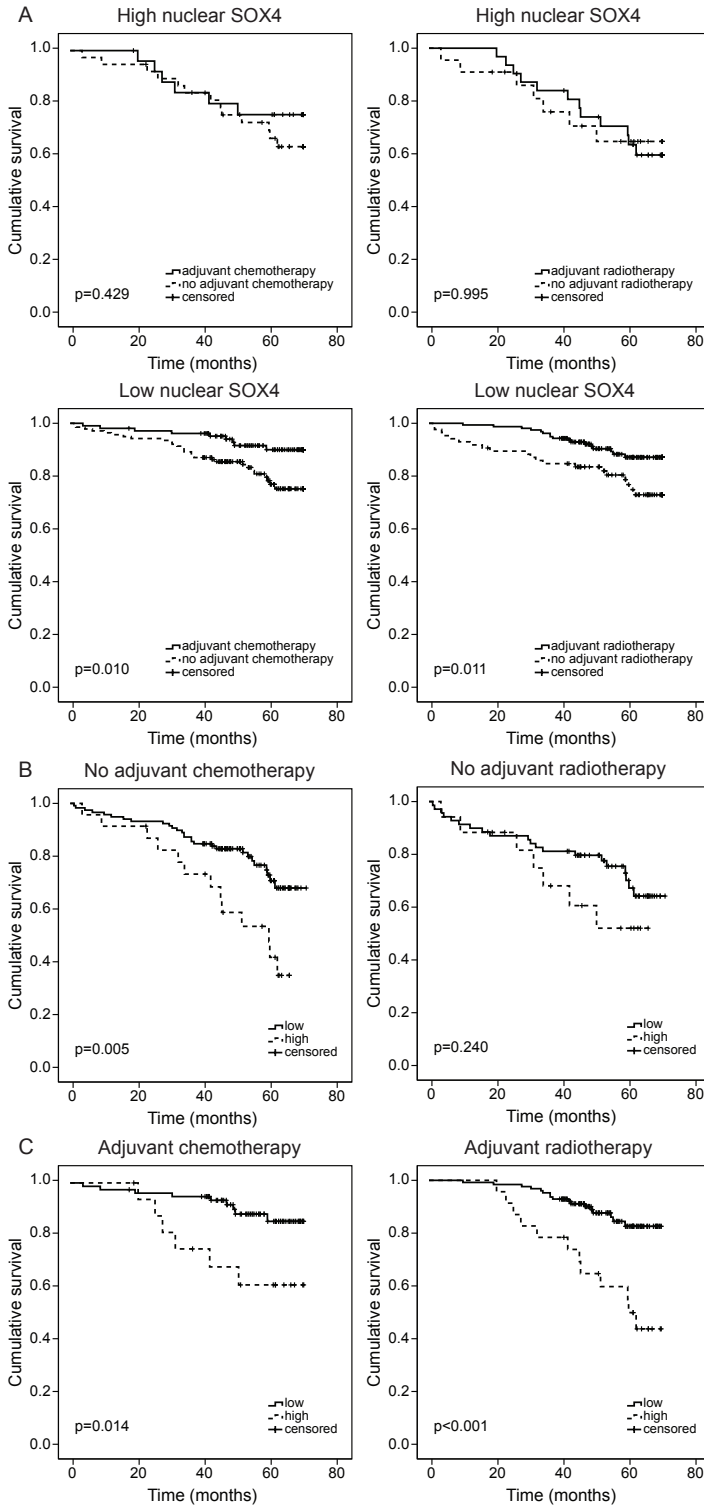


**Figure 3. Overall survival curves for patients with high or low nuclear SOX4 expression in relation to adjuvant therapy.**

(A) Overall survival of patients with high or low nuclear SOX4 in relation to adjuvant chemo- or radiotherapy.

(B) Overall survival of patients with high or low nuclear SOX4 in relation to not receiving adjuvant chemo- or radiotherapy.

(C) Overall survival of patients with high or low nuclear SOX4 in relation to receiving adjuvant chemo- or radiotherapy.

**Table 3.** Prognostic value of nuclear SOX4 expression and established prognosticators in relation to adjuvant therapy.

Feature	No adjuvant chemotherapy			No adjuvant radiotherapy			Adjuvant chemotherapy			Adjuvant radiotherapy		
	HR	95% CI	p-value	HR	95% CI	p-value	HR	95% CI	p-value	HR	95% CI	p-value
Type												
IDC	1.0 (ref)			1.0 (ref)			1.0 (ref)			1.0 (ref)		
ILC	0.945	0.449-1.990	0.882	0.432	0.161-1.163	0.097	0.068	0.011-0.443	<b>0.005</b>	0.661	0.252-1.734	0.400
Others	0.876	0.110-7.000	0.900	7.029	1.375-35.927	<b>0.019</b>	0.631	0.078-5.093	0.666	0.000	0.000	0.978
Grade												
1	1.0 (ref)			1.0 (ref)			1.0 (ref)			1.0 (ref)		
2	1.563	0.468-5.219	0.468	1.978	0.409-9.569	0.396	1.361	0.122-15.122	0.802	1.408	0.342-5.794	0.636
3	3.328	1.055-10.496	<b>0.040</b>	3.237	0.722-14.515	0.125	4.206	0.456-38.781	0.205	2.623	0.643-10.696	0.179
Tumor size												
pT1	1.0 (ref)			1.0 (ref)			1.0 (ref)			1.0 (ref)		
pT2	0.968	0.476-1968	0.928	1.054	0.444-2.499	0.905	1.089	0.354-3.348	0.882	0.757	0.313-1.829	0.536
pT3	1.307	0.521-3.279	0.568	6.130	1.731-21.709	<b>0.005</b>	6.258	1.426-27.474	<b>0.015</b>	1.215	0.45-3.278	0.700
Age	1.053	1.020-1.088	<b>0.002</b>	1.068	1.023-1.114	<b>0.003</b>	1.039	0.983-1.098	0.177	1.034	0.996-1.073	0.080
LN status												
Negative	1.0 (ref)			1.0 (ref)			1.0 (ref)			1.0 (ref)		
Positive	2.627	1.324-5.209	<b>0.006</b>	1.292	0.564-2.958	0.545	3.026	0.628-14.567	0.167	6.825	2.340-19.909	<b>&lt;0.001</b>
Nuclear SOX4												
Low	1.0 (ref)			1.0 (ref)			1.0 (ref)			1.0 (ref)		
High	1.670	0.803-3.469	0.170	1.546	0.622-3.846	0.348	4.132	1.626-10.499	<b>0.003</b>	3.049	1.462-6.358	<b>0.003</b>
Hormone therapy												
Not receiving	1.0 (ref)			1.0 (ref)			1.0 (ref)			1.0 (ref)		
Receiving	0.205	0.088-0.480	<b>&lt;0.001</b>	0.303	0.119-0.771	<b>0.012</b>	1.744	0.551-5.521	0.344	0.577	0.265-1.258	0.167
Radiotherapy												
Not receiving	1.0 (ref)			1.0 (ref)			1.0 (ref)			1.0 (ref)		
Receiving	0.854	0.426-1.710	0.656	0.337	0.113-1.006	0.051	0.337	0.113-1.006	0.051	0.458	0.167-1.258	0.130
Chemotherapy												
Not receiving	1.0 (ref)			1.0 (ref)			1.0 (ref)			1.0 (ref)		
Receiving	2.079	0.574-7.525	0.265	2.079	0.574-7.525	0.265	2.079	0.574-7.525	0.265	2.079	0.574-7.525	0.265

LN = lymph node; HR = Hazard rate; CI = Confidence interval

## Discussion

In addition to the established role of SOX transcription factors in vertebrate development, increasing evidence emerges that these factors can function as oncogenes or tumor suppressor genes [20-23]. The subgroup of SOXC-type transcription factors consisting of SOX4, SOX11, and SOX12 has been linked to multiple cancers, but the precise role of SOX4 in epithelial cancer is yet to be elucidated. Recently, SOX4 was shown to be associated with triple negative breast cancer and the induction of an EMT-like phenotype in breast cancer cells [25]. Further, overexpression of SOX4 in multiple cancers was correlated with resistance towards conventional adjuvant therapies by induction of DNA-repair and inhibition of apoptosis [29].

The aim of the present study was to identify the role of SOX4 in breast cancer in relation to prognosis and adjuvant therapy response. We found that expression of SOX4 was associated with high grade and high mitotic activity. Furthermore, SOX4 expression was higher in ILC compared to IDC. Since ILC lacks E-cadherin expression, SOX4 levels were expected to be higher than in IDC. However, pleomorphic ILC had significantly higher SOX4 expression than classical ILC, arguing that other factors in addition to loss of E-cadherin, (in)directly control SOX4 localization and expression. It has recently been described that regulation of SOX4 localization may occur through an interaction with plakoglobin ( $\gamma$ -catenin) which associates with adherens junction proteins such as cadherins [37]. In addition, SOX4 has been described to interact with  $\beta$ -catenin and has been demonstrated to potentiate Wnt-signaling [38]. The interaction of SOX4 with plakoglobin in the nucleus was observed to be dependent on Wnt3A signaling and resulted in a competition for binding with  $\beta$ -catenin and nuclear export of SOX4. Potentially tumor-specific loss of E-cadherin releases  $\beta$ -catenin and plakoglobin and thus modulates the localization of SOX4. Moreover, activation of the Wnt-signaling pathway has been linked to resistance to 5-FU in hepatocellular carcinoma [39], radiotherapy resistance in glioblastoma [40] and the generation of therapy-resistant cancer stem cell populations [41]. Possibly, SOX4-mediated potentiation of the Wnt-signaling pathway contributes to the therapy resistance phenotype in SOX4 high tumors [14].

In our study high nuclear SOX4 expression was independently associated with decreased survival of patients with both ILC and IDC. Furthermore, increased nuclear SOX4 expression predicted response to adjuvant chemotherapy and radiotherapy since only patients with low nuclear SOX4 responded to therapy. In the subgroup of patients receiving adjuvant therapy, nuclear SOX4 was also an independent prognostic factor. These findings suggest



that SOX4 may promote chemo- and radiotherapy resistance in breast cancer rather than sensitization as previously described for SOX4 in colorectal carcinoma [30]. The precise mechanism of SOX4-mediated resistance is largely unknown, while several studies have identified SOX4 transcriptional targets there is little overlap, potentially reflecting tumor-specific and context dependent mechanisms. However, the core of genes found e.g. *EGFR*, *VEGF* was rather linked to metastasis than to resistance [42, 43]. Nevertheless, two of the most well characterized SOX4 target genes *Tubulin- $\beta$ III* (*TUBB3*) and *TEAD2* have been linked to therapy resistance [10, 29]. *TUBB3* is an important factor in the acquired resistance to microtubule targeting agents [30], whereas the *TEAD2* transcription factor could impact on therapy resistance through modulation of the HIPPO-signaling pathway which is closely linked with therapy resistance in breast cancer and glioblastoma [44, 45]. It is thus possible that SOX4-mediated chemo- and radiotherapy resistance is dependent on its direct transcriptional regulation of yet to be identified resistance related target genes.

In conclusion, in this retrospective study, expression of nuclear SOX4 was associated with a more aggressive phenotype of both ductal and lobular breast cancer resulting in poor survival of affected patients. In addition, nuclear SOX4 seemed to independently predict resistance to adjuvant chemo- and radiotherapy. Since the chemotherapy regimens used differed over time and data on the exact combination of chemotherapeutics was not always available, no conclusions can be drawn according to type of chemotherapy and resistance upon SOX4 expression. In our view, based on our results, a second study where detailed information on various types of systemic adjuvant treatment, can be linked to SOX4 expression in the tumor, is warranted before any definite conclusions can be drawn towards clinical implications of SOX4 expression. If the data will be confirmative, targeting SOX4 could become a potential new avenue in the treatment of cancer.

## Acknowledgements

This work was supported by an unrestricted research grant of AEGON Inc.

## References

1. DeSantis C, Siegel R, Bandi P and Jemal A. Breast cancer statistics, 2011. *CA Cancer J Clin* 2011; 61(6): 409-18.
2. Howlader N, Noone A, Krapcho M, *et al.* SEER Cancer Statistics Review, 1975-2009, based on November 2011 SEER data submission. 2012.
3. Integraal Kanker Centrum Nederland. Incidentie van invasieve tumoren (1989-2010). [www.cijfersoverkanker.nl](http://www.cijfersoverkanker.nl). Accessed: 13 May 2012.
4. Autier P, Boniol M, La Vecchia C, *et al.* Disparities in breast cancer mortality trends between 30 European countries: retrospective trend analysis of WHO mortality database. *BMJ* 2010; 341:c3620.
5. Otto SJ, Fracheboud J, Verbeek AL, *et al.* Mammography screening and risk of breast cancer death: a population-based case-control study. *Cancer Epidemiol Biomarkers Prev* 2012; 21(1):66-73.
6. Singletary SE. Surgical margins in patients with early-stage breast cancer treated with breast conservation therapy. *Am J Surg* 2002; 184(5):383-93.
7. Integraal Kanker Centrum Nederland. Sterfte aan kanker (1989-2010). [www.cijfersoverkanker.nl](http://www.cijfersoverkanker.nl). Accessed: 13 May 2012.
8. Rhodes DR, Yu J, Shanker K, *et al.* Large-scale meta-analysis of cancer microarray data identifies common transcriptional profiles of neoplastic transformation and progression. *Proc Natl Acad Sci U S A* 2004; 101(25):9309-14.
9. Vervoort SJ, van Boxtel R and Coffey PJ. The role of SRY-related HMG box transcription factor 4 (SOX4) in tumorigenesis and metastasis: friend or foe? *Oncogene*; 2012. accepted.
10. Dy P, Penzo-Mendez A, Wang H, *et al.* The three SoxC proteins--Sox4, Sox11 and Sox12--exhibit overlapping expression patterns and molecular properties. *Nucleic Acids Res* 2008; 36(9):3101-17.
11. Maschhoff KL, Anziano PQ, Ward P and Baldwin HS. Conservation of Sox4 gene structure and expression during chicken embryogenesis. *Gene* 2003; 320:23-30.
12. Tanaka S, Kamachi Y, Tanouchi A, *et al.* Interplay of SOX and POU factors in regulation of the Nestin gene in neural primordial cells. *Mol Cell Biol* 2004; 24(20):8834-46.
13. Schilham MW, Oosterwegel MA, Moerer P, *et al.* Defects in cardiac outflow tract formation and pro-B-lymphocyte expansion in mice lacking Sox-4. *Nature* 1996; 380(6576):711-4.
14. Bhattaram P, Penzo-Mendez A, Sock E, *et al.* Organogenesis relies on SoxC transcription factors for the survival of neural and mesenchymal progenitors. *Nat Commun* 2010; 1:9.
15. Pece S, Tosoni D, Confalonieri S, *et al.* Biological and molecular heterogeneity of breast cancers correlates with their cancer stem cell content. *Cell* 2010; 140(1):62-73.
16. Hunt SM and Clarke CL. Expression and hormonal regulation of the Sox4 gene in mouse female reproductive tissues. *Biol Reprod* 1999; 61(2):476-81.
17. Van der Flier LG, Sabates-Bellver J, Oving I, *et al.* The Intestinal Wnt/TCF Signature. *Gastroenterology* 2007; 132(2):628-32.
18. Lioubinski O, Muller M, Wegner M and Sander M. Expression of Sox transcription factors in the developing mouse pancreas. *Dev Dyn* 2003; 227(3):402-8.
19. van de Wetering M, Oosterwegel M, van Norren K and Clevers H. Sox-4, an Sry-like HMG box protein, is a transcriptional activator in lymphocytes. *EMBO J* 1993; 12(10):3847-54.
20. de Bont JM, Kros JM, Passier MM, *et al.* Differential expression and prognostic significance of SOX genes in pediatric medulloblastoma and ependymoma identified by microarray analysis. *Neuro Oncol* 2008; 10(5):648-60.
21. Aaboe M, Birkenkamp-Demtroder K, Wiuf C, *et al.* SOX4 expression in bladder carcinoma: clinical aspects and in vitro functional characterization. *Cancer Res* 2006; 66(7):3434-42.
22. Jafarnejad SM, Wani AA, Martinka M and Li G. Prognostic significance of Sox4 expression in human cutaneous melanoma and its role in cell migration and invasion. *Am J Pathol* 2010; 177(6):2741-52.
23. Wang C, Zhao H, Lu J, *et al.* Clinicopathological significance of SOX4 expression in primary gallbladder carcinoma. *Diagn Pathol* 2012; 7:41.

24. Tavazoie SF, Alarcon C, Oskarsson T, *et al.* Endogenous human microRNAs that suppress breast cancer metastasis. *Nature* 2008; 451(7175):147-52.
25. Zhang J, Liang Q, Lei Y, *et al.* SOX4 induces epithelial-mesenchymal transition and contributes to breast cancer progression. *Cancer Res* 2012; 72(17):4597-608.
26. Graham JD, Hunt SM, Tran N and Clarke CL. Regulation of the expression and activity by progestins of a member of the SOX gene family of transcriptional modulators. *J Mol Endocrinol* 1999; 22(3):295-304.
27. Huang YW, Liu JC, Deatherage DE, *et al.* Epigenetic repression of microRNA-129-2 leads to overexpression of SOX4 oncogene in endometrial cancer. *Cancer Res* 2009; 69(23):9038-46.
28. Boyer J, Allen WL, McLean EG, *et al.* Pharmacogenomic identification of novel determinants of response to chemotherapy in colon cancer. *Cancer Res* 2006; 66(5):2765-77.
29. Chetty C, Dontula R, Gujrati M, Dinh DH and Lakka SS. Blockade of SOX4 mediated DNA repair by SPARC enhances radioresponse in medulloblastoma. *Cancer Lett* 2012; 323(2):188-98.
30. Pan X, Zhao J, Zhang WN, *et al.* Induction of SOX4 by DNA damage is critical for p53 stabilization and function. *Proc Natl Acad Sci U S A* 2009; 106(10):3788-93.
31. Elston CW and Ellis IO. Pathological prognostic factors in breast cancer. I. The value of histological grade in breast cancer: experience from a large study with long-term follow-up. *Histopathology* 1991; 19(5):403-10.
32. van der Groep P, Bouter A, van der Zanden R, *et al.* Distinction between hereditary and sporadic breast cancer on the basis of clinicopathological data. *J Clin Pathol* 2006; 59(6):611-7.
33. Vermeulen JF, van de Ven RA, Ercan C, *et al.* Nuclear kaiso expression is associated with high grade and triple-negative invasive breast cancer. *PLoS One* 2012; 7(5):e37864.
34. Vermeulen JF, van Brussel AS, van der Groep P, *et al.* Immunophenotyping invasive breast cancer: paving the road for molecular imaging. *BMC Cancer* 2012; 12(1):240.
35. van Diest PJ. No consent should be needed for using leftover body material for scientific purposes. *For BMJ* 2002; 325(7365):648-51.
36. Kornegoor R, Verschuur-Maes AH, Buerger H, *et al.* Molecular subtyping of male breast cancer by immunohistochemistry. *Mod Pathol* 2012; 25(3):398-404.
37. Finak G, Bertos N, Pepin F, *et al.* Stromal gene expression predicts clinical outcome in breast cancer. *Nat Med* 2008; 14(5):518-27.
38. Gluck S, Ross JS, Royce M, *et al.* TP53 genomics predict higher clinical and pathologic tumor response in operable early-stage breast cancer treated with docetaxel-capecitabine +/- trastuzumab. *Breast Cancer Res Treat* 2012; 132(3):781-91.
39. Noda T, Nagano H, Takemasa I, *et al.* Activation of Wnt/beta-catenin signalling pathway induces chemoresistance to interferon-alpha/5-fluorouracil combination therapy for hepatocellular carcinoma. *Br J Cancer* 2009; 100(10):1647-58.
40. Kim Y, Kim KH, Lee J, *et al.* Wnt activation is implicated in glioblastoma radioresistance. *Lab Invest* 2012; 92(3):466-73.
41. de Sousa EM, Vermeulen L, Richel D and Medema JP. Targeting Wnt signaling in colon cancer stem cells. *Clin Cancer Res* 2011; 17(4):647-53.
42. Herbst RS. EGFR inhibition in NSCLC: the emerging role of cetuximab. *J Natl Compr Canc Netw* 2004; 2 Suppl 2:S41-51.
43. Sitohy B, Nagy JA and Dvorak HF. Anti-VEGF/VEGFR therapy for cancer: reassessing the target. *Cancer Res* 2012; 72(8):1909-14.
44. Lai D, Ho KC, Hao Y and Yang X. Taxol resistance in breast cancer cells is mediated by the hippo pathway component TAZ and its downstream transcriptional targets Cyr61 and CTGF. *Cancer Res* 2011; 71(7):2728-38.
45. Xu Y, Stamenkovic I and Yu Q. CD44 attenuates activation of the hippo signaling pathway and is a prime therapeutic target for glioblastoma. *Cancer Res* 2010; 70(6):2455-64.

## Supplementary data

**Table S1.** Clinicopathological characteristics of 452 breast cancer patients studied for the expression of SOX4.

Feature	Grouping	N or value	%
Age (years)	Mean	61	
	Range	28-88	
Histological type	IDC	301	66.6
	ILC	123	27.2
	Other	28	6.2
Tumor size	pT1	202	44.7
	pT2	197	43.6
	pT3	50	11.1
	Not available	3	0.6
Histological grade	1	80	17.7
	2	160	35.4
	3	195	43.1
	Not available	17	3.8
MAI <sup>#</sup>	≤ 12	230	50.9
	≥ 13	222	49.1
Lymph node status	Negative*	220	48.7
	Positive**	212	46.9
	Not available	20	4.4

<sup>#</sup>: per 2 mm<sup>2</sup>; \*: negative = N0 or N0(i+); \*\*:positive = ≥N1mi (according to TNM 7<sup>th</sup> edition, 2010)

**Table S2.** Correlation of cytoplasmic and total SOX4 expression with clinicopathological and molecular features of invasive breast cancer.

Feature	Cytoplasmic SOX4 expression			Total SOX4 expression		
	Low N (%)	High N (%)	p-value	Low N (%)	High N (%)	p-value
Histological type						
IDC	149 (49.5)	152 (50.5)		86 (28.4)	217 (71.6)	
ILC	97 (80.2)	24 (19.8)		49 (39.8)	74 (60.2)	
Other	13 (46.4)	15 (53.6)	<b>&lt;0.001</b>	11 (39.3)	17 (60.7)	0.051
Histological grade						
1	51 (63.8)	29 (36.2)		42 (52.5)	38 (47.5)	
2	91 (57.2)	68 (42.8)		55 (34.0)	107 (66.0)	
3	102 (52.6)	92 (47.4)	0.228	36 (18.5)	159 (81.5)	<b>&lt;0.001</b>
Tumor size						
pT1	108 (53.7)	93 (46.3)		70 (34.7)	132 (65.3)	
pT2	115 (58.7)	81 (41.3)		59 (29.6)	140 (70.4)	
pT3	34 (68.0)	16 (32.0)	0.171	15 (30.0)	35 (70.0)	0.535
MAI (per 2mm <sup>2</sup> )						
≤ 12	136 (59.4)	93 (40.6)		97 (42.2)	133 (57.8)	
≥ 13	123 (55.7)	98 (44.3)	0.423	47 (21.2)	175 (78.8)	<b>&lt;0.001</b>
Lymph node status						
Positive	115 (54.5)	96 (45.5)		59 (27.7)	154 (72.3)	
Negative	137 (62.3)	83 (37.7)	0.102	82 (37.1)	139 (62.9)	<b>0.036</b>
Molecular classification						
Luminal	212 (56.5)	163 (43.5)		127 (33.6)	251 (66.4)	
HER2-driven	11 (64.7)	6 (35.3)		4 (23.5)	13 (76.5)	
Basal/TN	36 (62.1)	22 (37.9)	0.607	15 (25.4)	44 (74.6)	0.339
ERα						
Positive	210 (56.8)	160 (43.2)		127 (34.0)	246 (66.0)	
Negative	49 (61.2)	31 (38.8)	0.461	19 (23.5)	62 (76.5)	0.064
PR						
Positive	141 (53.0)	125 (47.0)		83 (31.0)	185 (69.0)	
Negative	117 (63.9)	66 (36.1)	<b>0.021</b>	62 (33.5)	123 (66.5)	0.568
HER2						
Positive	27 (61.4)	17 (38.6)		14 (31.1)	31 (68.9)	
Negative	231 (57.0)	174 (43.0)	0.581	131 (32.1)	277 (67.9)	0.892
E-cadherin						
Positive	142 (47.5)	157 (52.5)		81 (26.8)	221 (73.2)	
Negative	87 (75.7)	28 (24.3)	<b>&lt;0.001</b>	43 (37.1)	73 (62.9)	<b>0.040</b>

**Table S3.** Correlation of nuclear SOX4 expression with clinicopathological features of IDC and ILC.

Feature	Nuclear SOX4 expression IDC			Nuclear SOX4 expression ILC		
	Low N (%)	High N (%)	p-value	Low N (%)	High N (%)	p-value
Histological grade						
1	50 (94.3)	3 (5.7)		22 (100.0)	0 (0.0)	
2	86 (89.6)	10 (10.4)		40 (80.0)	10 (20.0)	
3	113 (79.6)	29 (20.4)	<b>0.013</b>	20 (45.5)	24 (54.5)	<b>&lt;0.001</b>
Tumor size						
pT1	134 (89.9)	15 (10.1)		33 (80.5)	8 (19.5)	
pT2	109 (82.0)	24 (18.0)		34 (65.4)	18 (34.6)	
pT3	14 (82.4)	3 (17.6)	0.142	20 (69.0)	9 (31.0)	0.265
MAI (per 2mm <sup>2</sup> )						
≤ 12	129 (92.1)	11 (7.9)		65 (87.8)	9 (12.2)	
≥ 13	130 (80.7)	31 (19.3)	<b>0.004</b>	23 (46.9)	26 (53.1)	<b>&lt;0.001</b>
Lymph node status						
Positive	125 (86.2)	20 (13.8)		36 (66.7)	18 (33.3)	
Negative	124 (85.5)	21 (14.5)	0.866	46 (74.2)	16 (25.8)	0.374
Molecular classification						
Luminal	207 (87.0)	31 (13.0)		84 (71.8)	33 (28.2)	
HER2-driven	15 (93.7)	1 (6.3)				
Basal/TN	37 (78.7)	10 (21.3)	0.216	4 (66.7)	2 (33.3)	0.786
ERα						
Positive	206 (87.3)	30 (12.7)		82 (71.9)	32 (28.1)	
Negative	53 (81.5)	12 (18.5)	0.236	6 (66.7)	3 (33.3)	0.736
PR						
Positive	149 (87.6)	21 (12.4)		56 (69.1)	25 (30.9)	
Negative	110 (84.0)	21 (16.0)	0.361	31 (75.6)	10 (24.4)	0.455
HER2						
Positive	34 (89.5)	4 (10.5)		1 (25.0)	3 (75.0)	
Negative	225 (85.6)	38 (14.4)	0.514	86 (72.9)	32 (27.1)	0.071

# Ten

**Summary and future perspectives**

## Summary of the thesis

The first part of the thesis focuses on biomarkers for molecular imaging of breast cancer. In **chapter 2** the prevalence of hypoxia-related markers CAIX, GLUT1, CXCR4, and IGF1-R in breast cancer and their potential for molecular imaging strategies is described in a comprehensive systematic review with meta-regression. We found that hypoxia markers are significantly less frequently expressed in invasive lobular cancer (ILC) compared to invasive ductal carcinoma (IDC). Furthermore, the prevalence of CAIX, GLUT1, and CXCR4 expression was significantly higher in grade 3 breast cancers, whereas IGF1-R expression was significantly lower in grade 3 cancers. Meta-regression showed that studies using tissue microarrays (TMAs) had a significantly lower pooled prevalence of CAIX and GLUT1 compared to studies using whole slides. Although TMAs are convenient for evaluation of large patient cohorts, the value for assessment of hypoxia (and other) markers needs to be reconsidered given significant differences between prevalences found in our meta-analysis. Furthermore, studies should also incorporate data on expression patterns in normal breast tissue, benign lesions, and DCIS, as such information is currently essentially lacking in the literature.

**Chapter 3** reports expression profiles of membrane-bound markers for molecular imaging in histological and molecular subtypes of female breast cancer. We demonstrate that a panel of membrane markers is required to obtain a high 'detection' rate, because the most abundantly expressed tumor-specific marker (GLUT1) was present in only 20% of breast cancers. Further, a panel consisting of tumor-specific markers was less sensitive in ILC and low grade IDC. Moreover, we show that tumor-to-normal ratios of less tumor-specific markers are not caused by increased expression of the marker on cancer cells, but are the result of increased cellularity of the cancer compared to normal breast epithelium. These less tumor-specific markers increased the 'detection' rate of lobular and low grade breast cancer up to 80%. Therefore, one of the current challenges is to identify tumor-specific markers for detection of ILC, but CD44v6 seems to be potentially quite useful.

In **chapter 4**, the growth factor receptor expression profile of male breast cancer is described, suggesting that IGF1-R, expressed in 40% of male breast cancers, is the driving receptor in male breast cancer. Like in female breast cancer, tumor-specific markers i.e. growth factor receptors and hypoxia markers are too infrequently expressed in male breast cancer for molecular imaging strategies. A panel of markers consisting of CD44v6, EGFR, IGF1-R, HER2, and GLUT1 supplemented with FGFR2 and CAXII was equally sensitive in 'detecting' male and female breast cancer.



**Chapter 5** explores whether identified markers for imaging of breast cancer could be useful for image-guided surgery of ductal carcinoma *in situ* (DCIS) using molecular imaging, and whether expression differs between DCIS and adjacent invasive breast cancer. The expression of HER2 is known to be higher in DCIS, but we found GLUT1, IGF1-R, and CAXII expression to be 3-fold higher in DCIS compared to invasive breast cancer. The resulting ‘detection’ rate of DCIS was over 90% and not different between pure DCIS and DCIS with adjacent invasive breast cancer.

In **Chapter 6** we show for the first time in a preclinical study that optical imaging using CD44v6-specific antibodies has sufficient sensitivity for non-invasive and intra-operative imaging of DCIS-like lesions *in vivo*. Due to limited tumor penetration of antibody-based tracers to the first 2-3 cell layers aligning stroma and blood vessels, smaller tracers will be even better applicable for detection of DCIS and other poorly vascularized malignancies.

The second part of the thesis focused on markers determining aggressiveness, metastasis, and predicting therapy resistance of breast cancer. The role of the transcription factor Kaiso in breast cancer is described in **chapter 7**. We show that nuclear Kaiso was predominantly found in IDC, while cytoplasmic Kaiso expression was linked to ILC. The expression of nuclear Kaiso correlated with high grade, loss of estrogen receptor and is highly expressed in triple negative breast cancer. In addition, Kaiso was frequently found in BRCA1-associated breast cancer. We show that p120-catenin is important for the nuclear localization of Kaiso and transcriptional repression of Kaiso targets *in vitro*. Although Kaiso’s target genes in breast cancer are unknown, this suggests that Kaiso may function as an oncogene in IDC through inhibition of tumor suppressor gene expression whereas in ILC, Kaiso might harbor tumor suppressor functions by p120-mediated relieve of transcriptional repression of oncogenic target genes.

The role of FER kinase in breast cancer metastasis is described in **chapter 8**. In highly metastatic cells we could show that downregulation of FER kinase inhibits migration, invasion and anchorage independence. The pronounced phenotype of FER kinase depleted cells was accompanied by changes in gross morphology, the formation of stress fibers, and focal adhesions. Further, in mouse models we determined that downregulation of FER kinase attenuates tumor growth and controls distant metastasis formation. Finally, we found that FER expression is a hallmark of aggressive breast cancer and an independent predictor of decreased patient survival.

**Chapter 9** reports SOX4 expression in breast cancer. SOX4 is abundantly expressed in various cancers and functions as a tumor suppressor or oncogene depending on the cellular context. In breast cancer, SOX4 expression drives tumor metastasis towards lung and bone. We found that nuclear SOX4 was highly expressed in 18% of breast cancers, especially in pleomorphic ILC, and correlated with grade in both IDC and ILC. Further, nuclear SOX4 expression was a prognostic factor for poor survival and served as an independent predictor of resistance to chemotherapy and radiotherapy. These findings suggest that SOX4 may promote chemo- and radiotherapy resistance rather than sensitization as previously described, although the precise mechanism of SOX4-mediated resistance is still to be elucidated.

## Future Perspectives

Molecular imaging with optical tracers rapidly developed into a clinically approved imaging modality for image-guided surgery. However, the number of clinically approved tumor-specific tracers is limited and several clinical trials are currently conducted with targeted imaging tracers. For targeted molecular imaging thorough patient selection is required since the targets are heterogeneously expressed across histological and molecular types of breast cancer, e.g. for HER2-specific tracers only 10-15% of patients will be eligible. In addition, molecular imaging also opens up the possibility to determine the molecular characteristics of breast cancer prior to surgery or to evaluate and adjust adjuvant therapy regimes, which is in particularly valuable for metastatic disease. As previously shown by Hoefnagel et al [1], in 5.2% of patients with metastatic breast cancer HER2 status differed between the primary breast cancer and the metastases, resulting that these patients received incorrect therapy. Therefore, molecular assessment of HER2 status of the metastases by molecular imaging might complement or replace taking biopsies of metastatic sites.

For breast cancer screening a panel of markers is required, but limited tumor penetration of antibodies might hamper the detection of DCIS and other poorly vascularized malignancies. Size reduction of imaging tracers holds promise here due to better diffusion. Prime candidates are tumor-specific VHHs (15kDa antibody fragments consisting of only the Vh domain of the heavy-chain-only antibodies from camelids), since VHHs are stable, non-immunogenic, and can be engineered into larger multivalent tracers [2, 3]. For screening of breast cancer combining multiple tumor-specific VHHs into a single imaging tracer, might be key for imaging of breast cancer with a panel of membrane markers.

The process of breast cancer metastasis and acquired resistance to systemic adjuvant therapies is still poorly understood. We identified that FER kinase and SOX4 are involved in these processes. Preliminary results indicate that SOX4 depletion results in a similar phenotype as FER kinase knockdown and that FER kinase and SOX4 are highly correlated in invasive breast cancer ( $p < 0.001$ ). All together this suggests that FER kinase and SOX4 are in the same biological pathway. Future experiments will therefore focus on whether SOX4 and FER kinase are functionally linked and whether FER kinase expression is effecting therapy resistance.

Comparable to the effect of SOX4 overexpression in breast cancer, tumor hypoxia has been shown to induce resistance to systemic therapy [4, 5]. Preliminary data reveal that nuclear SOX4 was significantly associated with known hypoxia markers HIF1 $\alpha$ , CAIX, and CAXII in clinical specimens. Furthermore, culturing cell lines under hypoxic conditions increased SOX4 expression 2-6 fold on the mRNA and protein level, resulting in upregulation of *TEAD2*, a SOX4 target gene that has been linked to therapy resistance. These data suggest that hypoxia might directly increase SOX4 expression, which could reveal novel mechanisms of induced therapy resistance.

## References

1. Hoefnagel LD, van de Vijver MJ, van Slooten HJ, *et al.* Receptor conversion in distant breast cancer metastases. *Breast Cancer Res* 2010; 12(5):R75.
2. Dolk E, van Vliet C, Perez JM, *et al.* Induced refolding of a temperature denatured llama heavy-chain antibody fragment by its antigen. *Proteins* 2005; 59(3):555-64.
3. Roovers RC, Vosjan MJ, Laeremans T, *et al.* A biparatopic anti-EGFR nanobody efficiently inhibits solid tumour growth. *Int J Cancer* 2011; 129(8):2013-24.
4. Brahimi-Horn MC, Chiche J and Pouyssegur J. Hypoxia and cancer. *J Mol Med (Berl)* 2007; 85(12):1301-7.
5. Semenza GL. Targeting HIF-1 for cancer therapy. *Nat Rev Cancer* 2003; 3(10):721-32.





# Addendum

Nederlandse samenvatting

Dankwoord

About the Author

List of Publications

*J. P. ...*

## Nederlandse samenvatting

In 2010 werd bij 13.257 vrouwen en 94 mannen borstkanker vastgesteld. Hiermee is borstkanker de meest voorkomende vorm van kanker bij vrouwen. Het aantal nieuwe gevallen van borstkanker in Nederland neemt elk jaar gestaag toe door de toegenomen levensverwachting en vanwege de leeftijdsopbouw van de Nederlandse samenleving. Dit betekent dat ongeveer 1 op 8 vrouwen en 1 op 1.000 mannen borstkanker krijgt. Ondanks dat elk jaar meer patiënten de diagnose borstkanker krijgen, blijft het aantal patiënten dat overlijdt aan borstkanker in Nederland stabiel: per jaar ongeveer 3.200 vrouwen en 32 mannen. Het stadium waarin de kanker wordt vastgesteld is van groot belang voor de overleving van borstkanker. De prognose van patiënten met een borsttumor kleiner dan 2 cm zonder uitzaaiingen naar de lymfeklieren (stadium 1) is goed: 98% van de patiënten is na vijf jaar nog in leven. Daarentegen is de prognose van patiënten met uitzaaiingen naar andere organen (stadium 4) erg ongunstig (5-jaars overleving is ongeveer 16%). Door verbeterde behandeling en eerdere diagnose van borstkanker is de 5-jaars overleving toegenomen tot 86% in de afgelopen 20 jaar.

In Nederland worden de meeste nieuwe gevallen van de borstkanker ontdekt door middel van mammografie zoals uitgevoerd tijdens het bevolkingsonderzoek. Door invoering van digitale mammografie wordt borstkanker vaker in een eerder stadium ontdekt, wat tot grotere overlevingskansen leidt. Een voorloperstadium van borstkanker, ductaal carcinoom *in situ*, is steeds vaker een reden om tot een operatie over te gaan. Het grootste nadeel van mammografie is dat de gevoeligheid in bepaalde patiënten te wensen overlaat. Hierdoor zijn andere beeldvormende technieken zoals MRI noodzakelijk om een diagnose te stellen.

Nieuwe ontwikkelingen om borstkanker te ontdekken, vinden plaats op het gebied van de moleculaire beeldvorming. Moleculaire beeldvorming houdt in dat visualisatie, karakterisering en metingen van biologische processen op een moleculair of cellulair niveau plaatsvindt en dat kwantificering van de meting in de tijd mogelijk is. Voorbeelden hiervan zijn MRI, PET, echo en optische beeldvorming. In 2000 werd door Ntziachristos en anderen aangetoond dat de opname van ICG (indocyanine green; een stofje dat na belichting infrarood licht gaat uitzenden, ook wel tracer genoemd) in borstkanker overeenkwam met MRI-beelden. Hieruit bleek dat ICG geschikt was als moleculaire tracer voor optische beeldvorming van borstkanker. Echter, ICG is niet specifiek en stabiel genoeg om tumoren met een hoge resolutie te kunnen ontdekken. Verbeterde stoffen zoals IRDye800CW zijn stabiel en kunnen tumorspecifiek gemaakt worden door ze te koppelen aan antilichamen. Het aantal antilichamen dat is goedgekeurd voor klinische doeleinden is echter beperkt.

Behalve verbeterde beeldvorming heeft het ontwikkelen van specifieke therapieën de overlevingskansen voor patiënten met borstkanker doen toenemen. Na het ontrafelen van de moleculaire karakteristieken van borstkanker in de afgelopen 20 jaar, is de behandeling steeds meer toegespitst op de tumorkarakteristieken van de individuele patiënt. Daardoor wordt hormoontherapie enkel gegeven wanneer hormoonreceptoren in de tumorcellen aanwezig zijn. Dit geldt ook voor behandeling met Herceptin, dat enkel bij overexpressie van de tumormarker HER2 effectief is. Daarnaast wordt er veel onderzoek gedaan naar de therapeutische mogelijkheden van andere markers zoals EGFR, IGF1-R en VEGF. Therapie die zich richt op specifieke markers, vergt een uitgebreide patiëntselectie. Wanneer de expressie van de marker waarop de therapie gebaseerd is verminderd, heeft dit direct negatieve gevolgen voor de effectiviteit van de behandeling. Om de behandeling te optimaliseren, kan gebruik gemaakt worden van tumorspecifieke antilichamen (met daaraan gekoppeld bijvoorbeeld IRDye800CW) om zo de target expressie op verschillende momenten te bepalen. Diagnostische beeldvorming is daarom in de toekomst niet meer los te zien van therapie.

## Deel 1 Moleculaire markers voor beeldvorming van borstkanker

Het eerste deel van het proefschrift gaat over nieuwe markers voor moleculaire beeldvorming. In **hoofdstuk 2** wordt een literatuurstudie beschreven over de expressie (hoeveel en hoe vaak een eiwit voorkomt) van hypoxia (zuurstoftekort) markers in borstkanker. Verschillen tussen de studies met betrekking tot de gebruikte methodes was groot. Wij hebben gevonden dat in tegenstelling tot invasief ductaal carcinoom (IDC, de meest voorkomende vorm van borstkanker), invasief lobulair carcinoom (ILC, verantwoordelijk voor 10-15% van alle borstkankers) bijna nooit hypoxia markers tot expressie brengt. Daarnaast was de prevalentie van hypoxia markers in borstkanker afhankelijk van de gebruikte methode.

In **hoofdstuk 3** wordt de expressie van verschillende markers in borstkanker beschreven. Hierin laten we zien dat meerdere tumorspecifieke markers noodzakelijk zijn om borstkanker in hoge mate te kunnen detecteren. De meest voorkomende marker (GLUT1) was maar in 20% van alle borstkankers aanwezig. Daarnaast waren de tumorspecifieke markers minder geschikt voor detectie van ILC en laaggradig (minder agressief) IDC. Markers die in het normale borstweefsel tot expressie komen, kwamen ook vaker tot expressie in ILC en laaggradig IDC. Dergelijke markers die voorkomen in zowel borstkanker als normaal borstweefsel kunnen bruikbaar zijn voor detectie van borstkanker, omdat de celdichtheid van kanker groter is dan van het omliggend normale borstweefsel. Zo is er voldoende verschil om borstkanker te kunnen onderscheiden.

**Hoofdstuk 4** beschrijft het expressiepatroon van groeifactorreceptoren in borstkanker bij mannen. In 40% van alle gevallen van borstkanker bij mannen kwam IGF1-R tot expressie. Daarmee kan IGF1-R de belangrijkste groeifactorreceptor zijn voor borstkankerontwikkeling bij mannen. Daarnaast hebben wij gevonden dat voor beeldvorming van borstkanker bij mannen een combinatie van markers noodzakelijk is.

Ductaal carcinoom *in situ* (DCIS), een voorloperstadium van borstkanker, komt vaak rond borstkanker voor. DCIS kan voor problemen zorgen tijdens borstbesparende operaties, omdat het niet te voelen is. Dit geeft het risico op een incomplete verwijdering en het (opnieuw) ontwikkelen van borstkanker. Moleculaire beeldvorming van DCIS tijdens de operatie zou de kans op een incomplete verwijdering kunnen beperken. In **hoofdstuk 5** hebben we gekeken of expressie van moleculaire markers in DCIS overeenkwam met die in borstkanker. De expressie was gelijk tussen patiënten met alleen DCIS en patiënten met DCIS en borstkanker. Wel kwamen verschillende markers tot drie keer vaker in DCIS tot expressie dan in de naastgelegen borstkanker. Kortom moleculaire markers zijn bruikbaar voor de detectie van zowel DCIS als borstkanker.

In **hoofdstuk 6** is in een muismodel onderzocht of DCIS met moleculaire optische beeldvorming detecteerbaar was. Hiervoor werden muizen geïnjecteerd met antilichamen gekoppeld aan IRDye800CW (een stof dat na belichting infrarood licht gaat uitzenden). De muizen zijn een week gevolgd om tumoren te lokaliseren op basis van het uitgezonden infrarode licht. Tumorspecifieke antilichamen waren vier uur na injectie in voldoende mate in de tumoren aanwezig om ze (non-invasief) te kunnen lokaliseren. Met controle antilichamen waren de tumoren niet detecteerbaar. Tijdens operatieve beeldvorming bleek dat non-invasieve beeldvorming de daadwerkelijke hoeveelheid antilichaam in de tumor onderschatte. Desondanks was DCIS met tumorspecifieke antilichamen zowel met non-invasieve als intra-operatieve beeldvorming detecteerbaar.

## **Deel 2 Markers die metastasering en therapieresistentie van borstkanker voorspellen**

Het tweede deel van het proefschrift gaat over markers die agressiviteit van borstkanker, metastasering (het proces van uitzaaien van borstkanker) en het niet meer werkzaam zijn van therapie voorspellen.

In **hoofdstuk 7** wordt het eiwit Kaiso beschreven. De lokalisatie van Kaiso blijkt samen te hangen met het type borstkanker: in IDC bevond Kaiso zich in de celkern terwijl in ILC Kaiso in het cytoplasma werd aangetroffen. Patiënten met veel Kaiso expressie in de kern hadden vaker een agressievere of erfelijke vorm van borstkanker.



De rol van het eiwit FER kinase in borstkanker staat centraal in **hoofdstuk 8**. In cellijnen die kunnen metastaseren hebben we aangetoond dat een verlaging van FER kinase expressie, migratie en invasie van tumorcellen beperkte. In muismodellen voor borstkanker werd aangetoond dat tumorcellen met verlaagde FER kinase expressie minder snel groeiden en minder tot geen metastases meer konden vormen in de longen, lever en bot. Daarnaast was hoge FER kinase expressie een kenmerk van agressieve borstkanker en hadden patiënten met hoge FER kinase expressie een slechtere overleving en vaker uitzaaiingen.

**Hoofdstuk 9** bespreekt de rol van SOX4 in borstkanker. SOX4 is een eiwit dat veelvuldig tot expressie komt in kanker. In borstkanker zorgt SOX4 er mede voor dat borstkanker kan uitzaaien naar longen en bot. Wij hebben gevonden dat SOX4 expressie in de kern vaker voorkomt in agressieve vormen van borstkanker. Deze patiënten hadden een slechtere prognose, omdat ze niet op de gebruikelijke chemo- en radiotherapie reageerden.

### **Toekomstperspectieven**

Moleculaire beeldvorming met tumorspecifieke markers ontwikkelt zich snel tot een klinisch toegepaste techniek voor beeldgeleide chirurgie. Echter, tumorspecifieke markers komen niet in elk type borstkanker tot expressie, waardoor uitgebreide patiëntselectie noodzakelijk is. Naast beeldgeleide chirurgie zijn er andere klinische toepassingen van moleculaire beeldvorming, zoals het bepalen van de tumorkarakteristieken en het evalueren en aanpassen van chemo- en radiotherapie op basis van metastases. Daarmee zou moleculaire beeldvorming het nemen van biopten van de metastases kunnen vervangen of van aanvullende waarde kunnen zijn.

Het proces van metastasering en resistentie tegen chemo- en radiotherapie is niet duidelijk. In dit proefschrift hebben we twee eiwitten beschreven FER kinase en SOX4, die betrokken zijn bij metastasering en therapieresistentie. Uit voorlopige resultaten is gebleken dat verminderde SOX4 expressie tot een identiek fenotype leidt als verminderde FER kinase expressie. Daarnaast is FER kinase en SOX4 expressie aan elkaar gekoppeld. Vervolgexperimenten zijn noodzakelijk om uit te zoeken hoe FER kinase en SOX4 elkaar beïnvloeden en of FER kinase van invloed is op therapieresistentie.

Vergelijkbaar met SOX4 expressie in borstkanker leidt hypoxia (zuurstoftekort) tot therapieresistentie. Wanneer cellijnen onder hypoxische omstandigheden groeiden, was SOX4 expressie verhoogd, wat leidde tot expressie van therapieresistentie geassocieerde genen. Vervolgexperimenten zijn noodzakelijk om dit verder te onderzoeken, maar deze data geven een eerste aanknopingspunt hoe hypoxia tot therapieresistentie kan leiden.

## Dankwoord

Er zijn vele mensen zonder wiens hulp ik dit proefschrift niet had kunnen voltooien. Graag wil ik iedereen, met wie ik heb samengewerkt, bedanken voor hun praktische bijdrage, danwel voor hun hulp of het tonen van interesse. Een aantal personen wil ik in het bijzonder noemen.

Prof. dr. P.J. van Diest. Beste Paul, jou ben ik veel dank verschuldigd, zeker nadat we op 14 mei 2010 besloten om mijn onderzoek te focussen op moleculaire markers voor beeldvorming in borstkanker. Een logisch begin was het analyseren van de expressie van markers in borstkanker specimens. Ik denk dat wij beiden niet hadden voorzien dat het in plaats van weken/maanden, anderhalf jaar zou duren en dat we ongeveer 17.000 TMA cores zouden bekijken. 'Do it bigger and better' in optima forma. Snel daarna kwam het (voorlopige) hoogtepunt toen we met een van die markers de eerste millimeter grootte borsttumoren met optische beeldvorming konden detecteren in een muis. Iets dat we lang niet voor mogelijk hadden gehouden en wat een mooi begin vormt om andere markers (pre)klinisch te valideren. Jouw betrokkenheid en enthousiasme, werken zeer aanstekelijk en heeft mij geholpen om tot dit proefschrift te komen. Dank je wel.

Prof. dr. E. van der Wall. Beste Elsen, ik wil je graag bedanken voor je betrokkenheid en klinische visie in mijn project, vaak was jouw input van doorslaggevend belang. Daarnaast stimuleerde je mij om translationeel onderzoek te plaatsen in de context: wat betekent het onderzoek/resultaat voor de patiënt met borstkanker, de vrouwen (en mannen) waar het uiteindelijk om gaat. Daarmee heb je (samen met Paul) mij laten ontdekken waar mijn interesse ligt, heel veel dank hiervoor.

Dr. P.W.B. Derksen. Beste Patrick, halverwege mijn promotietraject kwam je de afdeling versterken met jouw groep. Hoewel mijn project op dat moment inhoudelijk veranderde, was je inbreng van grote waarde en heeft het geleid tot een aantal papers die ook zijn opgenomen in dit proefschrift. Bedankt voor je begeleiding.

De leden van de beoordelingscommissie wil ik bedanken voor de tijd en moeite die u heeft genomen voor het beoordelen van mijn proefschrift.

Mijn collega's van de Breast Cancer Research groep: Iordanka, Aram, Robert Kornegoor, Petra, Cigdem, Laurien, Jolien, Jan, Yvonne, Pan, Cathy, Guus, Anoek, Ron, Eva, Milou, Robert van de Ven, Miranda, Marise, Mirthe, Annelies, Berna, Miangela en Jonathan

bedankt voor de samenwerking, waardevolle discussies en suggesties, het aandragen van nieuwe inzichten, het aanhoren van mijn onderzoeksfrustraties, maar zeker ook voor de gezelligheid op het lab en daarbuiten.

Naast de Breast Cancer Research groep, wil ik mijn (oud-)collega's van het Pathology Research Lab bedanken: Wendy (o.a. voor het runnen van het lab), Folkert, Stefanie, Lucas, Stefan, Dionne, Annette, Ka Wai, Roel Broekhuizen, Niels, Roel Goldschmeding, Johan, Ellen, Marc, Karijn, Robert, Geert, Danielle, Alexey, Julia, Kelly, Mariska en alle studenten voor de input, belangstelling en de goede sfeer.

Iedereen van de Moleculaire en Immunopathologie en de Biobank bedankt voor jullie hulp en interesse gedurende mijn onderzoek. In het bijzonder Domenico voor de assistentie bij het maken van de TMAs, Jan en Natalie voor het verwerken van mijn muismateriaal en het snijden van de coupes voor hoofdstuk 8. Een klus die niet snel vergeten zal worden, waardoor verschillende (micro)metastases zijn gevonden die anders gemist waren. Aad en Willem bedankt voor het opzoeken van de vele coupes. Willy bedankt voor alle logistieke hulp en het vinden van gaatjes in de overvolle agenda van Paul.

Graag zou de groep van Paul van Bergen en Henegouwen in het Kruij: Paul, Sabrina, Marta, Smiriti, Raimond, Jarno, Rachid, Chris en Alex bedanken voor hun hulp en belangstelling gedurende mijn onderzoek. Helaas is het door tijdgebrek er niet van gekomen om ook een nanobody te maken tegen een van mijn targets, wat ik wel gehoopt had. Wie weet gaat het er in de toekomst nog van komen...

Ik wil iedereen die betrokken is in het CTMM Mammoth consortium bedanken voor de input tijdens de meetings.

'Sometimes things just happen... and we call it miracles' is misschien ook wel van toepassing op het project SOX4 in borstkanker. Beste Stephin, wie had kunnen vermoeden dat wij de resultaten zouden gaan vinden zoals beschreven in hoofdstuk 9. Daarnaast lijkt de rol van SOX4 in therapieresistentie ook nog bevestigd te worden in *in vitro* experimenten. Ik heb je leren kennen als zeer gedreven onderzoeker en een prettig persoon om mee samen te werken. Ik wens je heel veel succes met je verdere onderzoek en ik hoop (nee, ik zorg) dat ik in mijn drukke schema ergens mogelijkheden vind om samen verder te bouwen aan bijvoorbeeld de relatie SOX4 en hypoxia.

Graag wil ik Sjoerd bedanken voor zijn inzet en hulp bij het tot stand komen van hoofdstuk 2.

Moleculaire beeldvorming in 'mijn' muizen was nooit van de grond gekomen zonder de inzet en toewijding van Arthur en Aram. Arthur, jouw inbreng is misschien het best te kwalificeren als onvervangbaar. Nadat de pilot met de daarvoor geoptimaliseerde animal imager op een grote teleurstelling uitdraaide, zorgde je ervoor dat er getest kon worden in het GDL met de voor klinische doeleinden geschikte camera (die het natuurlijk wel deed). Maar ook daarna was je zeer betrokken: van het regelen van software updates zodat er quantitative analyses gedaan konden worden, het mede opzetten en uitvoeren dan de proef, de analyses, tot samen vrijdagavond laat obducties doen in een uitgestorven donker GDL. Dit heeft geleid tot een mooi paper over CD44v6 imaging. Daarnaast ben ik je ook veel dank verschuldigd met betrekking tot hoofdstuk 2, zonder jouw inzet was het niet zo compleet geworden. Heel hartelijk bedankt voor alle hulp en ik hoop dat je nu snel de eerste patiënt kan gaan imagen.

Beste Aram, beste paranimf. Ik heb je leren kennen als een gedreven collega die fundamenteel biomedisch onderzoek ging doen naar niet de meest gemakkelijkste eiwitten voor moleculaire beeldvorming, CAIX en GLUT1. Ondanks de moeizame selecties van je nanobodies, bewonder ik je doorzettingsvermogen wat uiteindelijk tot werkende probes en bijbehorende prachtige resultaten heeft geleid in *in vivo* experimenten. Dat het gelukt is om met proof-of-principle experimenten, de klinische mogelijkheden en toepasbaarheid van hypoxia markers voor moleculaire beeldvorming aan te tonen, is iets waarop we toch wel (een klein beetje) trots mogen zijn. Naast je eigen probes, heb je een belangrijk aandeel gehad in moleculaire beeldvorming van CD44v6. Heel hartelijk bedankt hiervoor en heel veel succes met het afronden van je promotie.

Beste familie, opa en oma bedankt voor jullie belangstelling voor mijn onderzoek.

Beste Marije, mijn lieve zus, ik ben heel blij dat je mijn paranimf wilt zijn. Graag wil ik je bedanken voor de gezelligheid, je optimisme, de belangstelling voor mijn onderzoek en je hulp bij statistiek en bij de laatste loodjes van mijn proefschrift. Temeer omdat je in die periode zeer druk was met je eigen onderzoek en klinische stages. Heel veel succes met je promotie onderzoek.

Lieve pap en mam, ik ben jullie ontzettend dankbaar voor jullie liefde, de zorgeloze omgeving waar ik ben opgegroeid en de kansen die ik van jullie heb gekregen. Dank jullie wel voor jullie onvoorwaardelijke steun en vertrouwen.

## About the Author

Jeroen Vermeulen was born on December 8<sup>th</sup> 1984 in Gouda, The Netherlands. After graduating from the Coenecoop College in Waddinxveen (VWO), he started in 2003 his Bachelor Chemistry at Utrecht University. In 2006 he performed his thesis "*Effect of PI-TP $\alpha$  downregulation in C6 astrogloma on the survival of motor neurons*" at the Department of Biochemistry of Lipids and obtained his Bachelor of Science (cum laude).

In September 2006, Jeroen started with the Master Chemical Sciences, program Biomolecular Sciences at Utrecht University. He performed his 9 months internship at the Department of Membrane Enzymology supervised by Dr. Joost C.M. Holthuis on "*Relationship between P4 ATPase-catalysed lipid transport and vesicle formation*", followed by a 6 months internship at the Department of Cell Biology on "*Nanobody-induced internalisation and subcellular routing of EGFR.*" supervised by Dr. Paul M.P. van Bergen en Henegouwen en Dr. Rob C. Roovers. His Master thesis "*Flip or flop; the inner workings of a disease-related lipid pump*" was submitted to NWO in the context of the Toptalent-grant program. In September 2008, Jeroen obtained his Master of Science (cum laude).

Directly after obtaining his Master's degree, Jeroen started as a PhD-student at the Department of Pathology, University Medical Center Utrecht under supervision of Prof. Paul J. van Diest and Prof. Elsken van der Wall. In May 2010, his PhD-project changed to identification of targets for molecular imaging of breast cancer, of which the results are described in this thesis.

In September 2012 Jeroen started his study medicine to become a medical doctor.

## Curriculum Vitae

Jeroen Vermeulen werd geboren op 8 december 1984 te Gouda. Na het behalen van zijn VWO-diploma aan het Coenecoop College te Waddinxveen, startte hij in 2003 met zijn studie scheikunde aan de Universiteit Utrecht. In 2006 voltooide hij zijn Bachelorscriptie "*Effect of PI-TP $\alpha$  downregulation in C6 astroglioma on the survival of motor neurons*" bij het departement Biochemie van Lipiden en behaalde hij zijn Bachelor of Science (cum laude).

Vervolgens begon Jeroen in september 2006 met de tweejarige Masteropleiding Biomolecular Sciences aan de Universiteit Utrecht. Bij het departement Membraan Enzymologie onder begeleiding van Dr. Joost C.M. Holthuis deed hij een negen maanden durende onderzoeksstage over "*Relationship between P4 ATPase-catalysed lipid transport and vesicle formation*". Hierna volgde een onderzoeksstage van zes maanden bij het departement Cell Biologie. Onder begeleiding van Dr. Paul M.P. van Bergen en Henegouwen en Dr. Rob C. Roovers deed hij onderzoek naar "*Nanobody-induced internalisation and subcellular routing of EGFR*". Zijn Masterthesis "*Flip or flop; the inner workings of a disease-related lipid pump*" werd ingediend bij NWO in het kader van het Toptalent-subsidie programma. In september 2008 behaalde hij zijn Master of Science (cum laude).

Direct na het behalen van zijn master begon Jeroen als promovendus bij de afdeling Pathologie in het UMC Utrecht onder begeleiding van Prof. Paul J. van Diest en Prof. Elsken van der Wall. In mei 2010 veranderde het onderwerp van zijn onderzoek naar het identificeren van mogelijke targets voor moleculaire beeldvorming van borstkanker. De resultaten hiervan zijn beschreven in dit proefschrift.

In september 2012 is Jeroen begonnen met zijn studie geneeskunde.

## List of Publications

J.F. Vermeulen, A.S.A. van Brussel, P. van der Groep, F.H.M. Morsink, P. Bult, E. van der Wall, P.J. van Diest, *Immunophenotyping invasive breast cancer: paving the road for molecular imaging*. BMC Cancer. 2012; 12(1): 240

J.F. Vermeulen\*, R.A.H. van de Ven\*, C. Ercan, P. van der Groep, E. van der Wall, P. Bult, M. Christgen, U. Lehmann, J. Daniel, P.J. van Diest, and P.W.B. Derksen, *Nuclear kaiso expression is associated with high grade and triple-negative invasive breast cancer*. PLOS One. 2012; 7(5): e37864

C. Ercan, J.F. Vermeulen, L.D.C. Hoefnagel, P. Bult, H. Buerger, P. van der Groep, E. van der Wall, P. J. van Diest, *HIF-1 $\alpha$  and NOTCH signaling in ductal and lobular carcinomas of the breast*. Cellular Oncology. 2012 Sept 25 [Epub ahead of print]

J.F. Vermeulen, A.S.A. van Brussel\*, A. Adams\*, W.P.Th.M. Mali, E. van der Wall, P.J. van Diest, P.W.B. Derksen, *Near-infrared fluorescence molecular imaging of ductal carcinoma in situ with CD44v6-specific antibodies in mice: a preclinical study*. Submitted

J.F. Vermeulen, R. Kornegoor, E. van der Wall, P.J. van Diest, *Differential expression of growth factor receptors and membrane-bound tumor markers for imaging in male and female breast cancer*. Submitted

J.F. Vermeulen, E. van der Wall, A.J. Witkamp, P.J. van Diest, *Expression of membrane markers for molecular imaging of ductal carcinoma in situ of the breast*. Submitted

I.A. Ivanova, J.F. Vermeulen, C. Ercan, J.M. Houthuijzen, F. Al Saig, E.J. Vlug, E. van der Wall, P.J. van Diest, M. Vooijs, P.W.B. Derksen, *FER kinase promotes breast cancer growth and metastasis through inhibition of cell adhesion and anchorage dependence*. Submitted.

E.J. Vlug, J.F. Vermeulen, P. Bult, P.J. van Diest, P.W.B. Derksen, *Nuclear expression of the transcriptional coactivator YAP is associated with invasive lobular breast cancer*. Submitted

G.M. Bol, V. Raman, P. van der Groep, J.F. Vermeulen, A.H. Patel, E. van der Wall, P.J. van Diest, *Expression of the RNA helicase DDX3 and the hypoxia response in breast cancer*. Submitted

B. van de Sluis, X. Mao, Y Zhai, A.J. Groot, J.F. Vermeulen, E. van der Wall, P.J. van Diest, M.H. Hofke, C. Wijmenga, L.W. Klomp, K.R. Cho, E.R. Fearon, M. Vooijs, E. Burstein, *COMMD1 disrupts HIF-1alpha/beta dimerization and inhibits human tumor cell invasion*. J Clin Invest. 2010 Jun;120(6):2119-30.

B. van de Sluis, A.J. Groot, J.F. Vermeulen, E. van der Wall, P.J. van Diest, C. Wijmenga, L.W. Klomp, M. Vooijs, *COMMD1 Promotes pVHL and O2-Independent Proteolysis of HIF-1α via HSP90/70*. PLOS One. 2009; 4(10): e7332